

Network mechanisms underlying motor control after ischemic stroke

Inauguraldissertation

zur Erlangung des Doktorgrades
der Humanwissenschaftlichen Fakultät
der Universität zu Köln
nach der Promotionsordnung vom 18.12.2018
vorgelegt von

Theresa Paul

aus
Siegen

Januar 2023

Diese Dissertation wurde von der Humanwissenschaftlichen Fakultät
der Universität zu Köln im August 2023 angenommen.

Acknowledgements

First and foremost, I would like to thank my supervisor and mentor, Dr. Lukas Volz, for his guidance and support throughout the past years. Your determination, your passion for research, and your ability to instill enthusiasm in others have been an inspiration for me. I'd like to thank you for your time, your never-ending support, and our long discussions. I learned a lot from you and I cannot thank you enough.

My sincere thanks also go to my colleagues, Valerie Wiemer and Frauke Esser, who shared this journey with me. Thank you for all your help and for creating a working environment that allowed me to thrive.

I would also like to express my gratitude to Prof. Dr. Gereon Fink who gave me the opportunity to conduct this research at the Department of Neurology at the University Hospital Cologne. Moreover, I would like to thank Prof. Dr. Jan Peters who agreed to supervise this project as a representative of the Department of Psychology.

Finally, I would also like to thank my family and friends. The last four years have been a rollercoaster of emotions and you were always there for me. Your support means the world to me and I could not have done it without you.

Table of Contents

Abstract.....	1
Abbreviations	4
1. Introduction	6
2. Theoretical background.....	11
2.1. The human motor system	11
2.1.1. The corticospinal tract	11
2.1.2. The extrapyramidal system.....	13
2.1.3. Functional role of cortical motor regions	15
2.1.4. Functional role of subcortical motor regions.....	15
2.1.5. Cortical interactions during upper limb movement.....	18
2.2. Motor recovery after stroke.....	18
2.2.1. Principles of motor recovery	18
2.2.2. Characterizing motor deficits	20
2.2.3. The ipsilesional corticospinal tract.....	23
2.2.4. Alternative motor output pathways	26
2.2.5. Cortico-cortical structural connectivity	27
2.2.6. Functional interactions of cortical brain regions in stroke recovery	28
3. Objectives.....	32
4. Methods.....	36
4.1. Principles of magnetic resonance imaging.....	36
4.2. Diffusion MRI	37
4.2.1. The pulsed gradient spin echo sequence	37
4.2.2. Acquisition schemes and reconstruction	38
4.2.3. Measuring microstructural integrity	41
4.2.4. Compartmentwise anisotropy	42
4.3. Functional MRI	44
4.3.1. Preprocessing.....	45

4.3.2.	First- and second-level analyses.....	46
4.3.3.	Effective connectivity.....	47
4.3.4.	Functional connectivity	49
4.4.	Behavioral motor assessment.....	50
4.4.1.	National Institutes of Health Stroke Scale (NIHSS)	50
4.4.2.	Motricity Index (MI)	50
4.4.3.	Action Research Arm Test (ARAT).....	51
4.4.4.	Jebsen Taylor Test of Hand Function (JTT).....	51
4.4.5.	Relative grip strength	52
5.	Empirical section.....	53
5.1.	The role of corticospinal and extrapyramidal pathways in motor impairment after stroke	54
5.2.	Corticospinal premotor fibers facilitate complex motor control after stroke.....	76
5.3.	Basal but not complex motor control relies on interhemispheric structural connectivity after stroke.....	100
5.4.	Early motor network connectivity after stroke: An interplay of general reorganization and state-specific compensation.....	130
6.	General discussion.....	164
6.1.	Study-specific key findings.....	164
6.2.	Advantages of compartmentwise anisotropy in stroke	165
6.3.	Extrapyramidal output pathways.....	167
6.4.	Descending output from premotor regions.....	169
6.5.	Cortico-cortical structural connectivity.....	171
6.6.	Cortico-cortical information integration	173
6.7.	Clinical implications	174
6.8.	Limitations	176
6.9.	Future perspectives.....	179
6.10.	Conclusion.....	181

7. References	183
8. Personal contributions	211

Abstract

Motor impairment is one of the most common symptoms in ischemic stroke. While many patients partially regain lost functions due to plastic changes to the structural and functional architecture of brain networks, recovery is often incomplete, making stroke a leading cause of long-term disability worldwide. Thus, a better mechanistic understanding of motor recovery seems crucial to inform future plasticity-enhancing treatment approaches aiming at improving stroke outcome. The studies summarized in the present thesis therefore aimed at furthering our mechanistic insights into motor network reorganization in acute and chronic stroke patients.

In study 1, we focused on the role of different descending motor pathways on distinct aspects of motor control. While previous studies have frequently linked the integrity of the corticospinal tract (CST) assessed by means of diffusion magnetic resonance imaging (dMRI)-based anisotropy to the level of motor impairment, several limitations hinder its clinical application as a biomarker. From a methodological perspective, the estimation of anisotropy in crossing or kissing fibers, i.e., voxels containing more than one dominant fiber direction, constitutes a challenge when quantifying the integrity of fiber tracts such as the CST. Moreover, alternative output pathways such as the extrapyramidal system partially compensate for lesion-induced deficits, limiting the potential of CST anisotropy to predict motor functions. To address these issues, we applied a novel compartmentwise analysis approach that classifies voxels according to the number of dominant intra-voxel fiber directions. This allowed for a more accurate estimation of microstructural CST integrity by focusing on descending fibers represented by one-directional voxels. Our results provide direct evidence for secondary degenerative processes often referred to as Wallerian degeneration occurring along the entire length of the ipsilesional CST, which were correlated with basal and complex upper and lower limb performance. We further identified specific extrapyramidal brainstem structures involved in basal motor control of the upper and lower limb post-stroke. The lack of a difference between patients and age-matched control subjects across all extrapyramidal compartments suggests that the premorbid level of the extrapyramidal system rather than reorganization processes impact motor control after stroke, highlighting that extrapyramidal tracts may serve as a structural reserve after CST damage.

Study 2 addressed the role of corticospinal output fibers descending from the primary motor cortex (M1) and various premotor areas. It is well-known that premotor areas influence motor commands, yet previous research has mostly focused on cortico-cortical interactions and

mostly neglected their direct descending output to the spinal level. By applying our compartmentwise analysis approach introduced in study 1, we computed tractwise anisotropy of corticospinal output tracts descending from different premotor regions and M1 and assessed its relationship with basal and complex motor control. While M1 subtract anisotropy correlated with both aspects of motor control, anisotropy of premotor subtracts was primarily associated with complex motor skills. Thus, M1 output seemed to be a prerequisite for any form of muscle activation, whereas descending premotor output signals primarily shaped complex motor control during reaching and grasping movements. According to a subgroup analysis, premotor areas might additionally take on a vicarious function in more severely affected patients and also facilitate residual basal motor control.

In study 3, we turned to cortico-cortical structural connectivity. While functional magnetic resonance imaging (fMRI) findings commonly highlight the importance of cortico-cortical interactions in motor control after stroke, studies on structural connectivity within the cortical motor network remain sparse. Therefore, we generated normative cortico-cortical tract templates using data from the Human Connectome Project (HCP) and computed tractwise anisotropy between cortical motor regions. Both ipsilesional premotor-M1 and M1-M1 structural connectivity was strongly associated with motor impairment. While complex motor control depended on ipsilesional CST integrity, the association with basal motor control persisted when controlling for CST anisotropy. Thus, complex motor control strongly relies on ipsilesional descending motor signals, whereas basal motor output might be relayed through an alternative route via the contralesional M1 to access contralesional CST fibers. Especially patients who underwent substantial recovery seemed to exploit this alternative route.

Finally, study 4 utilized fMRI-data from acute stroke patients to conduct the first direct comparison of resting-state functional and task-related effective connectivity. Previous studies in stroke patients have frequently shown a relationship between both ipsilesional premotor-M1 and interhemispheric M1-M1 connectivity assessed via both approaches. This raises the question whether both kinds of motor network connectivity reflect similar aspects of altered information integration. While measures of motor network resting-state functional and task-related effective connectivity were not correlated, we observed a fundamental difference between intrahemispheric and interhemispheric connectivity when including task-related functional connectivity as an additional methodological approach. Intrahemispheric connectivity seemed to depend on the activation state, whereas interhemispheric connectivity was state-independent. Therefore, interhemispheric connectivity after stroke likely relied on more general, overarching principles that could be captured in both activation states. In contrast,

reorganization of ipsilesional connectivity might be state- and task-dependent. Of note, both connectivity approaches explained a substantial amount of behavioral variance, highlighting their potential for clinical applications aiming at decoding motor impairment and recovery thereof in acute stroke patients.

Taken together, our findings offer novel insights into mechanisms underlying motor control after stroke. First, they provide evidence for Wallerian degeneration along the length of the ipsilesional CST, which has a detrimental effect on motor performance. Interestingly, our results also indicate that the mechanistic compensation of these deficits differs between basal and complex motor control. Complex motor skills seem to rely primarily on premotor-M1 connections as well as corticospinal CST fibers descending from premotor regions. In contrast, the compensation of basal motor control might rely on extrapyramidal tracts as well as interhemispheric M1-M1 connectivity, which might help to relay signals via transcallosal fibers and the contralesional M1 and CST to the spinal level.

From a clinical perspective, our results hold important implications for the quest to identify biomarkers which allow the prediction of post-stroke recovery as well as the development of personalized treatment options. Based on our results, future biomarker research should not only focus on the integrity of the ipsilesional CST as commonly suggested in the literature, but should consider ipsilesional CST integrity, extrapyramidal structures, and cortico-cortical structural and functional connectivity in concert to achieve a more holistic description of the stroke-afflicted motor system. With respect to the improvement of therapeutic interventions, it might be beneficial to choose cortical target regions for plasticity-enhancing transcranial magnetic stimulus (TMS) interventions based on the structural reserve provided by the corticospinal fibers. Premotor regions with richer descending fiber structures might be better suited to take on a vicarious function and relay motor signals to the spinal level.

Abbreviations

ARAT	Action research arm test
BMS	Bayesian model selection
BOLD	blood-oxygenation level dependent
CSF	cerebrospinal fluid
CST	corticospinal tract
DCM	Dynamic Causal Modelling
dMRI	diffusion magnetic resonance imaging
DSI	diffusion spectrum imaging
DTI	diffusion tensor imaging
EMG	electromyography
FA	fractional anisotropy
fMRI	functional magnetic resonance imaging
FM-UE	Fugl-Meyer upper extremity
FWHM	full width at half maximum
gFA	generalized FA
GLM	general linear model
GM	grey matter
GQI	generalized q-sampling imaging
GSR	global signal regression
HARDI	high angular resolution imaging
HCP	Human Connectome Project
HRF	hemodynamic response function
iTBS	intermittent theta burst stimulation
JTT	Jebsen Taylor test of hand function
M1	primary motor cortex
MEP	motor-evoked potential
MI	motricity index
MNI	Montreal Neurological Institute
NIHSS	National Institutes of Health Stroke Scale
ODF	orientation distribution function
PCA	principal component analysis
PLIC	posterior limb of the internal capsule
PMd	dorsal premotor cortex

PMv	ventral premotor cortex
RF	radiofrequency
ROI	region of interest
rTMS	repetitive TMS
SMA	supplementary motor area
TE	time to echo
TMS	transcranial magnetic stimulation
TR	repetition time
WM	white matter

1. Introduction

With more than 12 million new cases per year, stroke remains a major cause of death and long-term disability worldwide (Feigin et al., 2021). While improved interventional therapy options have led to an increasing number of stroke survivors (Goyal et al., 2016; Thomalla et al., 2018), the number of people suffering from stroke-related disabilities is constantly rising (Feigin et al., 2021; Grefkes & Fink, 2020). Considering that 80% of stroke patients exhibit motor deficits in the acute (Bonita & Beaglehole, 1988) and 65% in the chronic stage (Dobkin, 2005), finding novel interventions to enhance motor recovery seems crucial. As the development of such therapeutic strategies strongly depends on a sound understanding of the processes facilitating motor recovery, this thesis aims at elucidating the underlying mechanisms and exploring their implications for clinical practice.

In general, there are two possible mechanisms that can lead to the occurrence of a stroke. Only about 10% are caused by intracranial bleeding, e.g., due to the rupture of a blood vessel, commonly referred to as *hemorrhagic* (Chauhan & DeBette, 2016). The remaining 90% are considered *ischemic* and result from the occlusion of a blood vessel (Andersen et al., 2009). Due to the disruption of blood flow during acute ischemia, the corresponding vascular territory is deprived of oxygen and the affected brain tissue is irreversibly damaged. While this tissue cannot be recovered, many patients are still able to regain lost functions in the following months post-stroke. The question how this is possible has been debated for over two centuries now, yet the underlying mechanisms are still not fully understood. Given our current state of knowledge, the widely accepted answer would be that recovery can be achieved by means of *plasticity*, which describes the brain's remarkable ability to compensate the loss of specialized neural tissue by adapting its structural and functional architecture. This process is thought to involve both local changes in spatial proximity to the lesion as well as remote reorganization processes on a network level (Grefkes & Ward, 2014; Nudo, 2006a).

Just like our current understanding of lesion-induced changes and possible compensatory mechanisms is closely intertwined with our understanding of the brain as a complex and interconnected system, previous theories on functional compensation closely reflect the mechanistic understanding of the brain at a given time. In the 17th and 18th century, the brain was believed to consist of two perfectly symmetrically organized hemispheres (Bichat, 1805; Finger, 2009; Wigan, 1844; Willis, 1664). Following this logic, proponents of *redundancy theories* advocated that the intact hemisphere should be able to carry out all functions after one hemisphere had been injured (Finger, 2009). The noted inability of the intact hemisphere to fully compensate for lost functions was generally attributed to an imbalance

between both hemispheres, which helped to explain adverse outcomes after unilateral brain damage.

This view was eventually refuted when Paul Broca discovered that aphasia was caused by lesions to a specific cortical area in the left hemisphere (Broca, 1863). The ensuing reports on functional deficits caused by focal left hemispheric cortical lesions led the field to adopt the notion of *functional specialization* of cortical regions and hemispheres (Finger, 2009). Importantly, these specialized regions were not regarded as isolated entities, but scientists acknowledged early on that a brain lesion could also affect distant but connected brain areas (Boes et al., 2015; Brown-Séguard, 1875). Based on this idea, von Monakow coined the term *diaschisis*. It describes symptoms related to a dysfunction of remote areas not directly affected by the lesion as a result of alterations in excitatory or inhibitory inputs from lesioned tissue to the remote region (Carrera & Tononi, 2014; von Monakow, 1914). During the alleviation of diaschisis, the function of the remote region is reinstated by substitution of excitatory or inhibitory inputs resulting from reorganizational processes (Carrera & Tononi, 2014).

Combining the logic of remote effects with the notion of functionally specialized cortical regions, the scientific community witnessed an increasing popularity of so-called *vicariation theories* starting in the second half of the 19th century (Finger, 2009). At the core of these theories stood the belief that the functional loss incurred by damage to a functionally specialized brain region could be compensated by another brain region originally not involved in this particular task. Using a double-lesion approach in which researchers induced a second lesion after (partial) recovery from ablation of the cortical hand or limb representation, the functional relevance of ipsilesional tissue for motor recovery could be directly demonstrated: Mapping the cortical representations using intracranially applied electric currents showed a cortical remapping of muscle groups to perilesional tissue in developing animals alongside motor recovery (Kennard, 1936, 1938; Soltmann, 1876). As these results could not be replicated in the adult cortex, cortical plasticity was believed to be limited to the developing brain (Finger, 2009; Kennard, 1936; Sherrington & Grunbaum, 1901).

First evidence of plasticity in the adult brain was reported by Glees and Cole who observed cortical remapping of the thumb representation in the fully-developed macaque cortex (Glees & Cole, 1950). However, a paradigm shift was only achieved years later when Michael Merzenich and his group published a series of experiments showing remapping in adult macaque monkeys after digit amputation (Merzenich et al., 1984) and in response to behavioral learning (Nudo, Milliken, et al., 1996; Nudo, Wise, et al., 1996). The occurrence of cortical map changes was strongly use-dependent, suggesting that the critical factor driving cortical

remapping was training rather than age (Nudo, 2003; Nudo, Milliken, et al., 1996; Nudo, Wise, et al., 1996). Approximately 100 years after the idea of vicariation had been born, these findings ushered in a new era of plasticity research and spurred the interest in recovery-related reorganization processes (Dancause & Nudo, 2011). At the same time, groundbreaking technical and methodological innovations helped to rapidly advance our knowledge on the functioning of the human motor system.

With the advent of functional magnetic resonance imaging (fMRI) it became possible to non-invasively identify brain regions involved in a given task or in responding to a stimulus (Bandettini et al., 1992; Kwong et al., 1992; Ogawa et al., 1992). By measuring region-specific neural activation based on the blood-oxygenation level dependent (BOLD) signal it provided researchers with the opportunity to non-invasively record activity in the living human brain (Ogawa et al., 1990). A fundamental observation was that the execution of various tasks commonly entailed the simultaneous activation of several remote brain areas. Thus, the concept of functional integration was adopted ascribing human behavior to arise from the interactions of multiple brain regions (Friston, 1994). In line with this view, researchers no longer tried to pinpoint a particular brain area responsible for vicariation, but rather attributed functional recovery to a network of several interconnected regions (Grefkes & Fink, 2011).

Especially the emergence of new modelling approaches to quantify brain network connectivity paved the way for an improved understanding of mechanisms underlying motor recovery. In general, one needs to distinguish between *functional* and *effective connectivity*. While functional connectivity describes temporal correlations between low-frequency BOLD signal fluctuations of different brain regions at rest (Biswal et al., 1995), effective connectivity quantifies the influence one region exerts over another during task execution and is commonly assessed by means of Dynamic Causal Modelling (DCM; Friston et al., 2003). Interestingly, both approaches suggest similar network mechanisms to contribute to motor recovery. On the one hand, information integration between premotor areas and ipsilesional M1 seems to play a crucial role in motor recovery, yet the exact processes through which premotor areas impact motor control post-stroke remain incompletely understood. Similarly, a growing body of evidence emphasizes that the contralesional M1 is in some way related to functional motor outcome, but it still remains unclear whether the commonly observed overactivation should be considered maladaptive or vicarious. Hence, the role of the contralesional hemisphere remains a topic of ongoing scientific debate.

In addition to these fMRI findings, a new line of research has emerged trying to predict residual motor functions based on structural information. While only a limited number of

studies has focused on cortico-cortical *structural connectivity* between the core motor regions implicated by fMRI-studies, there is a growing body of evidence tying structural damage of the corticospinal tract (CST) – the main output pathway of the motor system – to residual motor function (Koch et al., 2016). To date, the most promising approach to quantify the integrity of fiber pathways is based on diffusion MRI (dMRI), which estimates the *microstructural integrity* of white matter tissue based on the diffusion of water molecules (Basser, 1995). However, methodological limitations inherent to dMRI as well as functional motor system reorganization compensating for the lesion-induced CST degeneration hinder a reliable prediction of motor recovery on the level of individual patients.

In summary, the informational wealth obtained through different neurophysiological readouts led to today's understanding of motor recovery as a multifaceted concept that relies on various interacting mechanisms. Despite those advancements, the underlying processes are still not fully understood, and many clinically relevant questions remain unanswered to date. This is reflected in a consensus paper published by leading stroke experts in 2017, who identified (i) how to assess a patient's potential for recovery and (ii) how to tailor therapeutic interventions to maximize the functional outcome for each patient as the most pressing questions from a clinical perspective (Boyd et al., 2017). To answer these questions, we need to further our understanding of the mechanisms underlying motor recovery. Hence, mechanistic studies need to elucidate these pathophysiological mechanisms to inform the design of subsequent large-scale clinical trials with the goal to improve therapeutic interventions.

In line with this notion, the present thesis aims to advance our understanding of stroke-related changes to the motor network. Using state-of-the-art imaging approaches, we investigated structural and functional reorganization processes in four separate studies while focusing on distinct aspects of motor control. First, we addressed the role of different descending motor pathways in motor control of basal and complex movements via a novel dMRI analysis approach. In study 2, we used this newly established methodological dMRI approach to answer the question whether premotor areas can influence different motor control policies via descending corticospinal output signals. Next, we turned to cortico-cortical interactions. In study 3, we addressed whether structural connectivity of premotor-M1 as well as interhemispheric M1-M1 fiber tracts was differentially involved in various aspects of motor control and whether these cortico-cortical compensation processes were associated with the degree ipsilesional CST damage. In the fourth and final study, we compared functional and effective connectivity of this cortical motor network in the acute phase post-stroke to investigate whether both reflect similar (i.e., general) or differential (i.e., activation state-dependent)

aspects of motor network reorganization. Thus, the present thesis constitutes an attempt to draw a more complete picture of post-stroke motor control that integrates both cortico-cortical interactions and descending motor output and thereby advances our mechanistic understanding of motor control and recovery after stroke.

2. Theoretical background

In the following section, I will outline the theoretical concepts relevant for the present thesis. First, a brief overview will be provided of the anatomical structures involved in the generation of voluntary movements and their functional interactions. Then, I will proceed by describing different overarching mechanisms through which the human brain is thought to regain motor function after stroke-inflicted damage. Finally, I will illustrate how these mechanisms apply to different aspects of motor control by focusing on descending motor pathways as well as distinct cortico-cortical interactions.

2.1. The human motor system

The execution of voluntary movements relies on an intricate network of various cortical and subcortical areas, their interconnecting fiber tracts as well as descending output pathways that relay signals from their cortical origin to the spinal level. The central cortical region for the generation of motor signals is M1, the primary motor cortex. It is densely interconnected with various cortical premotor areas including the supplementary motor area (SMA), the dorsal premotor cortex (PMd) and the ventral premotor cortex (PMv). Subcortical structures such as the cerebellum and basal ganglia are further involved in feedback and feedforward loops with M1 that help to modulate and fine-tune ongoing movements. Several descending pathways relay motor signals to the spinal level from where they reach peripheral muscles (Baker, 2011; Lemon, 2008).

2.1.1. The corticospinal tract

The corticospinal tract is considered the most important descending output pathway (Lemon, 2008). More than half of its fibers emerge from large pyramidal cells located in cortical layer V of M1 in the precentral gyrus (Geyer et al., 2000; Lemon, 2008). Axons of these so-called upper motor neurons descend and form the CST. After travelling through the corona radiata, the descending CST fibers converge and form a densely packed bundle projecting through the posterior limb of the internal capsule (PLIC). From there, they travel further down through the cerebral peduncles and the ventral pons and afterwards form the medullary pyramids. Approximately 85% of CST fibers cross over to the opposite side into the lateral columns of the spinal cord in the pyramidal decussation, which is located at the height of the cervicomedullary junction, i.e., the intersection between medulla and spinal cord (Blumenfeld, 2010). The remaining 15% proceed ipsilaterally, forming the anterior CST. Axons finally

synapse onto lower motor neurons in the anterior horn, either monosynaptically or indirectly via interneurons. Notably, monosynaptic projections to spinal motor neurons are unique to primates and are thought to enable fine motor control and higher degrees of manual dexterity (Bortoff & Strick, 1993; Heffner & Masterton, 1975; Strick et al., 2021). Lower motor neurons transmit efferent signals to peripheral muscles where a reaction is generated via the release of acetylcholine (for a schematic presentation of the upper and lower motor neuron of the CST, please refer to Figure 1). As the lateral CST mainly controls distal muscle groups of the arm and leg of the contralateral side of the body, its lower motor neurons predominantly exit at the cervical and lumbosacral enlargements (Blumenfeld, 2010). In contrast, the anterior CST innervates bilateral axial and girdle muscles and therefore terminates mostly at the cervical and upper thoracic cord (Blumenfeld, 2010; Kwon et al., 2011).

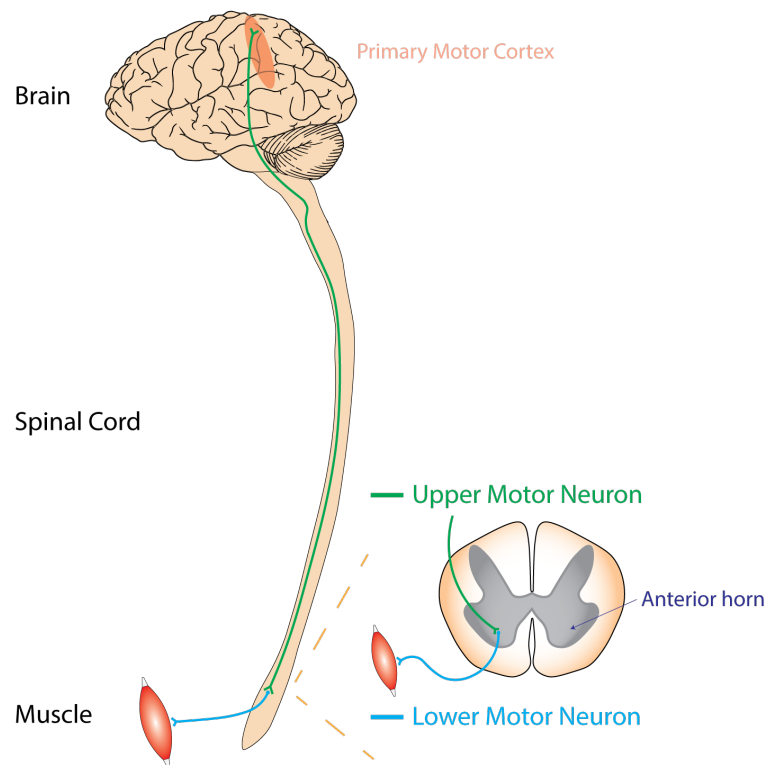


Figure 1: Schematic representation of the corticospinal tract (CST). Motor signals descend from cortical areas where the upper motor neuron originates. Forming the CST, upper motor neurons descend to the spinal level where they synapse onto lower motor neurons. Lower motor neurons then transmit signals to peripheral muscles. The image was adapted from https://commons.wikimedia.org/wiki/File:UMN_vs_LMN.png.

Importantly, even though a vast proportion of studies focus on M1 as the origin of descending motor commands, only approximately one third of all corticospinal fibers emerge from M1 (Strick et al., 2021). The remaining fibers originate mostly from premotor areas including SMA, PMv, and PMd as demonstrated by invasive tracer studies in monkeys (Dum & Strick, 1991; Galea & Darian-Smith, 1994; Nudo & Masterton, 1990). Given the substantial amount of corticospinal neurons located in premotor areas, it can be assumed that premotor areas may directly contribute to the generation of movements via their efferent fibers and do not necessarily need to relay information through M1 to reach the spinal level. Therefore, corticospinal fibers originating from premotor areas seem to be in a prime position to transmit motor signals to the spinal level after damage to M1 or its descending fibers.

2.1.2. The extrapyramidal system

The corticospinal system is complemented by several other descending motor tracts. These tracts originate at the level of the brainstem yet receive rich projections from various cortical areas. According to their termination pattern on the spinal level, a ventromedial and dorsolateral motor system can be distinguished (Lemon, 2008; Figure 2).

The ventromedial system includes the reticulospinal, tectospinal, and vestibulospinal tracts, which descend from the brainstem reticular formation, superior colliculus, and vestibular complex. Their fibers descend bilaterally and terminate in the ventromedial intermediate zone of the spinal cord (Blumenfeld, 2010; Lemon, 2008). The traditional and widely accepted view is that the ventromedial tracts innervate bilateral axial and girdle muscles, thereby facilitating postural stability as well as control of head, neck and proximal limb movements (Lawrence & Kuypers, 1968b). However, more recent findings have demonstrated monosynaptic projections of the reticulospinal tract to finger flexors, suggesting a potential additional influence on distal limb control (Baker, 2011). In line with this notion, it has recently been shown that the population-averaged firing rate of neurons located in the reticular formation is associated with the level of force contraction of the hand (Glover & Baker, 2022). Interestingly, while output from the reticulospinal tract seemed to code for the level of strength, output from pyramidal neurons of the CST matched more fine-grained adjustments. Thus, the reticulospinal tract seems to become increasingly important for distal motor control with the recruitment of higher levels of muscle strength.

The dorsolateral rubrospinal pathway emerges from the red nucleus and decussates in the ventral tegmental midbrain. It terminates in the dorsolateral region of the intermediate zone of the spinal cord to control movements of the contralateral extremities as demonstrated in

various animal studies (Blumenfeld, 2010; K uchler et al., 2002; Lemon, 2008). While this anatomical pattern has recently been confirmed in humans using diffusion tensor imaging (DTI)-based fiber tracking (Yang et al., 2011), its functional role in humans remains unclear (Cheney et al., 1991; de Oliveira-Souza, 2012). While most studies consider the rubrospinal tract as vestigial in humans (Blumenfeld, 2010), some studies suggest that it might take on a compensatory role after CST lesions by transmitting motor output signals to the spinal level, thereby helping to circumvent the damaged CST (Ruber et al., 2012; Takenobu et al., 2014).

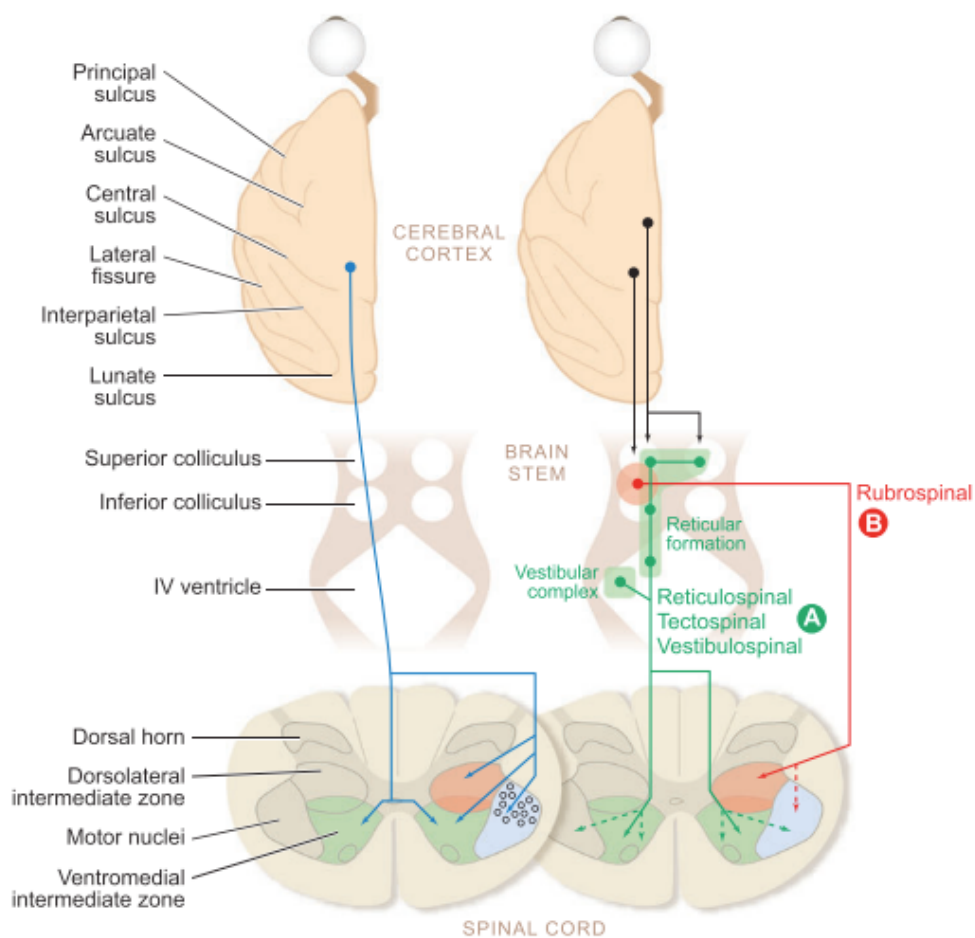


Figure 2: Corticospinal tract and extrapyramidal motor pathways. Corticospinal projections are depicted in blue on the left. The extrapyramidal pathways can be classified into a ventromedial system including reticulospinal, tectospinal, and vestibulospinal tracts (shown in green), and a dorsolateral system consisting of the rubrospinal tract (depicted in red). The extrapyramidal system receives projections from cortical areas shown in black. Adapted from Lemon, 2008.

2.1.3. Functional role of cortical motor regions

Building the functional core of the human motor system, M1 is located at the interior wall of the central sulcus and extends to the dorsal precentral gyrus (for the anatomical locations of cortical motor regions, see Figure 3A). It is somatotopically organized with the size of the cortical representation depending on the complexity of the represented muscle groups (Penfield & Boldrey, 1937). While the lower limbs are represented in the medial part of M1, the upper limbs are located more laterally.

M1 is complemented by various secondary motor regions located in the frontal lobe including SMA, PMd, PMv, and cingulate motor areas, which impact motor control through excitatory inputs to M1 and via descending motor fibers (Chouinard & Paus, 2006; Dum & Strick, 1991). The SMA is thought to support the execution of sequential movements (Gerloff et al., 1997) as well as the timing and temporal organization of movements (Lara et al., 2018; Macar et al., 2004) and initiation of upper limb movements (Bannur & Rajshekhar, 2000). Conversely, PMv and PMd are essential for reaching and grasping movements (Rizzolatti & Luppino, 2001; Schubotz & Von Cramon, 2003). While the PMv facilitates the positioning of fingers around objects, the PMd supports controlled reaching movements by coordinating the sequential recruitment of muscles (Davare, 2006). Notably, these premotor areas also show a somatotopic organization with a clear differentiation between proximal and distal limb representations (He et al., 1995).

Moreover, various higher-order regions also impact motor control. For example, prefrontal areas are involved in planning or inhibiting planned movements and monitoring motor execution (Corbetta & Shulman, 2002; Grafton & Volz, 2019). Moreover, parietal brain regions are crucial for coordinated hand movements and object manipulation as they facilitate visuomotor integration by giving rise to spatial representations of oneself and the environment (Corbetta & Shulman, 2002; Grafton & de C. Hamilton, 2007; Grefkes et al., 2004; Grefkes & Fink, 2005).

2.1.4. Functional role of subcortical motor regions

In addition to the aforementioned cortical areas, several subcortical regions contribute to the control of ongoing motor actions including the basal ganglia and the cerebellum (Figure 3B). The basal ganglia consist of the striatum (with caudate nucleus and putamen), the globus pallidus (divided into an internal and external segment), subthalamic nucleus and substantia nigra (Alexander & Crutcher, 1990; Smith et al., 1998). Especially the putamen receives rich projections from cortical areas. From there, signals are transmitted to the internal and external

globus pallidus and the substantia nigra from where they are relayed back to the motor cortex via thalamic nuclei (Alexander & Crutcher, 1990). Thereby, a closed loop system is formed between motor cortex and basal ganglia, which is considered crucial for the selection, facilitation, and inhibition of motor actions (Alexander & Crutcher, 1990; Friend & Kravitz, 2014). Moreover, it plays a critical role in motor and reinforcement learning by chunking individual actions into movement sequences (Graybiel, 1998) and influencing motor control in response to motivational factors (Turner & Desmurget, 2010).

A similar closed loop architecture has been described for cortico-cerebellar interactions (Allen & Tsukahara, 1974; Middleton, 2000). Here, cortical motor signals are relayed through brainstem nuclei to the cerebellum, where they primarily project to the intermediate and lateral zones of the contralateral cerebellum (Allen & Tsukahara, 1974; Ramnani, 2006; Stoodley & Schmahmann, 2010). Reciprocal signals are transmitted from the anterior part of the cerebellum via the thalamus back to the cerebral cortex, closing the cortico-cerebellar loop (Ramnani, 2006; Stoodley & Schmahmann, 2010). The functional role of this system lies in the online-control and fine-tuning of ongoing movements (Allen & Tsukahara, 1974; Shadmehr et al., 2010). The cerebellum is thought to implement an internal forward model that predicts the consequences of specific motor commands. The comparison of these predictions with real-time feedback enables the adjustment of movements and adaptation of motor control policies via error-based learning (Shadmehr et al., 2010).

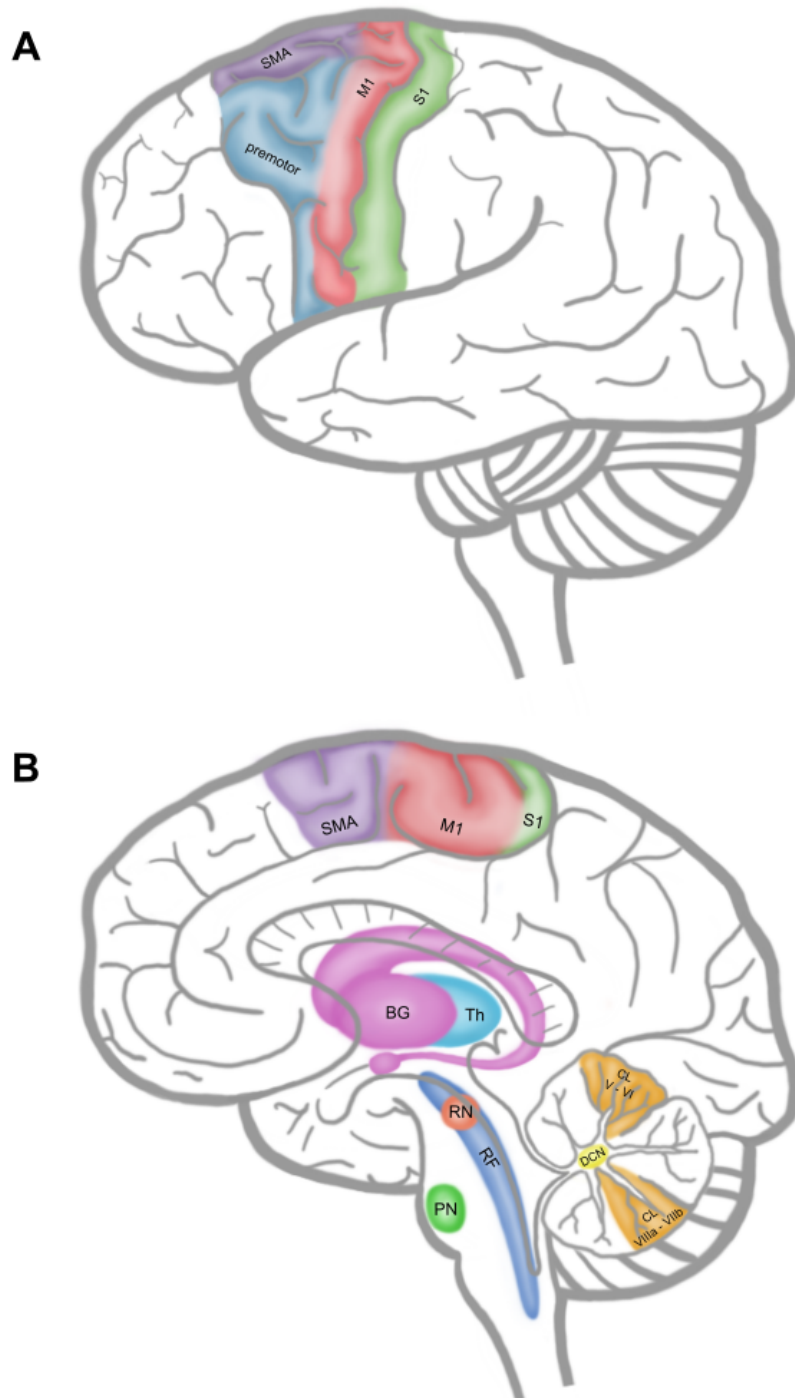


Figure 3: Cortical and subcortical motor areas. The brain regions depicted here play a major role in motor control. A) M1: primary motor cortex, SMA: supplementary motor area, premotor: premotor cortex, S1: primary somatosensory cortex; B) BG: basal ganglia, Th: thalamus, RN: red nucleus, RF: reticular formation, PN: pontine nuclei, DCN: deep cerebellar nuclei, CL: cerebellar lobule. The localization of regions was based on textbooks and atlases (Blumenfeld, 2010; Diedrichsen, 2006; Diedrichsen et al., 2009; Trepel, 2017).

2.1.5. Cortical interactions during upper limb movement

When investigating unilateral hand movements using fMRI, healthy participants usually exhibit pronounced neural activation in cortical regions contralateral to the moving hand as well as in the ipsilateral cerebellum (Pool et al., 2013, 2014). Directional influences between core regions of the cortical motor system have been assessed by means of DCM analyses, revealing a robust pattern of interregional coupling across studies (Grefkes, Eickhoff, et al., 2008; Pool et al., 2013, 2014; Volz, Eickhoff, et al., 2015). In particular, studies unanimously describe excitatory couplings from premotor areas onto the *active* M1 (i.e., contralateral to the moving hand) with concurrent inhibition of the *inactive* M1 (i.e., ipsilateral to the moving hand) by premotor areas and the active M1. In other words, while the active M1 generating motor signals receives driving inputs, it simultaneously inhibits its inactive homolog. Thus, the successful execution of unilateral hand movements relies on the balanced interplay of various motor areas, which can be severely disrupted by damage to one or several network elements.

2.2. Motor recovery after stroke

The ability to perform voluntary movements is something that we usually take for granted. Getting up in the morning, preparing coffee, reaching effortlessly for a mug and moving it with great precision to our mouth are just ordinary activities for us until the finely tuned system underlying those motions comes out of balance. Many people experiencing a stroke suddenly become aware of how dependent we are on our ability for motor control as motor deficits including hemiparesis or hemiplegia rank among the most commonly observed symptoms (Dobkin, 2005). While hemiparesis refers to unilateral movement deficits or weakness of the upper or lower limb, the term hemiplegia describes its complete paralysis (Krakauer & Carmichael, 2017). As already outlined in the introduction, (partial) recovery from these deficits is possible due to plastic changes in the motor system that typically unfold over time.

2.2.1. Principles of motor recovery

While neither the outcome nor the timeline of the recovery process of a given patient can be reliably predicted, some overarching principles have been identified that apply to different phases of the recovery process. In an attempt to standardize the time window for each of these phases across different studies, the *Stroke Recovery and Rehabilitation Roundtable Taskforce* suggested a reference framework that classifies different stages post-stroke (Bernhardt et al., 2017). In their consensus paper, they classified the first 24 hours as the hyperacute phase, day 1 to 7 as the acute phase, the time from 7 days to 3 months as the early

subacute phase, months 4 to 6 as the late subacute phase and the time from 6 months onward as the chronic phase (Figure 4). While this classification supplies a useful framework to make results more comparable across studies, the recovery process should not be viewed as a sequence of fixed events but rather as a continuous and non-linear process characterized by interindividual differences between patients (Grefkes & Fink, 2020).

In the first hours after infarct onset, the restriction of blood flow and the associated lack of oxygen leads to cell death in the affected tissue. From a therapeutic perspective, the aim in this acute phase is immediate recanalization of the compromised blood vessel, which has become possible through the introduction of novel treatment options in the early 2000s (Goyal et al., 2016; Thomalla et al., 2018). During the first hours after stroke onset, thrombolytic medication can be administered and clots blocking large proximal arteries can be mechanically removed via thrombectomy to minimize the loss of brain tissue. As acute motor impairment correlates with motor outcome in the chronic stage, these first few hours are critical for a patient's long-term trajectory (Stinear et al., 2012, 2017; van der Vliet et al., 2020).

Importantly, lesion-induced functional impairments do not exclusively stem from the loss of tissue due to the lesion itself but also arise from the subsequent dysfunction of structurally and functionally connected regions that are deprived of excitatory or inhibitory inputs as captured by the concept of diaschisis (Carrera & Tononi, 2014; Dancause & Nudo, 2011; von Monakow, 1914). Symptoms arising from diaschisis can partially subside in the acute phase as diaschisis alleviates. In parallel, the infarction sets into motion a cascade of different processes that are thought to induce plasticity on the molecular, cellular, and systems level (Cassidy & Cramer, 2017; Nudo, 2006b, 2013). Mechanisms including axonal sprouting, dendritic growth, formation of synaptic connections and a heightened expression of growth-related genes and proteins have been found to facilitate a period of increased plasticity in the acute and subacute phase post-stroke (Bernhardt et al., 2017; Cassidy & Cramer, 2017). This endogenous aspect of recovery is commonly referred to as *spontaneous recovery* and parallels processes known from animal studies that can also occur in the absence of training (Cassidy & Cramer, 2017; Tower, 1940). These naturally occurring processes can be enhanced by training interventions that exploit the malleable state of the motor system to optimize its functional reorganization. After an early window of heightened plasticity, motor recovery usually decreases when approaching the chronic stage until it reaches a plateau, whereas recovery in other domains might continue (Bernhardt et al., 2017; Langhorne et al., 2011).

When describing recovery, restitution of function is often differentiated from functional compensation. Restitution refers to “real recovery”, i.e., the return to physiological functioning

of the limb as observed in healthy individuals, and is mostly achieved during the phase of heightened plasticity (Bernhardt et al., 2017). The further the patient advances into the chronic stage, the more he or she starts to rely on compensational strategies (Cirstea & Levin, 2000). In other words, instead of using physiological movements from their premorbid repertoire, stroke patients adapt alternative patterns instead. Improvements in the execution of complex motor tasks in the chronic stage and increased independence despite the absence of heightened plasticity can largely be attributed to such compensational strategies.

In summary, the improvement of motor functions after stroke can be attributed to three major factors: (i) the alleviation of diaschisis, i.e., the subsiding effect of the lesion on remote regions, (ii) restitution of function in form of spontaneous recovery, and (iii) compensatory mechanisms. Empirically distinguishing these parallel processes is extremely difficult and the relative contribution of each aspect depends on numerous factors such as the time post-stroke and individual features of each patient. Considering the complexity of the recovery process, the question arises how motor impairment and recovery thereof can be quantified in a meaningful way, which ideally allows to identify the underlying mechanism of recovery.

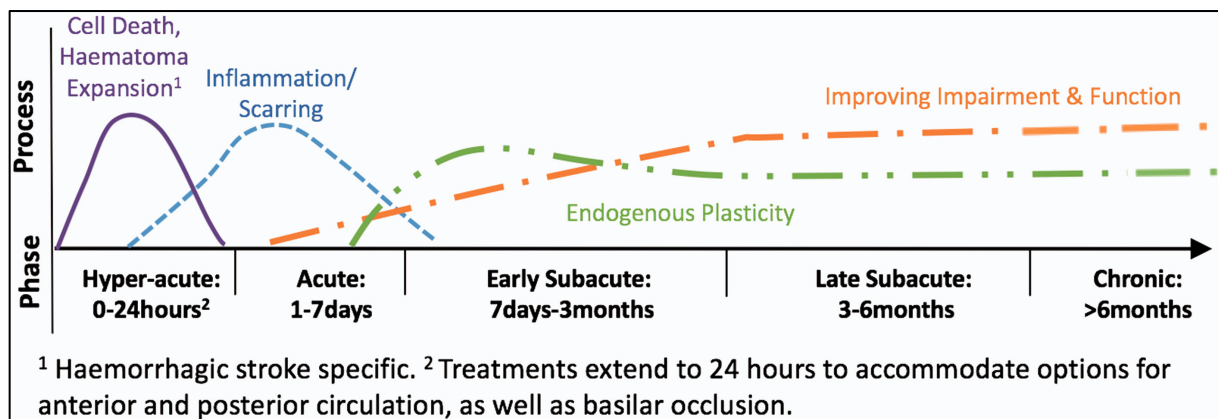


Figure 4: Time course of motor recovery. The recovery process after stroke as classified by the *Stroke Recovery and Rehabilitation Roundtable Taskforce*. Adapted from Bernhardt et al., 2017.

2.2.2. Characterizing motor deficits

Of note, the exact symptoms associated with hemiparesis of the upper limb can fundamentally differ between patients. While one patient might have difficulties reaching towards or grasping an object, another might only notice his or her deficit when trying to use fine motor skills like writing. Yet another might already experience severe difficulties when attempting to simply lift the affected arm. As a consequence, quantifying motor deficits in a

way that meaningfully reflects a patient's deficit while simultaneously capturing interindividual differences is a challenging endeavor.

A helpful concept to quantify upper limb motor deficits lies in categorizing deficits along two gradients: (i) proximal-to-distal muscle groups and (ii) gross-to-fine motor control (Lang et al., 2005; McMorland et al., 2015). Both themes can already be found in early animal studies investigating the effects of pyramidotomy on upper limb functions in monkeys (Beck & Chambers, 1970; Lawrence & Kuypers, 1968a; Tower, 1940) and have since been adopted in various scales quantifying post-stroke motor control (Fugl-Meyer et al., 1975; Jebsen et al., 1969; Lyle, 1981; Wade, 1989). Importantly, while the occurrence of specific motor deficits is not limited to a particular point in time post-stroke, the dissemination of specific symptoms is thought to show a distinct temporal pattern. While proximal and distal muscle groups tend to be equally affected early after stroke (Lang et al., 2005), the motor system seems to recover proximal functions more easily (Tower, 1940). With respect to the second gradient, i.e., gross-to-fine motor control, gross weakness dominates stroke symptoms in the early phase post-stroke, while problems with fine motor control often only become apparent as more severe symptoms subside. This phenomenon is reflected by large clinical trials using grip strength as their primary outcome measure (Hensel et al., 2019) as well as in clinical bedside assessments such as the National Institutes of Health Stroke Scale (NIHSS), which contains rather coarse items to assess motor function such as lifting and holding up the arm against gravity (Brott et al., 1989). Of note, deficits in more complex motor control such as fine motor control or reach-to-grasp movements are not adequately captured by these measures. Thus, more fine-grained test batteries are needed for mildly-to-moderately affected or well-recovered patients.

These more elaborate motor tests can be grouped into two different categories capturing either *restitution of function* or *compensation*, two interacting strategies employed by the motor system to counteract stroke-related deficits (see also section 2.2.1.). To gain a better understanding of how these underlying mechanisms manifest on a behavioral level, it is helpful to introduce the concept of *muscle synergies*. Of note, the term muscle synergies is used to describe different concepts depending on the context (McMorland et al., 2015; Roh et al., 2015).

In the motor control literature, muscle synergies commonly refer to the recruitment of a specific group of muscles in a stable spatiotemporal pattern (d'Avella, 2009; Roh et al., 2015). Movements are generated by flexibly combining these synergies rather than selecting each muscle command individually. To avoid confusion, I will refer to this concept as *motor primitives* rather than muscle synergies throughout this text. From a mathematical standpoint, motor primitives can be considered as a form of dimensionality reduction to generate motor

commands more efficiently by reducing the degrees of freedom. Support for this notion stems from the mathematical decomposition of motor cortical spiking data recorded from macaques that exhibited the same recurring pattern as the simultaneously recorded forelimb muscular activity (Overduin et al., 2015). Thus, the spatiotemporal pattern of distal muscle activity was reflected at the cortical level, representing a motor primitive.

As a result of a brain lesion, certain motor primitives might not be available anymore, which means that the motor system is lacking relevant building blocks. Restitution of function would involve re-building the pre-existing motor primitives, which give rise to physiological patterns of muscle activation as observed in healthy individuals. Thus, the resulting movement would feature premorbid qualities in terms of speed, accuracy and smoothness and thus would not be distinguishable from the movement of a healthy individual (Nudo, 2013).

An alternative definition of muscle synergies - which I will be using throughout this thesis - refers to stereotypical patterns of co-activation of specific muscles and ensuing coupling across different joints during a given movement (McMorland et al., 2015). Simply put, there is considerable redundancy with various combinatory options to achieve a certain task. For example, when repeatedly dunking a tea bag into hot water of a cup, one could either keep the elbow and forearm steady and only move the hand and wrist, or one could fix the wrist while moving the forearm up and down by flexing and extending the elbow. This redundancy of the motor system is particularly relevant for motor recovery. Of note, activities of daily living like reaching or grasping movements rely on the complex interplay of various muscle groups and therefore constitute a challenge for the recovering motor system. As the muscle synergy that a patient used to employ in a given task might not be available anymore, the motor system is forced to generate a new motor synergy within the realm of the imposed pathophysiological constraints. In other words, activities of daily living can be mastered using compensatory strategies and do not necessarily require the neurobiological restitution of function in the form of known motor primitives (Cirstea & Levin, 2000).

Thus, tests imitating activities of daily living can be used to probe a patient's capacity for compensation (Lyle, 1981). Exemplary test items include filling water from one glass to another, picking up beans with a spoon, or picking up a marble using a pinch grip. Throughout this dissertation, I will refer to these aspects as *complex motor control*. In contrast, an approximation of restitution of function may be achieved by focusing on isolated movements of individual muscle groups. Many tests in this category include strength to quantify the level of restitution. An example of different strength levels would be extending the arm and holding it up (i) against gravity or (ii) against force exerted by the examiner. The same principle can

also be applied to more distal muscle groups by asking the patients to hold a piece of paper between index finger and thumb (i) without any intervention or (ii) against the tug of the examiner. In the following, I will refer to such aspects of motor control primarily relying on restitution of function as *basal motor control*.

With this interplay between restitution and compensation in mind, it seems crucial to differentiate basal and complex aspects of motor control when assessing residual motor function and motor recovery in stroke patients over time. However, in practice, many studies simply rely on a single measure of motor performance. While this is understandable considering the time constraints when testing stroke patients, it limits our mechanistic understanding of motor recovery and hinders a direct comparison of results obtained across studies.

2.2.3. The ipsilesional corticospinal tract

Having established a general framework to track the time course of recovery as well as a basic understanding of how different aspects of motor impairment can be quantified, I will now present the current state of knowledge on how plastic changes observed on a system's level can lead to the recovery of motor functions.

Given that many patients presenting with hemiparesis after stroke exhibit lesions affecting the CST, there is a plethora of studies focusing on the relationship between the extent of CST damage and the level of residual motor function (Koch et al., 2016). The simplest way to quantify CST damage lies in delineating the lesion on a structural scan and then calculating the overlap between the normalized lesion mask and a normative CST template. Studies applying this approach have consistently reported negative correlations between the percentage of CST damage and behavioral performance measures, with increasing lesion load featured by patients exhibiting lower levels of residual motor control (Koch et al., 2016). However, quantifying CST damage by means of a lesion overlap ignores a critical aspect: Lesions to narrower CST sections in which fibers are more densely packed tend to result in more severe motor impairment than a lesion of equal size that is located in a wider CST section. To address this problem, a so-called weighted CST lesion load can be computed that emphasizes lesions to "CST bottlenecks" such as the PLIC or the brainstem (Feng et al., 2015). This is achieved by weighting each axial slicewise lesion overlap by the ratio of the maximum cross-sectional CST area divided by the cross-sectional area of a given slice.

While this approach accounts for the narrowing of the CST as it descends downwards, another important aspect is still missed: CST dysfunction is not only explained by damage to the tissue directly affected by the lesion, but also by the fact that axons passing through the

lesion deteriorate over time. This process of secondary deterioration is commonly referred to as *Wallerian degeneration* (Conforti et al., 2014). In other words, while a lesion might only affect a relatively small proportion of the CST, this lesion may induce a secondary degenerative loss of axons along the entire length of the tract. Given that a lesion overlap only takes into account the direct impact of the lesion, it is not able to capture the effects of Wallerian degeneration. To circumvent this problem, several studies used DTI to quantify CST integrity based on anisotropy. Anisotropy is a measure of the underlying white matter tissue's *microstructural integrity* and is commonly used to quantify fiber coherence (Basser, 1995). The more coherently fibers are oriented, i.e., the better they align, the higher the anisotropy measure. Importantly, reduced anisotropy is not necessarily the result of lesion-induced degeneration but can also stem from methodological limitations of estimating anisotropy in regions with crossing or kissing fibers that contain voxels with more than one dominant fiber direction such as the corona radiata (Basser et al., 1994; for a detailed discussion of the methodological limitations, please see section 4.2.4). In consequence, computing anisotropy across the entire length of the CST might yield misleading results. Region of interest (ROI)-based approaches that focus on specific parts of the CST containing densely packed, parallel running fibers help to alleviate the problem (Kim et al., 2018), yet there is no clear consensus on which anatomical section to use. Some studies extracted anisotropy measures from the CST on the level of the pons (Puig et al., 2010, 2013) or the section between mesencephalon and cerebral peduncle (Cheng et al., 2021; Schulz, Koch, et al., 2015; Schulz et al., 2017b), while others placed ROIs in the cerebral peduncle (Doughty et al., 2016; Thomalla et al., 2004) or in the PLIC (Borich et al., 2012, 2014; Jayaram et al., 2012; Puig et al., 2011), or used a combination of these ROIs (Yu et al., 2009). While such ROI-based approaches help to circumvent the problem of having to estimate anisotropy in multidirectional voxels, they simultaneously introduce new pitfalls. First, stroke patients are typically older individuals featuring considerable degrees of age-related brain atrophy in addition to stroke-induced damage. Despite the fact that age-related white matter atrophy is a rather global phenomenon not selectively affecting descending fibers (Kelley et al., 2021), certain parts of the brain are especially prone to age-related degeneration processes with the PLIC being one of them (Hsu et al., 2008; Salat et al., 2005). Second, due to the limited number of voxels within the typically used ROIs, common issues such as a suboptimal normalization of patients' diffusion images or partial volume effects can heavily bias the extraction of anisotropy measures (Moura et al., 2019). ROI-based approaches therefore introduce considerable sampling biases, raising the need for improved approaches to quantify anisotropy in descending tracts.

Notably, many of the studies cited above defined the CST as a tract descending from M1, thereby ignoring large portions of the CST that emerge from premotor areas. While using a wider CST template that accounts for CST fibers descending from both M1 and premotor areas yields a more accurate representation of actual CST fibers, analyzing corticospinal “subtracts” individually might hold valuable information regarding the descending output from various premotor regions. A small number of studies have adopted this approach so far (Archer et al., 2016; Ito et al., 2021; Liu et al., 2020; Phan et al., 2013; Riley et al., 2011; Schulz et al., 2012), but the somewhat inconsistent results do not yet paint a clear picture of the functional relevance of each of these fiber tracts.

An alternative readout for CST integrity can be achieved by means of transcranial magnetic stimulation (TMS), a form of non-invasive brain stimulation. During TMS, a coil positioned on the scalp generates a strong and rapidly changing magnetic fields, which in turn induces electrical currents perpendicular to the magnetic field (Barker et al., 1985; Klomjai et al., 2015). By applying a single TMS-pulse over M1, it is possible to evoke a twitch in contralateral muscles represented by the stimulated part of M1. This motor-evoked potential (MEP) can be read out via electromyography (EMG) and the intensity needed to elicit a motor response can be quantified, commonly referred to as the *cortical excitability*. After stroke-induced damage to the CST, MEPs typically decrease in amplitude implying that cortical excitability of the ipsilesional M1 decreases (Di Lazzaro et al., 2008; McDonnell & Stinear, 2017; Traversa et al., 1998). In general, patients in whom an MEP can be elicited in the acute stage post-stroke tend to have a higher chance for functional recovery (Stinear et al., 2012).

Of note, according to the consensus paper of the Stroke Recovery and Rehabilitation Roundtable from 2017, CST damage is considered the only valid biomarker for motor outcome to date (Boyd et al., 2017). In particular, they suggest quantifying CST damage in one of the following ways: (i) lesion overlap, (ii) DTI-based measures, or (iii) MEP-status. However, it should be noted that CST damage is still far from perfect as a biomarker for motor recovery. While it consistently yields moderate to strong correlations with motor outcome on the group level, individual predictions still lack the necessary reliability to warrant use in clinical practice (Boyd et al., 2017). Besides the methodological limitations described above, another underlying reason might be that CST damage can be partially compensated by alternative structures. Thus, while using the ipsilesional CST as a predictor might adequately capture direct effects of the lesion as well as Wallerian degeneration, cortico-cortical structures or alternative descending pathways might help to relay motor output signals via alternative routes and thereby contribute to motor control.

2.2.4. Alternative motor output pathways

After CST damage, the motor system might use alternative descending pathways to relay motor signals to the spinal level (Cleland & Madhavan, 2021). For example, non-crossing fibers of the contralesional CST seem strategically situated to convey excitatory inputs to the affected limb. In line with this view, anisotropy of the contralesional CST has been related to the level of motor impairment (Borich et al., 2012; Schaechter et al., 2009). However, in comparison to studies on the ipsilesional CST, evidence regarding the contralesional CST remains sparse.

A more widely discussed alternative for descending motor signals to circumvent the ipsilesional CST is the extrapyramidal system. Historically, a compensatory role of the extrapyramidal system was already introduced in relation to the return of rudimentary motor functions in monkeys after bilateral pyramidotomy (Lawrence & Kuypers, 1968a, 1968b; Tower, 1940). Since then, the role of the reticulospinal and rubrospinal tracts in facilitating post-stroke motor control has been a topic of on-going debate. While there seems to be a consensus that the extrapyramidal system has a functional relevance for post-stroke motor control, our mechanistic understanding remains coarse and whether its impact is beneficial or detrimental for motor performance is still heavily debated. In line with the notion that the reticulospinal tract mostly synapses on proximal muscle groups, several studies have suggested a compensatory role in locomotion and gross upper limb movements (Guo et al., 2019; Peters et al., 2021; Ruber et al., 2012; Takenobu et al., 2014). Conversely, others argue that an upregulated extrapyramidal system results in a maladaptive increase in flexor synergies, which may hinder the recruitment of individual digits and might even lead to spasticity (McPherson et al., 2018; Owen et al., 2017). This view is supported by a recent study in macaque monkeys, which reports an imbalance between forearm flexor and extensor muscles due to a selective flexor strengthening after CST injury (Zaaimi et al., 2012). In this sense, increased muscle strength may be achieved at the cost of individualized movements.

Moreover, previous dMRI-studies have not been able to resolve whether extrapyramidal anisotropy is subject to change after stroke. Whereas some studies indicated increased anisotropy in reticulospinal and rubrospinal tracts after stroke (Karbasforoushan et al., 2019; Ruber et al., 2012; Takenobu et al., 2014), other studies reported a decrease in extrapyramidal anisotropy (Guo et al., 2019). Thus, the functional role of extrapyramidal tracts in post-stroke motor control remains largely unknown. Moreover, it remains to be seen whether extrapyramidal tracts undergo reorganization processes to contribute to motor control or whether the variable influences across patients stem from the premorbid constitution of

extrapyramidal tracts that may serve as a structural reserve without the need for prior reorganization (Di Pino et al., 2014).

2.2.5. Cortico-cortical structural connectivity

While the role of descending pathways in stroke recovery has been widely discussed, literature on the relevance of cortico-cortical fiber tracts for motor recovery post-stroke remains scarce. In general, there are two possible approaches to analyze structural connectivity and its relationship to motor performance. One approach lies in using an atlas-based whole-brain parcellation to compute connectivity between predetermined region pairs, which usually results in a large number of connections neither limited nor tailored to the motor system. While exploratory analyses applying graph-theoretical and machine learning approaches to such whole-brain connectivity measures have been able to explain motor performance after stroke (Egger et al., 2021; Koch et al., 2021; Schlemm et al., 2020), the results do not allow for a conclusive interpretation regarding specific cortico-cortical connections for several reasons. First, the sheer number of connections in previous atlas-based analyses makes it impossible to isolate the particular influence of a single region pair. Second, the commonly used atlases do not specifically identify individual premotor regions like SMA, PMv or PMd, but use rather generic parcellations instead. Third, structural whole-brain connectivity usually relies on streamline count to quantify connectivity (Bullmore & Sporns, 2009), which is not a reliable measure in individuals with considerable age-related brain atrophy.

Using an alternative approach, several studies have quantified structural connectivity in a more hypothesis-driven manner as tractwise anisotropy between core motor regions. A commonly reported finding in these studies is a correlation between anisotropy of the corpus callosum extending between bilateral M1 and motor impairment (Chen & Schlaug, 2013; Hayward et al., 2022; Lindenberg et al., 2012; Peters et al., 2018; Radlinska et al., 2012; Stewart et al., 2017; Takenobu et al., 2014; Wang et al., 2012). Moreover, some studies also found an association of motor performance with ipsilesional premotor-M1 structural connectivity, yet reported mixed findings regarding specific connections (Peters et al., 2018; Schulz, Braass, et al., 2015; Schulz, Koch, et al., 2015; Schulz et al., 2017b). Possible explanations for the diverging reports regarding the role of specific premotor-M1 connections might lie in the heterogeneity of utilized patient cohorts and their particular lesion distributions. Given the relatively small sample sizes of the aforementioned studies, certain premotor areas may have played a more prominent role in motor recovery in a particular cohort. Alternatively, mixed findings might also stem from the way motor performance was quantified, which significantly

differed between studies. For instance, Schulz and colleagues calculated a composite motor score via a principal component analysis (PCA) based on the measures grip force, pinch force and finger tapping speed ratio. The authors reported a correlation with the ipsilesional PMd-M1 connection, but found no association with PMv-M1 or SMA-M1 (Schulz, Braass, et al., 2015). In a paper published in the same year, the same group of authors used a different approach to quantify motor performance in the form of the Fugl-Meyer upper extremity (FM-UE)-score (Fugl-Meyer et al., 1975) instead of finger tapping speed, thereby shifting the focus towards more basal aspects of motor control (Schulz, Koch, et al., 2015). In contrast to their previous findings, they reported a significant association between motor performance and the PMv-M1 connection. Conversely, Peters and colleagues used several separate motor tests and observed significant correlations with the SMA-M1 but not PMv-M1 connection (Peters et al., 2018). Interestingly, these associations only emerged for grip strength and dexterity, but not for the motricity index (MI), which probes the execution of specific muscle synergies. The motor tests used might hence have a significant impact on the relevance of particular premotor regions and their connections to the ipsilesional M1.

Then again, the role of specific premotor regions might change as a function of reorganization with more pronounced CST damage potentially resulting in a more extensive change in functional architecture. In line with this view, a study featuring a relatively large sample size of 56 subacute stroke patients suggests that the microstructural integrity of the PMv-M1 connection might only be critical for motor performance in patients with extensive CST damage (Schulz et al., 2017b). Thus, when investigating the relationship between ipsilesional premotor-M1 connections and different aspect of motor performance considering the extent of CST damage might help to offer valuable insights into reorganization processes after stroke.

2.2.6. Functional interactions of cortical brain regions in stroke recovery

From a functional perspective, unilateral hand movements of healthy subjects are accompanied by strong lateralization of neural activation to cortical motor regions contralateral to the moving hand (Grefkes, Eickhoff, et al., 2008; Pool et al., 2013). Conversely, acute stroke patients commonly show pronounced bihemispheric activation during movements of the affected hand and a general increase in the level of activation compared to healthy controls (Gerloff et al., 2006; Hensel et al., 2021; Rehme, Fink, et al., 2011; Rehme et al., 2012; Ward et al., 2003). As recovery progresses and motor function returns, this bilateral activation pattern typically recedes to a more physiological pattern of lateralized and less widespread activation

(Rehme et al., 2012; Tombari et al., 2004; Ward et al., 2003). According to a meta-analysis of more than 20 experiments including a variety of different tasks, good motor outcome coincides with a reinstatement of such a physiological activation pattern resembling what can be observed in healthy subjects, whereas the persistence of bilateral activation in the chronic stage has been linked to poor motor outcome (Rehme et al., 2012). Interestingly, an increase in neural activation as well as some degree of activation in the ipsilateral hemisphere has also been described in healthy volunteers in relation to increasing task demands (Buetefisch et al., 2014; Cramer et al., 2002; Pool et al., 2013, 2014). The observed overactivation might hence be interpreted as increased efforts of the motor system to compensate for increasing control demands either evoked by increasing task difficulty or the effect of the lesion.

However, mere changes in BOLD activation do not warrant conclusions regarding the functionality of the underlying region. In order to infer its functional role, more advanced modelling approaches are needed that enable us to infer the causal relationship between different brain regions (Grefkes & Ward, 2014). As described above, a common approach to probe directional interactions lies in estimating DCM-based effective connectivity. DCM studies in stroke patients commonly report decreased excitation of the ipsilesional M1 by premotor regions in the acute and subacute phase post-stroke (Grefkes, Nowak, et al., 2008; Hensel et al., 2021; Rehme, Eickhoff, et al., 2011) that normalizes alongside recovery (Rehme, Eickhoff, et al., 2011). Stronger ipsilesional premotor-M1 coupling in the acute phase has been related to increased recovery over the following three to six months and to better motor outcome in the chronic phase (Rehme, Eickhoff, et al., 2011). Thus, excitatory input from premotor areas to the ipsilesional M1 seems to be beneficial for motor performance after stroke.

In contrast, the role of functional interactions between bilateral M1 remains a topic of ongoing debate. Supportive interactions have been reported by DCM studies in the acute and early subacute phase. Specifically, patients featured reduced inhibition of the contralesional M1 by the ipsilesional M1 in the first 72 hours after stroke and subsequently increased excitatory input from the contralesional M1 to the ipsilesional M1 after 10 to 14 days (Rehme, Eickhoff, et al., 2011). In the late subacute phase, Grefkes and colleagues observed an additional inhibitory influence from the contralesional M1 onto the ipsilesional M1 in relation to the severity of motor impairment (Grefkes, Nowak, et al., 2008). Of note, patients featuring pronounced inhibition of the ipsilesional M1 during paretic hand movements suffered from more severe motor deficits (Grefkes, Nowak, et al., 2008). Thus, these inhibitory influences exerted by the contralesional onto the ipsilesional M1 were interpreted to be maladaptive. Support for such maladaptation of interhemispheric interactions in the late subacute stage

derives from several TMS studies (Grefkes et al., 2010; Murase et al., 2004). Finally, in the chronic stage, patients with persistent deficits exhibit *increased inhibition of the ipsilesional M1* with a simultaneous *decreased inhibition of the contralesional M1* (Di Pino et al., 2014; Rehme, Eickhoff, et al., 2011; Volz, Sarfeld, et al., 2015).

Taken together, these findings suggest a beneficial influence of the contralesional M1 early after stroke that may turn into a maladaptive inhibitory influence if its overactivation persists into the chronic phase. However, this simplistic view is challenged by results from online TMS studies, which emphasize that the role of the contralesional M1 is highly task-specific. By temporarily inducing a “virtual lesion” to the contralesional M1 during task execution, the authors probed its functional role in different tasks. Interfering with the contralesional M1 in acute stroke patients led to an improvement in finger tapping frequency, but had no effect on grip strength or a simple reaction time task performed with the paretic hand (Volz et al., 2017). Moreover, in contrast to the DCM-results reported above, online TMS studies have reported a supportive role of the contralesional M1 for the execution of specific tasks such as sequenced finger movements (Lotze et al., 2006) and grasping speed (Hensel et al., 2022) in chronic stroke patients.

In conclusion, interhemispheric M1-M1 connectivity seems to be critical for motor performance after stroke, yet the functional impact of this connection strongly depends on the time since stroke, the degree of motor impairment, and the underlying motor task. Moreover, DCM studies consistently report a reduction in intrahemispheric excitatory coupling from premotor areas onto the affected M1 that re-increases alongside motor recovery.

Interestingly, connections that appear to be crucial for task execution also correlate with motor impairment when investigating the post-stroke motor network at rest. Network dynamics at rest are generally investigated by focusing on spontaneous fluctuations in the fMRI BOLD signal in a relatively low frequency range below 0.1 Hz (Raichle, 2009). In the healthy brain, the time course of these fluctuations shows a coherent pattern within regions of known functional brain networks. For example, correlating the resting-state time course of spontaneous BOLD fluctuations within the motor system typically reveals robust correlations between bilateral M1 and individual premotor regions (Biswal et al., 1995; Pool et al., 2015).

After motor stroke, measures of resting-state functional connectivity are altered in a stereotypically evolving temporal pattern (Lee et al., 2017; Park et al., 2011; van Meer et al., 2010, 2012; Xu et al., 2014; Zheng et al., 2016). Both rodent and human studies have reported reduced interhemispheric connectivity between primary sensorimotor regions in the first few days post-stroke that was correlated with the degree of motor impairment. This initial decline

is usually followed by a subsequent re-increase over the course of several weeks alongside the recovery of motor functions until it stabilizes in the chronic stage. While resting-state connectivity normalizes in patients featuring good recovery with close to normal motor functions in the chronic stage, it remains chronically reduced in patients suffering from lasting motor impairments. Moreover, increased intrahemispheric resting-state connectivity between premotor areas and M1 have repeatedly been linked to poor motor performance (Bonkhoff et al., 2020; Lee et al., 2017; Rehme, Volz, Feis, Bomilcar-Focke, et al., 2015).

In summary, interhemispheric M1-M1 as well as ipsilesional premotor–M1 connectivity have been linked to residual motor function after stroke during task performance and at rest. These connections might therefore be of particular relevance for motor recovery after stroke and should be examined from a functional and structural perspective.

3. Objectives

The aim of the present thesis was to improve our understanding of mechanisms underlying motor network reorganization after stroke. To this end, we investigated structural and functional properties of the stroke-afflicted motor network in four different studies. In study 1 to 3, we used a novel approach to quantify tractwise anisotropy in a cohort of 25 chronic stroke patients. Given the conceptual difference between the compensation of basal and complex motor skills, we distinguished between distinct aspects of motor control on a behavioral level and assessed their relationship with different descending tracts and cortico-cortical connections. In study 4, we compared fMRI-based functional and effective connectivity in a sample of 26 acute stroke patients to infer whether distinct aspects of early motor network reorganization are differentially captured depending on the activation state of the network (rest vs. task). Thereby, we aimed to address the following questions:

1. Which role do different descending motor pathways play for distinct aspects of motor control after stroke?

Study 1: The role of corticospinal and extrapyramidal pathways in motor impairment after stroke, *Brain Communications*, 2023

The level of motor impairment after stroke has frequently been linked to the structural integrity of the ipsilesional CST, which is considered a promising biomarker for motor recovery (Boyd et al., 2017). In particular, the degree of Wallerian degeneration of the CST as assessed by means of dMRI-based anisotropy has been shown to relate to residual motor function (Koch et al., 2016). However, several limitations hinder the application of CST anisotropy as a biomarker in clinical practice. First, methodological limitations inherent to dMRI impede the correct estimation of anisotropy in crossing or kissing fibers, i.e., voxels with more than one dominant fiber direction. Second, ageing-related atrophy confounds the estimation of anisotropy in elderly stroke patients, especially in commonly used ROI-based approaches that focus on CST sections with densely packed fibers such as the PLIC. Third, reorganization processes and vicariation by intact brain structures partially compensate for lesion-induced motor impairment, which limits the predictive power of CST anisotropy. Fourth, assessment of behavioral impairment varies between different studies, hindering the comparison of findings across studies. To address these issues, we used diffusion spectrum imaging (DSI) combined with a novel compartmentwise analysis approach that categorizes white matter (WM) according to the number of trackable directions within a given voxel

(Volz et al., 2018). This allowed us to assess the relationship of basal and complex upper and lower limb motor impairment with anisotropy derived from the entire length of the CST, which constitutes an improved measure for Wallerian degeneration. We further investigated the role of the extrapyramidal system in motor control to account for compensatory influences of alternative descending fibers. Moreover, we used a young and an age-matched control group to delineate ageing- and stroke-related effects. Thus, study 1 introduces a novel analysis framework for dMRI after stroke that overcomes several shortcomings of previous dMRI approaches.

2. Do premotor areas influence basal and complex motor control via their descending corticospinal fibers after stroke?

Study 2: Corticospinal premotor fibers facilitate complex motor control after stroke,
Submitted

Premotor areas are known to influence motor control after stroke through cortico-cortical interactions, yet a possible compensatory role of their direct corticospinal projections remains poorly understood (Grefkes & Ward, 2014; Hartwigsen & Volz, 2021). These direct projections might enable the transmission of motor output signals to the spinal level in case of damage to the main corticospinal output pathway descending from M1. We therefore used the compartmentwise analysis approach introduced in study 1 to address the question whether premotor areas facilitate motor control via their corticospinal fibers. To this end, we computed tractwise anisotropy of descending corticospinal fibers emerging from M1, PMd, PMv, and SMA and assessed its relationship with basal and complex motor control. The differentiation between distinct aspects of motor control in combination with a subgroup analysis that differentiated between different levels of motor impairment offered the opportunity to clarify previous contradictory findings regarding the role of specific CST subtracts after stroke.

3. Are premotor-M1 and interhemispheric M1-M1 structural connections differentially involved in various aspects of post-stroke motor control? Do cortico-cortical compensation processes depend on ipsilesional CST integrity?

Study 3: Basal but not complex motor control relies on interhemispheric structural connectivity after stroke, *medRxiv preprint*, Uploaded November 2022

Having focused on descending motor output pathways in the first two studies, we turned to cortico-cortical structural connectivity in study 3. While fMRI studies have repeatedly highlighted the relevance of changes in functional interactions between cortical motor areas (Grefkes & Ward, 2014), studies on structural connectivity of the cortical motor network remain sparse (Koch et al., 2016). Of note, given the close relationship between structural and functional connectivity in the healthy human brain (Rubinov & Sporns, 2010), structural connectivity might be a valuable predictor of motor control after stroke. From a mechanistic perspective, the structural state of the motor network might predetermine its potential to undergo successful functional reorganization. To answer these questions, we performed fiber tracking between a network of cortical motor areas based on a normative Human Connectome Project (HCP)-data set (Yeh et al., 2018). The thereby generated tract templates were used to extract tractwise anisotropy from cortico-cortical connections and the ipsilesional CST in chronic stroke patients and healthy controls. In line with previous fMRI findings, we probed for a relationship of basal and complex motor skills with premotor-M1 and M1-M1 connectivity. As cortico-cortical interactions have been shown to depend on the severity of ipsilesional CST damage (Schulz et al., 2017b), we tested for a potential influence of ipsilesional CST integrity on cortico-cortical structure-function relationships.

4. Do resting-state functional and task-related effective connectivity capture similar aspects of information integration in the stroke-afflicted cortical motor network? Which of these modalities is better suited to capture motor impairment post-stroke?

Study 4: Early motor network connectivity after stroke: An interplay of general reorganization and state-specific compensation, *Human Brain Mapping*, 2021

Functional interactions between cortical motor areas after stroke have frequently been assessed using fMRI-based resting-state functional or task-related effective connectivity. Both approaches indicate changes to premotor-M1 and interhemispheric M1-M1 connectivity after stroke, which are related to motor impairment (Golestani et al., 2013;

Grefkes & Ward, 2014; Park et al., 2011; Rehme, Eickhoff, et al., 2011; Volz, Sarfeld, et al., 2015). Thus, the question arises whether both approaches reflect similar aspects of altered information integration contributing to motor network reorganization. On the one hand, general changes in inter-regional interactions may be similarly captured across different brain states. On the other hand, task-specific compensation may be visible during movement execution but not at rest. With regard to clinical applications, a highly relevant question lies in whether resting-state functional or task-related effective connectivity is better suited to explain behavioral variance in motor performance. Therefore, we conducted the first direct comparison of task-related effective connectivity and resting-state functional connectivity in a network of cortical motor regions in early subacute stroke patients. The focus on functional interactions between cortical regions complements the structural analyses from study 3 and offers additional insights into the mechanisms underlying functional recovery.

4. Methods

To assess network mechanisms underlying motor control after stroke, the studies summarized in this thesis used various approaches to quantify connectivity between brain regions. In the following, I will give an overview over these approaches. After briefly introducing the main principles of MRI, I will provide an introduction to dMRI, describe challenges related to the estimation of structural connectivity and outline how we addressed these challenges using a novel compartmentwise analysis approach combined with diffusion DSI. Next, I will describe the physiological underpinnings of fMRI and outline how resting-state functional connectivity and task-related effective connectivity can be calculated. I will end this chapter by introducing and summarizing the standardized tests used to assess different aspects of motor control.

4.1. Principles of magnetic resonance imaging

Magnetic resonance imaging was first developed in the 1970s (Lauterbur, 1973). It relies on the magnetic properties of protons in hydrogen nuclei (Bartels et al., 2012). When placed in the static magnetic field of the MRI scanner (longitudinal magnetic field or B_0), the spins of these protons align with the magnetic field and precess with the so-called Larmor frequency, which is proportional to the strength of the magnetic field (Hylton & Crooks, 1991). Next, a second magnetic field in the form of a short 90° radiofrequency (RF) pulse equal to the Larmor frequency is applied that excites the protons, causing them to flip and briefly align with this transverse magnetic field. Upon termination of the radio frequency pulse, the protons return into their previous orientation, thereby emitting energy that can be recorded by a receiver coil. The exponential process by which the signal decays is commonly referred to as relaxation (Hylton & Crooks, 1991). While the time T_1 describes the recovery of longitudinal magnetization (i.e., the re-alignment of protons with the longitudinal magnetic field), the time T_2 describes transverse relaxation (i.e., the time it takes protons to de-phase, i.e., to lose coherence). Based on different T_1 and T_2 latencies, tissue classes can be distinguished. Of note, the combination of different repetition times (TR; time between successive radio frequency pulses) and times to echo (TE; time from radio frequency pulse to signal recording) results in different types of images with specific characteristics. For example, while T_1 -weighted images with relatively short TRs and TEs offer great anatomical detail, T_2 -weighted images with relatively long TRs and TEs are particularly suited for the detection of lesioned tissue (Bartels et al., 2012; Zimny et al., 2015).

4.2. Diffusion MRI

The properties of WM structures can be investigated using dMRI (Basser, 1995). dMRI relies on measuring the diffusion of water molecules over time (Beaulieu, 2002, 2014). Diffusion can be described as Brownian motion, i.e., the random translational motion of a molecule driven by its inherent thermal energy (Basser & Özarslan, 2014; Beaulieu, 2002; Le Bihan et al., 2006). The motion of a group of particles can be described by a three-dimensional Gaussian distribution initially introduced by Albert Einstein (Einstein, 1905). In this framework, the likelihood that a certain freely moving molecule will travel a certain distance depends on the mass of the molecule as well as the temperature and viscosity of the surrounding medium.

However, in the human brain, water molecules are constrained in their motion by the surrounding brain tissue. In consequence, the distance covered by a molecule is shorter than in a free medium and strongly depends on the structure of the surrounding tissue (Le Bihan et al., 2006). Moreover, while diffusion in free water is isotropic (i.e., molecular motion is equal in all directions), diffusion in the brain is highly anisotropic (i.e., the motion is greater in certain directions than in others). As molecular movement along axons is faster and more likely than in a direction perpendicular to axonal fibers, the motion of water molecules can be used to draw inferences about the underlying WM microstructure (Le Bihan et al., 2006).

4.2.1. The pulsed gradient spin echo sequence

This leads to the question how MRI sequences can be adapted to visualize the displacement of water molecules over time. dMRI relies on adaptations of the *pulsed gradient spin echo sequence* developed by Stejskal and Tanner (Stejskal & Tanner, 1965). In their pioneering work published in 1965, they combined an RF pulse pair of 90° and 180° with two gradient pulses of equal magnitude along the same axis, one applied prior to and one after the second RF pulse (cf. Figure 5). This results in following phase changes:

The first 90° RF pulse causes a phase alignment and an increase in the MR signal. The subsequent gradient pulse causes a magnetic field varying linearly in strength along the gradient axis (Jones, 2014). This results in a phase difference between different protons based on their position along this axis (Basser & Özarslan, 2014; Le Bihan et al., 2006). Next, the 180° RF pulse is applied to refocus the spins, followed by the second gradient pulse of equal amplitude, duration, and direction. From a conceptual perspective, applying a second gradient pulse equal to the first one after an 180° refocusing pulse can be equated with applying a gradient pulse of the same amplitude and duration but of opposite polarity directly after the first gradient pulse

(Jones, 2014). Consequently, motionless spins will be rephased into their initial state, thereby reversing the effect of the first gradient. However, given the movement of molecules taking place between the first and second gradient pulse, the phase will not return to its prior orientation. This phase dispersion leads to an attenuation in MRI signal. As a result, the signal intensity will be lower in tissue with more pronounced movement of water molecules such as cerebral spinal fluid than in tissues with less motion such as grey matter (GM; Bassler & Özarslan, 2014).

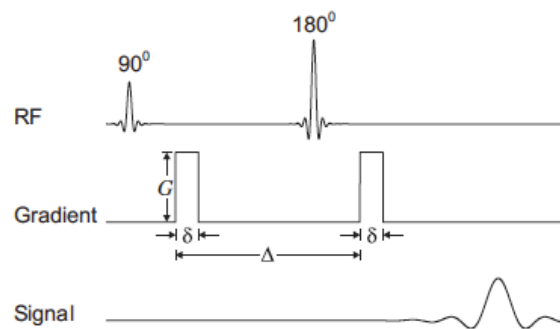


Figure 5: Schematic representation of a dMRI pulsed field gradient spin echo sequence. This approach was originally developed by Stejskal & Tanner who combined two radiofrequency pulses (RF) with two gradient pulses of equal magnitude along the same axis (Stejskal & Tanner, 1965). Adapted from Bassler & Özarslan, 2014.

4.2.2. Acquisition schemes and reconstruction

Of note, the pulse sequence just described only provides information about molecular movement in one particular direction (Basser, 1995). Given that the signal intensity is higher when applied with the fiber direction than when applied perpendicular to it, the pulse sequence has to be repeated numerous times with varying gradient directions (called *b-vectors*) to infer information about three-dimensional molecular displacements in anisotropic tissue (Basser, 1995; Sivapatham & Melhem, 2011). Further gradient characteristics are determined by the *b-value*, which contains information about gyromagnetic ratio (a characteristic of the underlying nucleus), the pulse width, the gradient amplitude and the temporal spacing (Stejskal & Tanner, 1965). dMRI acquisition schemes differ in terms of their number and combinations of distinct *b-vectors* and *b-values*. Based on the signal recorded with these different *acquisition schemes*, the underlying fiber orientations per voxel can be reconstructed by fitting a diffusion or fiber model to each voxel (O'Donnell & Pasternak, 2015). Notably, the range of possible *reconstruction methods* strongly depends on the sampling scheme. What can be confusing is the fact that some terms denoting specific acquisition schemes can also refer to a particular reconstruction method as for example the commonly used expression DTI.

DTI is the most basic and at the same time most widely used three-dimensional sampling scheme, which is usually applied in combination with the homonymic reconstruction method. Directionality of diffusion is modelled as a tensor in the shape of an ellipsoid (Basser et al., 1994; cf. Figure 6A). Utilizing a tensor model allows to characterize molecular displacement over time from as low as six recorded oblique gradient directions (Basser, 1995; Basser et al., 1994; Descoteaux, 2015). Of note, DTI relies on the assumption of Gaussian diffusion and - given the restricted possible shapes of the tensor - can only model one underlying fiber population. This becomes problematic in voxels containing kissing or crossing fibers with more than one dominant diffusion direction where diffusion processes can no longer be approximated by a Gaussian distribution (Descoteaux, 2015).

To address this problem, more advanced acquisition schemes rely on a way higher number of gradient directions that sample richer data as a basis for more elaborate reconstruction methods (Pesce et al., 2021; Wedeen et al., 2008; see Figure 7 for examples of different sampling schemes). For example, spherical shell methods such as high angular resolution imaging (HARDI) or Q-ball imaging sample a large number of points allocated on a single shell (defined by the b-value). Even more sophisticated approaches such as multi-shell HARDI rely on several b-value shells with usually more than 60 directions each and thereby sample a large number of directions from different spheres (Descoteaux, 2015). Alternatively, DSI samples from a cartesian grid and thereby aims at evenly covering the relevant space (Descoteaux, 2015; Wedeen et al., 2005). While this approach minimizes sampling biases, it also requires a large number of individual images through the combination of different b-values with numerous b-vectors. As this results in a relatively long acquisition time, DSI was long considered unfeasible for clinical populations (Descoteaux, 2015; Pesce et al., 2021). To circumvent this problem, studies included in the present thesis used a custom protocol relying on a novel DSI-based compressed sensing approach that significantly reduces the acquisition time to only 11 minutes by selectively sampling fewer points.

While it is technically possible to apply DTI reconstruction to data sampled via these advanced approaches (Figure 6C), this would discard the wealth of detailed information on intra-voxel diffusivity. Therefore, numerous different reconstruction techniques have been developed that can be grouped into two broad categories, namely mixture model-based techniques that incorporate biophysical assumptions about the WM microstructure and model-free techniques (Descoteaux, 2015). Common to all these approaches is the description of intra-voxel diffusion by a general function rather than the tensor known from DTI reconstruction (Wedeen et al., 2008). In the present thesis, we used generalized q-sampling imaging (GQI), a

model-free approach that produces an orientation distribution function (ODF) per voxel (Yeh et al., 2010; Figure 6B and D). This approach is particularly beneficial when assessing microstructural tissue integrity in voxels with multiple dominant fiber directions as will be discussed in the following section (Jin et al., 2019; for a comparison of DTI- vs. ODF-based methods, see Figure 6).

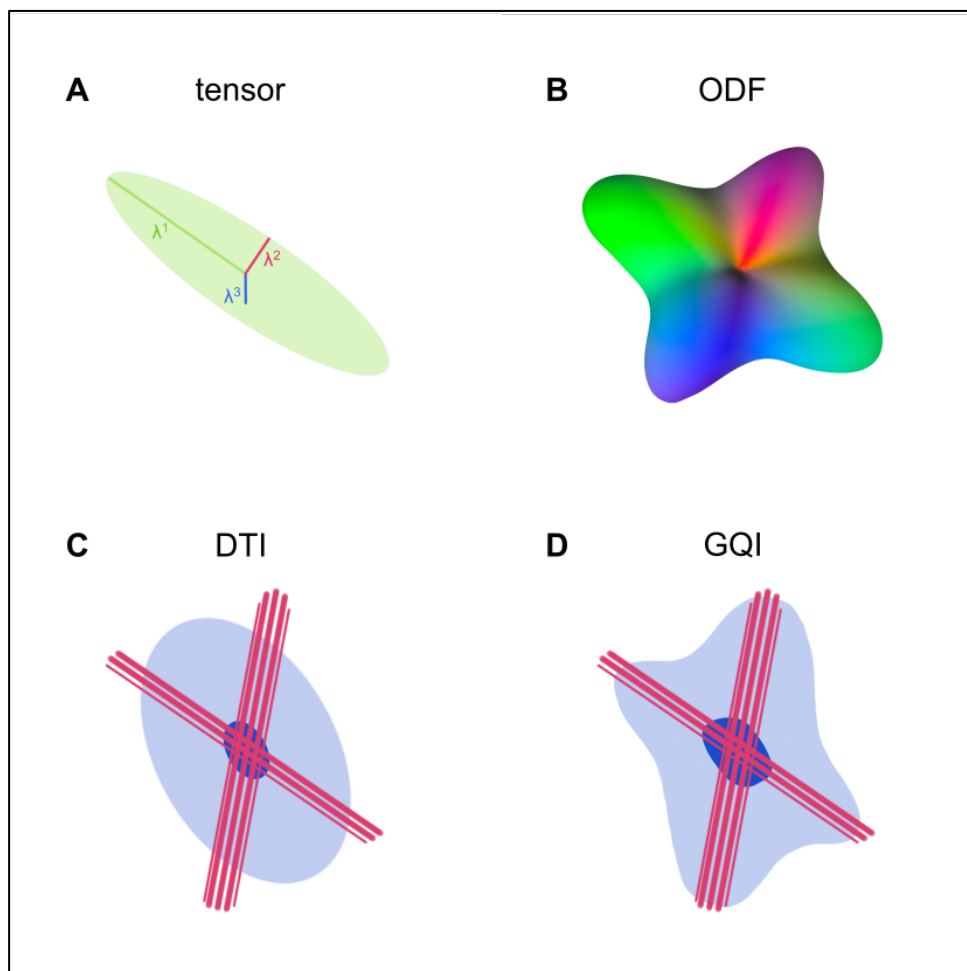


Figure 6: Difference between DTI and GQI reconstruction. A) Schematic representation of a DTI tensor relying on the assumption of Gaussian diffusion. B) Schematic representation of an orientation distribution function (ODF) as an example for a model-free approach. In C and D, the implications of choosing DTI vs. GQI reconstruction are shown in the case of voxels featuring two dominant fiber directions (fibers are visualized in pink). C) DTI is not able to differentiate the two underlying fiber directions based on the tensor model. D) In contrast, the ODF-based GQI-reconstruction accounts for the two underlying fiber directions. The idea for the visualization of DTI and GQI reconstruction is based on the DSI studio manual (https://dsi-studio.labsolver.org/doc/how_to_interpret_dmri.html)

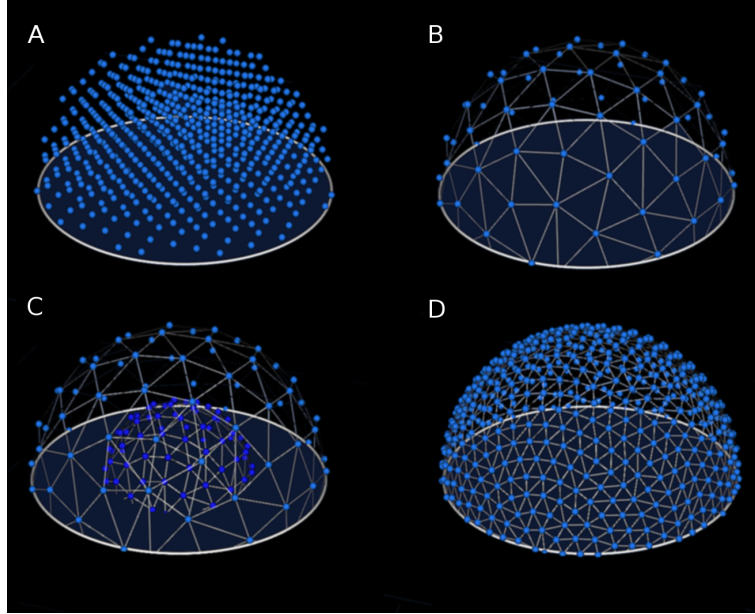


Figure 7: Schematic representation of different dMRI acquisition schemes. The figure contains acquisition schemes of different approaches to sample diffusion data based on a cartesian grid evenly covering the entire space (A) or based on one or multiple spheres (B-D). A) Diffusion spectrum imaging (DSI) with 604 directions sampled on a cartesian grid, B) High angular resolution imaging (HARDI) with a single shell of 65 directions, C) HARDI with 2 shells of 65 directions, D) Q-Ball Imaging with 515 directions. Adapted from Garyfallidis, 2012.

4.2.3. Measuring microstructural integrity

The microstructural integrity of WM tissue can be characterized by anisotropy, a voxelwise scalar measure of diffusion properties (Beaulieu, 2014). Anisotropy estimates can be calculated from reconstructed dMRI data based on voxelwise diffusion represented as tensors or ODFs (Bammer, 2003; Hagmann et al., 2006; Seunarine & Alexander, 2013). For DTI data, anisotropy is commonly quantified as fractional anisotropy (FA), which measures the fraction of the tensor attributable to anisotropic diffusion (Basser, 1995; Basser & Pierpaoli, 1996; Jones, 2008). FA can be computed by dividing the standard deviation of the eigenvalues of the tensor by their root mean squared error:

$$FA = \frac{std(\lambda)}{rms(\lambda)} = \sqrt{\frac{3 \sqrt{(\lambda_1 - \bar{\lambda})^2 + (\lambda_2 - \bar{\lambda})^2 + (\lambda_3 - \bar{\lambda})^2}}{2 \sqrt{\lambda_1^2 + \lambda_2^2 + \lambda_3^2}}}$$

where λ_1 , λ_2 , and λ_3 are the eigenvalues of the tensor and $\bar{\lambda}$ is the mean of all eigenvalues (Basser, 1995; Jones, 2008; Tuch, 2004). A major limitation of FA lies in the

inaccurate estimation of anisotropy in voxels with more than one dominant fiber direction. In these voxels, anisotropy will be systematically underestimated as the differing main directions cancel each other out (Descoteaux et al., 2006).

This problem is alleviated by computing anisotropy based on dMRI data reconstructed with more advanced model-free approaches that resolve multiple intra-voxel directions by representing diffusion via an ODF. By extending the formula for FA, a scalar can be computed based on model-free reconstruction methods termed generalized FA (gFA), which is computed as:

$$gFA = \frac{std(\psi)}{rms(\psi)} = \sqrt{\frac{n \sum_{i=1}^n (\psi(u_i) - \bar{\psi})^2}{(n-1) \sum_{i=1}^n \psi(u_i)^2}}$$

where ψ is the ODF, $\bar{\psi}$ the mean of the ODF and u_i the u_i th direction of the ODF (Tuch, 2004).

4.2.4. Compartmentwise anisotropy

However, even gFA cannot adequately resolve the problem of crossing or kissing fibers (Volz et al., 2018), which is especially problematic when trying to characterize stroke-related changes in CST anisotropy. As described above, a CST lesion leads to Wallerian degeneration, which is thought to result in the deterioration of descending fibers along the CST. However, voxels sampled from the CST do not only contain descending fibers, but also a multitude of crossing fibers. As a consequence, a CST lesion may have differential effects depending on the sampling location (cf. Figure 8). For example, in CST sections mostly comprising parallel-running fibers such as the PLIC, most voxels will contain only one main fiber direction. Deterioration of descending fibers will therefore cause a decline in anisotropy, as the main direction becomes smaller. Conversely, for voxels containing more than one dominant fiber direction, lesion-induced changes in anisotropy are less obvious. For example, in two-directional voxels, a deterioration of descending fibers may lead to a decrease in one of the dominant directions, while the other directions remain constant. This might lead to a paradoxical overall increase in anisotropy despite the decrease in diffusivity along descending fibers. Alternatively, depending on the magnitude of diffusivity in the remaining intact directions, anisotropy might also decrease or remain similar. Thus, changes in diffusivity that selectively affect one fiber direction as in case of Wallerian degeneration cannot be reliably estimated.

To circumvent this problem, we applied a novel compartmentwise analysis approach in studies 1 to 3, which classifies voxels according to their number of intra-voxel fiber directions (Volz et al., 2018). The deterministic templates were generated based on multi-shell HARDI data sets from 630 subjects of the HCP. By applying these compartment masks to gFA-maps of individual stroke patients, we were able to assess descending CST fibers in isolation by focusing solely on one-directional voxels.

Of note, the compartmentwise analysis approach did not only facilitate the assessment of descending fibers, but also helped to estimate cortico-cortical structural connectivity. In general, there are two ways to quantify structural connectivity between two brain regions, either by streamline count or by tractwise anisotropy. However, the number of streamlines assessed via fiber tracking is known to produce a large amount of false positive connections and is particularly challenging in stroke patients due to the severe ageing-related WM atrophy (Schilling et al., 2019; Thomas et al., 2014; Zalesky et al., 2016). We therefore chose to extract tractwise anisotropy, which is achieved by overlaying a binary normative tract template on an individual patient’s mask. To improve the signal-to-noise ratio, we additionally applied a compartment mask to focus our analyses on one-directional voxels, thereby mitigating the contamination of gFA by multi-directional voxels.

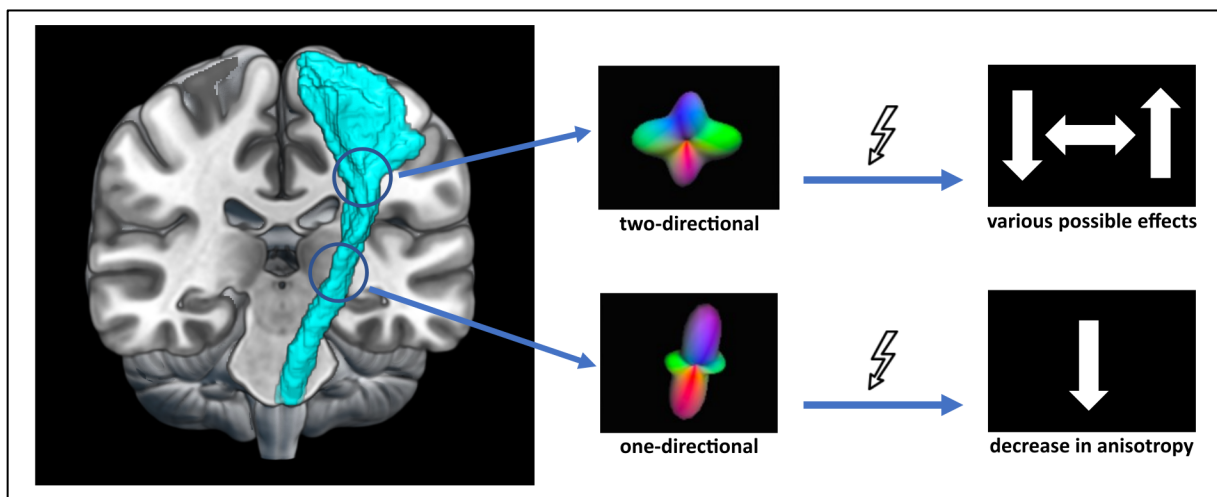


Figure 8: One- and two-directional voxels within the CST. In the posterior limb of the internal capsule (PLIC), fibers are densely packed with parallel orientations (lower blue circle). Thus, in case of deteriorating descending fibers, gFA decreases. In contrast, two-directional voxels (upper blue circle) might exhibit various different effects in response to the deterioration of one diffusion direction. Depending on the organization of the remaining directions and their ratio in comparison to the damaged one, gFA might either decrease, remain similar, or increase. Note that the underlying fiber directions are captured by the orientation distribution function (ODF) presented in the middle column.

4.3. Functional MRI

fMRI offers the unique opportunity to non-invasively investigate neural activation of the living human brain with high spatial resolution. Measures of brain activity are based on the BOLD signal, which reflects the ratio of diamagnetic oxygenated to paramagnetic deoxygenated hemoglobin (Ogawa et al., 1990). Changes in this ratio lead to measurable alterations in magnetic field inhomogeneities that are recorded as BOLD signal. Consequently, BOLD activity primarily reflects a vascular signal. However, as it exhibits strong (time-delayed) correlations with local field potentials (i.e., the electrical signal generated by local brain activity), the BOLD signal is thought to closely reflect neural activity (Logothetis et al., 2001).

The change in BOLD signal over time can be approximated by a mathematical model called the hemodynamic response function (HRF; Figure 9; Buxton et al., 1998). First, neural activation along with the related increase in metabolic consumption causes an increase in deoxyhemoglobin, which leads to an initial decrease in BOLD signal (Buxton et al., 1998; Fox et al., 1988). The subsequent increase in blood flow and volume exceeds the oxygen consumption within this area, resulting in a subsequent local surplus of oxyhemoglobin that causes an increase in BOLD signal (Ogawa et al., 1990). Before returning to baseline, the HRF typically features a post-stimulus undershoot (for a review on possible explanations for this phenomenon, please see van Zijl et al., 2012).

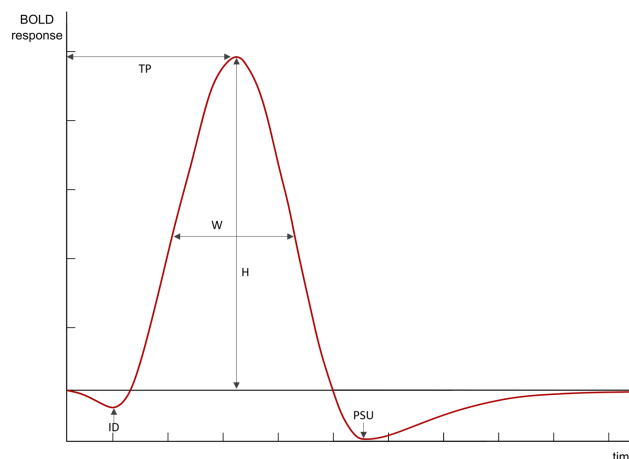


Figure 9: Hemodynamic response function (HRF). The HRF describes BOLD signal changes over time. First, task demands lead to an increase in deoxyhemoglobin, which leads to an initial dip (ID). The subsequent oversupply of blood results in a relative increase in oxyhemoglobin, which is reflected by an increase in BOLD signal. Before returning to baseline level, a post-stimulus undershoot (PSU) in BOLD activity can be observed. Thus, the shape of the HRF is determined by the time to peak (TP), the height of the response (H), the width of the HRF at half its maximum height (W), the initial dip (ID), and the PSU. Adapted from Poldrack et al., 2011 and Ashby, 2011.

4.3.1. Preprocessing

In order to prepare the data for subsequent analyses, several preprocessing steps are usually carried out. In this section, I will describe these steps and explain the motivation behind them.

Slice-timing correction: Due to technical constraints, an fMRI volume has to be recorded in various consecutive slices, meaning that not all slices of an image are acquired simultaneously. The maximum time between two slices is determined by the repetition time of the pulse sequence (TR). To address the discrepancy in the time of acquisition within a single image, it is possible to interpolate the data in all other slices in relation to a reference slice (Henson et al., 1999; Sladky et al., 2011). However, as modern multi-band scanners can acquire multiple slices simultaneously, this step is becoming increasingly obsolete.

Head motion correction: Recording an fMRI timeseries usually takes several minutes and subjects will inevitably move their head while lying in the scanner. As a consequence, the same anatomical point is not represented by the same voxel across the timeseries. Therefore, all images in a timeseries need to be realigned to a reference image using a rigid body transformation (Poldrack et al., 2011). Since the head can move along each of the three axes via translation or rotation, using a rigid body transformation yields six realignment parameters (Ashby, 2011).

Coregistration: The process of aligning the structural and functional scans is usually referred to as *coregistration*. This step is significantly more difficult than the realignment of fMRI volumes as structural and functional images usually differ in terms of their contrast and spatial resolution (Ashby, 2011). Thus, a voxel in one image does not necessarily feature a one-to-one corresponding voxel in the other. To solve this problem, current approaches mainly rely on mutual information, a concept adopted from the field of information theory that tries to identify the degree of statistical dependence between two variables (Ashby, 2011). Of note, after completion of the registration process, functional and structural images are spatially aligned and exhibit identical spatial resolution.

Spatial normalization: For group-level analyses, the images of each subject have to be transferred to a common space, referred to as *spatial normalization*. The most frequently used common space was developed by the Montreal Neurological Institute (MNI) based on the average of a large number of healthy individuals, therefore termed *MNI space* (Fonov et al., 2009). Due to the interindividual anatomical variability, affine linear registrations are insufficient as they do not allow to warp anatomical differences to a target image. Therefore, nonlinear registration methods are typically used for spatial normalization (Friston et al., 1995;

Poldrack et al., 2011). As structural images are easier to register to MNI space due to their higher anatomical detail and spatial resolution, the transformation matrix obtained by normalizing a structural image is usually applied to normalize the functional data.

Spatial smoothing: Smoothing is achieved by applying a Gaussian kernel to the BOLD signal (Ashby, 2011). Thereby, the BOLD value in a given voxel is replaced by a weighted average of its surrounding voxels. The degree of smoothing is determined by the size of the Gaussian kernel, usually defined as its full width at half maximum (FWHM). Smoothing basically results in a “blurring” of the data, which helps to improve the signal-to-noise ratio by removing high-frequency fluctuations. This makes it easier to detect changes at a larger spatial scale, i.e., changes extending across numerous neighboring voxels. Moreover, smoothing alters the distribution of the underlying data towards normality, which is a prerequisite for various subsequent statistical analyses often relying on normality assumptions.

Temporal filtering: To separate signal from noise, *temporal filtering* is applied. Task-related signal is commonly filtered using a high-pass filter at 1/128 Hz to eliminate the low frequency drift of the scanner (Poldrack et al., 2011). Conversely, as resting-state signals lie within the low-frequency range, a band-pass filter retaining only frequencies between 0.01 and 0.08 Hz is typically applied (Fox & Raichle, 2007).

4.3.2. First- and second-level analyses

For the first-level (i.e., individual subject-level) analysis of BOLD timeseries, a general linear model (GLM) is defined. The GLM relies on the assumption of a linear time invariant BOLD signal. Here, time invariant means that a shift of the stimulus presentation to a later point in time will lead to a respective delay of the hemodynamic response (Poldrack et al., 2011). Using a mass-univariate approach, a GLM is computed for each voxel individually to model the BOLD timeseries as a linear combination of weighted regressors and an error term. Regressors are determined through the convolution of a stimulus function containing the timing of each experimental condition with a model of the HRF (Kiebel & Holmes, 2004; see Figure 9 for an example of a canonical HRF). To account for motion-related variance in the data, realignment parameters obtained during head motion correction and their derivatives can be included as covariates into the model (Friston et al., 1998). The estimated parameters for each voxel, i.e., regression weights, can be tested for statistical significance using for example t- or F-tests. The result is a statistical parametric map showing clusters of BOLD activity in form of t- or F-values usually thresholded to reflect significant differences in activation across conditions. For group-level inference, the parameter estimates obtained for each condition of

interest can be entered into a second-level analysis. Given that each voxel is tested individually for statistical significance, results need to be corrected for multiple comparisons (Poldrack et al., 2011).

4.3.3. Effective connectivity

Effective connectivity measures the influence one brain region exerts over another and is therefore a popular approach to investigate causal interactions on a network level (Friston, 1994). Assessing effective connectivity based on fMRI-data represents a particular challenge due to the indirect nature of the BOLD signal and model assumptions needed to infer causal interactions. Specifically, hemodynamic changes in response to an increase in neural activation exhibit a region-specific time delay that is not accounted for in most methodological approaches aiming at estimating effective connectivity. Instead, approaches such as structural equation modelling simply consider the observed BOLD timeseries rather than the latent activation (Stephan & Friston, 2010).

In 2003, Karl Friston proposed a solution to this problem when he published his first paper on DCM (Friston et al., 2003). DCM relies on a generative model that can be used to infer hidden neuronal states from the measured brain activity (Friston et al., 2003). It combines a model of neural dynamics with the inversion of a biophysical forward model (Stephan & Friston, 2010). The biophysical model used in DCM is an extension of the so-called Balloon model that captures the association between neuronal activity and vascular changes in form of an HRF (cf. Figure 9; Buxton et al., 1998). On the level of the underlying neural signal, the model of neural dynamics describes changes in neural activity within the system over time, which is summarized by the following differential equation (Friston et al., 2003):

$$\frac{dz}{dt} = \left[A + \sum_j^m u_j B^{(j)} \right] z + Cu$$

In this equation, u represents the experimental input and z the neuronal activity. A , B , and C denote three matrices containing coupling parameters that capture the rates of change in neural activity due to synaptic influences (Stephan et al., 2010). Matrix A reflects endogenous connectivity, i.e., intrinsic coupling in the absence of any experimental perturbations. Matrix B contains changes in coupling induced by the j^{th} input and therefore reflects context-dependent connectivity changes modulated by the experimental condition. Finally, matrix C captures extrinsic influences, i.e., changes in endogenous coupling caused by direct inputs into the

system. Of note, these coupling parameters can be either positive or negative, indicating facilitatory or inhibitory influences. Using an iterative Bayesian algorithm, both the hemodynamic and neural coupling parameters are estimated based on the region-specific BOLD timeseries. The fitted DCM minimizes the discrepancy between estimated and observed BOLD signal fluctuations within the constraints of pre-specified model priors, restricting hemodynamic parameter estimates to a physiologically plausible distribution and using conservative shrinkage priors for estimates of neural coupling parameters (Friston et al., 2003; Penny et al., 2004).

Since DCM is a hypothesis-driven approach that relies on a priori assumptions about the anatomical regions and their structural connections, defining different neurobiologically plausible models to explore the space of potential network configurations underlying a specific task is a crucial analysis step. Previous research on motor network connectivity has mostly relied on a cortical network of core motor regions including M1 and various premotor regions, sometimes complemented by the visual cortex V1 due to the required visuo-motor integration in various tasks (Grefkes, Eickhoff, et al., 2008; Grefkes, Nowak, et al., 2008; Pool et al., 2013; Rehme, Eickhoff, et al., 2011; Volz, Eickhoff, et al., 2015). To extract the activation timeseries of a specific motor region, subject-specific coordinates can be determined based on the activation observed in the motor task (e.g., finger tapping or fist closure movements). The first eigenvariate is extracted within a sphere around the local activation maximum of each region and entered into the DCM. For model definition, the matrices A, B, and C need to be specified according to the a priori formulated hypotheses. In line with tracing studies in monkeys, anatomical connections between all motor regions can be assumed, leading to a fully connected A matrix (Pool et al., 2013). For the B matrices, different options for modulatory influences are usually considered differing in terms of complexity. Of note, the number of B matrices is determined by the number of experimental conditions as they reflect condition-specific changes in effective connectivity. Including movements of the affected and unaffected hand in stroke patients thus requires two B matrices. Matrix C considers the influence of driving inputs to the motor system that is commonly either set to the visual cortex if included or alternatively to premotor regions. After having estimated parameters for all evoked models, Bayesian model selection (BMS) can be applied to identify the model with the best balance between model fit and complexity based on the maximum log model evidence, with the model evidence $p(y|m)$ being the probability of obtaining the observed data y given the model m (Penny et al., 2004; Stephan et al., 2009; Stephan & Friston, 2010).

In study 4, we used DCM to quantify effective connectivity within a network of six cortical motor regions to infer stroke-related network interactions. The resulting coupling parameters for each region pair were compared with the respective functional connectivity measures. I will therefore outline the basic principles of functional connectivity analyses in the next section.

4.3.4. Functional connectivity

Functional connectivity describes inter-regional correlations of neuronal variability (Fox & Raichle, 2007). While some studies have investigated functional connectivity based on task-related BOLD activity, it is typically computed from resting-state data, i.e., data recorded in the absence of a specific task. Resting-state analyses emerged in the late 1990s as a new way to investigate network interactions by focusing on spontaneous fluctuations in the ultra-slow frequency range (Biswal et al., 1995; Raichle, 2009). Of note, regions exhibiting correlated activity during rest often resemble known functional networks, i.e., sets of brain regions activated by a particular task such as motor performance or attention (Damoiseaux et al., 2006; Fox & Raichle, 2007).

When computing functional resting-state connectivity, it is important to consider that artifacts such as head motion can cause spurious correlations (Power et al., 2012; van Dijk et al., 2012). Moreover, unlike in task-related analyses, the relevant signal in resting-state analyses lies in the low-frequency range, which means it is heavily susceptible to scanner drift (Bright et al., 2017). To account for this problem, known confounds can be entered as nuisance regressors into a regression model to predict the preprocessed timeseries data, yielding denoised timeseries data in form of the residuals of the model fit (Bright et al., 2017). Commonly used nuisance regressors include the six head motion parameters, their first derivatives, and mean signal extracted from WM or cerebrospinal fluid (CSF; Power et al., 2014; Satterthwaite et al., 2013). The use of the mean global signal derived from all voxels, termed global signal regression (GSR), is a heavily debated approach in resting-state analyses (Murphy & Fox, 2017). While some consider it a valid method to efficiently remove head motion-related noise (Power et al., 2014), others argue that it might lead to spurious negative correlations in functional connectivity analyses (Murphy et al., 2009). In light of this controversy, resting-state analyses in the present thesis were performed both with and without GSR. To focus functional connectivity analyses on the signal of interest, the BOLD timeseries has to be temporally band-pass filtered, retaining only fluctuations from 0.01 to 0.08 Hz (Biswal et al., 1995). Then, timeseries data are extracted for a given ROI and the first eigenvariate (or sometimes the mean)

is determined across all voxels for each TR. Next, Pearson correlations are computed for the resulting values with either each voxel in the brain (seed-to-whole-brain analyses) or with the eigenvariate (or mean) derived from another ROI (seed-to-seed analyses). The resulting correlation coefficients are Fisher's z-transformed and denote the connectivity strength. To characterize functional connectivity between cortical motor regions in study 4, we relied on the latter approach of seed-to-seed analyses as this allowed for a direct comparison with DCM-based effective connectivity computed within a network comprising identical ROIs for both approaches.

4.4. Behavioral motor assessment

For the assessment of motor control, standardized tests addressing distinct aspects of motor function were used. In the chronic cohort, we differentiated between basal and complex motor control by using the Motricity Index (MI) and Action Research Arm Test (ARAT), respectively. Recovery was quantified based on the change in the NIHSS upper extremity score from the acute to the chronic stage. In the acute sample, we quantified global motor performance as a composite motor score by extracting the first principal component from a principal component analysis (PCA) based on the ARAT, Jebsen Taylor test of hand function (JTT), and relative grip strength, thereby generating a relatively broad measure that generalizes across different aspects of motor control (Rehme, Eickhoff, et al., 2011).

4.4.1. National Institutes of Health Stroke Scale (NIHSS)

The NIHSS is the international standard measure to assess impairment in clinical practice in a bedside manner. It features a high inter-rater reliability, but is a coarse measure that does not capture subtle deficits (Brott et al., 1989). While it assesses 11 categories in total including domains such as the level of consciousness, visual field deficits or facial paralysis, we focused exclusively on the upper extremity item. It requires the patient to lift the arms to 90° and assigns points according to impairment severity (0 = no drift, 1 = drift, 2 = cannot resist gravity, 3 = no effort against gravity, 4 = no movement).

4.4.2. Motricity Index (MI)

The MI consists of an upper and lower limb scale and probes the ability to perform isolated movements that do not require complex multi-joint coordination (Demeurisse et al., 1980). Upper limb performance is assessed using the items shoulder abduction, elbow flexion, and pinch grip. Lower limb performance relies on the items hip flexion, knee extension, and

dorsiflexion. Each item is scored on a six-point scale according to the level of ability to perform a given movement. It is considered a valid and reliable instrument that is comparatively fast to perform (Bohannon, 1999; Collin & Wade, 1990). Measuring basal, isolated movements, each item can be considered to reflect the retrieval of a motor primitive.

4.4.3. Action Research Arm Test (ARAT)

The ARAT requires patients to manipulate objects of different sizes and weights with varying difficulties, thereby aiming to reflect activities of daily living (Lyle, 1981). It consists of the subscales grasp (6 items: e.g., lifting up wooden blocks of different sizes and placing them on an elevated surface), grip (4 items: e.g., pouring water from one glass to another), pinch (6 items: e.g., manipulating marbles with a pinch grip) and gross movement (3 items, e.g., placing the hand on top of the head). Points are assigned according to the quality of the performed movement on a four-point scale. The ARAT features high reliability and validity, but can lead to ceiling effects in the grasp and gross movement scales in well-recovered patients (Hsieh et al., 1998; Nijland et al., 2010). Given its reliance on multi-joint movements, the ARAT captures aspects of complex motor control.

4.4.4. Jebsen Taylor Test of Hand Function (JTT)

The JTT is a speeded test that requires participants to perform complex motor tasks resembling activities of daily living as quickly as possible (Jebsen et al., 1969). The items include (1) writing (printing a 24-letter sentence), (2) simulated page turning (turning over 3×5-inch cards), (3) picking up small objects (specifically pennies, paper clips, and bottle caps), (4) eye-hand coordination (stacking checkers on top of each other), (5) simulated feeding (handling kidney beans with a spoon), (6) picking up empty cans, and (7) picking up weighted cans (1 lb).

Each item is scored according to the time needed for completion, which minimizes ceiling effects commonly observed in other tests like the MI or ARAT. Due to the severe difficulties patients experience when having to write with their non-dominant hand the item writing was not performed. In line with previous research, the maximum time allowed for an item was 120 seconds (Duncan et al., 1998). The maximum time was also assigned when a patient was unable to perform a certain item.

4.4.5. Relative grip strength

Maximum grip strength was assessed using a handgrip dynamometer. Patients performed three presses with each hand, alternating between the affected and unaffected hand across trials. To account for interindividual differences in strength level, we used relative grip strength rather than absolute values. Relative grip strength was defined as the ratio of mean grip strength of the affected to mean grip strength of the unaffected hand. Of note, relative grip strength is a relatively simple motor control problem as it only requires maximum contraction of finger flexors. However, unlike the MI, it does not require the individualized control of specific muscle groups, but strongly relies on flexor synergies instead. Therefore, motor deficits like spasticity or finger enslaving, i.e., the inability to move an individual finger without unintentionally producing force in other fingers (Abolins et al., 2020), are not captured by relative grip strength.

5. Empirical section

Study 1:

Paul, T., Cieslak, M., Hensel, L., Wiemer, V. M., Grefkes, C., Grafton, S. T., Fink, G. R., & Volz, L. J. (2023). The role of corticospinal and extrapyramidal pathways in motor impairment after stroke. *Brain Communications*, 5(1).
<https://doi.org/10.1093/braincomms/fcac301>

Study 2:

Paul, T., Cieslak, M., Hensel, L., Wiemer, V. M., Grefkes, C., Tscherpel, C., Grafton, S. T., Fink, G. R., & Volz, L. J. (2023). Corticospinal premotor fibers facilitate complex motor control after stroke. *Submitted*.

Study 3:

Paul, T. †, Wiemer, V. M. †, Hensel, L., Cieslak, M., Grefkes, C., Tscherpel, C., Grafton, S. T., Fink, G. R., & Volz, L. J. Basal but not complex motor control relies on interhemispheric structural connectivity after stroke. *MedRxiv preprint*. Uploaded November 2022.

Study 4:

Paul, T., Hensel, L., Rehme, A. K., Tscherpel, C., Eickhoff, S. B., Fink, G. R., Grefkes, C., & Volz, L. J. (2021). Early motor network connectivity after stroke: An interplay of general reorganization and state-specific compensation. *Human Brain Mapping*, 42(16), 5230–5243. <https://doi.org/10.1002/hbm.25612>

5.1. The role of corticospinal and extrapyramidal pathways in motor impairment after stroke

Theresa Paul, Matthew Cieslak, Lukas Hensel, Valerie M. Wiemer, Christian Grefkes,
Scott T. Grafton, Gereon R. Fink, Lukas J. Volz

Brain Communications, Volume 5, Issue 5, 2023

<https://doi.org/10.1093/braincomms/fcac301>

BRAIN COMMUNICATIONS

The role of corticospinal and extrapyramidal pathways in motor impairment after stroke

 Theresa Paul,¹  Matthew Cieslak,²  Lukas Hensel,¹  Valerie M. Wiemer,¹
 Christian Grefkes,^{1,3}  Scott T. Grafton,⁴  Gereon R. Fink,^{1,3} and  Lukas J. Volz¹

Anisotropy of descending motor pathways has repeatedly been linked to the severity of motor impairment following stroke-related damage to the corticospinal tract. Despite promising findings consistently tying anisotropy of the ipsilesional corticospinal tract to motor outcome, anisotropy is not yet utilized as a biomarker for motor recovery in clinical practice as several methodological constraints hinder a conclusive understanding of degenerative processes in the ipsilesional corticospinal tract and compensatory roles of other descending motor pathways. These constraints include estimating anisotropy in voxels with multiple fibre directions, sampling biases and confounds due to ageing-related atrophy. The present study addressed these issues by combining diffusion spectrum imaging with a novel compartmentwise analysis approach differentiating voxels with one dominant fibre direction (one-directional voxels) from voxels with multiple fibre directions. Compartmentwise anisotropy for bihemispheric corticospinal and extrapyramidal tracts was compared between 25 chronic stroke patients, 22 healthy age-matched controls, and 24 healthy young controls and its associations with motor performance of the upper and lower limbs were assessed. Our results provide direct evidence for Wallerian degeneration along the entire length of the ipsilesional corticospinal tract reflected by decreased anisotropy in descending fibres compared with age-matched controls, while ageing-related atrophy was observed more ubiquitously across compartments. Anisotropy of descending ipsilesional corticospinal tract voxels showed highly robust correlations with various aspects of upper and lower limb motor impairment, highlighting the behavioural relevance of Wallerian degeneration. Moreover, anisotropy measures of two-directional voxels within bihemispheric rubrospinal and reticulospinal tracts were linked to lower limb deficits, while anisotropy of two-directional contralateral rubrospinal voxels explained gross motor performance of the affected hand. Of note, the relevant extrapyramidal structures contained fibres crossing the midline, fibres potentially mitigating output from brain stem nuclei, and fibres transferring signals between the extrapyramidal system and the cerebellum. Thus, specific parts of extrapyramidal pathways seem to compensate for impaired gross arm and leg movements incurred through stroke-related corticospinal tract lesions, while fine motor control of the paretic hand critically relies on ipsilesional corticospinal tract integrity. Importantly, our findings suggest that the extrapyramidal system may serve as a compensatory structural reserve independent of post-stroke reorganization of extrapyramidal tracts. In summary, compartment-specific anisotropy of ipsilesional corticospinal tract and extrapyramidal tracts explained distinct aspects of motor impairment, with both systems representing different pathophysiological mechanisms contributing to motor control post-stroke. Considering both systems in concert may help to develop diffusion imaging biomarkers for specific motor functions after stroke.

- 1 Medical Faculty, University of Cologne, and Department of Neurology, University Hospital Cologne, 50937 Cologne, Germany
- 2 Department of Psychiatry, Perelman School of Medicine, University of Pennsylvania, Philadelphia, PA 19104, United States of America
- 3 Institute of Neuroscience and Medicine, Cognitive Neuroscience (INM-3), Research Centre Juelich, 52425 Juelich, Germany
- 4 Department of Psychological & Brain Sciences, University of California, Santa Barbara, CA 93106, United States of America

Correspondence to: Lukas J. Volz, M.D.
Department of Neurology, University of Cologne
Kerpener Str. 62, 50937 Cologne, Germany
E-mail: lukas.volz@uk-koeln.de

Received May 13, 2022. Revised September 01, 2022. Accepted November 17, 2022. Advance access publication November 21, 2022

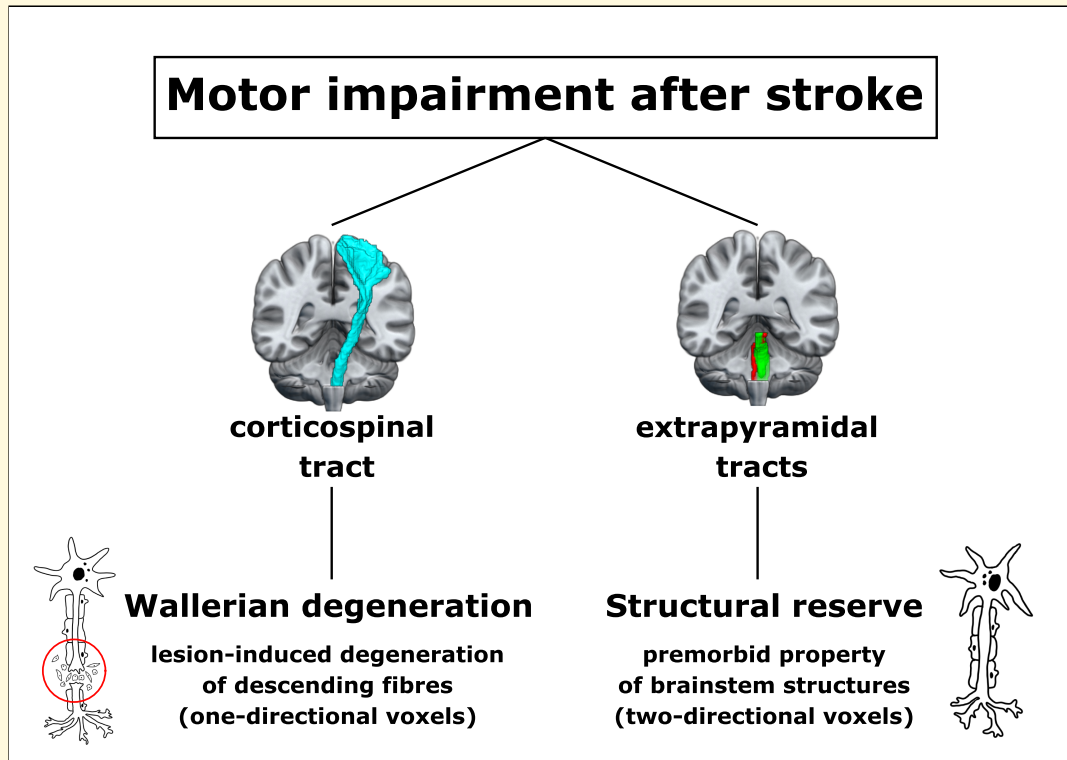
© The Author(s) 2022. Published by Oxford University Press on behalf of the Guarantors of Brain.

This is an Open Access article distributed under the terms of the Creative Commons Attribution License (<https://creativecommons.org/licenses/by/4.0/>), which permits unrestricted reuse, distribution, and reproduction in any medium, provided the original work is properly cited.

Keywords: diffusion spectrum imaging; Wallerian degeneration; recovery of function; anisotropy; structural reserve

Abbreviations: CP = cerebral peduncle; CST = corticospinal tract; dMRI = diffusion magnetic resonance imaging; DSI = diffusion spectrum imaging; DTI = diffusion tensor imaging; FA = fractional anisotropy; gFA = generalized fractional anisotropy; ODF = orientation distribution function; PLIC = posterior limb of the internal capsule; reticuloST = reticulospinal tract; ROI = region of interest; rubroST = rubrospinal tract; WM = white matter

Graphical Abstract



Introduction

Stroke-related motor deficits are often caused by damage to the corticospinal tract (CST) and associated white matter (WM) changes are frequently assessed using anisotropy derived from diffusion MRI (dMRI). Studies commonly report a relationship between decreased anisotropy in various parts of the ipsilesional CST and the severity of motor impairment of the upper¹⁻³ and lower limbs,⁴⁻⁶ highlighting anisotropy as a promising biomarker for motor recovery post-stroke.³ However, anisotropy measures have yet to find their way into clinical practice as individual predictions of motor impairment and recovery remain challenging for several reasons.

First, most studies use a single measure of motor impairment, hindering a differentiated analysis of various aspects of motor performance. Second, it remains unknown which biological processes may underlie changes in anisotropy or give rise to the correlation between CST anisotropy and motor behaviour, rendering conclusive mechanistic interpretations

difficult. In line with the notion that the degree of anisotropy reduction reflects the extent of structural damage—often referred to as *microstructural integrity*—lower CST anisotropy coincides with more severe motor impairment.¹ Given that this correlation can still be observed when calculating anisotropy without including the lesion itself, a commonly held view is that this association is driven by *Wallerian degeneration* of descending fibres, a process that describes how axons passing through the lesion degenerate over time.⁷ However, several methodological limitations hinder a confirmation of this notion as previous dMRI studies primarily relied on fractional anisotropy (FA) derived from diffusion tensor imaging (DTI). DTI cannot adequately resolve multiple fibre directions within a given voxel,⁸ yielding misleading FA estimates for multi-directional voxels entailing crossing or kissing fibres.^{9,10} Numerous studies have circumvented this issue by focusing the analyses on specific parts of the CST, which contain densely packed, parallel-running descending fibres,¹¹ therefore thought to reflect the extent of Wallerian degeneration.¹² Commonly used regions of interest (ROIs) include the pons,^{13,14} the cerebral peduncle (CP),^{15,16} or the posterior

limb of the internal capsule (PLIC).¹⁷⁻¹⁹ Unfortunately, such ROI-based approaches introduce new pitfalls. First, the limited number of voxels within the typically used ROIs aggravates sampling biases.² Moreover, stroke patients usually feature considerable degrees of ageing-related WM atrophy²⁰ in addition to stroke-induced damage, with certain parts of the brain such as the PLIC being especially prone to ageing-related degeneration.^{21,22} Thus, ageing-related confounds might bias the quantification of Wallerian degeneration, especially when applying ROI-based approaches. Taken together, this leads to the question whether ipsilesional CST anisotropy is primarily reflective of Wallerian degeneration, which would emphasize its potential as biomarker, or whether ageing-related degeneration and methodological limitations may bias the commonly observed correlation with motor performance.

A third aspect that hinders the usage of ipsilesional CST anisotropy as a biomarker is the motor system's ability to compensate for CST damage via alternate fibre tracts not directly affected by the lesion. Therefore, a patient may not necessarily have to rely on spared fibres of the lesioned CST alone. Specifically, non-crossing fibres of the contralesional CST²³ or bihemispheric extrapyramidal pathways including the reticulospinal (reticuloST) and rubrospinal tract (rubroST)^{1,5} may compensate for ipsilesional CST damage by supporting basal motor skills via their projections to proximal arm and leg muscles. However, mixed findings hinder a conclusive interpretation of their role in motor control post-stroke. While some studies argue that extrapyramidal pathways successfully support gross motor performance, others ascribe a potential maladaptive influence to an upregulated extrapyramidal system, leading to a dysfunctional increase in flexor synergies.^{24,25} While an increase in anisotropy has been conceptualized as an upregulation of the extrapyramidal system caused by structural reorganization post-stroke,²⁶⁻²⁸ other studies could not replicate this finding, even reporting a decrease in anisotropy.²⁹⁻³¹ Thus, the question arises whether the frequently observed association between extrapyramidal tract anisotropy and motor behaviour is a result of structural changes in the extrapyramidal system or whether subjects with a relatively high premorbid level of extrapyramidal anisotropy are better equipped to compensate for CST deficits through reliance on their structural reserve.³² Notably, the assessment of anisotropy in extrapyramidal tracts suffers from the same limitations as described above for the CST, rendering the interpretation of anisotropy in the extrapyramidal system challenging.

In sum, a better understanding of the mechanisms underlying degeneration of the CST and behavioural compensation of specific motor functions via alternate motor pathways is crucial to pave the way for the usage of anisotropy as a biomarker in clinical care. To address these issues, we assessed chronic stroke patients using motor tests that differentiate various aspects of motor performance and included age-matched and young controls to discern ageing- and stroke-related WM degeneration. Diffusion spectrum imaging (DSI) was employed to better resolve multiple diffusion directions per voxel.³³ Anisotropy was conceptualized as

generalized fractional anisotropy (gFA), which allowed us to quantify the magnitude of multiple intravoxel directions.³⁴ Moreover, a compartmentwise analysis approach that differentiates voxels according to their number of trackable directions¹⁰ (cf. Fig. 1) enabled us to separately analyze voxels containing one-directional or multi-directional fibres.

By focusing on voxels containing only one dominant fibre direction, we assessed anisotropy of descending fibres along the length of the entire ipsilesional CST, overcoming the limitations of ROI-based approaches. Assuming that the correlation with motor impairment was genuinely driven by Wallerian degeneration, we hypothesized a positive correlation between motor performance and anisotropy mainly driven by one-directional CST voxels. Given the seminal role of the CST, we expected this correlation to emerge for both basal and complex motor skills of the upper and lower limbs. In line with the hypothesis that other descending motor tracts can partially compensate stroke-related deficits in gross motor control,^{4,26,28,29} we expected anisotropy within contralesional CST and extrapyramidal tracts to be linked to basal arm and leg functions. We further hypothesized a combination of alternate motor pathways and ipsilesional CST to explain more behavioural variance than the latter alone as motor performance ultimately depends on both degenerative and compensatory processes. Finally, if compensation was the result of an upregulation of the extrapyramidal system caused by structural reorganization, we would expect an increase in anisotropy in patients compared with age-matched controls, whereas no group difference would imply the reliance on a structural reserve instead.

Materials and methods

Subjects

Twenty-five chronic stroke patients (20 male, 5 female, mean age = 66.68, std = 11.25; mean time post-stroke 33.05 months with a range from 10.57 to 81.57 months) formerly hospitalized at the University Hospital Cologne, Department of Neurology, 22 healthy age-matched controls (16 male, 6 female, mean age = 67.05, std = 6.59), and 24 healthy young control subjects recruited at the University of California, Santa Barbara (8 male, 16 female, mean age = 22.29, std = 3.66) were included in this study (see [Supplementary Table 1](#) for patient information, [Fig. 2](#) for a lesion overlay). For patients, inclusion criteria were as follows: (i) first-ever ischaemic stroke before 6 months or more; (ii) initial hand motor deficit; and (iii) age 40–90 years. Exclusion criteria were as follows: (i) any contraindications to MRI; (ii) cerebral haemorrhage; (iii) bihemispheric infarcts; (iv) reinfarction or any other neurological disease; as well as (v) persistence of severe aphasia or neglect. We further ensured that patients did not exhibit any pronounced orthopaedic conditions that could have prevented a proper assessment of residual motor impairment. All participants provided informed consent prior to participation. The local ethics committee approved the study carried out under the declaration of Helsinki.

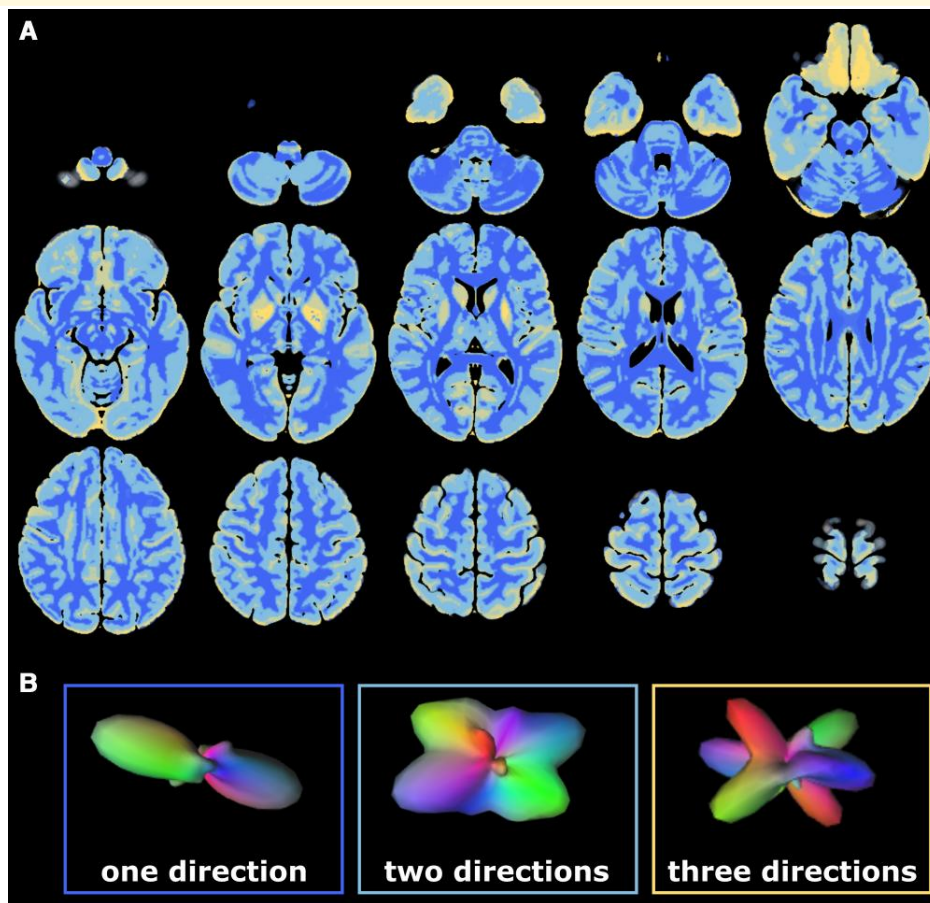


Figure 1 Deterministic brain mask for whole-brain compartmentalization. (A) The mask was created by Volz et al. based on 630 subjects from the Human Connectome Project.¹⁰ Each colour represents a single compartment containing voxels with a certain number of trackable directions [dark blue = one direction, light blue = two directions, yellow = three (or more) directions]. Images depicted in (A) were created based on the nifti-file published by Volz et al.¹⁰ (B) The number of trackable directions was determined based on the underlying ODF within a given voxel, which can simultaneously depict several diffusion directions. Depending on the number of peaks exceeding a certain threshold, each voxel was assigned to a specific compartment representing the number of trackable intravoxel directions. Exemplary ODFs with different numbers of peaks are shown in (B).

Motor tests

The Motricity Index (MI) was assessed in each patient to determine basal motor performance focusing on individual joints of the upper and lower limbs.³⁵ For motor skills representing activities of daily living, we used the Action Research Arm Test (ARAT), including the subscales grasp, grip, pinch and gross movements.³⁶ Thus, we covered a wide range of motor functions ranging from basal to complex motor control with widely used valid and reliable tests.³⁷⁻³⁹

MRI acquisition

At both scanning sites, fMRI data were recorded using a Siemens MAGNETOM Prisma 3 Tesla scanner equipped with a 64-channel head coil (Siemens Medical Solutions, Erlangen, Germany). Of note, identical scanning protocols were used at both locations, rendering a potential bias

introduced by varying scanning sites highly unlikely. DSI scans were sampled with a spatial resolution of $1.8 \times 1.8 \times 1.8 \text{ mm}^3$ with b_{max} -value of 5000 s/mm^2 , 128 diffusion directions and 10 additional b_0 s for *post hoc* movement correction (TR = 4300 ms, TE = 96 ms, FoV = 262 mm). In addition, T_1 -weighted images (TR = 2500 ms, TE = 2.22 ms, FoV = 241 mm, 208 axial slices, voxel size = $0.94 \times 0.94 \times 0.94 \text{ mm}^3$) and T_2 -weighted images (TR = 3200 ms, TE = 0.566 ms, FoV = 241 mm, 208 axial slices, voxel size = $0.94 \times 0.94 \times 0.94 \text{ mm}^3$) were acquired.

MRI preprocessing

Preprocessing was performed using QSIPrep 0.13.0RC1,⁴⁰ based on Nipype 1.6.0.⁴¹ The exact workflow is described in the printout from QSIPrep: The T_1 -weighted (T_{1w}) image was corrected for intensity non-uniformity using N4BiasFieldCorrection as implemented in ANTs 2.3.1⁴² and

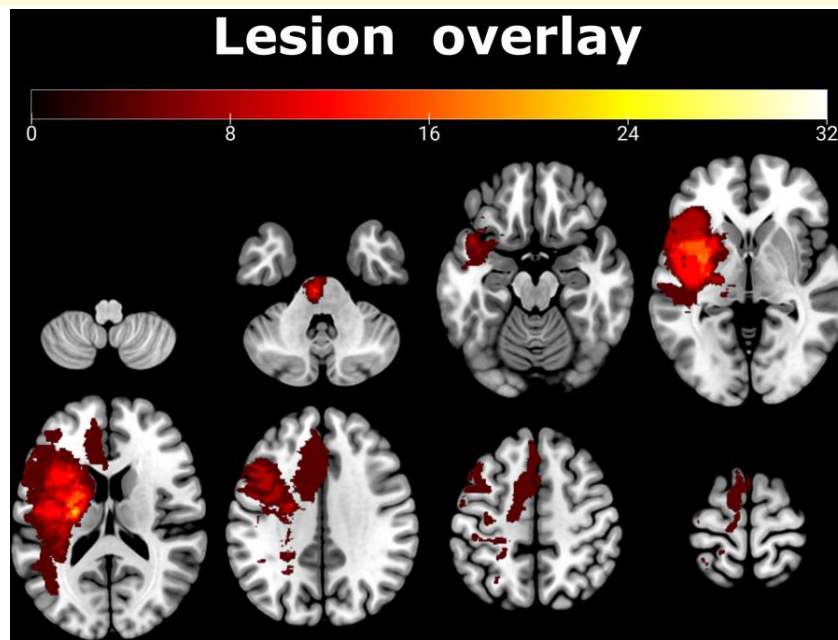


Figure 2 Lesion overlay showing affected voxels across all 25 patients in the left hemisphere (indicated as a percentage). Please note that lesions affecting the right hemisphere were flipped to the left for ease of comparison. The maximum overlap was observed within the internal capsule.

used as T_1w reference throughout the workflow. The T_1w reference was then skull-stripped with `antsBrainExtraction`, using OASIS as a target template. Spatial normalization to the ICBM 152 Nonlinear Asymmetrical template version 2009c⁴³ was performed through nonlinear registration with `antsRegistration` (ANTs 2.3.1),⁴⁴ using brain-extracted versions of both T_1w volume and template. Brain tissue segmentation of CSF, WM and grey matter was performed on the brain-extracted T_1w using FAST as implemented in FSL.⁴⁵

For diffusion data preprocessing, any images with a b -value $< 100 \text{ s/mm}^2$ were treated as a $b=0$ image. MP-PCA denoising as implemented in MRtrix3's `dwi denoise`⁴⁶ was applied with a 5-voxel window. B1 field inhomogeneity was corrected using `dwi bias correct` from MRtrix3 with the N4 algorithm.⁴² After B1 bias correction, the mean intensity of the DWI series was adjusted so all the mean intensity of the $b=0$ images matched across each separate DWI scanning sequence. Motion correction was performed using `3dSHORE` as implemented in QSIPrep.⁴⁷ The DWI time series were re-sampled to ACPC, generating a preprocessed DWI run in ACPC space with 1.8 mm isotropic voxels.

DSI-reconstruction

Diffusion orientation distribution functions (ODFs) were reconstructed using generalized q -sampling imaging⁴⁸ with a ratio of mean diffusion distance of 1.25. Next, individual gFA maps were created and normalized to the MNI standard space using ANTs.

Lesion masking and whole-brain compartmentalization

For patient data, lesion masks were drawn on individual T_2 -weighted images using MRICron (www.sph.sc.edu/comd/rorden/Mricron) and applied to patients' gFA-maps, thereby excluding direct lesion effects on gFA from further analyses to focus on secondary degeneration (cf. Fig. 3A). In case of right-hemispheric lesions, masks and gFA-maps were flipped along the mid-sagittal plane to ensure that all lesions were located in the left hemisphere, thereby rendering group comparisons possible.⁵⁰⁻⁵² Moreover, individual WM-masks derived from QSIPrep were applied to each subject's gFA-map, excluding non-WM voxels from further analyses. A deterministic mask denoting the number of trackable directions per voxel (constructed using $n=630$ HCP data sets)¹⁰ was used to compartmentalize whole-brain gFA maps (cf. Fig. 1). Compartmentwise mean gFA values [(i) all voxels; voxels with (ii) one; (iii) two; and (iv) three fibre directions] were extracted from the motor tracts of interest (CST, rubroST, reticuloST) as defined in the HCP tractography atlas⁴⁹ (cf. Fig. 3B, Supplementary Figure 1). To focus on descending fibres and exclude the widespread cortical inputs to the reticuloST, the reticuloST mask was trimmed, retaining only the part of the tract below $z=-7$. This ensured that reticuloST and rubroST masks commenced on the same z -level, ruling out systematic differences between the extrapyramidal masks. In order to avoid a sampling bias induced by different numbers of voxels in left- and right-hemispheric masks, we constructed symmetric masks by

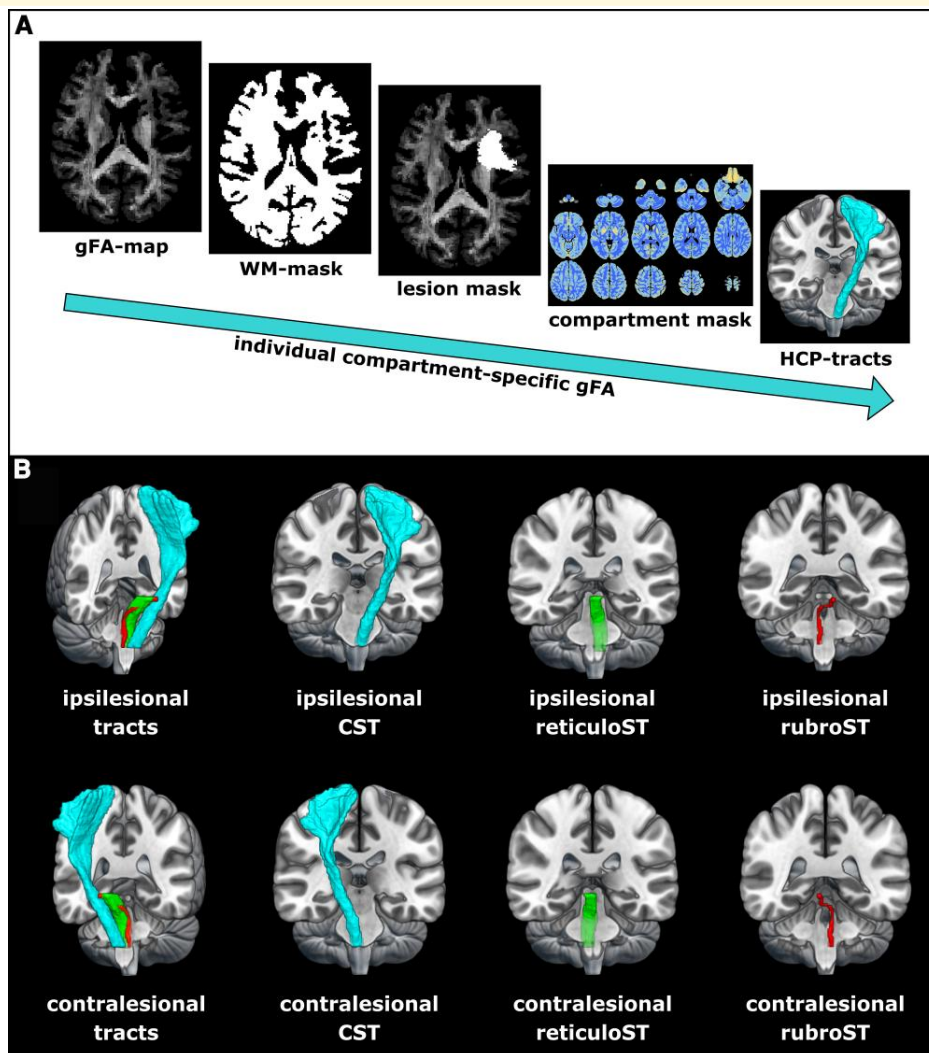


Figure 3 Extraction of compartment-specific tractwise gFA. **(A)** Workflow to obtain compartment-specific gFA values per tract. First, voxels containing WM were extracted from each subject's normalized gFA-map using individual WM tissue classifications as derived from QSIprep. For patient data, lesion masks were applied to focus the analysis on secondary degeneration processes rather than the assessment of anisotropy within the lesion. A deterministic compartment mask was applied to categorize all voxels according to the number of trackable directions.¹⁰ Mean gFA was extracted for descending motor tracts as defined by the HCP tractography atlas.⁴⁹ **(B)** Motor tracts derived from the HCP tractography atlas⁴⁹ used for gFA extraction. Note that 'ipsilesional' is defined by the origin of the tract superior to its decussation. Symmetric masks were used to ensure an equal number of voxels in each hemisphere, reducing potential sampling biases.

flipping left-hemispheric masks along the mid-sagittal plane and applied the resulting masks to the right hemisphere. A considerable overlap with other major fibre tracts such as the superior longitudinal fasciculus was excluded by visual inspection (cf. [Supplementary Figure 2](#)).

Statistical analyses

Differentiating stroke and ageing-related effects

To differentiate between ageing- and stroke-related effects, we compared the three subject groups across different

compartments for the left and right CST. We computed a mixed ANOVA with the between factor group (levels: patients, age-matched controls, young controls) and the within factor compartment [levels: all (all voxels), one (one-directional voxels), two (two-directional voxels)] for the left and right CST. All assumptions for performing the ANOVA were met. A Greenhouse–Geisser correction was applied where appropriate. *Post hoc* pairwise *t*-tests were used to test for the following differences: (i) compartment all: patients versus old controls; (ii) compartment one: patients versus old controls; (iii) compartment two: patients versus old controls; (iv) compartment all: young versus old controls; (v) compartment one: young versus old controls; and (vi) compartment two: young versus old controls.

Results of *post hoc* tests were FDR-corrected for the number of comparisons.

Probing for extrapyramidal anisotropy differences

By comparing patients and age-matched controls with respect to mean gFA derived from extrapyramidal tracts, we probed for a potential reorganization of the extrapyramidal system. We computed a mixed ANOVA with the between factor group (levels: patients, age-matched controls) and the within factor compartment [levels: all (all voxels), one (one-directional voxels), two (two-directional voxels)]. A Greenhouse–Geisser correction was applied where appropriate.

Explaining motor impairment: ipsilesional CST

In order to probe for a possible relationship with behaviour, we computed simple linear regressions with mean gFA derived from the ipsilesional CST as predictor and ARAT, MI arm or MI leg as the outcome variable. Next, we repeated these analyses using mean gFA derived from one- or two-directional voxels as predictors. Moreover, according analyses were performed using the compartment-specific asymmetry index as predictor, which was determined as $\text{asymmetry} = [\text{mean gFA}(\text{unaff CST}) - \text{mean gFA}(\text{aff CST})] / [\text{mean gFA}(\text{unaff CST}) + \text{mean gFA}(\text{aff CST})]$.⁵³ This step was implemented to improve the signal-to-noise ratio by accounting for the individual ageing-related level of atrophy.^{16,53} To compare our current results with more conventional ROI-based approaches, we computed regression models using gFA derived from (i) all voxels contained in the PLIC^{17–19} and (ii) voxels that fell into the CST section from the mesencephalon to the CPs (z from -25 to -20).⁵⁴ As previous research has shown that the microstructural integrity of the CST and motor impairment exhibit a stronger relationship in patients with persisting motor deficits,^{4,55} we repeated the compartmentwise analyses for a non-fully recovered subgroup as defined by an ARAT score < 57 .³⁶ For each step, all P -values were FDR-corrected for the number of comparisons.

Explaining motor impairment: contralesional CST and extrapyramidal pathways

The role of alternative motor pathways in motor function after stroke was assessed through linear regression analyses. To test for a relationship with basal motor performance, five linear regression models were computed with the MI arm score as the outcome variable and contralesional CST, ipsilesional reticuloST, contralesional reticuloST, ipsilesional rubroST or contralesional rubroST as the predictor variable. The resulting P -values were FDR-corrected for the number of comparisons. These analyses were carried out for mean gFA derived from (i) all voxels; (ii) one-directional voxels; and (iii) two-directional

voxels. The same procedure was repeated for the ARAT score and the MI leg score as outcome variable to probe for a potential relationship with the performance of activities of daily living or lower limb performance, respectively. Next, we tested for shared variance between alternative motor pathways and the ipsilesional CST by entering mean gFA values derived from extrapyramidal tracts that correlated with motor performance as predictor variables into the regression model containing gFA derived from one-directional ipsilesional CST voxels. To rule out multicollinearity of predictor variables, we probed for a correlation between extrapyramidal anisotropy of two-directional voxels and CST anisotropy of one-directional voxels. An overlay of all four extrapyramidal tracts was created to test whether compartment two of the four tracts captured a high number of identical voxels.

Results

Ageing- versus stroke-related CST anisotropy

For the ipsilesional CST, we found a significant main effect of group ($F(2, 68) = 32.28$, $P < 0.001$, generalized $\eta^2 = 0.44$) and compartment ($F(1.05, 71.56) = 2178.42$, $P < 0.001$, generalized $\eta^2 = 0.84$), as well as an interaction between group and compartment ($F(2.10, 71.56) = 19.77$, $P < 0.001$, generalized $\eta^2 = 0.09$). *Post hoc* independent sample t -tests showed that patients featured reduced gFA values within the ipsilesional CST compared with age-matched controls when considering all voxels within the CST mask ($t(45) = -2.65$, $P = 0.013$, FDR-corrected). This difference was attributable to voxels containing only one fibre direction ($t(45) = -3.66$, $P = 0.001$, FDR-corrected), while two-directional voxels showed no difference ($t(45) = 0.41$, $P = 0.684$, FDR-corrected; cf. Fig. 4A). At the same time, young and old controls differed with respect to all levels of the factor compartment (all $P < 0.001$, FDR-corrected), indicating that the age-related difference could be objectified in all compartments, affecting both one- and two-directional voxels. For the contralesional CST, we found a main effect of group ($F(2, 68) = 19.24$, $P < 0.001$, generalized $\eta^2 = 0.34$) and a main effect of compartment ($F(1.06, 71.80) = 3756.75$, $P < 0.001$, generalized $\eta^2 = 0.86$). There was no interaction between group and compartment ($F(2.11, 71.80) = 2.41$, $P = 0.094$). While patients and age-matched controls did not differ with respect to mean gFA in any compartment ($P > 0.1$), young and elderly control subjects differed across all compartments ($P < 0.01$, FDR-corrected; cf. Fig. 4B). Thus, while stroke-related changes in anisotropy were specific to the ipsilesional CST, ageing-related degeneration affected the CST in both hemispheres.

Anisotropy in the extrapyramidal system

For the extrapyramidal system entailing bihemispheric reticuloST and rubroST, there was a main effect of

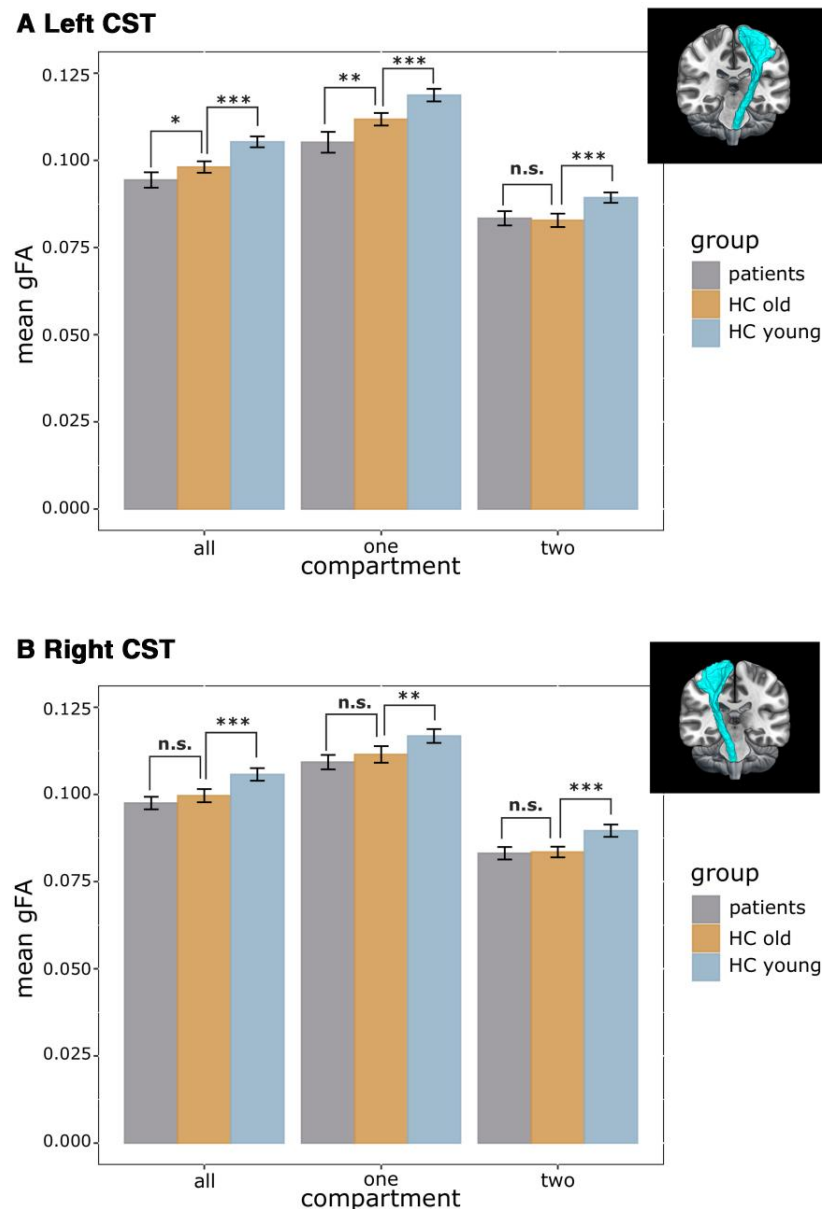


Figure 4 Group differences per compartment. Results of a mixed ANOVA with the between factor group (levels: patients, age-matched controls, young controls) and the within factor compartment [levels: all (all voxels), one (one-directional voxels), two (two-directional voxels)] for **(A)** the ipsilesional CST and **(B)** the contralesional CST. **(A)** Left (ipsilesional) CST: While young and old controls differed across all compartments, patients and age-matched controls differed for compartment 1 but not for compartment 2. Thus, ageing-related changes occurred across the entire left CST entailing both one- and two-directional voxels, while stroke-related decreases in gFA were driven by one-directional voxels. **(B)** Right (contralesional) CST: In line with findings for the left CST, young and old controls differed across all compartments, yet there was no difference between patients and age-matched controls. *Post hoc* two-sided *t*-tests were used to further investigate significant effects. Significance thresholds: *** $P < 0.001$, ** $P < 0.01$, * $P < 0.05$ (FDR-corrected for multiple comparisons). Error bars represent two standard errors.

compartment ($F(1.01, 45.29) = 656.22$, $P < 0.001$, generalized $\eta^2 = 0.38$) but no main effect of group ($F(1,45) = 0.01$, $P = 0.913$) or interaction between group and compartment ($F(1.01,45.29) = 0.78$, $P = 0.381$), indicating that patients and age-matched controls did not differ with respect to extrapyramidal anisotropy.

Ipsilesional CST degeneration explains motor impairment

Mean gFA values derived from all voxels of the ipsilesional CST significantly explained upper limb impairment as measured by the ARAT ($R^2 = 34.61$, $P = 0.006$, FDR-corrected)

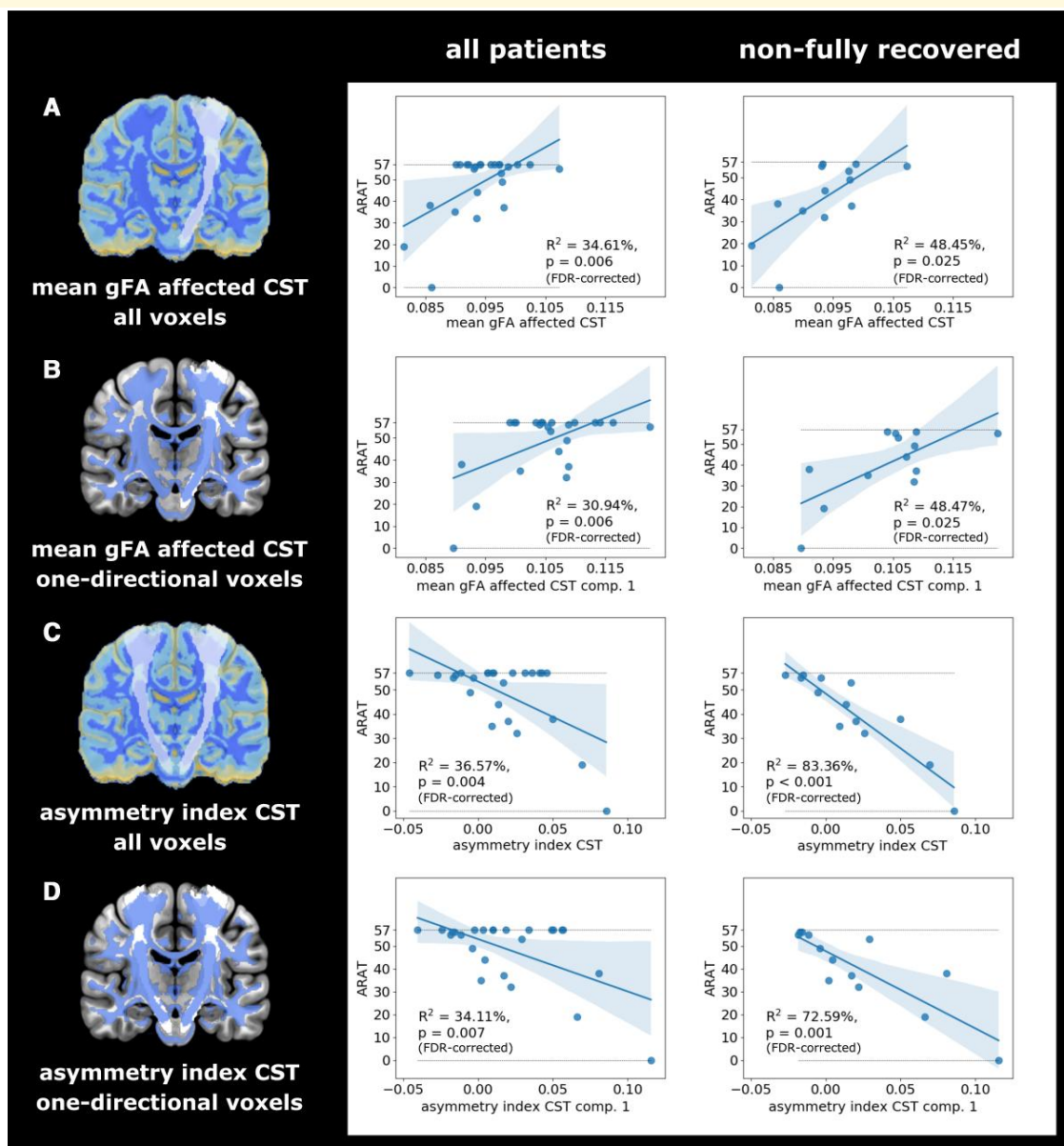


Figure 5 Regression analyses for the association between different gFA-based CST measures and ARAT motor scores. **(A)** Mean gFA values within the ipsilesional CST explained motor impairment for the entire cohort and to an even higher degree for the non-fully recovered subgroup. **(B)** By obtaining the mean gFA value from one-directional voxels within the ipsilesional CST, it becomes evident that the association between anisotropy and motor performance was driven by descending fibres. Note that the mean taken from two-directional voxels did not significantly explain motor performance ($P > 0.2$, FDR-corrected). **(C)** To improve the signal-to-noise ratio, we calculated the asymmetry index that accounts for the subject-specific level of atrophy by considering both the affected and unaffected CST. Across all CST voxels, we observed a significant association with the ARAT score for the entire sample and the non-fully recovered subgroup. **(D)** Entering the asymmetry index from one-directional voxels as the predictor into the regression models yielded a similar ratio of explained variance as in **(C)**.

or MI arm ($R^2 = 28.9\%$, $P = 0.008$, FDR-corrected) (cf. Fig. 5). The regression model containing MI leg as the outcome variable showed a trend towards significance ($R^2 = 15.25\%$, $P = 0.054$, FDR-corrected). Repeating the analyses with only one-directional voxels showed that the results were indeed driven by descending fibres (ARAT: $R^2 = 30.94\%$, $P = 0.006$; MI arm: $R^2 = 31.94\%$, $P = 0.010$; MI

leg: $R^2 = 17.71\%$, $P = 0.036$, FDR-corrected). Regression models using mean gFA derived from compartment two did not reach significance (all $P > 0.2$, FDR-corrected; for a summary of all results see Supplementary Table 3). Using the asymmetry index based on the entire CST as the predictor yielded a slightly higher percentage of explained variance for the ARAT ($R^2 = 36.57\%$, $P = 0.004$, FDR-corrected) but not

for MI arm ($R^2 = 28.10\%$, $P = 0.010$, FDR-corrected) or MI leg ($R^2 = 11.21\%$, $P = 0.102$, FDR-corrected). Increased explained variance was also observed when computing the asymmetry index for one-directional voxels (ARAT: $R^2 = 34.11\%$, $P = 0.007$; MI arm: $R^2 = 31.78\%$, $P = 0.005$; MI leg: $R^2 = 16.01\%$, $P = 0.048$, FDR-corrected). Of note, using gFA derived from one-directional voxels outperformed conventional ROI-based approaches which rely on anisotropy from voxels regardless of their directional compartment (for detailed results see [Supplementary Table 2](#)).

When exclusively considering patients with persisting motor deficits and repeating the analyses for this non-fully recovered subgroup, the ratio of explained variance increased for all models, when using mean gFA across all voxels (ARAT: $R^2 = 48.45\%$, $P = 0.025$; MI arm: $R^2 = 40.77\%$, $P = 0.028$; MI leg: $R^2 = 29.12\%$, $P = 0.057$, FDR-corrected) or gFA extracted from one-directional voxels (ARAT: $R^2 = 48.47\%$, $P = 0.025$; MI arm: $R^2 = 46.22\%$, $P = 0.016$; MI leg: $R^2 = 35.11\%$, $P = 0.033$, FDR-corrected), as well as the asymmetry index derived from all voxels (ARAT: $R^2 = 83.36\%$, $P < 0.001$; MI arm: $R^2 = 63.08\%$, $P = 0.002$; MI leg: $R^2 = 50.88\%$, $P = 0.006$, FDR-corrected) or one-directional voxels (ARAT: $R^2 = 72.59\%$, $P = 0.001$; MI arm: $R^2 = 63.08\%$, $P = 0.002$; MI leg: $R^2 = 52.47\%$, $P = 0.005$, FDR-corrected).

Extrapyramidal pathways explain motor impairment

While neither the contralesional CST nor any of the extrapyramidal tracts explained variance in ARAT scores in any compartment ($P > 0.7$, FDR-corrected), the rubroST descending from the contralesional hemisphere showed a significant relationship with the MI arm score for two-directional voxels ($R^2 = 25.94\%$, $P = 0.047$, FDR-corrected) and a trend towards significance when using all voxels ($R^2 = 22.18$, $P = 0.087$, FDR-corrected). For the MI leg score, all extrapyramidal tracts explained variance in motor performance when using two-directional voxels (all $P < 0.05$), but not the contralesional CST (cf. [Table 1](#), [Supplementary Table 3](#), and [Fig. 6A-D](#)). Notably, the two-directional voxels of the four extrapyramidal tracts barely overlapped, with only seven voxels being included in all four masks, indicating that the explained variance observed for the different tracts was not driven by the same set of overlapping voxels (cf. [Fig. 6E-G](#)).

To assess whether the extrapyramidal system's anisotropy may reflect a compensatory mechanism, i.e. may hold additional information on motor outcome exceeding that of the ipsilesional CST, we tested whether the extrapyramidal system explained additional behavioural variance when combined with the ipsilesional CST. Adding mean gFA derived from compartment 2 of any of the extrapyramidal tracts as an additional variable to anisotropy derived from one-directional ipsilesional CST voxels into a regression model significantly increased the amount of explained variance for the MI leg score, underlining the independence

Table 1 Linear regression results of the motricity index leg score for alternative motor output pathways using mean gFA derived from two-directional voxels

Predictor	R ²	P (FDR)
Contralesional CST	1.11%	0.616
Ipsilesional reticuloST	19.14%	0.036
Contralesional reticuloST	21.85%	0.046
Ipsilesional rubroST	21.77%	0.031
Contralesional rubroST	27.37%	0.036

of extrapyramidal tracts from the ipsilesional CST (all R^2 values $> 38\%$, $P < 0.01$, cf. [Supplementary Table 4](#)). Concerning the shared variance between ipsilesional CST and extrapyramidal system in the prediction of gross upper limb performance, the combination of mean gFA derived from compartment 1 of the ipsilesional CST and compartment 2 of the contralesional rubroST led to a significantly higher ratio of explained variance than any of the two tracts alone ($R^2 = 51.02\%$, $P < 0.001$). Of note, individual predictor variables were not correlated, ruling out biases due to multicollinearity (cf. [Supplementary Figure 3](#)).

Discussion

Using DSI data combined with a compartmentwise analysis approach that differentiates the number of fibre directions per voxel, we found that decreased anisotropy following stroke primarily affected one-directional voxels of the ipsilesional CST while ageing-related degeneration was observed across all directional compartments. In line with numerous previous findings, ipsilesional CST anisotropy explained motor performance across many functional domains, which entirely relied on one-directional voxels representing descending fibres. Thus, our data provide direct evidence for Wallerian degeneration occurring throughout the entire ipsilesional CST and underline the seminal pathophysiological role of Wallerian degeneration for various aspects of motor function. However, the ipsilesional CST cannot be considered the sole descending motor pathway involved in motor control post-stroke: anisotropy of extrapyramidal tracts was associated with specific aspects of motor impairment, highlighting function-specific compensatory roles of distinct pathways. While the contralesional rubroST was indicative of gross motor control of the arm, bihemispheric rubroST and reticuloST were related to lower limb motor function. Importantly, the relationship between extrapyramidal tracts and motor performance only emerged when focusing on voxels containing two fibre directions, which may explain contradictory findings of previous studies. Of note, stroke patients did not differ from age-matched controls regarding anisotropy in extrapyramidal tracts, suggesting that functional compensation through extrapyramidal pathways does not rely on reorganization of these tracts but rather reflects an aspect of the structural reserve of the motor system as discussed below.

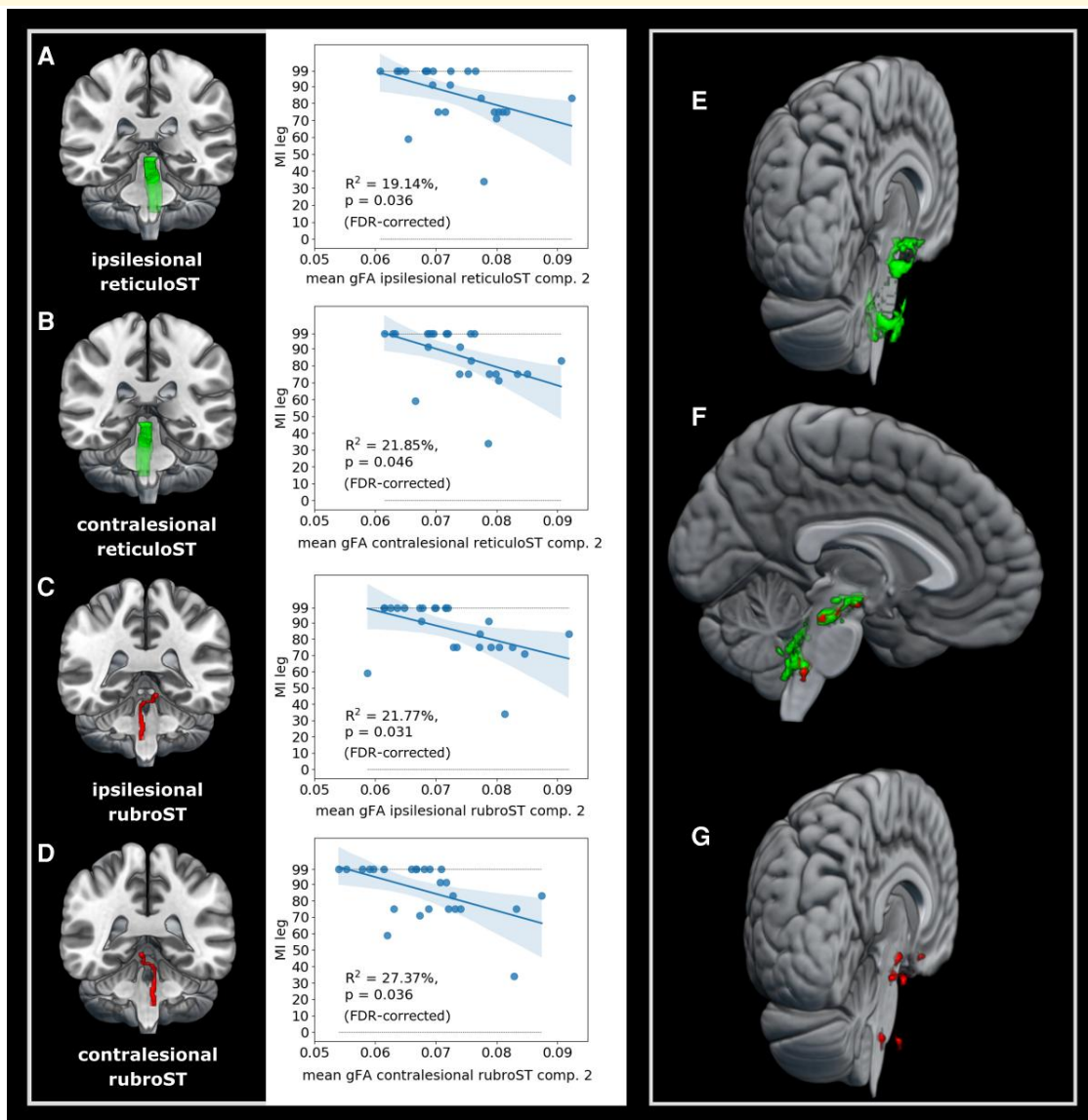


Figure 6 Explained variance by mean gFA derived from two-directional voxels of extrapyramidal pathways for the motricity index lower extremity scores. Note that there was a robust negative relationship between leg impairment and gFA derived from two-directional voxels within the (A) ipsilesional reticuloST, (B) contralesional reticuloST, (C) ipsilesional rubroST, and (D) contralesional rubroST. Of note, compartment 2 voxels of the reticuloST (E) and rubroST (G) did not contain many overlapping voxels (F).

Structural CST alterations in stroke and ageing

Using a compartmentwise approach, we aimed to disentangle the drivers of anisotropy changes in chronic stroke patients to further elucidate the potential of anisotropy in descending motor tracts to explain motor control after stroke. In line with our hypotheses, the expected decline in anisotropy in the ipsilesional CST compared with age-matched controls was limited to voxels containing one-directional, i.e. descending fibres, and could not be observed in the contralesional CST (cf. Fig. 4). Conversely, age-related

differences between the young and old control group manifested themselves in bilateral CSTs regardless of the number of intravoxel directions, which nicely fits the notion that ageing represents a global phenomenon affecting more than just descending fibre tracts.²⁰ Thus, the compartmentwise analysis approach allowed us to differentiate ageing- and stroke-related anisotropy changes. Of note, decreased ipsilesional CST anisotropy in stroke patients compared with age-matched controls was only evident in one-directional voxels, highlighting Wallerian degeneration as the main driver of anisotropy changes in descending ipsilesional CST fibres. The pivotal influence of Wallerian degeneration on anisotropy

changes post-stroke clarifies why previous research has frequently linked the integrity of ipsilesional CST fibres to motor impairment. For instance, Schaechter *et al.*²³ investigated differences between chronic stroke patients and healthy controls by comparing FA curves extracted along the ipsilesional CST starting from the precentral gyrus down to the CP. Their results indicate that poorly recovered stroke patients feature significantly decreased FA values in the ipsilesional CST between the height of the PLIC and CP. Parts of this CST section have repeatedly been used as ROIs to investigate stroke-related WM abnormalities and their association with motor impairment. As Pierpaoli *et al.*¹¹ point out, this particular stretch of the CST is characterized by densely packed descending fibres without any significant association tracts passing through. In other words, it mainly consists of descending fibres which we captured as one-directional voxels in our analyses.

Interestingly, our results suggest that focusing on descending fibres along the entire CST might increase the sensitivity for certain aspects of motor performance: When using all CST voxels, mean gFA significantly explained motor impairment of the upper but not the lower limb. However, lower limb deficits could also be explained when exclusively including one-directional voxels. Moreover, the significant association between gFA in the ipsilesional CST and motor impairment of the upper limb was entirely driven by one-directional voxels: While mean gFA derived from one-directional voxels accounted for almost the same amount of explained variance as all CST voxels combined, two-directional voxels did not show any association with motor impairment. Of note, these effects were intensified for the non-fully recovered subgroup, which is in line with previous studies reporting more severe WM changes and better predictions of motor performance in patients with more pronounced motor deficits.^{4,55} The ratio of explained variance was even higher when using the asymmetry index and thereby accounting for a patient's individual level of ageing-related atrophy.

Importantly, the present findings do not only underline the applicability of a DSI-based compartmentwise approach but also offer a possible solution to the problem of arbitrary ROI selection since focusing on descending fibres allowed us to include the entire length of the CST into our analysis. Moreover, using one-directional voxels from the entire length of the ipsilesional CST may also help to reduce ageing-related confounds commonly introduced when focusing on regions heavily affected by ageing-related atrophy such as the PLIC.^{21,22} In summary, anisotropy of one-directional ipsilesional CST fibres primarily reflects Wallerian degeneration of descending motor fibres which accounted for a large amount of variance in motor impairment across various domains of motor control. However, our current results also highlight that Wallerian degeneration of the ipsilesional CST should not be regarded as the only factor contributing to motor control after stroke, given the compensatory potential of other descending motor pathways.

Compensatory role of the extrapyramidal system

The role of the extrapyramidal system in motor recovery following stroke is a subject of ongoing debate, inspired by several studies reporting associations between motor impairment and extrapyramidal tract anisotropy. While some authors argue that increased reliance on the extrapyramidal system may help patients to recover successfully,^{4,29} others interpret their findings as maladaptive reorganization.^{24,27,28,56} These opposing interpretations are largely driven by the direction of the observed correlations between anisotropy and motor behaviour: positive correlations linking higher anisotropy to better motor performance are often construed as beneficial compensation, whereas negative correlations linking higher anisotropy to worse motor performance are commonly interpreted as maladaptive overcompensation caused by reorganization processes of the extrapyramidal tracts. A commonly held view is that the overcompensation may stem from an overactivation of extrapyramidal pathways resulting in increased flexor synergies, hindering the control of individual movements.^{24,25} Here, we exclusively observed negative associations between extrapyramidal anisotropy and motor performance of the arm and leg (cf. Fig. 6). Therefore, one may interpret our current findings as a maladaptive overcompensation by the extrapyramidal system. However, motor impairment across patients was exclusively explained by two-directional voxels which renders the interpretation more difficult. Two-directional voxels are characterized by two dominant directions which need to change to a different extent for gFA to either decrease or increase. Depending on the ratio of the two directions, even an underlying decrease in one direction could lead to an overall increase in gFA. For instance, if only the non-dominant direction in a two-directional voxel decreases while the dominant direction remains constant, the gFA value will increase. Following this logic, gFA values will not change at all when both fibre directions within a two-directional voxel change to the same extent. Thus, a higher or lower degree of anisotropy in two-directional voxels should not be mistaken for higher or lower microstructural integrity. In other words, higher or lower degrees of anisotropy in two-directional voxels cannot be functionally interpreted in a straightforward way, which may well account for previous contradictory findings. Therefore, future studies should focus on changes at the subvoxel level to further our understanding of the underlying pathophysiological mechanisms.

From a functional perspective, extrapyramidal pathways are thought to support gross motor function via their projections to proximal muscles of the arm and leg. In particular, the basal motor control by extrapyramidal tracts may stem from their ability to directly code for strength of muscle activation as recently observed for the reticular formation in monkeys.⁵⁷ Our current results are well in line with this notion, as reflected by their associations with MI scores of the

upper and lower limb but not for the ARAT. For the ARAT, higher scores can be achieved through compensatory strategies applied in daily life, which requires higher degrees of motor control and more complex motor skills.⁵⁸ The MI, on the other hand, assesses each joint individually. In other words, it relies on muscular strength and therefore reflects more basal demands on the motor system.^{59,60} Given the observed relationship between anisotropy of all four extrapyramidal tracts and the patients' ability to move individual joints as assessed using the MI, our current findings underline the potential involvement of extrapyramidal pathways in the recovery of gross motor function after stroke. This notion is supported by the fact that extrapyramidal pathways seemed to be independent of the ipsilesional CST as indicated by the increase in explained variance when combining CST and extrapyramidal anisotropy in a regression model explaining MI scores. These observations perfectly match previous reports indicating an additional explanation of variance in motor function by anisotropy of the reticuloST and rubroST independent of the ipsilesional CST.^{29,31} Thus, these findings are in line with the notion that both pyramidal and extrapyramidal tracts contribute independently to the execution and control of gross motor function. To further elucidate the mechanistical role of extrapyramidal tracts in motor control post-stroke, a seminal question lies in whether extrapyramidal tracts undergo stroke-induced reorganization or whether compensation may be determined by the premorbid level of descending motor output. Considering that we did not find a group difference between stroke patients and age-matched controls, a compensatory upregulation through structural changes of the extrapyramidal tracts seems less likely. Conversely, extrapyramidal anisotropy may rather indicate a structural reserve within those tracts the motor system may capitalize on to compensate for stroke-induced damage.³²

Anatomical foundations of extrapyramidal compensation

Having established a link between motor function and extrapyramidal integrity of two-directional voxels, the question arises which anatomical parts of the reticuloST and rubroST drove this observation. The reticuloST receives its cortical inputs from the primary motor cortex, as well as the premotor and supplementary motor areas⁶¹ and descends mostly ipsilaterally from the medial pontine and medullary reticular formation.⁶² The rubroST originates from the red nucleus at the level of the mesencephalon and receives inputs from an array of cortical areas and the cerebellum. It decussates at the level of the red nucleus and descends alongside the lateral CST.⁶³ While most fibres within the rubroST decussate, most of the reticuloST descends without crossing. Therefore, it seems striking that tracts from both hemispheres showed a similar relationship with motor performance. A potential explanation for this observation might derive from the limited number of crossing fibres in both

tracts.^{5,64} Considering the anatomical proximity of these crossing fibres and the relatively high overlap in explained variance in motor performance of all four tracts, one might assume that identical voxels were included in both tracts due to tracking inaccuracies or sampling biases. However, computing the overlap between all four masks yielded a negligible number of shared voxels.

When visualizing compartment two voxels (cf. Fig. 6E-G), clusters emerged at three different levels. Voxels located at the most superior level may potentially constitute input and output fibres from various nuclei. For example, anisotropy surrounding the red nucleus has been shown to correlate with motor impairment,^{4,26,28} supporting the notion that output properties of the red nucleus may contribute to motor control after stroke. Moreover, units in the pontine reticular formation of the cat discharge during motor activity even when deprived of any other stimulus inputs,⁶⁵ which highlights the involvement of the pontine reticular formation and the descending reticuloST for the generation of motor output. Second, various clusters can be seen close to the midline, where both rubroST and the reticuloST cross over to the other hemisphere. Whether the integrity of these crossings is vital for motor performance after stroke remains an interesting question for future research. Third, at the lowest level, a cluster of two-directional voxels may include fibres from cerebellar structures. Cortico-cerebellar pathways as well as the cerebellar peduncles have already been shown to relate to residual motor function after stroke,⁶⁶⁻⁶⁸ and it may thus be possible that the observed relationship with motor impairment was partially driven by fibres projecting to or from the cerebellum. In summary, our methodological approach helped to identify specific parts of the extrapyramidal system contributing to compensation of gross arm and leg movements after stroke, primarily comprising fibres crossing the midline, fibres potentially mitigating output from brain stem nuclei (such as the red nucleus) or interactions across different parts of the extrapyramidal system and cerebellum.

Limitations and future directions

One major limitation pertains to the limited sample size. However, we covered a wide range of motor deficits and lesion sizes and a sample of 25 stroke patients is well in the range of other hypothesis-driven fMRI studies.^{30,50,52} Thus, while a bigger sample would be desirable, our sample yields sufficient variability for the present analysis framework, resulting in meaningful effects of considerable sizes. Moreover, the focus on chronic stroke patients allowed us to draw conclusions regarding the effects of secondary degenerative processes and to assess the reorganized motor system. Further studies are warranted to quantify anisotropy changes in descending tracts longitudinally starting in the acute phase after stroke. As our findings suggest that compensatory processes in the extrapyramidal system rely on a patient's structural reserve rather than structural changes within the extrapyramidal tracts, estimating the propensity

of these tracts to compensate for lost functionality based on anisotropy measures might already be possible in the acute phase post-stroke. Moreover, the present study focused on structural alterations in descending tracts underlining their relationship with motor impairment. Given that compensatory mechanisms may also operate via alternative routes such as cortico-(sub)cortical interactions, extending the current analyses by assessing structural connectivity between different (sub)cortical areas may result in a more comprehensive picture.⁶⁹ Since motor impairment has also been shown to be closely related to functional connectivity between cortical motor regions,^{50,70-74} future research should try to elucidate the relationship between stroke-related changes in the structural and functional organization of the motor network.

Conclusion

By disentangling ageing from stroke-related effects via compartmentwise analyses, we provide direct evidence for Wallerian degeneration of the ipsilesional descending CST and its seminal role in various aspects of motor control of the upper and lower limbs. Anisotropy of the contralesional rubroST explained gross motor performance of the affected hand, while anisotropy within all extrapyramidal tracts located throughout the brainstem was linked to motor function of the lower limb in chronic stroke patients, supporting the notion of increased reliance on extrapyramidal pathways to support basal motor function after CST damage. Of note, all extrapyramidal tract findings were based on two-directional voxels which can be found in specific anatomical locations throughout the brainstem, potentially mitigating output of brainstem nuclei, signals crossing the midline and cerebellar influences. Since the highest ratio of explained variance was achieved when combining extrapyramidal pathways and ipsilesional CST anisotropy, clinical biomarkers should consider both the degeneration of the ipsilesional CST, as well as the compensation via the extrapyramidal system. From a mechanistic perspective, our findings suggest that compensatory processes in the extrapyramidal system reflect an aspect of structural motor reserve rather than reorganization of extrapyramidal tracts. In summary, anisotropy of descending motor pathways seems to be a promising marker for motor impairment post-stroke, especially when divided into compartments based on the number of trackable directions per voxel.

Funding

G.R.F. gratefully acknowledges support from the Marga and Walter Boll Stiftung, Kerpen, Germany. C.G. and G.R.F. are funded by the Deutsche Forschungsgemeinschaft (DFG, German Research Foundation)—Project-ID 431549029—SFB 1451. S.T.G. was supported by Cooperative Agreement W911NF-19-2-0026 from the US Army Research Office.

Competing interests

The authors report no competing interests.

Supplementary material

Supplementary material is available at *Brain Communications* online.

Data availability

Data are available from the corresponding author upon reasonable request.

References

1. Koch P, Schulz R, Hummel FC. Structural connectivity analyses in motor recovery research after stroke. *Ann Clin Transl Neurol.* 2016;3(3):233-244.
2. Moura LM, Luccas R, de Paiva JPQ, et al. Diffusion tensor imaging biomarkers to predict motor outcomes in stroke: A narrative review. *Front Neurol.* 2019;10(MAY):1-17.
3. Boyd LA, Hayward KS, Ward NS, et al. Biomarkers of stroke recovery: Consensus-based core recommendations from the stroke recovery and rehabilitation roundtable. *Int J Stroke.* 2017;12(5):480-493.
4. Peters DM, Fridriksson J, Richardson JD, et al. Upper and lower limb motor function correlates with ipsilesional corticospinal tract and red nucleus structural integrity in chronic stroke: A cross-sectional, ROI-based MRI study. *Tambasco N, ed. Behav Neurol.* 2021;2021:1-10.
5. Cleland BT, Madhavan S. Ipsilateral motor pathways to the lower limb after stroke: Insights and opportunities. *J Neurosci Res.* 2021;99(6):1565-1578.
6. Jayaram G, Stagg CJ, Esser P, Kischka U, Steinar J, Johansen-Berg H. Relationships between functional and structural corticospinal tract integrity and walking post stroke. *Clin Neurophysiol.* 2012;123(12):2422-2428.
7. Conforti L, Gilley J, Coleman MP. Wallerian degeneration: An emerging axon death pathway linking injury and disease. *Nat Rev Neurosci.* 2014;15(6):394-409.
8. Basser PJ, Mattiello J, LeBihan D. MR Diffusion tensor spectroscopy and imaging. *Biophys J.* 1994;66(1):259-267.
9. Descoteaux M, Angelino E, Fitzgibbons S, Deriche R. Apparent diffusion coefficients from high angular resolution diffusion imaging: Estimation and applications. *Magn Reson Med.* 2006;56(2):395-410.
10. Volz LJ, Cieslak M, Grafton ST. A probabilistic atlas of fiber crossings for variability reduction of anisotropy measures. *Brain Struct Funct.* 2018;223(2):635-651.
11. Pierpaoli C, Barnett A, Pajevic S, et al. Water diffusion changes in wallerian degeneration and their dependence on white matter architecture. *Neuroimage.* 2001;13(6):1174-1185.
12. Kim B, Fisher BE, Schweighofer N, et al. A comparison of seven different DTI-derived estimates of corticospinal tract structural characteristics in chronic stroke survivors. *J Neurosci Methods.* 2018;304:66-75.
13. Puig J, Pedraza S, Blasco G, et al. Wallerian degeneration in the corticospinal tract evaluated by diffusion tensor imaging correlates with motor deficit 30 days after middle cerebral artery ischemic stroke. *Am J Neuroradiol.* 2010;31(7):1324-1330.

14. Puig J, Blasco G, Daunis-I-Estadella J, *et al.* Decreased corticospinal tract fractional anisotropy predicts long-term motor outcome after stroke. *Stroke*. 2013;44(7):2016-2018.
15. Thomalla G, Glauche V, Koch MA, Beaulieu C, Weiller C, Röther J. Diffusion tensor imaging detects early wallerian degeneration of the pyramidal tract after ischemic stroke. *Neuroimage*. 2004;22(4):1767-1774.
16. Doughty C, Wang J, Feng W, Hackney D, Pani E, Schlaug G. Detection and predictive value of fractional anisotropy changes of the corticospinal tract in the acute phase of a stroke. *Stroke*. 2016;47(6):1520-1526.
17. Borich MR, Mang C, Boyd LA. Both projection and commissural pathways are disrupted in individuals with chronic stroke: Investigating microstructural white matter correlates of motor recovery. *BMC Neurosci*. 2012;13(1):107.
18. Puig J, Pedraza S, Blasco G, *et al.* Acute damage to the posterior limb of the internal capsule on diffusion tensor tractography as an early imaging predictor of motor outcome after stroke. *Am J Neuroradiol*. 2011;32(5):857-863.
19. Borich MR, Brown KE, Boyd LA. Motor skill learning is associated with diffusion characteristics of white matter in individuals with chronic stroke. *J Neurol Phys Ther*. 2014;38(3):151-160.
20. Kelley S, Plass J, Bender AR, Polk TA. Age-Related differences in white matter: Understanding tensor-based results using fixel-based analysis. *Cereb Cortex*. 2021;31(8):3881-3898.
21. Salat DH, Tuch DS, Greve DN, *et al.* Age-related alterations in white matter microstructure measured by diffusion tensor imaging. *Neurobiol Aging*. 2005;26(8):1215-1227.
22. Hsu JL, Leemans A, Bai CH, *et al.* Gender differences and age-related white matter changes of the human brain: A diffusion tensor imaging study. *Neuroimage*. 2008;39(2):566-577.
23. Schaechter JD, Perdue KL, Wang R. Structural damage to the corticospinal tract correlates with bilateral sensorimotor cortex reorganization in stroke patients. *Neuroimage*. 2008;39(3):1370-1382.
24. Owen M, Ingo C, Dewald JPA. Upper extremity motor impairments and microstructural changes in bulbospinal pathways in chronic hemiparetic stroke. *Front Neurol*. 2017;8(JUN):1-10.
25. McPherson JG, Chen A, Ellis MD, Yao J, Heckman CJ, Dewald JPA. Progressive recruitment of contralateral cortico-reticulospinal pathways drives motor impairment post stroke. *J Physiol*. 2018;596(7):1211-1225.
26. Takenobu Y, Hayashi T, Moriwaki H, Nagatsuka K, Naritomi H, Fukuyama H. Motor recovery and microstructural change in rubro-spinal tract in subcortical stroke. *NeuroImage Clin*. 2014;4:201-208.
27. Karbasforoushan H, Cohen-Adad J, Dewald JPA. Brainstem and spinal cord MRI identifies altered sensorimotor pathways post-stroke. *Nat Commun*. 2019;10(1):3524.
28. Ruber T, Schlaug G, Lindenberg R. Compensatory role of the cortico-rubro-spinal tract in motor recovery after stroke. *Neurology*. 2012;79(6):515-522.
29. Guo J, Liu J, Wang C, *et al.* Differential involvement of rubral branches in chronic capsular and pontine stroke. *NeuroImage Clin*. 2019;24(154):102090.
30. Lindenberg R, Zhu LL, Rüber T, Schlaug G. Predicting functional motor potential in chronic stroke patients using diffusion tensor imaging. *Hum Brain Mapp*. 2012;33(5):1040-1051.
31. Schulz R, Park E, Lee J, *et al.* Synergistic but independent: The role of corticospinal and alternate motor fibers for residual motor output after stroke. *NeuroImage Clin*. 2017;15(April):118-124.
32. Di Pino G, Pellegrino G, Assenza G, *et al.* Modulation of brain plasticity in stroke: A novel model for neurorehabilitation. *Nat Rev Neurol*. 2014;10(10):597-608.
33. Wedeen VJ, Hagmann P, Tseng WYI, Reese TG, Weisskoff RM. Mapping complex tissue architecture with diffusion spectrum magnetic resonance imaging. *Magn Reson Med*. 2005;54(6):1377-1386.
34. Tan ET, Marinelli L, Sperl JI, Menzel MI, Hardy CJ. Multi-directional anisotropy from diffusion orientation distribution functions. *J Magn Reson Imaging*. 2015;41(3):841-850.
35. Demeurisse G, Demol O, Robaye E. Motor evaluation in vascular hemiplegia. *Eur Neurol*. 1980;19(6):382-389.
36. Lyle RC. A performance test for assessment of upper limb function in physical rehabilitation treatment and research. *Int J Rehabil Res*. 1981;4(4):483-492.
37. Collin C, Wade D. Assessing motor impairment after stroke: A pilot reliability study. *J Neurol Neurosurg Psychiatry*. 1990;53(7):576-579.
38. Hsieh CL, Hsueh IP, Chiang FM, Lin PH. Inter-rater reliability and validity of the action research arm test in stroke patients. *Age Ageing*. 1998;27(2):107-113.
39. Nijland R, van Wegen E, Verbunt J, van Wijk R, van Kordelaar J, Kwakkel G. A comparison of two validated tests for upper limb function after stroke: The wolf motor function test and the action research arm test. *J Rehabil Med*. 2010;42(7):694-696.
40. Cieslak M, Cook PA, He X, *et al.* QSIPrep: An integrative platform for preprocessing and reconstructing diffusion MRI data. *Nat Methods*. 2021;18(7):775-778.
41. Gorgolewski K, Burns CD, Madison C, *et al.* Nipype: A flexible, lightweight and extensible neuroimaging data processing framework in python. *Front Neuroinform*. 2011;5(August):1-15.
42. Tustison NJ, Avants BB, Cook PA, *et al.* N4ITK: Improved N3 bias correction. *IEEE Trans Med Imaging*. 2010;29(6):1310-1320.
43. Fonov V, Evans A, McKinstry R, Almli C, Collins D. Unbiased non-linear average age-appropriate brain templates from birth to adulthood. *Neuroimage*. 2009;47:S102.
44. Avants BB, Epstein CL, Grossman M, Gee JC. Symmetric diffeomorphic image registration with cross-correlation: Evaluating automated labeling of elderly and neurodegenerative brain. *Med Image Anal*. 2008;12(1):26-41.
45. Zhang Y, Brady M, Smith S. Segmentation of brain MR images through a hidden markov random field model and the expectation-maximization algorithm. *IEEE Trans Med Imaging*. 2001;20(1):45-57.
46. Veraart J, Novikov DS, Christiaens D, Ades-aron B, Sijbers J, Fieremans E. Denoising of diffusion MRI using random matrix theory. *Neuroimage*. 2016;142(1):394-406.
47. Merlet SL, Deriche R. Continuous diffusion signal, EAP and ODF estimation via compressive sensing in diffusion MRI. *Med Image Anal*. 2013;17(5):556-572.
48. Yeh FC, Wedeen VJ, Tseng WYI. Generalized q-sampling imaging. *IEEE Trans Med Imaging*. 2010;29(9):1626-1635.
49. Yeh FC, Panesar S, Fernandes D, *et al.* Population-averaged atlas of the macroscale human structural connectome and its network topology. *Neuroimage*. 2018;178(April):57-68.
50. Volz LJ, Sarfeld AS, Diekhoff S, *et al.* Motor cortex excitability and connectivity in chronic stroke: A multimodal model of functional reorganization. *Brain Struct Funct*. 2015;220(2):1093-1107.
51. Grefkes C, Nowak DA, Eickhoff SB, *et al.* Cortical connectivity after subcortical stroke assessed with functional magnetic resonance imaging. *Ann Neurol*. 2008;63(2):236-246.
52. Rehme AK, Eickhoff SB, Wang LE, Fink GR, Grefkes C. Dynamic causal modeling of cortical activity from the acute to the chronic stage after stroke. *Neuroimage*. 2011;55(3):1147-1158.
53. Stinear CM, Barber PA, Smale PR, Coxon JP, Fleming MK, Byblow WD. Functional potential in chronic stroke patients depends on corticospinal tract integrity. *Brain*. 2006;130(Pt 1):170-180.
54. Schulz R, Koch P, Zimmerman M, *et al.* Parietofrontal motor pathways and their association with motor function after stroke. *Brain*. 2015;138(7):1949-1960.
55. Guggisberg AG, Nicolo P, Cohen LG, Schnider A, Buch ER. Longitudinal structural and functional differences between proportional and poor motor recovery after stroke. *Neurorehabil Neural Repair*. 2017;31(12):1029-1041.

56. Choudhury S, Shobhana A, Singh R, et al. The relationship between enhanced reticulospinal outflow and upper limb function in chronic stroke patients. *Neurorehabil Neural Repair*. 2019; 33(5):375-383.
57. Glover IS, Baker SN. Both corticospinal and reticulospinal tracts control force of contraction. *J Neurosci*. 2022;42(15): 3150-3164.
58. Krakauer JW, Carmichael ST. *Broken movement*. The MIT Press; 2017.
59. Bohannon RW. Motricity Index scores are valid indicators of paretic upper extremity strength following stroke. *J Phys Ther Sci*. 1999; 11(2):59-61.
60. Sunderland A, Tinson D, Bradley L, Hewer RL. Arm function after stroke. An evaluation of grip strength as a measure of recovery and a prognostic indicator. *J Neurol Neurosurg Psychiatry*. 1989;52(11): 1267-1272.
61. Keizer K, Kuypers HGJM. Distribution of corticospinal neurons with collaterals to the lower brain stem reticular formation in monkey (macaca fascicularis). *Exp Brain Res*. 1989;74(2): 311-318.
62. Sakai ST, Davidson AG, Buford JA. Reticulospinal neurons in the pontomedullary reticular formation of the monkey (macaca fascicularis). *Neuroscience*. 2009;163(4):1158-1170.
63. Snell RS. *Clinical neuroanatomy*. 7th ed.: Lippincott Williams & Wilkins; 2010.
64. Jankowska E, Edgley SA. How can corticospinal tract neurons contribute to ipsilateral movements? A question with implications for recovery of motor functions. *Neurosci*. 2006;12(1):67-79.
65. Siegel JM, McGinty DJ. Pontine reticular formation neurons: Relationship of discharge to motor activity. *Science (80-)*. 1977; 196(4290):678-680.
66. Schulz R, Frey BM, Koch P, et al. Cortico-Cerebellar structural connectivity is related to residual motor output in chronic stroke. *Cereb Cortex*. 2017;27(1):635-645.
67. Guder S, Frey BM, Backhaus W, et al. The influence of cortico-cerebellar structural connectivity on cortical excitability in chronic stroke. *Cereb Cortex*. 2020;30(3):1330-1344.
68. Soulard J, Huber C, Baillieux S, et al. Motor tract integrity predicts walking recovery. *Neurology*. 2020;94(6):e583-e593.
69. Koch PJ, Park CH, Girard G, et al. The structural connectome and motor recovery after stroke: Predicting natural recovery. *Brain*. 2021;144(7):2107-2119.
70. Grefkes C, Ward NS. Cortical reorganization after stroke. *Neuroscientist*. 2014;20(1):56-70.
71. Volz LJ, Rehme AK, Michely J, et al. Shaping early reorganization of neural networks promotes motor function after stroke. *Cereb Cortex*. 2016;26(6):2882-2894.
72. Park C hyun H, Chang WH, Ohn SH, et al. Longitudinal changes of resting-state functional connectivity during motor recovery after stroke. *Stroke*. 2011;42(5):1357-1362.
73. Carter AR, Astafiev S V, Lang CE, et al. Resting state inter-hemispheric fMRI connectivity predicts performance after stroke. *Ann Neurol*. 2009;67(3):365-375.
74. Paul T, Hensel L, Rehme AK, et al. Early motor network connectivity after stroke: An interplay of general reorganization and state-specific compensation. *Hum Brain Mapp*. 2021;42(16):5230-5243.

Supplement

Supplementary Tables

Supplementary Table 1: Patient demographics. Our patient cohort comprised 12 fully recovered and 13 non-fully recovered patients as determined by the ARAT-score (fully recovered = 57 points, non-fully recovered < 57 points).

<i>subject</i>	<i>sex</i>	<i>affected hemisphere</i>	<i>ARAT</i>	<i>MI-arm</i>	<i>MI-leg</i>
1	m	l	19	65	59
2	f	r	57	83	83
3	m	r	38	76	75
4	f	r	56	91	75
5	m	l	57	99	91
6	m	l	35	92	99
7	f	l	32	77	83
8	f	r	57	76	75
9	m	r	49	91	99
10	f	l	56	76	75
11	m	r	57	91	99
12	m	l	57	99	99
13	m	l	55	92	91
14	m	r	57	99	99
15	m	r	57	99	99
16	m	r	53	99	99
17	m	l	55	92	99
18	m	l	44	83	75
19	m	r	37	84	75
20	m	l	57	99	99
21	m	l	57	99	99
22	m	l	0	34	34
23	m	r	57	99	71
24	m	l	57	99	99
25	m	r	57	99	99

Supplementary Table 2: Comparison of compartmentwise and ROI-based approaches. The first column depicts results when using one-directional voxels from the entire length of the CST. This is contrasted by two conventional ROI-based approaches using either the section from the mesencephalon to the cerebral peduncle (CP; z-level -25 to -20) or the posterior limb of the internal capsule (PLIC; z-level -5 to 20).

one-directional CST voxels			mesencephalon to CP			PLIC		
DV	R2	p(FDR)	DV	R2	p(FDR)	DV	R2	p(FDR)
ARAT	0.309	0.006	ARAT	0.081	0.500	ARAT	0.339	0.007
MI-arm	0.319	0.010	MI-arm	0.017	0.800	MI-arm	0.187	0.046
MI-leg	0.177	0.036	MI-leg	0.003	0.789	MI-leg	0.044	0.313

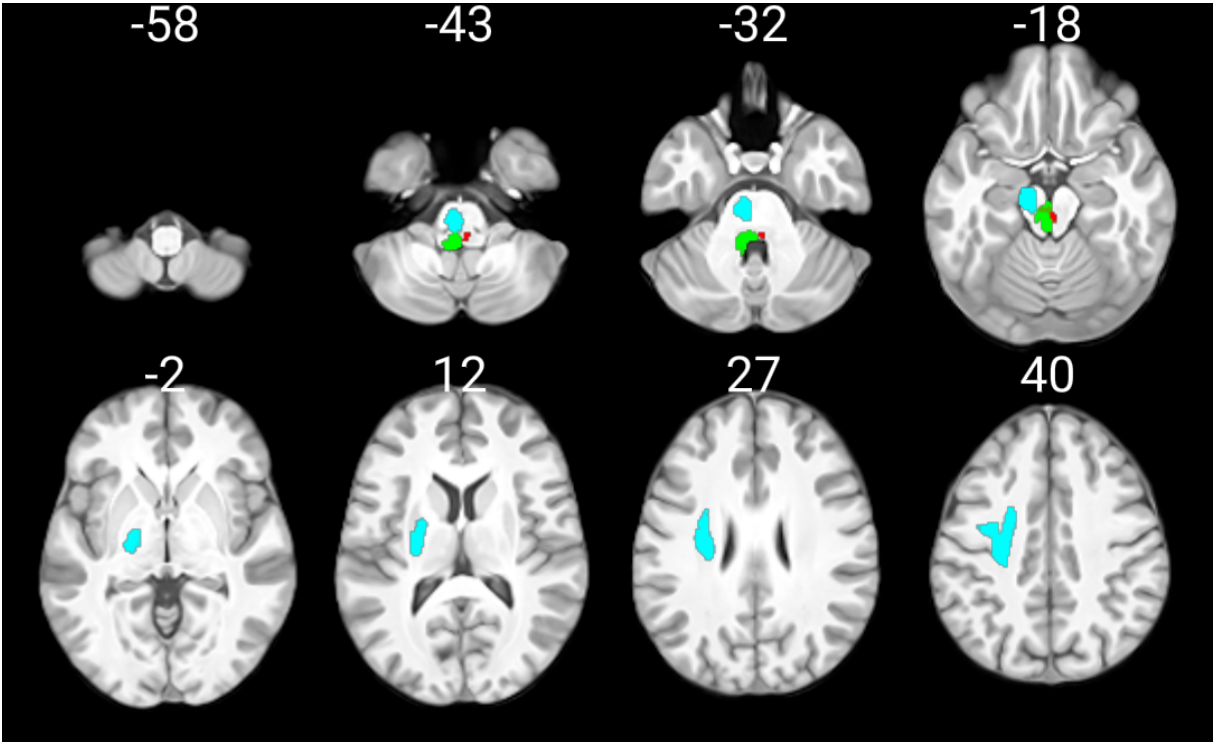
Supplementary Table 3: Overview of regression results. Behavioral variance in motor impairment is explained by compartment-wise anisotropy from descending motor tracts. Bold font indicates significance after FDR-correction.

all voxels				one-directional voxels				two-directional voxels			
DV	predictor	R2	p (FDR)	DV	predictor	R2	p (FDR)	DV	predictor	R2	p (FDR)
ARAT	il CST	0.346	0.006	ARAT	il CST	0.309	0.006	ARAT	il CST	0.126	0.243
MI-arm	il CST	0.289	0.008	MI-arm	il CST	0.319	0.010	MI-arm	il CST	0.059	0.364
MI-leg	il CST	0.152	0.054	MI-leg	il CST	0.177	0.036	MI-leg	il CST	0.010	0.638
ARAT	CST asym	0.366	0.004	ARAT	CST asym	0.341	0.007	ARAT	CST asym	0.141	0.193
MI-arm	CST asym	0.281	0.010	MI-arm	CST asym	0.318	0.005	MI-arm	CST asym	0.056	0.380
MI-leg	CST asym	0.112	0.102	MI-leg	CST asym	0.160	0.048	MI-leg	CST asym	0.000	0.925
ARAT	cl CST	0.000	0.956	ARAT	cl CST	0.001	0.892	ARAT	cl CST	0.006	0.890
ARAT	il RST	0.004	1.293	ARAT	il RST	0.002	1.054	ARAT	il RST	0.011	1.533
ARAT	cl RST	0.000	1.188	ARAT	cl RST	0.003	1.307	ARAT	cl RST	0.007	1.147
ARAT	cl rubroST	0.086	0.776	ARAT	cl rubroST	0.074	0.941	ARAT	cl rubroST	0.091	0.719
ARAT	il rubroST	0.005	1.852	ARAT	il rubroST	0.012	1.522	ARAT	il rubroST	0.001	0.871
MI-arm	cl CST	0.000	0.939	MI-arm	cl CST	0.000	0.936	MI-arm	cl CST	0.004	0.752
MI-arm	il RST	0.083	0.407	MI-arm	il RST	0.071	0.494	MI-arm	il RST	0.090	0.240
MI-arm	cl RST	0.055	0.432	MI-arm	cl RST	0.033	0.638	MI-arm	cl RST	0.124	0.211
MI-arm	cl rubroST	0.222	0.087	MI-arm	cl rubroST	0.184	0.161	MI-arm	cl rubroST	0.259	0.047
MI-arm	il rubroST	0.029	0.522	MI-arm	il rubroST	0.014	0.709	MI-arm	il rubroST	0.071	0.248
MI-leg	cl CST	0.008	0.676	MI-leg	cl CST	0.003	0.792	MI-leg	cl CST	0.011	0.616
MI-leg	il RST	0.133	0.121	MI-leg	il RST	0.100	0.205	MI-leg	il RST	0.191	0.036
MI-leg	cl RST	0.148	0.144	MI-leg	cl RST	0.123	0.215	MI-leg	cl RST	0.218	0.046
MI-leg	cl rubroST	0.176	0.184	MI-leg	cl rubroST	0.130	0.384	MI-leg	cl rubroST	0.274	0.036
MI-leg	il rubroST	0.133	0.092	MI-leg	il rubroST	0.088	0.187	MI-leg	il rubroST	0.218	0.031

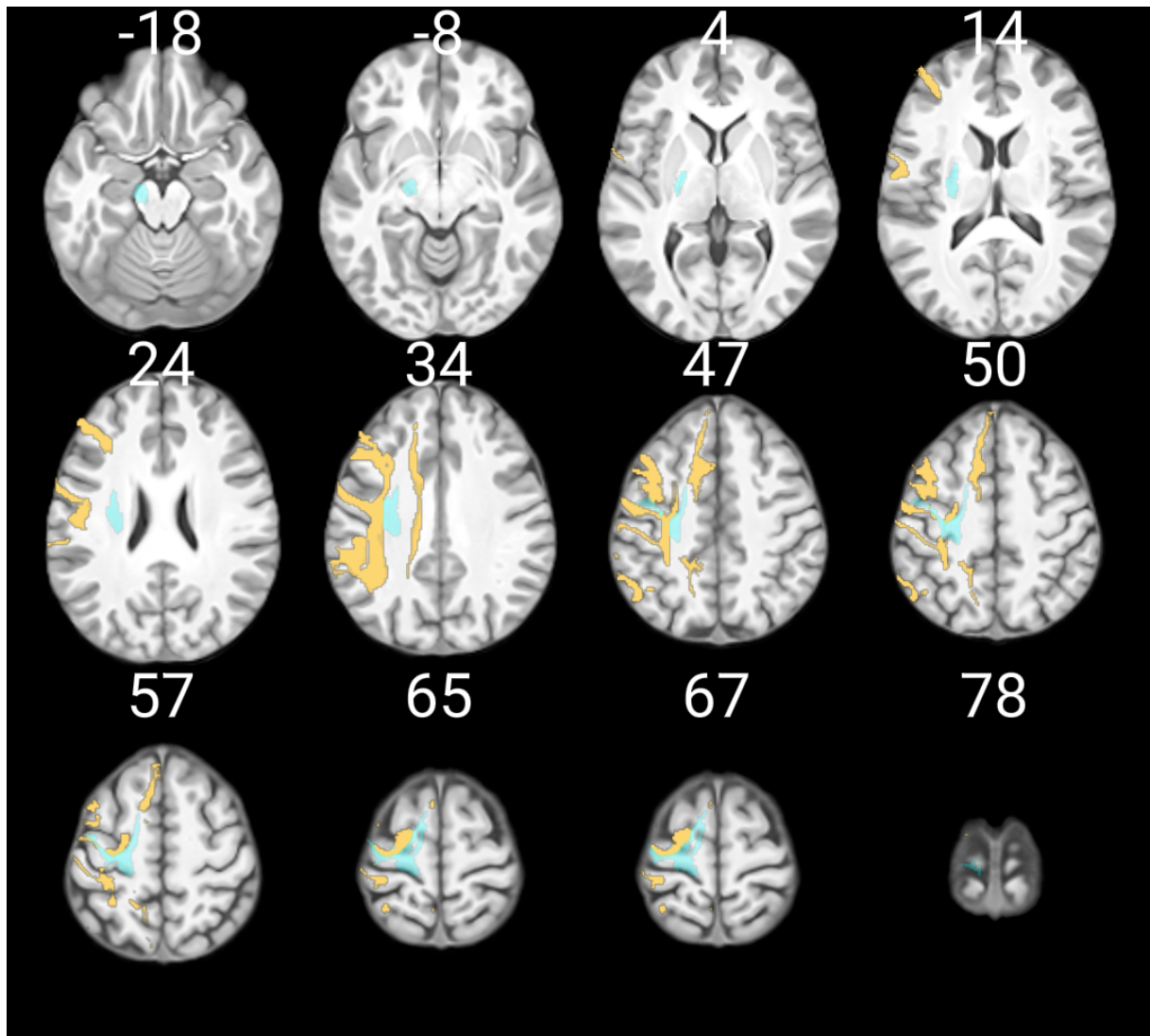
Supplementary Table 4: Linear regression results when combining gFA derived from one-directional voxels of the ipsilesional CST with gFA derived from two-directional extrapyramidal voxels. The results suggest that ipsilesional CST and extrapyramidal tracts were largely independent with respect to the explanation of behavioral variance in motor impairment. (*il = ipsilesional, cl = contralesional, CST = corticospinal tract, reticuloST = reticulospinal tract, rubroST = rubrospinal tract*)

DV	predictor 1	R ²	p	predictor 2	R ²	p
MI-arm	il CST	31.94%	0.003	cl rubroSt	51.02%	0.0004
MI-leg	il CST	17.71%	0.036	il reticuloST	38.86%	0.0045
MI-leg	il CST	17.71%	0.036	cl reticuloST	39.61%	0.0039
MI-leg	il CST	17.71%	0.036	il rubroST	38.94%	0.0044
MI-leg	il CST	17.71%	0.036	cl rubroST	39.85%	0.0037

Supplementary Figures

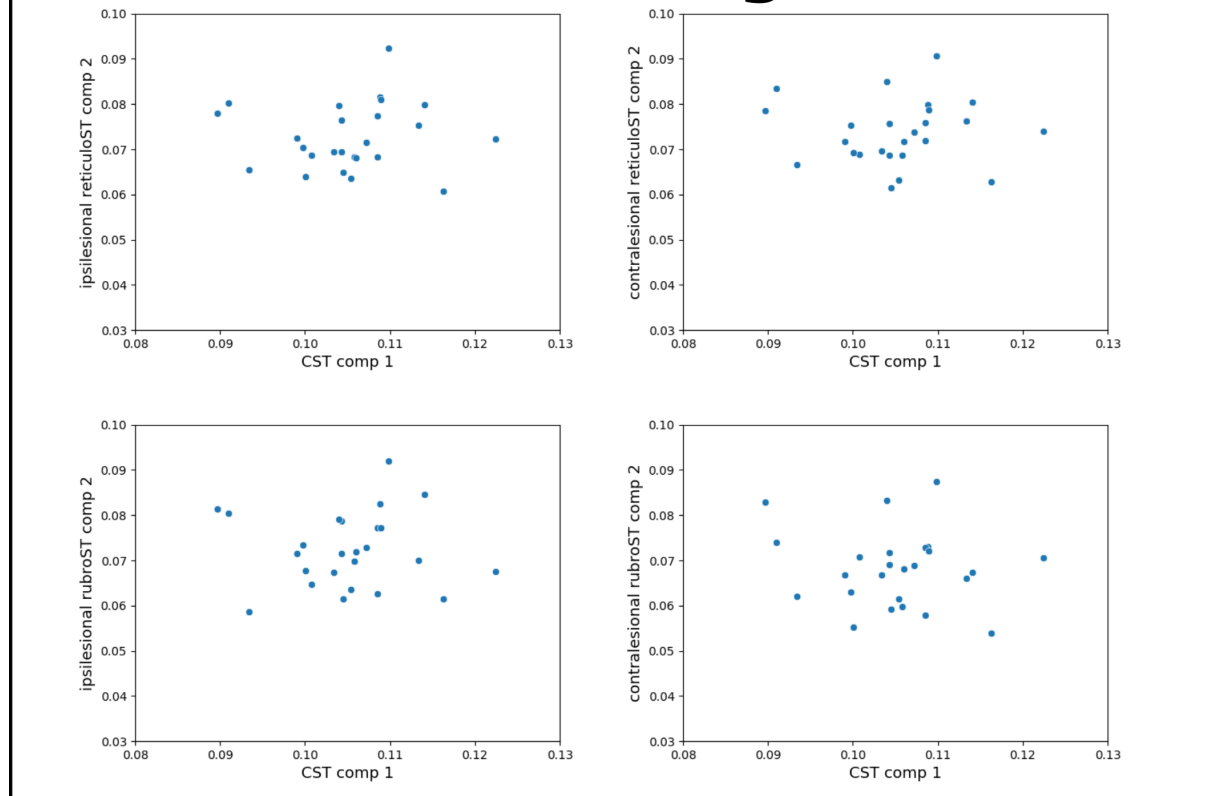


Supplementary Figure 1: Slicewise depiction of motor tracts descending from the left hemisphere. (*blue = corticospinal tract, green = reticulospinal tract, red = rubrospinal tract*)



Supplementary Figure 2: Slicewise depiction of superior longitudinal fasciculus (SLF, yellow) and corticospinal tract (CST, blue). To exclude a possible bias of our findings introduced by accidentally sampling SLF voxels when extracting gFA from the CST, axial slices were assessed for a potential overlap of both tracts. As depicted in this figure, there was no considerable overlap between both tracts.

Tractwise gFA



Supplementary Figure 3: Scatter plots of mean gFA derived from compartment 1 of the ipsilesional CST and compartment 2 of extrapyramidal tracts. The scatter plots indicate no correlation between those variables, ruling out multicollinearity between predictor variables as a potential bias that might hinder the interpretation of multiple linear regression models.

5.2. Corticospinal premotor fibers facilitate complex motor control after stroke

Theresa Paul, Matthew Cieslak, Lukas Hensel, Valerie M. Wiemer,
Caroline Tscherpel, Christian Grefkes, Scott T. Grafton,
Gereon R. Fink, Lukas J. Volz

Submitted

Corticospinal premotor fibers facilitate complex motor control after stroke

Theresa Paul, MSc¹, Matthew Cieslak, PhD², Lukas Hensel, MD¹, Valerie M. Wiemer, MSc¹, Caroline Tscherpel, MD¹, Christian Grefkes, MD^{1,3}, Scott T. Grafton, MD⁴, Gereon R. Fink, MD^{1,3}, Lukas J. Volz, MD¹

¹ Department of Neurology, University Hospital Cologne, Cologne, Germany

² Department of Psychiatry, Perelman School of Medicine, University of Pennsylvania, Philadelphia, PA, USA

³ Institute of Neuroscience and Medicine, Cognitive Neuroscience (INM-3), Research Centre Juelich, Juelich, Germany

⁴ Department of Psychological & Brain Sciences, University of California, Santa Barbara, CA, USA

Corresponding author:

Lukas J. Volz, M.D.

Department of Neurology, University of Cologne,

Kerpener Str. 62, 50937 Cologne, Germany

Email: Lukas.Volz@uk-koeln.de

Short title: Role of CST subtracts after motor stroke

Keywords: Diffusion spectrum imaging, corticospinal tract, motor recovery, structural connectivity, anisotropy

Abstract

Background and Objectives: The corticospinal tract (CST) is considered the most important motor output pathway comprising fibers from the primary motor cortex (M1) and various premotor areas. Damage to its descending fibers after stroke commonly leads to motor impairment. While premotor areas are thought to critically support motor recovery after stroke, the functional role of their corticospinal output for different aspects of post-stroke motor control remains poorly understood.

Methods: We assessed the differential role of CST fibers originating from premotor areas and M1 in the control of basal and complex motor skills using a novel diffusion imaging approach in chronic stroke patients.

Results: We observed a clear dissociation between the control of basal motor performance and more complex motor skills: While M1 subtract anisotropy was positively correlated with basal and complex motor skills, anisotropy of PMd, PMv, and SMA subtracts was exclusively associated with complex motor tasks. Interestingly, patients featuring persistent motor deficits additionally showed a positive association between premotor subtract integrity and basal motor control.

Discussion: While descending M1 output seems to be a prerequisite for any form of upper limb movements, complex motor skills critically depend on output from premotor areas after stroke. In severely affected patients, descending signals from premotor areas may also serve to flexibly compensate for the impairment of basal motor functions. In summary, our findings highlight the pivotal role of descending corticospinal output from premotor areas for motor control post-stroke which thus serve as prime candidates for future interventions to amplify motor recovery.

Introduction

Motor impairment after stroke is commonly caused by damage to the corticospinal tract (CST),¹ which comprises descending fibers originating from the primary motor cortex (M1) as well as various premotor areas.^{2,3} While the increased involvement of premotor regions in motor control after stroke is well-established,^{4,5,6} the functional role of CST projections from premotor areas remains largely unclear. Considering that premotor areas contribute a substantial amount of CST fibers descending to the spinal level,⁷ these premotor fibers seem readily situated to facilitate motor control after stroke via descending signals.⁸ Previous studies analyzing CST subtracts originating from premotor areas⁹⁻¹⁷ support this notion yet report inconclusive findings regarding the differential involvement of distinct tracts emerging from ventral and dorsal premotor areas (PMv, PMd) as well as supplementary motor area (SMA). Possible explanations for this inconsistency lie in the differing ways in which tract integrity was quantified and in differing assessments of motor performance across studies. Of note, most studies relied on CST lesion overlaps rather than diffusion MRI (dMRI) to quantify tract integrity.^{9,11,13-17} This systematically overestimates tract integrity by precluding the analysis of secondary degeneration of axons passing through the lesion, i.e., *Wallerian degeneration*.^{1,18} Moreover, the limited number of dMRI studies have focused on selective parts of the CST rather than assessing anisotropy along the entire length of each CST subtract.^{10,12} Thus, it remains unknown whether corticospinal output from distinct premotor areas and M1 differentially contributes to aspects of basal and complex motor control after stroke.

From an anatomical perspective, tracer studies in macaque monkeys suggest that each premotor area holds a unique efferent system facilitating distinct aspects of hand and arm motor control.¹⁹ Thus, the functional roles of descending fibers are likely tied to the functional specialization of each premotor area: The SMA is thought to support the execution of sequential movements²⁰ as well as the timing^{21,22} and initiation of upper limb movements.²³ Conversely, the PMv and PMd are essential for reaching and grasping movements.^{24,25} Thus, one might expect that the compensatory potential arises from a regions functional specialization which would predestine premotor areas to support complex hand movements after stroke. Alternatively, premotor areas might more flexibly support different aspects of motor control depending on the stroke-induced impairment allowing them to contribute to a wide range of movements outside their physiological repertoires including basal muscle activation.

To address these questions, we captured the functional specificity of primary and premotor areas in post-stroke reorganization using a battery of standardized tests to differentiate basal

and complex motor skills of the upper limb. The integrity of CST subtracts originating from M1 and premotor areas (PMv, PMd, and SMA) was quantified by means of anisotropy extracted from the entire length of each subtract in chronic stroke patients. We hypothesized that CST fibers emerging from M1 are sufficient to carry out basal motor functions. In contrast, more elaborate motor skills of the paretic hand likely rely on an interplay of descending signals from M1 and premotor areas, in particular PMv and PMd, given their pivotal role in carrying out reaching and grasping movements in healthy individuals.

Methods

Sample

Twenty-five chronic stroke patients (20 male, 5 female, mean age=66.68, std=11.25) formerly hospitalized at the University Hospital Cologne, Department of Neurology and 22 healthy age-matched controls (16 male, 6 female, mean age=67.05, std=6.59) were included (Supplementary Table 1). Inclusion criteria were (1) first-ever ischemic stroke at least six months earlier, (2) unilateral hand motor deficit in the acute post-stroke phase, and (3) age 40 to 90 years. Exclusion criteria were (1) contraindications to MRI, (2) cerebral hemorrhage, (3) bihemispheric infarct lesions, (4) re-infarct or other preexisting neurological diseases, as well as (5) severe aphasia or neglect. All participants provided informed written consent. The study was approved by the ethics committee of the Medical Faculty at the University of Cologne and carried out in accordance with the declaration of Helsinki. The current patient cohort was included in a previous publication on the differential role of descending and crossing fibers in the corticospinal and extrapyramidal system in ageing and after stroke.¹⁸ Of note, all analyses presented in the present study are novel and there is no overlap with this previous publication.

Behavioral testing

While isolated movements involving only a limited amount of muscle groups do not require complex interjoint coordination, more complex forms of motor control, e.g., involving object manipulation impose higher demands on the human motor system as they require the integration of several motor synergies and offer multiple degrees of freedom.²⁶ Thus, compensatory strategies employed by the stroke-afflicted motor system likely vary depending on the level of movement complexity. Unlike previous studies that only focused on one aspect of motor

control, we therefore differentially assessed basal and complex motor control in the present study. Complex motor performance representing activities of daily living was assessed through the Action Research Arm Test (ARAT) comprising the subscales grasp, grip, pinch, and gross movements.²⁷ The test involves tasks such as picking up wooden blocks, pouring water from one glass to another or lifting up small objects using a pinch grip. Thus, successful execution requires the interplay of various motor control policies. Conversely, basal movements were evaluated using the motricity index (MI)²⁸ which assesses the ability to execute an isolated movement against gravity or resistance, thereby testing simple synergies and muscle strength. The upper limb scale includes the items shoulder abduction, elbow flexion, and pinch grip. Thus, the MI evaluates the execution of individual motor primitives rather than complex motor skills. Importantly, while both scales include the item pinch grip, the level of complexity varies: While the MI assesses pinch grip as an isolated movement, the ARAT requires participants to manipulate small marbles, thereby probing pinch grip in the form of a goal-directed object manipulation.

Tract characteristics

Another major limitation of previous studies on premotor CST fibers pertains to the quantification of tract damage. Many of the previous studies used their own templates for the quantification of lesion overlap or extraction of anisotropy, which oftentimes resulted in a considerable tract overlap of up to 80%.⁹ The only study relying on externally validated tract templates used binarized lesion information rather than dMRI and was therefore not able to capture Wallerian degeneration.¹⁴ To increase generalizability and validity, we based our analyses on tract templates that were developed and validated by an independent research group using an independent dataset (Figure 1).²⁹ The dataset included corticospinal subtracts emerging from M1, PMd, PMv, and SMA, as well as two sensorimotor tracts descending from the prefrontal area preSMA and the primary somatosensory cortex (S1). We included these additional tracts as ‘negative’ controls as they feature projections in close proximity to the CST without generating descending motor signals.

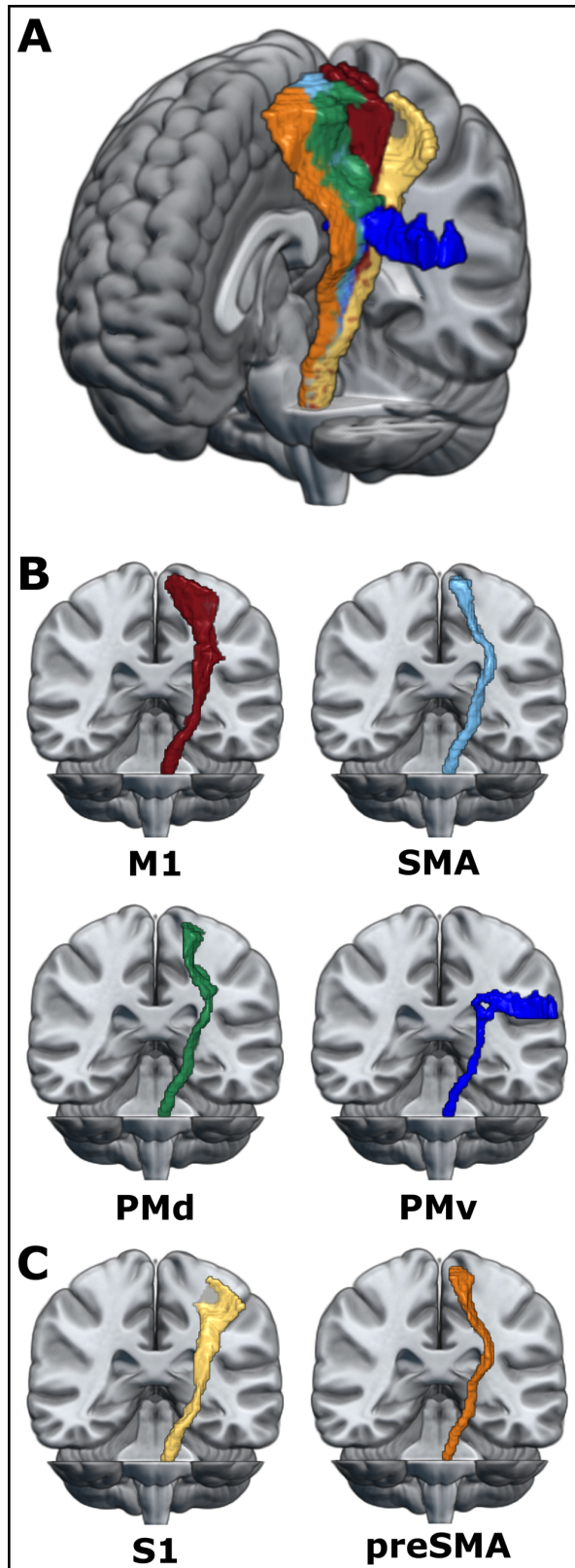


Figure 1: Overview of sensorimotor tracts. (A) Overview of all six sensorimotor tracts as defined in the sensorimotor area tract template (SMATT).²⁹ (B) Individual CST subtracts according to their cortical origin. (C) Additional sensorimotor tracts. Images were created in MRICroGL.³⁰ *MI* = primary motor cortex, *SMA* = supplementary motor area, *PMd* = dorsal premotor cortex, *PMv* = ventral premotor cortex, *S1* = primary somatosensory cortex

Acquisition and preparation of MRI data

Diffusion spectrum imaging (DSI), T1-weighted, and T2-weighted data were recorded using a Siemens MAGNETOM Prisma 3 Tesla scanner equipped with a 64-channel head coil (Siemens Medical Solutions, Erlangen, Germany). Image acquisition, the preprocessing workflow including motion and distortion correction in QSIPrep,³¹ and creation of individual gFA-maps were performed as described in detail elsewhere.¹⁸ Each patient's gFA-map was normalized to the ICBM 152 Nonlinear Asymmetrical template version 2009c³² using ANTs.³³ To focus all subsequent analyses on Wallerian degeneration of descending fibers,¹⁸ we applied the following masks to each subject's gFA-map: (i) Individual white matter (WM)-masks were used to limit the analysis to WM. (ii) Lesion masks drawn on T2-weighted images using MRICron were applied to focus on secondary degeneration by eliminating the impact of the lesion itself. (iii) To focus the analyses on descending fibers WM voxels were compartmentalized according to the number of trackable directions per voxel,³⁴ retaining only voxels with exactly one trackable direction for further analyses. CST-masks were taken from the sensorimotor area tract template (SMATT), which consists of high-resolution nifti-images of different sensorimotor tracts originating from six different cortical regions, namely M1, S1, PMv, PMd, SMA, and preSMA²⁹ (Figure 1). To match image dimensions of the gFA-maps, masks were coregistered to the underlying 1.25x1.25x1.25 mm³ MNI-template.

Tractwise correlations with motor performance

For each subject and tract, mean gFA-values were derived from all one-directional voxels (representing descending motor fibers¹⁸). Correlations were computed between the resulting tractwise values and ARAT scores as well as MI-arm scores. We further tested for correlations with the four ARAT subscales for tracts showing a significant relationship with the overall ARAT score to specify aspects of motor behavior supported by the given subtracts. To assess whether premotor subtracts also contributed to basal motor control in patients with persistent motor deficits (N=13), we tested for correlations between MI-arm scores and anisotropy of subtracts showing a significant association with the ARAT. The persistence of motor deficits was defined as an ARAT score of less than the maximum score of 57 points.²⁷ For each analysis, p-values were FDR-corrected to account for the number of comparisons. To address whether subtracts emerging from premotor areas explained behavioral variance independent from M1, we computed partial correlations between behavioral scores and premotor subtracts while

controlling for the influence of the M1 subtract. Similarly, we also computed partial correlations to assess the impact of premotor subtract integrity on the correlation between M1 subtract anisotropy and motor behavior.

Slicewise analyses along each tract

Previous research has commonly calculated CST anisotropy for pre-defined ROIs containing densely packed descending fibers.³⁵⁻³⁷ While these ROIs are thought to closely reflect Wallerian degeneration,³⁵ using voxels from the entire length of the CST has recently been shown to be better suited to predict motor behavior.¹⁸ Therefore, a compartmentwise approach was employed that utilizes voxels from the entire length of the CST. As upper CST sections might be influenced by other reorganization processes such as cortical remapping and axonal sprouting, slicewise correlation analyses were performed to assess which sections of each subtract drove the observed correlations between anisotropy and motor behavior. Thus, tract-specific mean gFA was computed per z-slice along the entire tract length based on one-directional voxels and subsequently correlated with ARAT and MI-arm scores.

Data availability statement

Data are available from the corresponding author upon reasonable request.

Results

Characterization of CST subtracts

According to a repeated-measures ANOVA with the factor tract (levels: M1, SMA, PMd, PMv, preSMA, S1), lesion load (i.e., the percentage of tract voxels affected by the lesion) did not differ significantly between tracts ($F(2.32,55.56)=0.76$, $p=.488$). Accordingly, all subtracts were affected to a similar degree across the group. For a tractwise lesion overlap of the descending motor subtracts, please see Figure 2.

To test whether lesions resulted in systematically reduced tractwise anisotropy compared to healthy age-matched controls, we computed a mixed ANOVA with the between factor group

(levels: patients, controls) and the within factor tract (levels: M1, SMA, PMd, PMv, preSMA, S1). Results showed a significant main effect of group ($F(1,45)=9.39, p=.004$, generalized $\eta^2=0.124$) and tract ($F(2.22,99.97)=51.84, p<.001$, generalized $\eta^2=0.270$) but no interaction effect ($F(2.22,99.97)=1.32, p=.270$). Post-hoc t-tests revealed either a significantly lower or a statistical trend towards lower gFA-values in patients compared to controls for all subtracts (all $p<.1$ after FDR-correction for multiple comparison), confirming that anisotropy was systematically reduced in patients. A Greenhouse-Geisser correction was applied where appropriate. In contrast, anisotropy derived from the right superior longitudinal fasciculus (SLF) did not differ between groups ($t(45)= -1.57, p=.124$), indicating that the difference was specific to the affected motor system rather than reflecting systematic differences between groups with regard to factors such as small vessel disease.

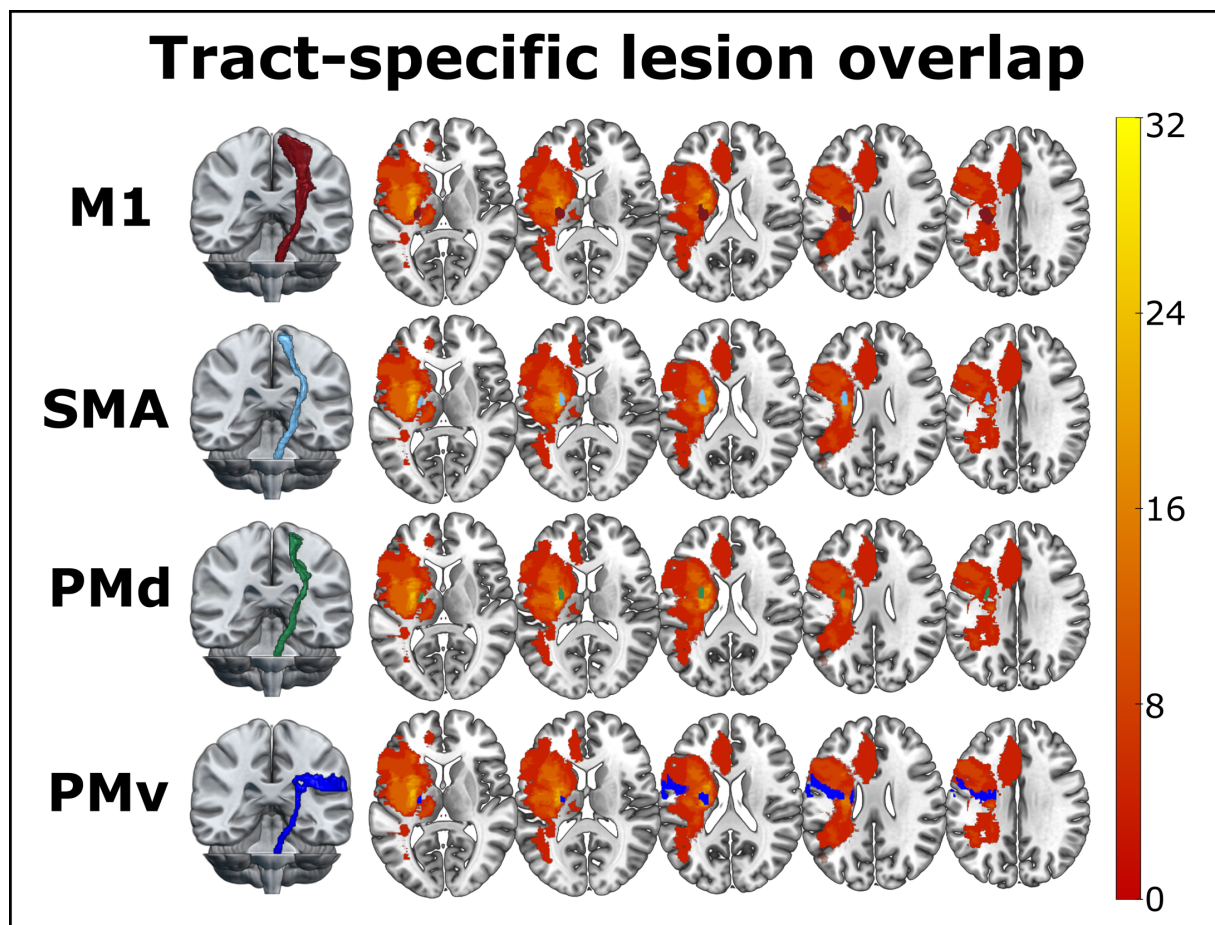


Figure 2: Tract-specific lesion overlap for CST subtracts descending from distinct motor areas. Lesion overlaps are shown for each CST subtract as a percentage across all subjects. The highest lesion overlap was observed in the posterior limb of the internal capsule (PLIC) with 32% of all patients affected.

Tractwise correlations with motor behavior

The MI-arm score was significantly associated with the M1 substract but not with substracts emerging from premotor areas, indicating that the control of individual limb movements was primarily related to M1 output integrity (Table 1). For complex motor skills assessed by the ARAT, we found significant correlations with motor performance for CST substracts originating from M1, PMd, PMv, and SMA. Thus, our results emphasize the importance of these premotor regions for shaping complex arm and hand movements (Table 1, Figure 3). Most substracts also showed significant associations with all ARAT subscales ($p < .05$, FDR-corrected; two tests yielded a p -value of $p = .055$ after FDR-correction, Supplementary Table 2).

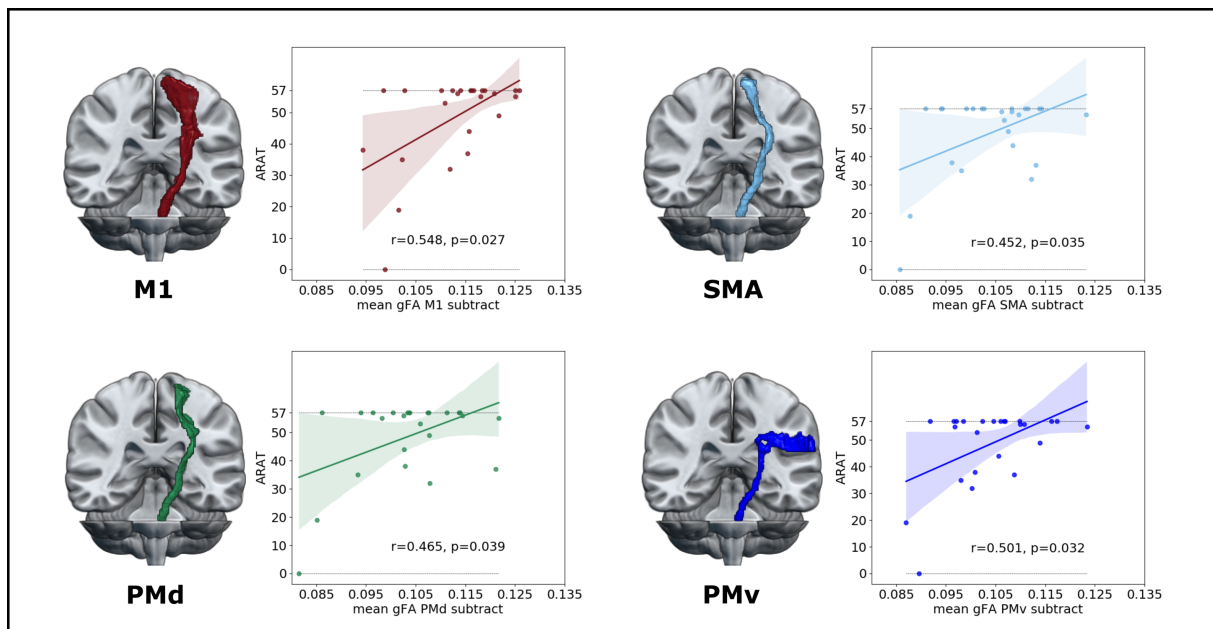


Figure 3: Correlations between anisotropy of CST substracts and complex motor skills. For each CST substract, mean gFA was derived from one-directional voxels along the entire tract length and correlations with the ARAT score were computed. All reported p -values are FDR-corrected for the number of comparisons. *M1* = primary motor cortex, *SMA* = supplementary motor area, *PMd* = dorsal premotor cortex, *PMv* = ventral premotor cortex

Table 1: Tractwise correlations between mean gFA derived from one-directional voxels and motor behavior. Bold font indicates significance after FDR-correction.

DV	predictor	R ²	Pearson r	p	p(FDR)
ARAT	M1	0.300	0.548	0.005	0.027
ARAT	PMd	0.216	0.465	0.019	0.039
ARAT	PMv	0.251	0.501	0.011	0.032
ARAT	S1	0.076	0.276	0.181	0.218
ARAT	SMA	0.204	0.452	0.023	0.035
ARAT	preSMA	0.063	0.250	0.228	0.228
MI-arm	M1	0.316	0.562	0.003	0.021
MI-arm	PMd	0.115	0.340	0.097	0.290
MI-arm	PMv	0.103	0.321	0.118	0.177
MI-arm	S1	0.073	0.271	0.190	0.228
MI-arm	SMA	0.107	0.327	0.111	0.221
MI-arm	preSMA	0.014	0.116	0.580	0.580

In contrast, patients suffering from persistent motor deficits also featured significant correlations between the MI-arm score and anisotropy of premotor subtracts, suggesting a contribution of premotor areas to basal motor performance exclusively in patients with persistent motor deficits (Table 2).

Table 2: Results for patients with persistent motor deficits. Tractwise correlations between mean gFA derived from one-directional voxels and motor behavior for each CST subtract. Bold font indicates significance after FDR-correction.

DV	predictor	R ²	Pearson r	p	p(FDR)
MI-arm	M1	0.354	0.595	0.032	0.043
MI-arm	PMd	0.421	0.649	0.016	0.033
MI-arm	PMv	0.325	0.570	0.042	0.042
MI-arm	SMA	0.477	0.691	0.009	0.036

Partial correlations assessing the association between premotor subtract integrity and complex motor performance, while controlling for the influence of the M1 subtract, were not significant after correction for multiple comparisons (all $p > .05$, FDR-corrected). Similarly, the association between M1 subtract anisotropy and complex motor skills did not remain significant when controlling for gFA derived from PMd, PMv, or SMA subtracts (all $p > .05$, FDR-corrected). These observations suggest a large degree of interdependence between M1 and premotor tract integrity for the execution of complex motor skills. In other words, the control of complex

motor skills seems to critically rely on descending signals from both M1 and PMd, PMv, and SMA.

Slicewise correlation analyses

To localize sections that were most indicative of motor performance for each CST subtract, we computed slicewise correlations between mean gFA derived from one-directional voxels and motor performance. Premotor subtractions originating from PMd, PMv, and SMA showed a consistent pattern of correlations with complex motor skills for the CST section extending from the internal capsule down to the mesencephalon (MNI z-levels -6 to 15). The M1 substract featured a highly similar pattern for correlations with basal and complex motor skills (MNI z-level -10 to 9). However, an additional section of significant correlations was observed for the M1 substract closer to the cortex (MNI z-levels 49 to 72; Figure 4).

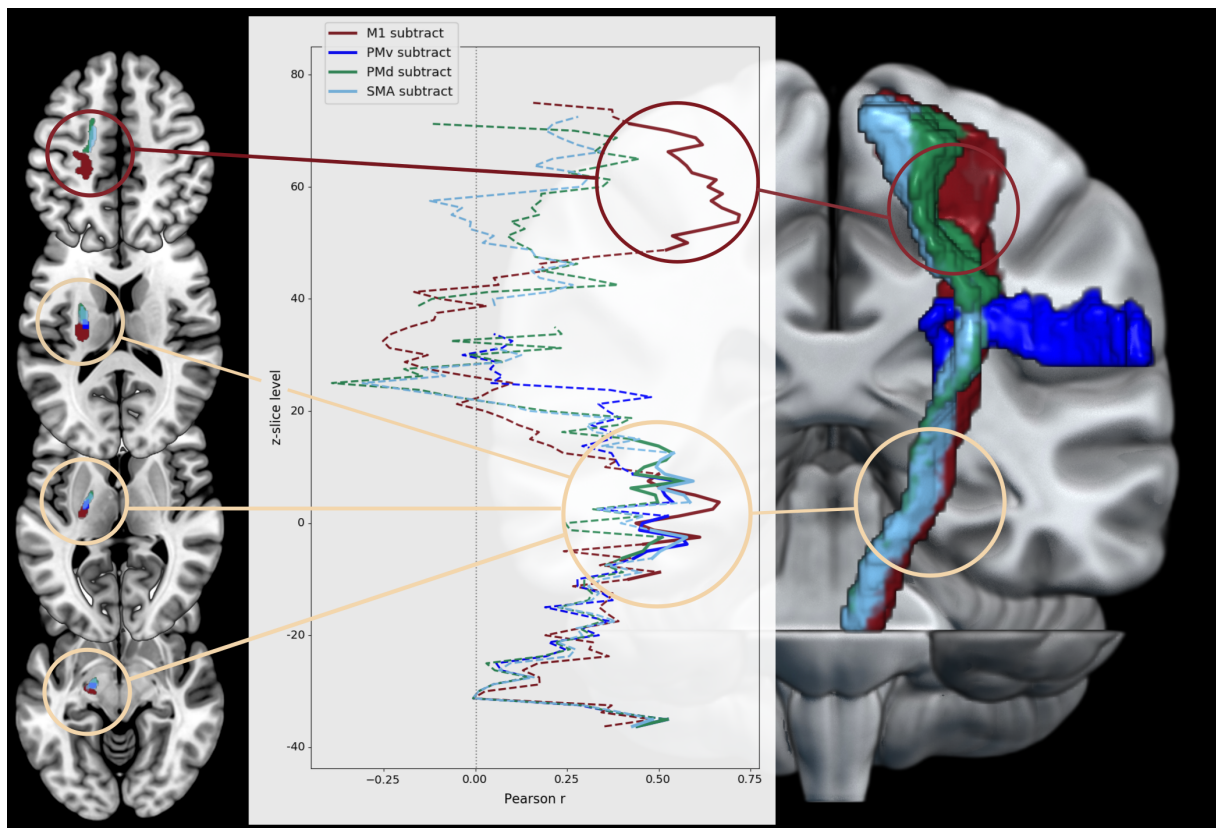


Figure 4: Slicewise correlations between mean anisotropy and complex motor skills. For subtractions originating from M1 (red), PMd (green), PMv (dark blue), and SMA (light blue), correlations between mean gFA and the ARAT were computed for each z-slice. A cluster of significant correlations emerged at the level of the internal capsule ranging down to the mesencephalon consistently across all subtractions. Only the M1 substract showed an additional section of significant correlations closer to the cortex in line with a potential cortical remapping. *M1 = primary motor cortex, SMA = supplementary motor area, PMd = dorsal premotor cortex, PMv = ventral premotor cortex*

Discussion

Premotor areas are considered key players facilitating motor network reorganization following stroke.⁴ For example, disturbing the activation of ipsilesional premotor areas by means of non-invasive brain stimulation has detrimental effects on motor performance after stroke.³⁸ Moreover, fMRI studies have frequently reported increased activation of premotor areas during movements of the paretic hand⁵ as well as correlations between motor impairment and resting-state or task-related connectivity within the core motor network including M1, SMA, PMv, and PMd.^{39,40} Thus, motor recovery may arise from functional reorganization of cortico-cortical interactions between premotor areas and M1 facilitated by dense cortico-cortical fibers linking these regions. However, the aforementioned cortical motor areas also feature direct projections to the spinal level.^{3,19,41,42} Therefore, the question arises whether premotor areas may facilitate post-stroke motor control not only via well-established cortico-cortical connections but also using their descending CST projections to the spinal level.

Functional role of premotor areas in post-stroke reorganization

In accordance with the notion that descending output from premotor regions is behaviorally relevant following stroke, previous studies have linked the integrity of descending premotor tracts to motor performance.^{9–14} However, to date, studies do not converge towards a clear pattern regarding the functional relevance of specific subtracts. Our present findings offer a possible explanation for the somewhat contradictory results of previous publications as they reveal a clear dissociation of basal and complex motor control: a patient's ability to move an individual limb as measured by the MI-arm score was exclusively correlated with M1 subtract integrity. Conversely, the successful performance of complex motor tasks resembling activities of daily living as measured by the ARAT was associated with subtractions descending from M1, PMd, PMv, and SMA (Figure 3).

Given that the integrity of the M1 subtract was associated with both basal and complex motor performance, our findings highlight the preeminent role of motor output from M1 which constitutes a prerequisite for the elicitation of any form of muscle activity. Further support for the necessity of residual M1 output stems from the fact that the association between premotor subtract anisotropy and complex motor skills was dependent on M1 tract integrity as suggested by the results of the partial correlation analyses. However, the fact that the correlation between M1 anisotropy and motor performance also did not remain significant when controlling for

premotor subtract anisotropy highlights that M1 output alone is not sufficient for the execution of sophisticated movements of the affected arm and hand. Instead, motor commands seem to be shaped by signals from PMv, PMd, and SMA. Considering the pivotal role of PMv and PMd for reaching and grasping movements,^{24,25} the reliance on descending PMv and PMd output in post-stroke motor control is well in line with their physiological roles in motor control of hand movements. For the somewhat unanticipated yet strong correlation between complex motor performance and anisotropy of the SMA subtract, three possible explanations should be considered. First, the functional role of the SMA including the performance of sequential movements and movement initiation²⁰⁻²³ might be instrumental for a wider range of tasks than initially assumed. Second, considering the significant association between M1-premotor effective connectivity and motor impairment after stroke,^{6,39} premotor areas including the SMA might serve as a “relay station” for M1 output. Following this logic, the SMA may receive motor commands from M1 via its cortico-cortical connections, thus offering an alternative route to bypass damaged descending M1 fibers. Third, the functional distinction of premotor areas may partially macerate as a feature of cerebral reorganization after stroke. This would allow the intact premotor areas to flexibly compensate functions of lesioned areas and their output tracts. Assuming this amount of flexibility, the functional role of a given premotor area may more heavily depend on the lesion and its secondary effects than its physiological role in motor control in the healthy brain. Of note, both a relay of M1 output through premotor areas as well as the flexible adoption of novel motor functions by premotor areas are well in line with our current findings, considering the significant correlation of premotor tract anisotropy with all ARAT subscales.²⁷ In sum, signals descending from premotor areas seem crucial for the successful execution of complex motor skills post-stroke, while direct descending output from M1 seems to be necessary for both basal and complex motor performance.

Compensation via premotor areas in patients with persistent deficits

The motor network of severely affected patients has been shown to be subject to more extensive reorganization processes.⁴³ Hence, premotor CST fibers may play a distinct and potentially more important role in the reorganized brain of such severely affected patients. In line with this notion, anisotropy derived from premotor subtracts originating from PMd, PMv, and SMA was linked to the MI-arm score in a subsample of patients with persistent motor deficits (Table 2). Thus, in more severely affected patients with persistent motor deficits, premotor pathways seem

to support basal individual limb movements. From a mechanistic perspective, this may be interpreted as a difference in cortico-cortical interactions: Basal motor commands that would normally be transmitted via the M1 subtract might be relayed from M1 to a premotor region in order to reach the spinal level via corticospinal premotor fibers. This view nicely matches previous reports of a correlation between basal motor performance and anisotropy of the cortical PMv-M1 connection in patients with pronounced CST damage,⁴⁴ thus suggesting an increased reliance on premotor areas via cortico-cortical connections following severe damage to descending M1 fibers. Hence, extensive damage to the M1 subtract might cause a shift in basal motor control from M1 towards premotor areas at the cortical level to capitalize on the intact or less affected CST fibers emerging from these premotor areas.

Relevant CST sections

While lower CST sections are thought to be a valid indicator of Wallerian degeneration, upper parts might also be influenced by cortical reorganization. Slicewise correlations between mean gFA and complex motor performance along the z-axis of each tract suggested that the CST section ranging from the internal capsule down to the mesencephalon emerged as the most important segment across all tracts (Figure 4). Notably, these particular sections are known to almost exclusively contain densely packed descending fibers⁴⁵ and to be indicative of motor performance after stroke.^{36,46,47} Of note, the correlation between basal motor skills and the M1-tract was also driven by z-slices closer to the cortex (Figure 4). A possible explanation for this finding might derive from cortical remapping of M1 motor functions from damaged to intact cortical tissue.^{43,48,49} In particular, axonal sprouting may result in novel efferent connections from remapped cortical areas to the CST. Alternatively, this observation may reflect the premorbid level of structural connectivity: patients with less aging-related atrophy may be able to draw on the structural reserve of descending and cortico-cortical motor network connections. While these mechanistic interpretations remain speculative, the additional section of relevant z-slices closer to the cortex underlines the importance to consider voxels from the entire length of the CST, which constitutes an important difference to previous ROI-based studies.^{10,12}

Limitations

Given that complex motor behavior correlated with subtracts originating from SMA, PMv, PMd, and M1, one might assume that a potential overlap between different subtracts within the PLIC biased these correlations. However, a relatively small number of overlapping voxels across subtracts within the PLIC renders a considerable sampling bias unlikely. Moreover, no association was observed between motor performance and anisotropy extracted from CST subtracts originating from preSMA or S1, corroborating the specificity of our findings. In particular, the preSMA has rich connections to regions of the prefrontal cortex and receives inputs from non-motor areas of the dentate nucleus and globus pallidus,⁵⁰ underlining its functional role as a prefrontal rather than premotor area. Given the relatively small sample size of our cohort, one might argue that lesion locations favoring a specific tract may have biased our findings. However, we observed that all subtracts were similarly affected, which renders such a bias highly unlikely. Moreover, one may assume that tractwise anisotropy is compromised by ageing-related atrophy and hence inadequately represents stroke-induced damage and degeneration. However, compared to age-matched controls we found a specific anisotropy decrease for CST subtracts but not unaffected tracts such as the SLF, further corroborating our results. Another limitation pertains to the quantification of behavior. While the MI and ARAT are adequate instruments to differentiate basal and complex motor skills, their scales are not suited to accurately capture functions specific to different premotor areas. Thus, future research is needed that relates distinct aspects of reach-to-grasp movements to the integrity of different CST subtracts.

Conclusion

We here demonstrate for the first time a distinct functional role of CST subtracts originating from M1 and premotor areas for basal motor performance and more complex motor skills after stroke. While descending signals from M1 were vital for both basal and complex movements, output from SMA, PMv, and PMd were relevant for the execution of complex motor skills in line with their physiological roles in motor control. However, premotor subtracts also showed an association with basal motor performance in patients with persistent motor deficits exclusively, emphasizing their potential functional flexibility in more severely affected patients. Thus, our current findings illustrate the flexibility of premotor areas to adopt new functional roles during post-stroke reorganization and suggest a functional relay of motor commands via descending premotor tracts after damage to M1 fibers. In conclusion, our results

underline the importance of corticospinal motor signals from premotor areas for stroke recovery and propagate the focus on premotor areas for therapeutic interventions.

Funding

GRF gratefully acknowledges support from the Marga and Walter Boll Stiftung, Kerpen, Germany. CG and GRF are funded by the Deutsche Forschungsgemeinschaft (DFG, German Research Foundation) – Project-ID 431549029-SFB1451. STG was supported by the Institute for Collaborative Biotechnologies under Cooperative Agreement W911NF-19-2-0026 with the Army Research Office.

Disclosures

None.

References

1. Koch PJ, Schulz R, Hummel FC. Structural connectivity analyses in motor recovery research after stroke. *Ann Clin Transl Neurol.* 2016;3(3):233-244. doi:10.1002/acn3.278
2. Nudo RJ, Masterton RB. Descending pathways to the spinal cord, IV: Some factors related to the amount of cortex devoted to the corticospinal tract. *J Comp Neurol.* 1990;296(4):584-597. doi:10.1002/cne.902960406
3. Galea MP, Darian-Smith I. Multiple Corticospinal Neuron Populations in the Macaque Monkey Are Specified by Their Unique Cortical Origins, Spinal Terminations, and Connections. *Cereb Cortex.* 1994;4(2):166-194. doi:10.1093/cercor/4.2.166
4. Grefkes C, Ward NS. Cortical Reorganization After Stroke. *Neurosci.* 2014;20(1):56-70. doi:10.1177/1073858413491147
5. Rehme AK, Eickhoff SB, Rottschy C, Fink GR, Grefkes C. Activation likelihood estimation meta-analysis of motor-related neural activity after stroke. *Neuroimage.* 2012;59(3):2771-2782. doi:10.1016/j.neuroimage.2011.10.023
6. Rehme AK, Eickhoff SB, Wang LE, Fink GR, Grefkes C. Dynamic causal modeling of cortical activity from the acute to the chronic stage after stroke. *Neuroimage.* 2011;55(3):1147-1158. doi:10.1016/j.neuroimage.2011.01.014
7. Strick PL, Dum RP, Rathelot JA. The Cortical Motor Areas and the Emergence of Motor Skills: A Neuroanatomical Perspective. *Annu Rev Neurosci.* 2021;44(1):425-447. doi:10.1146/annurev-neuro-070918-050216
8. Kantak SS, Stinear JW, Buch ER, Cohen LG. Rewiring the Brain. *Neurorehabil Neural Repair.* 2012;26(3):282-292. doi:10.1177/1545968311420845
9. Riley JD, Le V, Der-Yeghiaian L, et al. Anatomy of Stroke Injury Predicts Gains From Therapy. *Stroke.* 2011;42(2):421-426. doi:10.1161/STROKEAHA.110.599340
10. Schulz R, Park CH, Boudrias MH, Gerloff C, Hummel FC, Ward NS. Assessing the Integrity of Corticospinal Pathways From Primary and Secondary Cortical Motor Areas After Stroke. *Stroke.* 2012;43(8):2248-2251. doi:10.1161/STROKEAHA.112.662619
11. Phan TG, van der Voort S, Chen J, et al. Impact of corticofugal fibre involvement in subcortical stroke. *BMJ Open.* 2013;3(9):e003318. doi:10.1136/bmjopen-2013-003318
12. Archer DB, Misra G, Patten C, Coombes SA. Microstructural properties of premotor pathways predict visuomotor performance in chronic stroke. *Hum Brain Mapp.* 2016;37(6):2039-2054. doi:10.1002/hbm.23155
13. Liu J, Wang C, Qin W, et al. Corticospinal Fibers With Different Origins Impact Motor Outcome and Brain After Subcortical Stroke. *Stroke.* 2020;51(7):2170-2178. doi:10.1161/STROKEAHA.120.029508
14. Ito KL, Kim B, Liu J, et al. Corticospinal Tract Lesion Load Originating From Both Ventral Premotor and Primary Motor Cortices Are Associated With Post-stroke Motor Severity. *Neurorehabil Neural Repair.* Published online December 24, 2021:154596832110684. doi:10.1177/15459683211068441
15. Boccuni L, Meyer S, D'cruz N, et al. Premotor dorsal white matter integrity for the prediction of upper limb motor impairment after stroke. *Sci Rep.* 2019;9(1):19712. doi:10.1038/s41598-019-56334-w
16. Saltão da Silva MA, Baune NA, Belagaje S, Borich MR. Clinical Imaging-Derived Metrics of Corticospinal Tract Structural Integrity Are Associated With Post-stroke

- Motor Outcomes: A Retrospective Study. *Front Neurol.* 2022;13(February):1-13. doi:10.3389/fneur.2022.804133
17. Lin DJ, Cloutier AM, Erler KS, et al. Corticospinal Tract Injury Estimated From Acute Stroke Imaging Predicts Upper Extremity Motor Recovery After Stroke. *Stroke.* 2019;50(12):3569-3577. doi:10.1161/STROKEAHA.119.025898
 18. Paul T, Cieslak M, Hensel L, et al. The role of corticospinal and extrapyramidal pathways in motor impairment after stroke. *Brain Commun.* Published online November 21, 2022. doi:10.1093/braincomms/fcac301
 19. Dum RP, Strick PL. Motor areas in the frontal lobe of the primate. *Physiol Behav.* 2002;77(4-5):677-682. doi:10.1016/S0031-9384(02)00929-0
 20. Gerloff C, Corwell B, Chen R, Hallett M, Cohen LG. Stimulation over the human supplementary motor area interferes with the organization of future elements in complex motor sequences. *Brain.* 1997;120(9):1587-1602. doi:10.1093/brain/120.9.1587
 21. Macar F, Anton JL, Bonnet M, Vidal F. Timing functions of the supplementary motor area: an event-related fMRI study. *Cogn Brain Res.* 2004;21(2):206-215. doi:10.1016/j.cogbrainres.2004.01.005
 22. Lara AH, Cunningham JP, Churchland MM. Different population dynamics in the supplementary motor area and motor cortex during reaching. *Nat Commun.* 2018;9(1):2754. doi:10.1038/s41467-018-05146-z
 23. Bannur U, Rajshekhar V. Post operative supplementary motor area syndrome: clinical features and outcome. *Br J Neurosurg.* 2000;14(3):204-210. doi:10.1080/026886900408379
 24. Rizzolatti G, Luppino G. The Cortical Motor System. *Neuron.* 2001;31(6):889-901. doi:10.1016/S0896-6273(01)00423-8
 25. Davare M. Dissociating the Role of Ventral and Dorsal Premotor Cortex in Precision Grasping. *J Neurosci.* 2006;26(8):2260-2268. doi:10.1523/JNEUROSCI.3386-05.2006
 26. Cirstea MC, Levin MF. Compensatory strategies for reaching in stroke. *Brain.* 2000;123(5):940-953. doi:10.1093/brain/123.5.940
 27. Lyle RC. A performance test for assessment of upper limb function in physical rehabilitation treatment and research. *Int J Rehabil Res.* 1981;4(4):483-492. doi:10.1097/00004356-198112000-00001
 28. Demeurisse G, Demol O, Robaye E. Motor Evaluation in Vascular Hemiplegia. *Eur Neurol.* 1980;19(6):382-389. doi:10.1159/000115178
 29. Archer DB, Vaillancourt DE, Coombes SA. A Template and Probabilistic Atlas of the Human Sensorimotor Tracts using Diffusion MRI. *Cereb Cortex.* 2018;28(5):1685-1699. doi:10.1093/cercor/bhx066
 30. Rorden C, Brett M. Stereotaxic Display of Brain Lesions. *Behav Neurol.* 2000;12(4):191-200. doi:10.1155/2000/421719
 31. Cieslak M, Cook PA, He X, et al. QSIPrep: an integrative platform for preprocessing and reconstructing diffusion MRI data. *Nat Methods.* 2021;18(7):775-778. doi:10.1038/s41592-021-01185-5
 32. Fonov V, Evans A, McKinstry R, Almlí C, Collins D. Unbiased nonlinear average age-appropriate brain templates from birth to adulthood. *Neuroimage.* 2009;47:S102. doi:10.1016/S1053-8119(09)70884-5

33. Avants BB, Epstein CL, Grossman M, Gee JC. Symmetric diffeomorphic image registration with cross-correlation: evaluating automated labeling of elderly and neurodegenerative brain. *Med Image Anal.* 2008;12(1):26-41. doi:10.1016/j.media.2007.06.004
34. Volz LJ, Cieslak M, Grafton ST. A probabilistic atlas of fiber crossings for variability reduction of anisotropy measures. *Brain Struct Funct.* 2018;223(2):635-651. doi:10.1007/s00429-017-1508-x
35. Kim B, Fisher BE, Schweighofer N, et al. A comparison of seven different DTI-derived estimates of corticospinal tract structural characteristics in chronic stroke survivors. *J Neurosci Methods.* 2018;304:66-75. doi:10.1016/j.jneumeth.2018.04.010
36. Puig J, Pedraza S, Blasco G, et al. Acute Damage to the Posterior Limb of the Internal Capsule on Diffusion Tensor Tractography as an Early Imaging Predictor of Motor Outcome after Stroke. *Am J Neuroradiol.* 2011;32(5):857-863. doi:10.3174/ajnr.A2400
37. Borich MR, Brown KE, Boyd LA. Motor Skill Learning Is Associated With Diffusion Characteristics of White Matter in Individuals With Chronic Stroke. *J Neurol Phys Ther.* 2014;38(3):151-160. doi:10.1097/NPT.0b013e3182a3d353
38. Hartwigsen G, Volz LJ. Probing rapid network reorganization of motor and language functions via neuromodulation and neuroimaging. *Neuroimage.* 2021;224(October 2020):117449. doi:10.1016/j.neuroimage.2020.117449
39. Paul T, Hensel L, Rehme AK, et al. Early motor network connectivity after stroke: An interplay of general reorganization and state-specific compensation. *Hum Brain Mapp.* 2021;42(16):5230-5243. doi:10.1002/hbm.25612
40. Rehme AK, Grefkes C. Cerebral network disorders after stroke: evidence from imaging-based connectivity analyses of active and resting brain states in humans. *J Physiol.* 2013;591(1):17-31. doi:10.1113/jphysiol.2012.243469
41. Martino AM, Strick P. Corticospinal projections originate from the arcuate premotor area. *Brain Res.* 1987;404(1-2):307-312. doi:10.1016/0006-8993(87)91384-9
42. Macpherson J, Wiesendanger M, Marangoz C, Miles TS. Corticospinal neurones of the supplementary motor area of monkeys. *Exp Brain Res.* 1982;48(1):81-88. doi:10.1007/BF00239574
43. Olafson ER, Jamison KW, Sweeney EM, et al. Functional connectome reorganization relates to post-stroke motor recovery and structural and functional disconnection. *Neuroimage.* 2021;245(October):118642. doi:10.1016/j.neuroimage.2021.118642
44. Schulz R, Park E, Lee J, et al. Interactions Between the Corticospinal Tract and Premotor–Motor Pathways for Residual Motor Output After Stroke. *Stroke.* 2017;48(10):2805-2811. doi:10.1161/STROKEAHA.117.016834
45. Pierpaoli C, Barnett A, Pajevic S, et al. Water Diffusion Changes in Wallerian Degeneration and Their Dependence on White Matter Architecture. *Neuroimage.* 2001;13(6):1174-1185. doi:10.1006/nimg.2001.0765
46. Thomalla G, Glauche V, Koch MA, Beaulieu C, Weiller C, Röther J. Diffusion tensor imaging detects early Wallerian degeneration of the pyramidal tract after ischemic stroke. *Neuroimage.* 2004;22(4):1767-1774. doi:10.1016/j.neuroimage.2004.03.041
47. Doughty C, Wang J, Feng W, Hackney D, Pani E, Schlaug G. Detection and Predictive Value of Fractional Anisotropy Changes of the Corticospinal Tract in the Acute Phase of a Stroke. *Stroke.* 2016;47(6):1520-1526. doi:10.1161/STROKEAHA.115.012088

48. Ward N. Assessment of cortical reorganisation for hand function after stroke. *J Physiol.* 2011;589(23):5625-5632. doi:10.1113/jphysiol.2011.220939
49. Byrnes ML, Thickbroom GW, Phillips BA, Wilson SA, Mastaglia FL. Physiological studies of the corticomotor projection to the hand after subcortical stroke. *Clin Neurophysiol.* 1999;110(3):487-498. doi:10.1016/S1388-2457(98)00044-3
50. Akkal D, Dum RP, Strick PL. Supplementary Motor Area and Presupplementary Motor Area: Targets of Basal Ganglia and Cerebellar Output. *J Neurosci.* 2007;27(40):10659-10673. doi:10.1523/JNEUROSCI.3134-07.2007

Supplement

Supplementary Tables

Supplementary Table 1: Demographic and clinical patient information.

patient	sex	affected hemisphere	lesion location	ARAT	MI-arm	months since stroke
1	m	r	MCA (subcortical)	57	99	21
2	m	r	MCA (subcortical)	57	91	14
3	m	r	MCA (subcortical)	38	76	17
4	m	l	MCA (subcortical)	0	34	51
5	m	l	PCA (subcortical)	35	92	23
6	f	l	MCA (subcortical)	32	77	11
7	m	l	MCA (subcortical)	19	65	59
8	m	l	MCA (subcortical)	55	92	71
9	m	l	ACA/MCA (subcortical)	57	99	31
10	m	r	MCA (subcortical)	49	91	12
11	m	l	MCA (subcortical)	57	99	37
12	m	r	Brainstem	57	99	44
13	f	r	MCA (cortical)	56	91	55
14	m	r	MCA (cortical)	57	99	32
15	m	l	MCA (subcortical)	57	99	43
16	f	r	MCA (subcortical)	57	76	15
17	m	r	Brainstem	37	84	82
18	m	l	Brainstem	44	83	30
19	f	l	Brainstem	56	76	12
20	m	l	PCA (subcortical)	55	92	15
21	m	l	MCA (subcortical)	57	99	33
22	m	l	MCA (sub- & cortical)	57	99	25
23	m	r	MCA (subcortical)	53	99	35
24	f	r	Brainstem	57	83	20
25	m	r	MCA (subcortical)	57	99	23

Supplementary Table 2: Correlations between tractwise anisotropy of one-directional voxels and ARAT subscores. Please note that all test yielded significant results after FDR-correction except for two tests probing for an association between premotor tract anisotropy and gross movements.

DV	predictor	R2	Pearson r	p	p(FDR)
ARAT grasp	M1	0.251	0.501	0.011	0.043
ARAT gross	M1	0.239	0.488	0.013	0.035
ARAT grip	M1	0.290	0.538	0.006	0.044
ARAT pinch	M1	0.326	0.571	0.003	0.046
ARAT grasp	PMd	0.194	0.440	0.028	0.034
ARAT gross	PMd	0.155	0.394	0.051	0.055
ARAT grip	PMd	0.203	0.451	0.024	0.034
ARAT pinch	PMd	0.232	0.482	0.015	0.033
ARAT grasp	PMv	0.213	0.462	0.020	0.040
ARAT gross	PMv	0.212	0.460	0.021	0.037
ARAT grip	PMv	0.246	0.496	0.012	0.038
ARAT pinch	PMv	0.261	0.511	0.009	0.048
ARAT grasp	SMA	0.186	0.431	0.031	0.036
ARAT gross	SMA	0.151	0.389	0.055	0.055
ARAT grip	SMA	0.198	0.445	0.026	0.034
ARAT pinch	SMA	0.212	0.460	0.021	0.033

5.3. Basal but not complex motor control relies on interhemispheric structural connectivity after stroke

Theresa Paul[†], Valerie M. Wiemer[†], Lukas Hensel, Matthew Cieslak,
Caroline Tscherpel, Christian Grefkes, Scott T. Grafton,
Gereon R. Fink, Lukas J. Volz

[†]These authors contributed equally to this work.

MedRxiv preprint, Uploaded November 2023
<https://doi.org/10.1101/2022.10.04.22280666>

Basal but not complex motor control relies on interhemispheric structural connectivity after stroke

Theresa Paul, MSc^{1, †}, Valerie M. Wiemer, MSc^{1, †}, Lukas Hensel, MD¹, Matthew Cieslak, PhD², Caroline Tscherpel, MD¹, Christian Grefkes, MD, PhD^{1,3}, Scott T. Grafton, MD⁴, Gereon R. Fink, MD, PhD^{1,3}, Lukas J. Volz, MD¹

†These authors contributed equally to this work.

¹ Medical Faculty, University of Cologne, and Department of Neurology, University Hospital Cologne, Cologne, Germany

² Department of Psychiatry, Perelman School of Medicine, University of Pennsylvania, Philadelphia, PA, United States of America

³ Institute of Neuroscience and Medicine, Cognitive Neuroscience (INM-3), Research Centre Juelich, Juelich, Germany

⁴ Department of Psychological & Brain Sciences, University of California, Santa Barbara, CA, United States of America

Corresponding author:

Lukas J. Volz, M.D.

Department of Neurology, University of Cologne

Kerpener Str. 62, 50937 Cologne, Germany

Email: Lukas.Volz@uk-koeln.de

Running title

Structural connectivity in motor stroke

Keywords

cortical reorganization, cortical motor network, diffusion imaging

Number of words in abstract: 249

Number of words in main text: 4189

Number of figures: 4

Number of tables: 2

List of abbreviations

ARAT = Action Research Arm Test

BIC = Bayesian information criterion

cl = contralesional

CST = corticospinal tract

dMRI = diffusion magnetic resonance imaging

DSI = diffusion spectrum imaging

FDR = false discovery rate

gFA = generalized fractional anisotropy

il = ipsilesional

M1 = primary motor cortex

MI = Motricity Index

NIHSS = National Institutes of Health Stroke Scale

PMd = dorsal premotor cortex

PMv = ventral premotor cortex

ROI = region of interest

SMA = supplementary motor area

WM = white matter

Abstract

Objective: While ample evidence highlights that the ipsilesional corticospinal tract (CST) plays a crucial role in motor recovery after stroke, very few studies have assessed cortico-cortical motor connections with inconclusive results. Given their unique potential to serve as structural reserve enabling motor network reorganization, the question arises whether cortico-cortical connections may facilitate motor control depending on CST damage.

Methods: Diffusion spectrum imaging (DSI) and a novel compartmentwise analysis approach were used to quantify structural connectivity between bilateral cortical core motor regions in chronic stroke patients. Basal and complex motor control were differentially assessed.

Results: Both basal and complex motor performance were correlated with structural connectivity between bilateral premotor areas and ipsilesional primary motor cortex (M1) as well as interhemispheric M1-M1 connectivity. While complex motor skills depended on CST integrity, a strong association between M1-M1 connectivity and basal motor control was observed independent of CST integrity especially in patients who underwent substantial motor recovery. Harnessing the informational wealth of cortico-cortical connectivity facilitated the explanation of both basal and complex motor control.

Interpretation: We demonstrate for the first time that distinct aspects of cortical structural reserve enable basal and complex motor control after stroke. In particular, recovery of basal motor control is supported via an alternative route through contralesional M1 and non-crossing fibers of the contralesional CST. Our findings help to explain previous conflicting interpretations regarding a vicarious or maladaptive role of the contralesional M1 and highlight the potential of structural connectivity of the cortical motor network as a biomarker post-stroke.

Introduction

Diffusion MRI (dMRI) is commonly used to characterize white matter (WM) alterations associated with motor impairment following stroke.¹ It is well-established that the capacity for motor control depends on the “microstructural” integrity of descending motor tracts such as the ipsilesional CST.² At the same time, very little attention has been devoted to cortico-cortical structural connectivity, even though functional imaging studies suggest a pivotal role of interactions between cortical motor areas for motor performance in healthy individuals and stroke patients.^{3,4} Both resting-state functional connectivity and task-based effective connectivity have repeatedly been shown to relate to motor impairment in the acute and chronic stages post-stroke.⁵⁻⁸ Given the assumed structure-function relationships,⁹ structural connectivity of this cortical motor network might play a seminal role in motor control after stroke. From a mechanistic perspective, structural cortical connectivity may form the basis for altered network dynamics and hence reflect a patients’ structural reserve enabling motor recovery via functional reorganization.¹⁰

However, studies on cortico-cortical structure-function relationships remain surprisingly scarce. Existing evidence suggests that motor performance relates to structural connectivity between bilateral primary motor cortex (M1).¹¹⁻¹⁶ Studies investigating ipsilesional premotor-M1 connectivity have reported inconclusive findings.^{11,17,18} Moreover, data on the role of interhemispheric premotor-M1 connections are missing. While whole-brain analyses principally include these connections, typical atlas parcellations do not isolate known premotor areas, limiting their interpretability.^{19,20} Moreover, most studies commonly focus on either CST integrity or cortical connectivity. Hence, it remains unknown how post-stroke motor control is facilitated via reorganization based on structural connectivity of the cortical motor network or whether such reorganization depends on the extent of ipsilesional CST damage.

To address these issues, we assessed diffusion spectrum imaging (DSI) data in a sample of chronic stroke patients. Using a novel approach,²¹ compartmentwise generalized fractional anisotropy (gFA) was extracted from specific cortico-cortical tracts defined based on normative HCP data.²² Tracts were defined for a network of cortical motor areas. We systematically assessed the relationship of various cortico-cortical connections with basal and complex motor functions in chronic stroke patients. In line with functional and effective connectivity findings, we expected bilateral premotor - ipsilesional M1 and interhemispheric M1-M1 connectivity to be indicative of both basal and complex motor skills. Given that basal motor commands such as lifting the arm against gravity might potentially be compensated via alternative routes such

as non-crossing fibers of the contralesional CST,²³ we hypothesized a stronger dependence on ipsilesional CST integrity for complex than for basal motor skills. Importantly, all analyses were repeated while controlling for ipsilesional CST integrity. Finally, we addressed whether structural connectivity differed in patients with substantial motor recovery compared to patients with limited or no recovery from the acute to the chronic phase post-stroke. This approach allowed us to identify features of cortico-cortical structural connectivity associated with successful motor recovery. Advancing our mechanistic understanding of motor recovery will help to lay the foundation for targeted therapeutic interventions and to identify cortico-cortical connections as potential biomarkers.

Material and methods

Subjects

Twenty-five chronic stroke patients (mean age=66.68, std=11.25, 5 female, 20 male) formerly hospitalized at the University Hospital Cologne, Department of Neurology, were included (for detailed demographic and clinical information, see Supplementary Table 1). Inclusion criteria were (1) age between 40 and 90 years, (2) first-ever ischemic stroke more than six months ago and (3) initial unilateral impairment of upper limb motor function. Exclusion criteria were (1) any contraindications to MRI, (2) bihemispheric infarctions, (3) cerebral hemorrhage, (4) reinfarction or other neurological diseases, and (5) persistence of severe aphasia or neglect. All subjects provided informed consent. The study was approved by the ethics committee of the Medical Faculty of the University of Cologne and was conducted in accordance with the declaration of Helsinki. While data from the current patient cohort was included in a previous publication focusing on descending corticospinal and extrapyramidal pathways,²¹ there is no overlap with the current analyses assessing cortico-cortical connectivity.

Behavioral motor tests

To differentially quantify the impairment of basal and complex motor control involving proximal and distal arm movements, motor impairment was assessed using the Action Research Arm Test (ARAT)²⁴ and the Motricity Index (MI)-arm score.²⁵ The ARAT probes the execution of activities of daily living and therefore requires the complex interplay of motor synergies, emphasizing distal control of hand motor functions. In contrast, the MI-arm reflects more basal

motor control with a focus on proximal and some distal upper limb movements (Fig. 1). The universally used National Institutes of Health Stroke Scale (NIHSS)-arm subscore was used to quantify a patient's degree of motor recovery from the acute to the chronic stage post-stroke (holding arms 90° against gravity; levels 0: no drift, 1: drift, 2: arm falls before 10 s, 3: no effort against gravity, 4: no movement). *Substantial* recovery was defined as NIHSS-arm improvements of one point or more from the acute to the chronic stage (15 patients). Of note, the absence of a change in the NIHSS-arm score should not be equated with no recovery as the NIHSS cannot capture nuanced differences. In other words, a patient who is able to perform all NIHSS items flawlessly might still have difficulties performing certain aspects of the ARAT. Therefore, patients without an increase in the NIHSS-arm score are summarized as *non-substantial* recovery group (10 patients).

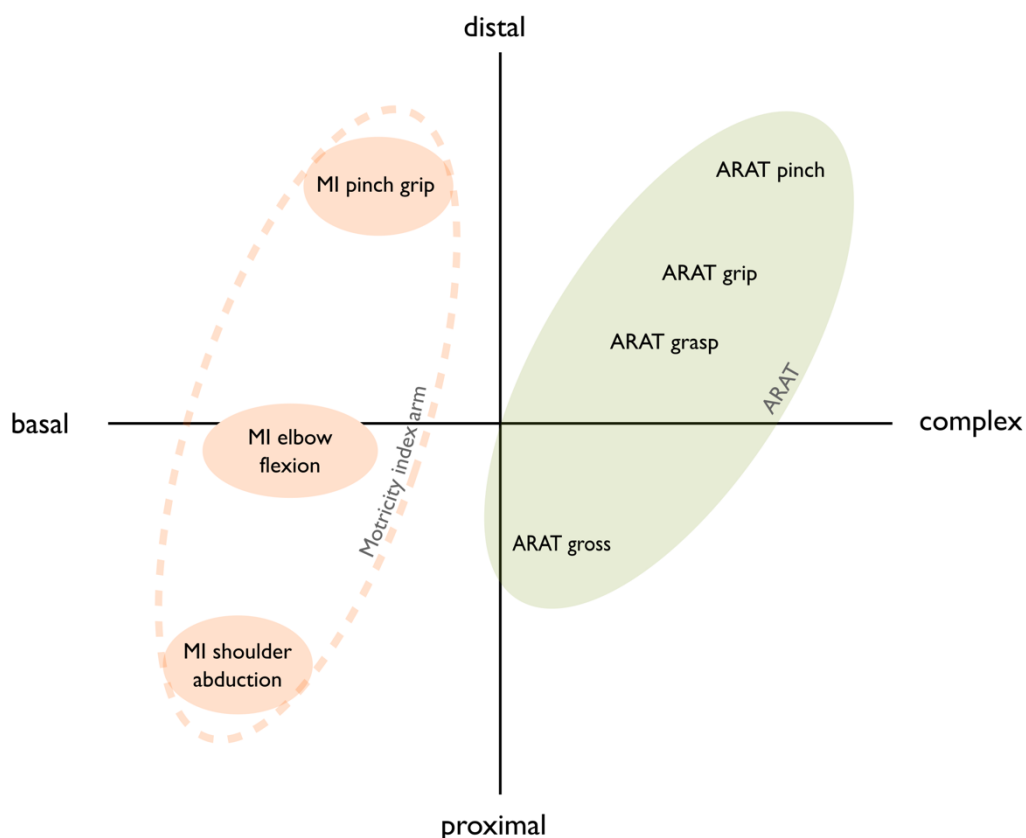


Figure 1: Schematic illustration of motor assessments via the Action Research Arm Test (ARAT) and Motricity Index (MI)-arm score. The MI-arm score (orange) reflects basal motor control of simple movements involving specific muscle synergies with a precise delineation of the reliance on required muscle groups for proximal to distal movements. Conversely, the ARAT (green) quantifies more complex motor control of the affected arm that requires the interplay of different motor control policies, closely reflecting activities of daily living.

MRI acquisition and preprocessing

MRI data were recorded using a Siemens MAGNETOM Prisma 3 Tesla scanner (Siemens Medical Solutions, Erlangen, Germany). Preprocessing of diffusion data was performed using QSIPrep²⁶ and gFA-maps were generated in DSI Studio (<https://dsi-studio.labsolver.org/>; for a detailed description see²¹). Individual gFA-maps were normalized to MNI-space using ANTS.²⁷ Lesion masks were drawn in MRIcron (www.sph.sc.edu/comd/rorden/MRIcron) and verified by a certified neurologist. Images with lesions affecting the right hemisphere were flipped along the mid-sagittal plane to facilitate group comparisons. To focus all subsequent analyses on WM voxels and exclude voxels located within the stroke lesion, gFA-maps were masked using both individual WM-masks derived from brain tissue segmentation and lesion masks.

Defining regions of the cortical motor network

As effective and functional connectivity within a motor network comprising core motor areas have frequently been linked to motor impairment after stroke,^{5-7,28} we accordingly included bilateral core motor areas such as M1, dorsal premotor cortex (PMd), ventral premotor cortex (PMv) and supplementary motor area (SMA). To define the location of the aforementioned areas, term-based fMRI meta-analyses were performed using the neurosynth.org database (<https://www.neurosynth.org/>) with search terms including “motor cortex”, “dorsal premotor”, “ventral premotor”, and “supplementary motor”. Derived activation patterns were used to define regions of interest (ROIs) for M1 (MNI coordinates left: -38/-22/60, right: 38/-22/60), PMd (left: -24/-6/62, right: 24/-6/62), PMv (left: -54/-1/22, right: 54/-1/22) and SMA (left: -4/-4/54, right: 4/-4/54).

Generation of tract templates

Fiber bundles connecting cortical motor regions were defined via deterministic fiber tracking as implemented in DSI Studio²⁹ using the HCP-1065 template based on diffusion data of 1065 healthy subjects.²² Deterministic fiber tracking was used to identify (1) intrahemispheric cortico-cortical fiber tracts between ipsilesional (il) M1 and ipsilesional premotor areas (ilPMd-ilM1, ilPMv-ilM1, ilSMA-ilM1), (2) interhemispheric cortico-cortical fiber tracts between ipsilesional M1 and contralesional (cl) premotor areas (clPMd-ilM1, clPMv-ilM1, clSMA-ilM1), as well as (3) the interhemispheric tract between bilateral M1 (clM1-ilM1; Fig. 2). Fiber

tracking was performed using the generated cortical ROIs, exclusion ROIs and an angular threshold of 50-90 degrees. Resulting tracts were manually trimmed and validated by a certified neurologist. To address whether potential associations between structural motor network connectivity and motor impairment were independent of CST integrity, we generated an additional CST mask originating from M1, PMd, PMv and SMA. Importantly, the CST is known to be slightly asymmetrical for the left and right hemispheres in healthy subjects.³⁰ Considering that right-hemispheric lesions were flipped to the left hemisphere, left- and right-hemispheric CST tracts were created and combined into a single mask after flipping the right-hemispheric tract along the mid-sagittal plane. Thereby we ensured that all relevant voxels were captured (Fig. 2).

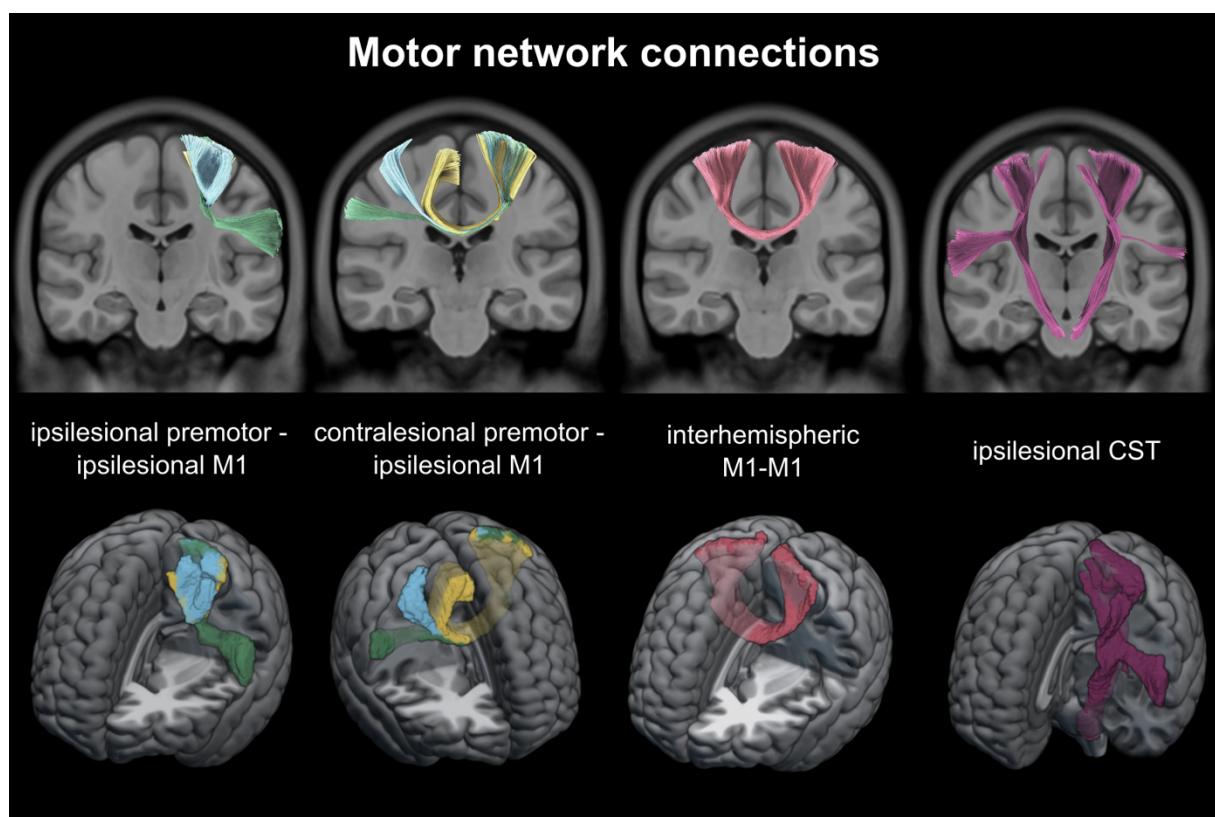


Figure 2: Cortico-cortical and descending motor network connections. Fiber tracts between core areas of the cortical motor network were created using deterministic fiber tracking based on the HCP1065-template²² in DSI Studio (upper row). Motor tract templates used for anisotropy extraction are depicted as overlays in MRICroGL (lower row). Note that for the ipsilesional CST, tracking was first performed in both hemispheres (upper row). Bilateral tracts were then combined into a single ipsilesional CST mask after flipping the right-hemispheric tract to the left (lower row). blue = connection with PMd, green = connection with PMv, yellow = connections with SMA, red = interhemispheric M1-M1 connection, purple = corticospinal tract.

Tractwise anisotropy

To quantify structural connectivity, diffusion data was compartmentalized using a DSI-based compartmentwise approach.³⁰ A deterministic mask was applied to whole-brain gFA-maps in order to differentiate voxels according to the number of trackable fiber directions.³⁰ This

approach has been shown to facilitate the analyses of anisotropy in stroke patients.²¹ Importantly, tractwise gFA-values were determined based on voxels with only one dominant fiber direction. Focusing the analyses on one-directional voxels helped us to overcome the methodological limitations of biased anisotropy estimations in voxels with multiple fiber directions (for a detailed discussion regarding the impact of compartmentalization on analyses of anisotropy, see ^{21,30}).

Structural connectivity and motor control after stroke

A potential relationship between anisotropy of cortico-cortical motor connections and different aspects of motor control after stroke was tested via Pearson correlations. To probe for relationships with basal motor control, correlations were computed between the MI-arm score and tractwise mean gFA. All p-values were FDR-corrected for multiple comparisons.³¹ To test for relationships with complex motor control, the analyses were repeated using the ARAT score.

To address the question whether the associations between cortico-cortical connectivity and motor control depended on CST damage, partial correlations were computed controlling for ipsilesional CST anisotropy. Importantly, CST integrity has also been related to the degree of motor recovery after stroke.¹ However, recovery is multifaceted, with good outcomes potentially deriving from various distinct mechanisms at the network level. For example, a small lesion may lead to mild initial impairment which yields a good outcome (almost) independent of the degree of recovery. On the other hand, patients with lesions involving a large amount of brain tissue suffering from severe initial impairment may recover substantially during rehabilitation, also resulting in a good outcome at the chronic stage. Therefore, we assessed the relationship between cortico-cortical motor network connectivity and motor outcome in a recovery-dependent manner. To this end, we divided the patient cohort into two subgroups featuring substantial or non-substantial upper limb recovery, as reflected by improvements in the NIHSS-arm score between the acute and chronic phases. Correlation analyses with basal motor outcome scores were repeated for both subgroups.

To make sure that results were not driven by the direct impact of the lesion, all correlation analyses were repeated after excluding specific tracts in subjects that showed an overlap of more than 10% between the lesion and the tract's one-directional voxels (N=3).

Stepwise linear backward regressions

Stepwise linear backward regressions based on the Bayesian information criterion (BIC, $k=\log(N)$, $N=25$) were computed to probe for the extent of explained variance in basal (MI-arm) and complex (ARAT) motor performance by the integrity of ipsilesional CST and cortico-cortical connectivity. For a better appraisal of the ratio of explained variance by the combined model, we separately assessed how much variance was accounted for by (i) cortico-cortical connectivity without the CST and (ii) CST anisotropy alone. As CST damage is considered a valid biomarker for motor impairment post-stroke,² the direct comparison is a good indicator for the suitability of cortico-cortical structural connectivity to potentially improve prediction of behavior.

Data availability statement

Data are available from the corresponding author upon reasonable request. Tract templates used for the extraction of tractwise anisotropy can be downloaded from the following link: <https://tinyurl.com/4ttnzsr>

Results

Correlation analyses

For both basal and complex upper limb motor control, positive correlations were observed with anisotropy of the homologous cIM1-ilM1 connection, all intrahemispheric premotor-ilM1 connections and interhemispheric cPMv-ilM1 and cSMA-ilM1 connections (all $p<.05$, FDR-corrected; for details see Table 1 and Fig. 3A). Thus, higher levels of anisotropy were found in patients featuring higher levels of basal and complex motor control of the stroke-affected arm. In general, correlations with tractwise anisotropy tended to be stronger for basal than for complex motor control. Our findings are in line with the notion that structural motor network connectivity between ipsilesional M1 and (i) bilateral premotor areas as well as (ii) contralesional M1 supports both basal and complex motor function of the paretic arm and hand in chronic stroke patients. Considering the prominent role of the CST in motor control, we next addressed the question whether the observed correlations were dependent on the level of CST integrity by means of partial correlations.

Partial correlation analyses

Partial correlation analyses were performed to control for the effect of ipsilesional CST integrity on tractwise correlations with motor behavior. For basal motor control, results of correlation analyses and partial correlations were highly similar (Table 1; Fig. 3). In particular, anisotropy of all intrahemispheric premotor-*ilM1* connections (all $r > .59$, $p < .006$, FDR-corrected) were associated with basal motor control (Fig. 3B). Regarding interhemispheric connectivity, *clPMv-*ilM1** ($r = .53$, $p = .013$, FDR-corrected) as well as M1-M1 connectivity ($r = .45$, $p = .040$, FDR-corrected) also remained significant when controlling for CST integrity. In summary, structural connectivity between the ipsilesional M1 and (i) all ipsilesional premotor areas, (ii) contralesional PMv as well as (iii) contralesional M1 was associated with basal motor control independent of ipsilesional CST integrity.

In contrast, correlations between cortico-cortical connections and complex motor control were not independent of ipsilesional CST integrity (Table 1; Fig. 3B). No significant partial correlations were observed after correction for multiple comparisons. Considering that some premotor-M1 connections showed an FDR-corrected trend towards significance when controlling for CST damage (Table 1), compensation via premotor-M1 connections seemed to show a less pronounced reliance on CST fibers than compensation via the interhemispheric M1-M1 connection. Of note, after excluding lesion-affected tracts, Pearson correlations as well as partial correlations yielded highly similar results, corroborating the robustness of our findings (Supplementary Table 2).

In summary, our findings outline the crucial role of ipsilesional CST integrity for complex motor control after stroke, as compensatory effects at the cortical level seem to be limited in case of substantial ipsilesional CST damage.

Table 1: Correlation analyses between different aspects of motor control and cortico-cortical connections. Analyses were carried out separately for (i) basal and (ii) complex motor control. Partial correlations assessed the relationship between motor control and tractwise anisotropy while controlling for ipsilesional CST integrity. Bold font indicates significance after FDR-correction ($p < .05$). Asterisks signify the following significance thresholds: *** $p < .001$, ** $p < .01$, * $p < .05$. Results are visualized in Fig. 3.

connection	basal motor control			
	Pearson correlations		partial correlations	
	r	p (FDR)	r	p (FDR)
homologous				
cMI-iMI	0.62	0.002**	0.45	0.040*
intrahemispheric				
iPMd-iMI	0.63	0.002**	0.59	0.006**
iPMv-iMI	0.72	<0.001***	0.65	0.004**
iSMA-iMI	0.54	0.009**	0.59	0.006**
interhemispheric				
cPMd-iMI	0.31	0.134	0.25	0.246
cPMv-iMI	0.53	0.009**	0.53	0.013*
cSMA-iMI	0.43	0.036*	0.31	0.172
	complex motor control			
homologous				
cMI-iMI	0.49	0.023*	0.26	0.246
intrahemispheric				
iPMd-iMI	0.51	0.023*	0.44	0.068
iPMv-iMI	0.59	0.013*	0.49	0.057
iSMA-iMI	0.49	0.023*	0.53	0.052
interhemispheric				
cPMd-iMI	0.28	0.183	0.21	0.332
cPMv-iMI	0.44	0.033*	0.42	0.068
cSMA-iMI	0.45	0.032*	0.33	0.160

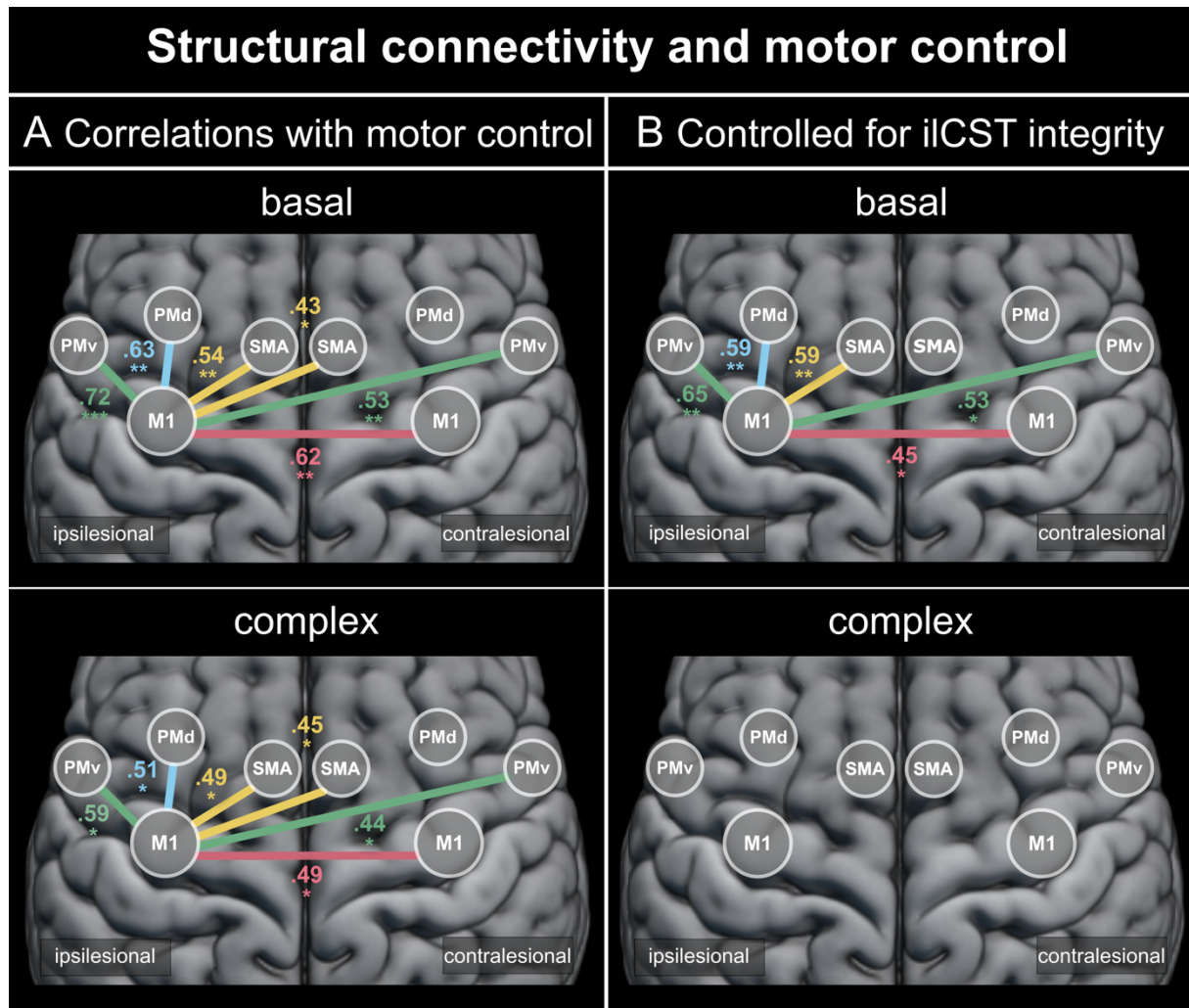


Figure 3: Association between structural motor network connectivity and motor control after stroke. Tractwise anisotropy of several cortico-cortical connections showed a significant association with basal or complex motor control. **(A)** Correlation coefficients of significant Pearson correlations. **(B)** Significant partial correlations of cortico-cortical connections with motor behavior when controlling for ipsilesional CST damage. All depicted connections were significant after FDR-correction for multiple comparisons ($p < .05$). Significance thresholds: *** $p < .001$, ** $p < .01$, * $p < .05$. *M1* = primary motor cortex, *PMd* = dorsal premotor cortex, *PMv* = ventral premotor cortex, *SMA* = supplementary motor area, *ilCST* = ipsilesional corticospinal tract

Motor network connectivity and motor recovery

Patients were divided into subgroups with ($N=15$) and without ($N=10$) substantial recovery of arm motor function to assess whether the degree of recovery impacted the association between structural motor connectivity and motor control. For patients featuring substantial recovery, basal motor control was strongly associated with mean anisotropy of the homologous cM1-*ilM1* tract ($r=.79$, $p=.003$, FDR-corrected; Table 2; Fig. 4A) but showed no significant association with premotor-M1 connectivity. Importantly, this association persisted when controlling for CST integrity ($r=.75$, $p=.016$, FDR-corrected).

Conversely, for patients showing no substantial recovery of arm motor function, the interhemispheric cIPMv-ilM1 connection ($r=.71$, $p=.036$, FDR-corrected) as well as intrahemispheric premotor-ilM1 connectivity was significantly correlated with motor control (all $r>.81$, $p<.011$, FDR-corrected; Table 2; Fig. 4A). Of note, no significant association was observed for the cIM1-ilM1 connection in patients without substantial recovery ($r=.44$, $p=.279$, FDR-corrected). When controlling for CST integrity, only the ilSMA-ilM1 connection yielded a significant correlation ($r=.87$, $p=.015$, FDR-corrected). Again, excluding directly affected cortico-cortical connections yielded highly similar results (Supplementary Table 3).

In summary, while patients with substantial motor recovery seemed to heavily rely on interhemispheric M1-M1 connectivity to ensure basal motor control, patients without substantial recovery of arm function featured no such association. Hence, our findings highlight an essential role of interhemispheric M1-M1 connectivity in motor recovery, which may serve as a critical route to recruit the intact contralesional motor network and its descending pathways to compensate for the lesion-induced impairment of motor control after stroke.

Table 2: Recovery-dependent subgroup analysis: Correlations analyses between basal motor control and cortico-cortical connections. Analyses were carried out separately for patients featuring (i) substantial or (ii) no substantial recovery as assessed by the difference in NIHSS-arm score in the acute and chronic stage. Partial correlations assessed the relationship between basal motor control and tractwise anisotropy while controlling for ipsilesional CST integrity. Bold font indicates significance after FDR-correction ($p < .05$). Asterisks signify the following significance thresholds: *** $p < .001$, ** $p < .01$, * $p < .05$. Results are visualized in Fig. 4.

connection	substantial recovery			
	Pearson correlations		partial correlations	
	r	p (FDR)	r	p (FDR)
homologous				
cIMI-iIMI	0.79	0.003**	0.75	0.016*
intrahemispheric				
iIPMd-iIMI	0.25	0.492	0.30	0.427
iIPMv-iIMI	0.58	0.081	0.55	0.153
iISMA-iIMI	0.05	0.862	0.19	0.549
interhemispheric				
cIPMd-iIMI	0.22	0.492	0.18	0.549
cIPMv-iIMI	0.31	0.467	0.34	0.416
cISMA-iIMI	0.50	0.139	0.42	0.325
	no substantial recovery			
homologous				
cIMI-iIMI	0.44	0.279	0.17	0.657
intrahemispheric				
iIPMd-iIMI	0.85	0.007**	0.77	0.053
iIPMv-iIMI	0.81	0.010*	0.73	0.060
iISMA-iIMI	0.90	0.003**	0.87	0.015*
interhemispheric				
cIPMd-iIMI	0.33	0.392	0.34	0.521
cIPMv-iIMI	0.71	0.036*	0.68	0.076
cISMA-iIMI	0.30	0.392	0.21	0.657

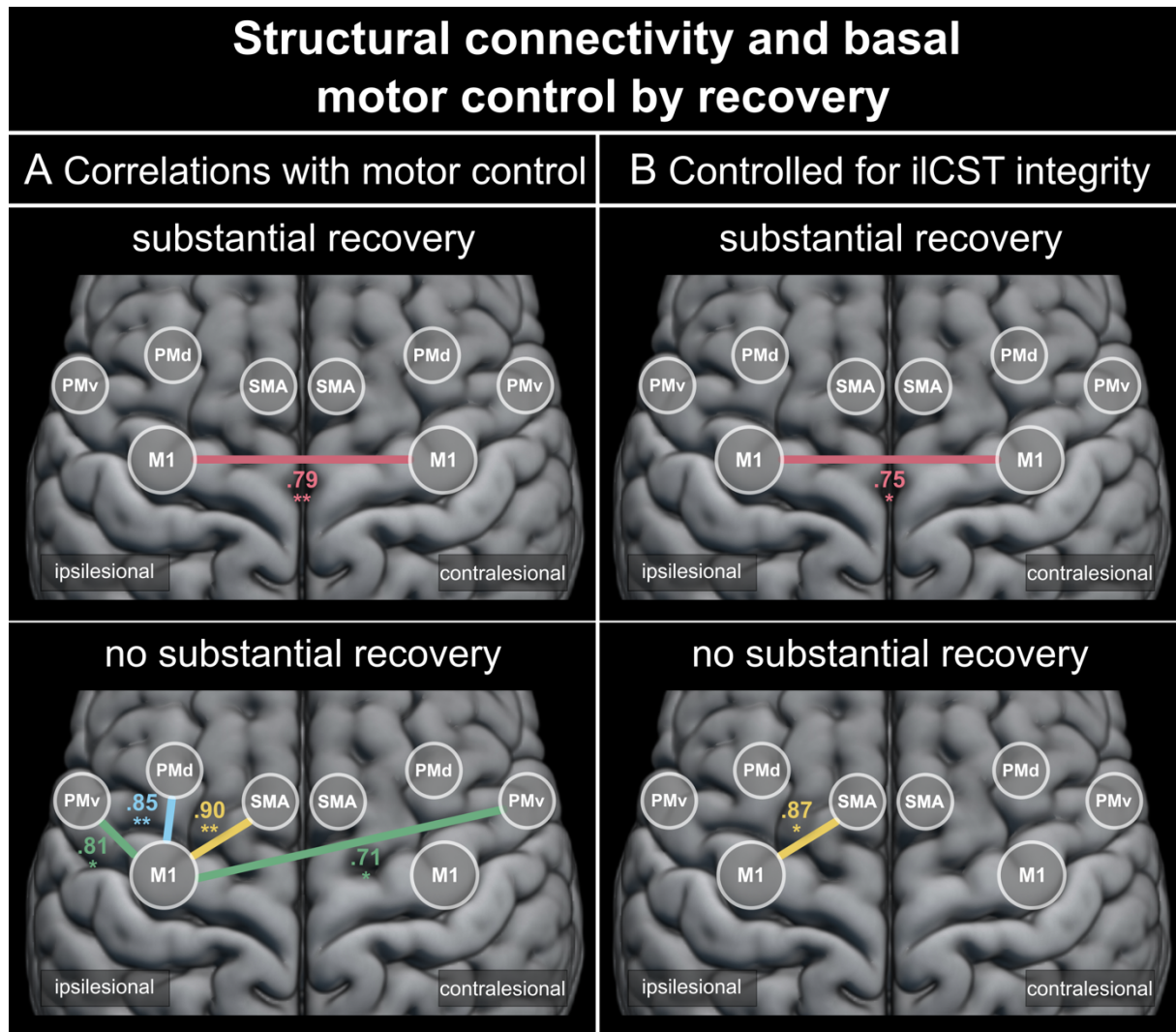


Figure 4: Recovery-dependent subgroup analysis: associations between structural motor network connectivity and basal motor control after stroke. (A) Significant Pearson correlations between tractwise anisotropy and basal or complex motor control for patients showing (i) substantial or (ii) no substantial recovery. (B) Significant partial correlations between tractwise anisotropy and basal motor control when controlling for ipsilesional CST integrity in patients featuring (i) substantial or (ii) no substantial recovery. Of note, only subjects featuring substantial recovery of arm motor function showed an association of interhemispheric M1-M1 connectivity with basal motor control, highlighting a compensatory role of transcallosal fibers. All depicted connections were significant after FDR-correction for multiple comparisons ($p < .05$). Significance thresholds: *** $p < .001$, ** $p < .01$, * $p < .05$. M1 = primary motor cortex, PMd = dorsal premotor cortex, PMv = ventral premotor cortex, SMA = supplementary motor area, iICST = ipsilesional corticospinal tract

Stepwise linear backward regressions

First, we assessed the propensity of CST integrity to explain behavioral impairment. For basal motor control, 28% of variance ($R^2 = 27.71\%$, adjusted $R^2 = 24.57\%$, $p = .007$, $BIC = 132.46$) was explained by the ipsilesional CST. A highly similar result was obtained for complex motor control ($R^2 = 27.77\%$, adjusted $R^2 = 24.63\%$, $p = .007$, $BIC = 130.88$). Stepwise backward regression models including cortico-cortical connections and ipsilesional CST integrity explained a high amount of variance for both basal and complex motor control. Specifically, 71% of variance in basal motor control ($R^2 = 71.01\%$, adjusted $R^2 = 65.22\%$, $p < .001$, $BIC = 119.27$) and 60% of variance in complex motor control ($R^2 = 60.17\%$, adjusted $R^2 = 46.90\%$,

$p=.006$, $BIC=132.09$) were captured. When excluding the ipsilesional CST and only using cortico-cortical connections to start the backward elimination process, the resulting model still explained a substantial amount of variance in basal motor control ($R^2=63.26\%$, adjusted $R^2=58.01\%$, $p<.001$, $BIC=121.98$). Conversely, while complex motor control was still explained significantly ($R^2=35.02\%$, adjusted $R^2=32.19\%$, $p=.002$, $BIC=128.24$), the ratio of explained variance in complex motor control considerably decreased after ipsilesional CST exclusion. Thus, the stepwise linear backward regression analyses showed that structural motor network connectivity holds valuable information on motor control across subjects. While basal motor control is readily explained by cortico-cortical connectivity, complex motor control crucially relies on ipsilesional CST integrity.

Discussion

Motor control is assumed to rely on a distributed network of cortical and subcortical motor areas, as well as its descending pathways such as the CST.³² At the cortical level, premotor areas are crucially involved in shaping motor commands in M1 via dense cortico-cortical connections.³³ After stroke-inflicted CST damage, the question arises how the motor network can reorganize its functional architecture to recover motor control. From a mechanistic perspective, stronger structural cortico-cortical connections may allow for a more flexible and efficient transmission of motor signals, thereby enabling increased influences of bilateral premotor areas onto ipsilesional M1.⁵ Alternatively, retrograde coupling from M1 onto premotor areas might also play a role in compensating motor control. In this case, output signals that cannot be transmitted through damaged CST fibers originating from M1 might be relayed via CST fibers descending from premotor areas or non-crossing contralesional CST fibers originating from contralesional M1. Of note, the interplay and functional significance of these proposed mechanisms remains largely unknown and has resulted in conflicting interpretations of previous findings. Given that recovery of basal and complex movements has been shown to differentially benefit from rehabilitation,³⁴ we hypothesized that both derive from distinct mechanisms.

Complex motor control

After stroke, intact structural connections are thought to enable the functional reorganization of motor network dynamics to facilitate recovery. In line with this assumption, we here observed significant correlations between complex motor skills and cortico-cortical connectivity from contralesional M1 and bilateral premotor areas to the ipsilesional M1 (Fig. 3A). However, when controlling for ipsilesional CST integrity, no significant correlations were observed between cortico-cortical motor connections and complex motor control (Fig. 3B). In other words, while partial correlations with intrahemispheric premotor-M1 connectivity showed a trend towards significance (Table 1), similar variance in complex motor control was captured by anisotropy of ipsilesional CST and cortico-cortical connectivity. An explanation for this observation may derive from previous results indicating that motor performance post-stroke critically relies on the task-dependent modulation of ipsilesional premotor-M1 connectivity.^{5,7} Hence, premotor areas may use intact structural cortico-cortical connections to enhance recruitment of the ipsilesional M1. However, the potential to adapt hand motor output signals on the cortical level may be critically limited in case of extensive CST damage, stressing the significance of ipsilesional CST integrity. This notion is well in line with earlier studies frequently reporting correlations between ipsilesional CST integrity and hand motor function.^{2,35-38} Moreover, our stepwise regression analyses performed best when including CST anisotropy in the starting model. In other words, the CST explained relevant behavioral variance in addition to the information contained in cortico-cortical connectivity. Thus, complex motor commands seem to critically rely on ipsilesional CST output signals.

Basal motor control

We conceptualized basal motor control as simple movements that require only basic control of specific muscle synergies such as lifting the arm against gravity. While previous diffusion imaging studies have not typically differentiated basal and complex motor control, more basal motor functions have previously been associated with varying features of ipsilesional premotor-M1^{11,17,18} as well as transcallosal M1-M1¹¹⁻¹⁴ structural connectivity, painting a rather inconclusive picture. We here observed associations of the MI-arm with anisotropy of all three ipsilesional premotor-M1 connections, interhemispheric premotor-M1 connectivity, and interhemispheric M1-M1 connectivity (Fig. 3A). From a mechanistic perspective, stronger structural cortico-cortical connections may allow for a more flexible and efficient transmission of motor signals, thereby enabling increased influences of bilateral premotor areas onto

ipsilesional M1.⁵ Alternatively, retrograde coupling from M1 onto premotor areas might also play a role in compensating basal motor skills. In this case, output signals that cannot be transmitted through damaged CST fibers originating from M1 might be relayed via CST fibers descending from premotor areas. Of note, partial correlation analyses keeping the influence of ipsilesional CST anisotropy constant revealed that associations between cortico-cortical connections and basal motor control were largely independent of CST integrity (Fig. 3B). In other words, basal motor performance showed less reliance on CST anisotropy than complex motor control. The fact that anisotropy between bilateral M1 was significantly associated with basal motor control but not complex motor control indicates that basal but not complex motor skills may be compensated via recruitment of the contralesional M1. Importantly, the contralesional M1 has access to alternative descending routes such as the intact contralesional CST which may relay motor output signals from ipsilesional M1.²³

Our findings thus highlight a differential role of interhemispheric M1-M1 structural connectivity for basal and complex motor control which helps to shed light on the heavily debated role of the contralesional M1. While some authors have argued that the contralesional M1 serves a vicarious role by contributing to motor control of the paretic hand,³⁹⁻⁴² other results favor a maladaptive influence of the contralesional M1.⁴³⁻⁴⁵ Maladaptation is frequently conceptualized to result from increased inhibitory influences exerted by the contralesional M1 onto the ipsilesional M1 as demonstrated by transcranial magnetic stimulation⁴⁴ and fMRI-based effective connectivity.^{43,46}

Conversely, the contralesional M1 may play a supportive role by (i) exerting facilitatory influences on the ipsilesional M1⁵ or by (ii) offering an alternative route for descending motor commands via the contralesional CST. As non-crossing CST fibers predominantly innervate proximal arm and shoulder muscles,³² this pathway is situated to support proximal arm and shoulder movements rather than fine motor control of the hand and fingers. Our current findings are perfectly in line with this notion as basal motor control involving proximal muscle groups but not complex motor control was associated with interhemispheric connectivity.

Moreover, our recovery-dependent results emphasize that interhemispheric M1-M1 connectivity constitutes a structural reserve for the reorganization of basal motor control. Patients featuring substantial recovery of motor function showed strong correlations between interhemispheric M1-M1 connectivity and basal motor control independent of ipsilesional CST integrity (Fig. 4). Support for this notion stems from Stewart and colleagues who reported anisotropy of callosal motor regions to be linked to (basal) motor control in patients with

favorable motor outcomes at the chronic stage.¹⁴ Hence, recovery of basal motor function seems to depend on a patient's ability to recruit the contralesional M1 via interhemispheric callosal fibers.

Clinical relevance

Our current findings highlight the potential of structural cortico-cortical motor network connectivity as a biomarker to predict motor impairment following stroke. Structural scans can be easily integrated into the clinical routine as they only require little patient compliance.^{47,48} For example, the DSI scanning protocol used in the present study offers a fast acquisition time of only 11 minutes. However, the reliable assessment of cortical-cortical connectivity via anisotropy is hindered by voxels with multiple fiber directions. To overcome this problem we employed a compartmentwise approach that differentiates voxels according to the number of trackable fiber directions.³⁰ Importantly, stepwise backward regression analyses yielded a high ratio of explained variance for both basal and complex motor skills, by far exceeding the ratio of explained variance achieved by CST integrity alone. Adding CST integrity as a variable to the starting model of the stepwise backward regression drastically increased the percentage of explained variance for complex motor control yet only yielded little additional explained variance for basal motor performance. Thus, a potential biomarker should ideally be task-specific and focus on cortico-cortical connectivity for basal motor skills while including cortico-cortical connectivity and CST integrity in concert for complex motor skills.

Limitations

A major limitation pertains to the limited sample size of 25 chronic stroke patients. While this sample size is not unusual for hypothesis-driven imaging studies in patient cohorts, a larger sample size would allow for additional analyses. Moreover, one might argue that our results may have been biased by lesions affecting cortico-cortical connections. However, most patients featured subcortical lesions that primarily affected the internal capsule. Thus, cortico-cortical tracts were hardly ever directly affected. Moreover, repeating the analyses without subjects showing a significant lesion overlap with specific cortico-cortical connections yielded highly similar results. Thus, a considerable lesion-induced bias seems unlikely.

Conclusion

Our current findings highlight the seminal importance of structural cortico-cortical motor network connectivity which serves as a structural reserve for distinct aspects of motor control post-stroke. Our data emphasize that complex motor control depends on an interplay of cortico-cortical information integration and descending motor commands via the ipsilesional CST. Thus, severe CST damage seems to preclude the control of complex motor functions of the paretic hand. Conversely, basal motor control can be successfully compensated via alternative routes: Interhemispheric pathways between bilateral M1 seem to play a crucial role in relaying motor commands to the contralesional motor cortex. This might help to access intact descending pathways such as non-crossing fibers of the contralesional CST.²³ Especially patients who underwent substantial recovery from the acute to the chronic stage post-stroke seemed to heavily rely on this route emphasizing its seminal role in functional reorganization of basal motor control. Finally, our results identified a combination of cortico-cortical structural connectivity and CST integrity as a possible biomarker for basal and complex motor functions after stroke which is emphasized by the high degree of explained behavioral variance when using both in concert.

Acknowledgements

GRF gratefully acknowledges support from the Marga and Walter Boll Stiftung, Kerpen, Germany. CG and GRF are funded by the Deutsche Forschungsgemeinschaft (DFG, German Research Foundation) – Project-ID 431549029 – SFB 1451. STG was supported by the Institute for Collaborative Biotechnologies under Cooperative Agreement W911NF-19-2-0026 with the Army Research Office.

Author contributions

TP, CG, STG, GRF and LJV contributed to the conception and design of the study. TP, VMW, LH and CT made substantial contributions to the acquisition of the data. TP, VMW, MC and LJV contributed to the analysis of the data. TP, VMW, STG and LJV contributed significantly to drafting the manuscript and figures. All authors have critically revised and finally approved the version of the paper to be published.

Potential conflicts of interest

The authors report no competing interests.

Supplementary material

Supplementary material is available online.

References

1. Koch P, Schulz R, Hummel FC. Structural connectivity analyses in motor recovery research after stroke. *Ann Clin Transl Neurol*. 2016;3(3):233-244. doi:10.1002/acn3.278
2. Boyd LA, Hayward KS, Ward NS, et al. Biomarkers of stroke recovery: Consensus-based core recommendations from the Stroke Recovery and Rehabilitation Roundtable. *Int J Stroke*. 2017;12(5):480-493. doi:10.1177/1747493017714176
3. Pool EM, Rehme AK, Fink GR, Eickhoff SB, Grefkes C. Network dynamics engaged in the modulation of motor behavior in healthy subjects. *Neuroimage*. 2013;82:68-76. doi:10.1016/j.neuroimage.2013.05.123
4. Grefkes C, Ward NS. Cortical Reorganization After Stroke. *Neurosci*. 2014;20(1):56-70. doi:10.1177/1073858413491147
5. Rehme AK, Eickhoff SB, Wang LE, Fink GR, Grefkes C. Dynamic causal modeling of cortical activity from the acute to the chronic stage after stroke. *Neuroimage*. 2011;55(3):1147-1158. doi:10.1016/j.neuroimage.2011.01.014
6. Rehme AK, Grefkes C. Cerebral network disorders after stroke: evidence from imaging-based connectivity analyses of active and resting brain states in humans. *J Physiol*. 2013;591(1):17-31. doi:10.1113/jphysiol.2012.243469
7. Paul T, Hensel L, Rehme AK, et al. Early motor network connectivity after stroke: An interplay of general reorganization and state-specific compensation. *Hum Brain Mapp*. 2021;42(16):5230-5243. doi:10.1002/hbm.25612
8. Golestani AM, Tymchuk S, Demchuk A, Goodyear BG. Longitudinal Evaluation of Resting-State fMRI After Acute Stroke With Hemiparesis. *Neurorehabil Neural Repair*. 2013;27(2):153-163. doi:10.1177/1545968312457827
9. Rubinov M, Sporns O. Complex network measures of brain connectivity: Uses and interpretations. *Neuroimage*. 2010;52(3):1059-1069. doi:10.1016/j.neuroimage.2009.10.003
10. Di Pino G, Pellegrino G, Assenza G, et al. Modulation of brain plasticity in stroke: A novel model for neurorehabilitation. *Nat Rev Neurol*. 2014;10(10):597-608. doi:10.1038/nrneurol.2014.162
11. Peters DM, Fridriksson J, Stewart JC, et al. Cortical disconnection of the ipsilesional primary motor cortex is associated with gait speed and upper extremity motor impairment in chronic left hemispheric stroke. *Hum Brain Mapp*. 2018;39(1):120-132. doi:10.1002/hbm.23829
12. Chen JL, Schlaug G. Resting State Interhemispheric Motor Connectivity and White Matter Integrity Correlate with Motor Impairment in Chronic Stroke. *Front Neurol*. 2013;4. doi:10.3389/fneur.2013.00178
13. Hayward K, Ferris JK, Lohse KR, et al. Observational Study of Neuroimaging Biomarkers of Severe Upper Limb Impairment After Stroke. *Neurology*. Published online May 12, 2022:1-42. doi:10.1212/WNL.0000000000200517
14. Stewart JC, Dewanjee P, Tran G, et al. Role of corpus callosum integrity in arm function differs based on motor severity after stroke. *NeuroImage Clin*. 2017;14:641-647. doi:10.1016/j.nicl.2017.02.023
15. Wang LE, Tittgemeyer M, Imperati D, et al. Degeneration of corpus callosum and

- recovery of motor function after stroke: A multimodal magnetic resonance imaging study. *Hum Brain Mapp.* 2012;33(12):2941-2956. doi:10.1002/hbm.21417
16. Lindenberg R, Zhu LL, Rüber T, Schlaug G. Predicting functional motor potential in chronic stroke patients using diffusion tensor imaging. *Hum Brain Mapp.* 2012;33(5):1040-1051. doi:10.1002/hbm.21266
 17. Schulz R, Braass H, Liuzzi G, et al. White matter integrity of premotor–motor connections is associated with motor output in chronic stroke patients. *NeuroImage Clin.* 2015;7:82-86. doi:10.1016/j.nicl.2014.11.006
 18. Schulz R, Park E, Lee J, et al. Interactions Between the Corticospinal Tract and Premotor–Motor Pathways for Residual Motor Output After Stroke. *Stroke.* 2017;48(10):2805-2811. doi:10.1161/STROKEAHA.117.016834
 19. Schlemm E, Schulz R, Bönstrup M, et al. Structural brain networks and functional motor outcome after stroke—a prospective cohort study. *Brain Commun.* 2020;2(1):1-13. doi:10.1093/braincomms/fcaa001
 20. Kalinosky BT, Schindler-Ivens S, Schmit BD. White matter structural connectivity is associated with sensorimotor function in stroke survivors. *NeuroImage Clin.* 2013;2(1):767-781. doi:10.1016/j.nicl.2013.05.009
 21. Paul T, Cieslak M, Hensel L, et al. The role of corticospinal and extrapyramidal pathways in motor impairment after stroke. *Brain Commun.* Published online 2022. doi:10.1093/braincomms/fcac301
 22. Yeh FC, Panesar S, Fernandes D, et al. Population-averaged atlas of the macroscale human structural connectome and its network topology. *Neuroimage.* 2018;178(April):57-68. doi:10.1016/j.neuroimage.2018.05.027
 23. Schaechter JD, Fricker ZP, Perdue KL, et al. Microstructural status of ipsilesional and contralesional corticospinal tract correlates with motor skill in chronic stroke patients. *Hum Brain Mapp.* 2009;30(11):3461-3474. doi:10.1002/hbm.20770
 24. Lyle RC. A performance test for assessment of upper limb function in physical rehabilitation treatment and research. *Int J Rehabil Res.* 1981;4(4):483-492. doi:10.1097/00004356-198112000-00001
 25. Demeurisse G, Demol O, Robaye E. Motor Evaluation in Vascular Hemiplegia. *Eur Neurol.* 1980;19(6):382-389. doi:10.1159/000115178
 26. Cieslak M, Cook PA, He X, et al. QSIPrep: an integrative platform for preprocessing and reconstructing diffusion MRI data. *Nat Methods.* 2021;18(7):775-778. doi:10.1038/s41592-021-01185-5
 27. Avants BB, Epstein CL, Grossman M, Gee JC. Symmetric diffeomorphic image registration with cross-correlation: evaluating automated labeling of elderly and neurodegenerative brain. *Med Image Anal.* 2008;12(1):26-41. doi:10.1016/j.media.2007.06.004
 28. Volz LJ, Sarfeld AS, Diekhoff S, et al. Motor cortex excitability and connectivity in chronic stroke: a multimodal model of functional reorganization. *Brain Struct Funct.* 2015;220(2):1093-1107. doi:10.1007/s00429-013-0702-8
 29. Yeh FC, Verstynen TD, Wang Y, Fernández-Miranda JC, Tseng WYI. Deterministic diffusion fiber tracking improved by quantitative anisotropy. *PLoS One.* 2013;8(11):1-16. doi:10.1371/journal.pone.0080713
 30. Volz LJ, Cieslak M, Grafton ST. A probabilistic atlas of fiber crossings for variability

- reduction of anisotropy measures. *Brain Struct Funct*. 2018;223(2):635-651. doi:10.1007/s00429-017-1508-x
31. Benjamini Y, Hochberg Y. Controlling the False Discovery Rate: A Practical and Powerful Approach to Multiple Testing. *J R Stat Soc Ser B*. 1995;57(1):289-300. doi:10.1111/j.2517-6161.1995.tb02031.x
 32. Lemon RN. Descending Pathways in Motor Control. *Annu Rev Neurosci*. 2008;31(1):195-218. doi:10.1146/annurev.neuro.31.060407.125547
 33. Strick PL, Dum RP, Rathelot JA. The Cortical Motor Areas and the Emergence of Motor Skills: A Neuroanatomical Perspective. *Annu Rev Neurosci*. 2021;44(1):425-447. doi:10.1146/annurev-neuro-070918-050216
 34. George SH, Rafiei MH, Borstad A, Adeli H, Gauthier L V. Gross motor ability predicts response to upper extremity rehabilitation in chronic stroke. *Behav Brain Res*. 2017;333(June):314-322. doi:10.1016/j.bbr.2017.07.002
 35. Puig J, Blasco G, Daunis-I-Estadella J, et al. Decreased Corticospinal Tract Fractional Anisotropy Predicts Long-term Motor Outcome After Stroke. *Stroke*. 2013;44(7):2016-2018. doi:10.1161/STROKEAHA.111.000382
 36. Stinear CM, Barber PA, Smale PR, Coxon JP, Fleming MK, Byblow WD. Functional potential in chronic stroke patients depends on corticospinal tract integrity. *Brain*. 2007;130(Pt 1):170-180. doi:10.1093/brain/awl333
 37. Lindenberg R, Renga V, Zhu LL, Betzler F, Alsop D, Schlaug G. Structural integrity of corticospinal motor fibers predicts motor impairment in chronic stroke. *Neurology*. 2010;74(4):280-287. doi:10.1212/WNL.0b013e3181ccc6d9
 38. Peters DM, Fridriksson J, Richardson JD, et al. Upper and Lower Limb Motor Function Correlates with Ipsilesional Corticospinal Tract and Red Nucleus Structural Integrity in Chronic Stroke: A Cross-Sectional, ROI-Based MRI Study. Tambasco N, ed. *Behav Neurol*. 2021;2021:1-10. doi:10.1155/2021/3010555
 39. Biernaskie J, Szymanska A, Windle V, Corbett D. Bi-hemispheric contribution to functional motor recovery of the affected forelimb following focal ischemic brain injury in rats. *Eur J Neurosci*. 2005;21(4):989-999. doi:10.1111/j.1460-9568.2005.03899.x
 40. Johansen-Berg H, Rushworth MFS, Bogdanovic MD, Kischka U, Wimalaratna S, Matthews PM. The role of ipsilateral premotor cortex in hand movement after stroke. *Proc Natl Acad Sci*. 2002;99(22):14518-14523. doi:10.1073/pnas.222536799
 41. Lotze M, Markert J, Sauseng P, Hoppe J, Plewnia C, Gerloff C. The role of multiple contralesional motor areas for complex hand movements after internal capsular lesion. *J Neurosci*. 2006;26(22):6096-6102. doi:10.1523/JNEUROSCI.4564-05.2006
 42. Rehme AK, Fink GR, von Cramon DY, Grefkes C. The Role of the Contralesional Motor Cortex for Motor Recovery in the Early Days after Stroke Assessed with Longitudinal fMRI. *Cereb Cortex*. 2011;21(4):756-768. doi:10.1093/cercor/bhq140
 43. Grefkes C, Nowak DA, Eickhoff SB, et al. Cortical connectivity after subcortical stroke assessed with functional magnetic resonance imaging. *Ann Neurol*. 2008;63(2):236-246. doi:10.1002/ana.21228
 44. Murase N, Duque J, Mazzocchio R, Cohen LG. Influence of interhemispheric interactions on motor function in chronic stroke. *Ann Neurol*. 2004;55(3):400-409. doi:10.1002/ana.10848
 45. Takeuchi N, Izumi SI. Maladaptive Plasticity for Motor Recovery after Stroke:

- Mechanisms and Approaches. *Neural Plast.* 2012;2012:1-9. doi:10.1155/2012/359728
46. Grefkes C, Nowak DA, Wang LE, Dafotakis M, Eickhoff SB, Fink GR. Modulating cortical connectivity in stroke patients by rTMS assessed with fMRI and dynamic causal modeling. *Neuroimage.* 2010;50(1):233-242. doi:10.1016/j.neuroimage.2009.12.029
 47. Horn U, Grothe M, Lotze M. MRI Biomarkers for Hand-Motor Outcome Prediction and Therapy Monitoring following Stroke. *Neural Plast.* 2016;2016:1-12. doi:10.1155/2016/9265621
 48. Bonkhoff AK, Grefkes C. Precision medicine in stroke: towards personalized outcome predictions using artificial intelligence. *Brain.* 2022;145(2):457-475. doi:10.1093/brain/awab439

Supplement

Supplementary Table 1: Demographic and clinical patient information. *f = female, m = male, l = left, r = right, MCA = middle cerebral artery, PCA = posterior cerebral artery, ACA = anterior cerebral artery*

patient	sex	lesion side	lesion location	ARAT	MI-arm	NIHSS-arm acute	NIHSS-arm chronic	substantial recovery	months since stroke
1	m	r	MCA (subcortical)	57	99	2	0	yes	21
2	m	r	MCA (subcortical)	57	91	4	1	yes	14
3	m	r	MCA (subcortical)	38	76	1	1	no	17
4	m	l	MCA (subcortical)	0	34	3	4	no	51
5	m	l	PCA (subcortical)	35	92	1	1	no	23
6	f	l	MCA (subcortical)	32	77	1	2	no	11
7	m	l	MCA (subcortical)	19	65	3	2	yes	59
8	m	l	MCA (subcortical)	55	92	4	1	yes	71
9	m	l	ACA/MCA (subcortical)	57	99	0	0	no	31
10	m	r	MCA (subcortical)	49	91	1	1	no	12
11	m	l	MCA (subcortical)	57	99	1	0	yes	37
12	m	r	Brainstem	57	99	0	1	no	44
13	f	r	MCA (cortical)	56	91	3	0	yes	55
14	m	r	MCA (cortical)	57	99	4	0	yes	32
15	m	l	MCA (subcortical)	57	99	1	0	yes	43
16	f	r	MCA (subcortical)	57	76	2	1	yes	15
17	m	r	Brainstem	37	84	3	1	yes	82
18	m	l	Brainstem	44	83	1	1	no	30
19	f	l	Brainstem	56	76	1	1	no	12
20	m	l	PCA (subcortical)	55	92	1	0	yes	15
21	m	l	MCA (subcortical)	57	99	4	1	yes	33
22	m	l	MCA (sub- & cortical)	57	99	1	0	yes	25
23	m	r	MCA (subcortical)	53	99	1	0	yes	35
24	f	r	Brainstem	57	83	1	1	no	20
25	m	r	MCA (subcortical)	57	99	4	0	yes	23

Supplementary Table 2: Correlation analyses between different aspects of motor control and cortico-cortical connections after tract-specific subject exclusion. For three patients, distinct cortico-cortical tracts were excluded because lesions affected a considerable proportion (>10%) of the tract's one-directional voxels. Analyses were carried out separately for (i) basal and (ii) complex motor control. Partial correlations assessed the relationship between motor control and tractwise anisotropy while controlling for ipsilesional CST integrity. Bold font indicates significance after FDR-correction ($p < .05$). Asterisks signify the following significance thresholds: *** $p < .001$, ** $p < .01$, * $p < .05$.

connection	basal motor control			
	Pearson correlations		partial correlations	
	r	p (FDR)	r	p (FDR)
homologous				
cMI-iMI	0.62	0.002**	0.45	0.040*
intrahemispheric				
iPMd-iMI	0.66	0.002**	0.61	0.005**
iPMv-iMI	0.74	<0.001***	0.67	0.003**
iSMA-iMI	0.63	0.002**	0.65	0.003**
interhemispheric				
cPMd-iMI	0.31	0.134	0.25	0.246
cPMv-iMI	0.56	0.007**	0.54	0.013*
cSMA-iMI	0.43	0.036*	0.31	0.172
	complex motor control			
homologous				
cMI-iMI	0.49	0.022*	0.26	0.246
intrahemispheric				
iPMd-iMI	0.53	0.018*	0.45	0.073
iPMv-iMI	0.60	0.015*	0.49	0.073
iSMA-iMI	0.56	0.015*	0.56	0.035*
interhemispheric				
cPMd-iMI	0.28	0.183	0.21	0.332
cPMv-iMI	0.46	0.029*	0.43	0.073
cSMA-iMI	0.45	0.029*	0.33	0.160

Supplementary Table 3: Recovery-dependent subgroup analysis: Correlation analyses between basal motor control and cortico-cortical connections after tract-specific subject exclusion. For three patients, distinct cortico-cortical tracts were excluded because lesions affected a considerable proportion (>10%) of the tract's one-directional voxels. Analyses were carried out separately for patients featuring (i) substantial or (ii) no substantial recovery as assessed by the difference in NIHSS-arm score in the acute and chronic stage. Partial correlations assessed the relationship between basal motor control and tractwise anisotropy while controlling for ipsilesional CST integrity. Bold font indicates significance after FDR-correction ($p < .05$). Asterisks signify the following significance thresholds: *** $p < .001$, ** $p < .01$, * $p < .05$.

connection	substantial recovery			
	Pearson correlations		partial correlations	
	r	p (FDR)	r	p (FDR)
homologous				
cIMI-ilMI	0.79	0.003**	0.75	0.016*
intrahemispheric				
iPMd-ilMI	0.31	0.397	0.33	0.387
iPMv-ilMI	0.62	0.079	0.58	0.166
iSMA-ilMI	0.16	0.582	0.26	0.467
interhemispheric				
cPMd-ilMI	0.22	0.492	0.18	0.549
cPMv-ilMI	0.35	0.390	0.36	0.387
cSMA-ilMI	0.50	0.139	0.42	0.325
	no substantial recovery			
homologous				
cIMI-ilMI	0.44	0.279	0.17	0.657
intrahemispheric				
iPMd-ilMI	0.85	0.007**	0.77	0.053
iPMv-ilMI	0.81	0.010*	0.73	0.060
iSMA-ilMI	0.90	0.003**	0.87	0.015*
interhemispheric				
cPMd-ilMI	0.33	0.392	0.34	0.521
cPMv-ilMI	0.71	0.036*	0.68	0.076
cSMA-ilMI	0.30	0.392	0.21	0.657

5.4. Early motor network connectivity after stroke: An interplay of general reorganization and state-specific compensation

Theresa Paul, Lukas Hensel, Anne K. Rehme, Caroline Tscherpel, Simon B. Eickhoff, Gereon R. Fink, Christian Grefkes, Lukas J. Volz



Human Brain Mapping, Volume 42, Issue 16, 2021

<https://doi.org/10.1002/hbm.25612>

RESEARCH ARTICLE

WILEY

Early motor network connectivity after stroke: An interplay of general reorganization and state-specific compensation

Theresa Paul¹ | Lukas Hensel¹ | Anne K. Rehme¹ | Caroline Tschempel¹ |
Simon B. Eickhoff^{2,3} | Gereon R. Fink^{1,4} | Christian Grefkes^{1,4}  | Lukas J. Volz^{1,4} 

¹Department of Neurology, University Hospital Cologne, Cologne, Germany

²Institute of Neuroscience and Medicine, Brain & Behaviour (INM-7), Research Centre Juelich, Juelich, Germany

³Institute of Systems Neuroscience, Medical Faculty, Heinrich Heine University Duesseldorf, Duesseldorf, Germany

⁴Institute of Neuroscience and Medicine, Cognitive Neuroscience (INM-3), Research Centre Juelich, Juelich, Germany

Correspondence

Lukas J. Volz, Department of Neurology, University of Cologne, Kerpener Str. 62, 50937 Cologne, Germany.
Email: lukas.volz@uk-koeln.de

Funding information

Deutsche Forschungsgemeinschaft, Grant/Award Numbers: 431549029-SFB 1451, RE3014/2-1; Horizon 2020 Framework Programme, Grant/Award Numbers: 785907 (HBP SGA2), 945539 (HBP SGA3); Marga and Walter Boll Stiftung

Abstract

Motor recovery after stroke relies on functional reorganization of the motor network, which is commonly assessed via functional magnetic resonance imaging (fMRI)-based *resting-state functional connectivity (rsFC)* or *task-related effective connectivity (trEC)*. Measures of either connectivity mode have been shown to successfully explain motor impairment post-stroke, posing the question whether motor impairment is more closely reflected by rsFC or trEC. Moreover, highly similar changes in ipsilesional and interhemispheric motor network connectivity have been reported for both rsFC and trEC after stroke, suggesting that altered rsFC and trEC may capture similar aspects of information integration in the motor network reflecting principle, state-independent mechanisms of network reorganization rather than state-specific compensation strategies. To address this question, we conducted the first direct comparison of rsFC and trEC in a sample of early subacute stroke patients ($n = 26$, included on average 7.3 days post-stroke). We found that both rsFC and trEC explained motor impairment across patients, stressing the clinical potential of fMRI-based connectivity. Importantly, intrahemispheric connectivity between ipsilesional M1 and premotor areas depended on the activation state, whereas interhemispheric connectivity between homologs was state-independent. From a mechanistic perspective, our results may thus arise from two distinct aspects of motor network plasticity: task-specific compensation within the ipsilesional hemisphere and a more fundamental form of reorganization between hemispheres.

KEYWORDS

brain network connectivity, dynamic causal modeling (DCM), ischemic stroke, motor network reorganization, resting-state fMRI

1 | INTRODUCTION

Motor recovery after stroke relies on various intra- and inter-hemispheric processes aiming at compensating the loss of specialized neural tissue, commonly referred to as *functional reorganization*

(Cramer, 2008). In humans, cerebral reorganization can be assessed by functional magnetic resonance imaging (fMRI) and specifically by the analysis of connectivity, that is, changes in inter-regional interactions (Grefkes & Fink, 2014). In particular, two fMRI-based connectivity approaches have frequently revealed changes in the motor network

This is an open access article under the terms of the Creative Commons Attribution-NonCommercial License, which permits use, distribution and reproduction in any medium, provided the original work is properly cited and is not used for commercial purposes.

© 2021 The Authors. *Human Brain Mapping* published by Wiley Periodicals LLC.

after stroke: *resting-state functional connectivity (rsFC)* and *task-related effective connectivity (trEC)*. rsFC is typically estimated via temporal correlations between time series of different brain regions recorded at rest. It can be easily acquired even in severely affected patients, but is highly susceptible to confounds such as head motion (Power et al., 2014; Thiel & Vahdat, 2015). trEC describes the causal influence one brain region exerts on another (Friston, 1994). It is commonly estimated during task performance using Dynamic Causal Modeling (DCM), a model-based framework conceptualizing connectivity as directed facilitatory or inhibitory influences (Buxton, Wong, & Frank, 1998; Friston, Harrison, & Penny, 2003; Stephan & Friston, 2010). While trEC enables more specific insights regarding the nature of connectivity and causality, results are highly task- and model-dependent, which may limit their generalizability (Friston et al., 2003).

Assessing motor network connectivity during unilateral hand movements in healthy subjects, DCM has repetitively shown positive, excitatory coupling from bilateral premotor areas onto the primary motor cortex (M1) contralateral to the moving hand and negative, inhibitory coupling from the contralateral to the ipsilateral M1 (Grefkes, Eickhoff, Nowak, Dafotakis, & Fink, 2008; Pool, Rehme, Fink, Eickhoff, & Grefkes, 2013; Rehme, Eickhoff, Wang, Fink, & Grefkes, 2011; Volz, Sarfeld, et al., 2015). In the acute and subacute phase post-stroke, the excitatory influence from ipsilesional premotor areas onto ipsilesional M1 has been reported to be reduced, resulting in decreased excitation of the ipsilesional M1 during paretic hand movements (Rehme, Eickhoff, et al., 2011). Moreover, the inhibitory influences typically observed from ipsilesional M1 and premotor areas onto contralesional M1 were attenuated (Rehme, Eickhoff, et al., 2011). Importantly, altered trEC has been linked to stroke-induced motor impairment: ipsilesional influences of premotor areas on M1 and interhemispheric inputs onto contralesional M1 were related to motor performance and functional recovery (Grefkes et al., 2010; Grefkes & Ward, 2014; Rehme, Eickhoff, et al., 2011; Volz, Sarfeld, et al., 2015). Motor network alterations assessed via rsFC feature a characteristic time-course of changes deemed to reflect functional reorganization (Grefkes & Fink, 2014). Interhemispheric rsFC between bilateral motor areas, especially between bilateral M1, first decreases and subsequently re-increases alongside functional recovery, thereby resembling interhemispheric trEC changes (Carter et al., 2009, 2012; Golestani, Tymchuk, Demchuk, & Goodyear, 2013; Park et al., 2011; van Meer et al., 2010, 2012; Zheng et al., 2016). Moreover, increased rsFC between ipsilesional premotor areas and M1 has been found post-stroke and has also been linked to behavioral performance in line with findings obtained from DCM studies (Lee et al., 2017; Rehme, Volz, Feis, Bomilcar-Focke, et al., 2015; Volz et al., 2016).

In summary, both approaches highlight changes in ipsilesional premotor–M1 as well as interhemispheric motor network connectivity in the subacute phase post-stroke that relate to motor performance of the paretic hand. However, it remains unclear whether rsFC or trEC is better suited to explain motor impairment in (sub)acute stroke with implications for potential clinical applications. From a mechanistic perspective, the similarity of post-stroke changes in motor network connectivity between rsFC and trEC leads to the question whether some

fundamental aspects of stroke-induced changes in information integration may be similarly captured during rest and task-performance, that is, in a state-independent fashion by both rsFC and trEC. Conversely, both approaches probe the brain during vastly different physiological states: while rsFC describes the brain during wakeful rest, trEC reflects network interactions underlying the performance of a given task, resulting in largely unrelated motor network rsFC and trEC in healthy subjects (Rehme, Eickhoff, & Grefkes, 2013).

To address these questions, we here for the first time directly compared rsFC and trEC in a group of 26 acute to early subacute stroke patients tested within the first two weeks post-stroke. First, we probed the potential of both connectivity approaches to explain variance in motor impairment. Considering that trEC-estimates are based on data recorded during the performance of an active motor task, we expected trEC to be more closely related to motor performance than rsFC. Next, we assessed which aspects of both connectivity approaches were best suited to explain motor performance. Considering previous findings after stroke, we hypothesized that interhemispheric M1–M1 connectivity would be particularly relevant for both rsFC and trEC (Carter et al., 2009, 2012; Golestani et al., 2013; Park et al., 2011; van Meer et al., 2010, 2012; Zheng et al., 2016), while the driving input from ipsilesional premotor areas onto the affected M1 should be of particular importance for trEC (Grefkes et al., 2010; Grefkes & Ward, 2014; Rehme, Eickhoff, et al., 2011; Volz, Sarfeld, et al., 2015).

Second, we tested for an association between rsFC and trEC: If rsFC and trEC indeed reflected similar state-general aspects of information integration within the stroke-afflicted motor network, we would expect rsFC and trEC to be associated across patients. In particular, connections that typically exhibit stroke-induced alterations at rest and during task performance such as ipsilateral premotor–M1 and interhemispheric M1–M1 may show similar changes and may thus be associated across patients. Finally, aiming to disentangle whether differences between rsFC and trEC can be ascribed to the activation state (task vs. rest) or the connectivity mode (functional vs. effective), we additionally computed task-related functional connectivity (trFC). If motor network changes observed after stroke were primarily driven by the activity state of the brain, we would expect trFC and trEC to be associated across patients. Alternatively, if connectivity estimates were rather mode-dependent than state-dependent, that is, assuming that the methodological approach used to compute connectivity heavily impacted our observations, one would expect to find a correlation between trFC and rsFC. Besides further elucidating the clinical potential of fMRI-based motor network connectivity estimates as biomarkers reflecting motor impairment, our findings help to more accurately interpret the commonly observed changes in rsFC and trEC after stroke.

2 | METHODS

2.1 | Data set

fMRI data analyzed here were initially obtained to assess the longitudinal effect of repeated intermittent theta-burst-stimulation (iTBS) on

the recovery of hand function and motor network reorganization (Volz et al., 2016). To rule out any confounding effects of the iTBS-intervention, we here only analyzed data obtained at baseline, that is, before iTBS was applied.

2.2 | Participants

Twenty-six first-ever ischemic stroke patients (mean age = 67 years, $SD = 13$, 9 females, 22 right-handed) were recruited from the University Hospital of Cologne, Department of Neurology (see Table S1 for demographic and lesion information). Inclusion criteria comprised age between 40 and 90 years, ischemic stroke as verified by diffusion-weighted magnetic resonance imaging (DWI) with a symptom onset within the past 2 weeks (average: 7.3 days ± 3.6 , one patient was included 16 days after stroke), unilateral hand motor impairment, no lesions affecting M1 hand representation or other cortical areas used in the network analysis, no severe aphasia, apraxia, or neglect, no visual field deficits or other neurological disorders. Exclusion criteria were defined as any contraindications to transcranial magnetic stimulation or MRI, infarcts in multiple territories, and hemorrhagic stroke. The study was carried out under the Declaration of Helsinki and had been approved by the local ethics committee of the University of Cologne. All subjects provided informed consent.

2.3 | Data acquisition

Participants underwent fMRI scans consisting of a resting-state sequence of 7 min and the subsequent performance of an active motor task. During the motor task, participants performed 20 blocks of unimanual rhythmically paced fist-closures. Each block lasted for 15 s, interrupted by breaks of 15 s (plus a temporal jitter of 1–2.5 s). Left- or right-hand-use was randomized across blocks.

Motor performance was assessed on the day of the fMRI scan using three different behavioral measures. First, as a robust parameter of basal hand motor performance, relative grip strength was determined as the ratio between the maximum grip strength of the affected and unaffected hand. We further included the Jebsen Taylor Test of Hand Function (JTT, Jebsen, Taylor, Trieschmann, Trotter, & Howard, 1969) and the Action Research Arm Test (ARAT, Lyle, 1981) as representations of more complex upper limb motor skills. For the JTT, each subtest was timed with a maximum time limit of 120 s, which was also assigned in case a subtask could not be performed (Duncan et al., 1998). In line with previous work (Rehme, Fink, von Cramon, & Grefkes, 2011), we computed a composite motor score by extracting the first principal component from a principal component analysis (PCA) comprising relative grip strength, ARAT, and JTT scores (explained variance by the first component = 90.95%), resulting in a measure that generalizes across different aspects of hand motor function with higher motor scores reflecting better performance.

fMRI data were recorded using a Siemens Trio 3.0 Tesla scanner (Siemens Medical Solutions, Erlangen, Germany). Resting-state images

were acquired using a gradient-echo-planar (EPI) imaging sequence with the following parameters: repetition time (TR) = 2,200 ms, echo time (TE) = 30 ms, field of view (FOV) = 200 mm, 33 slices, voxel size: $3.1 \times 3.1 \times 3.1 \text{ mm}^3$, 20% distance factor, flip angle = 90° , 184 volumes. EPI volumes during the motor task were recorded using the same parameters for a total of 283 volumes. The slices covered the whole brain extending from the vertex to lower parts of the cerebellum. DWI were recorded to determine the localization and extent of acute stroke lesions (TR = 5,100 ms, TE = 104 ms, FOV = 230 mm, 30 slices, voxel size = $1.8 \times 1.8 \times 3.0 \text{ mm}^3$).

2.4 | Processing of fMRI data

Preprocessing of all fMRI-sequences was carried out using Statistical Parametric Mapping (SPM, The Wellcome Centre for Human Neuroimaging, London, UK, <http://www.fil.ion.ucl.ac.uk/>). Scans of six patients with right-hemispheric lesions were flipped along the mid-sagittal plane to ensure that all lesions were consistently located in the left hemisphere. The first four EPIs of each session were discarded as dummy images. The remaining volumes were realigned to the mean image of each time series. Based on the DWI showing the greatest lesion extent, we created lesion masks using MRICron (www.sph.sc.edu/comd/rorden/MRICron), which were applied to the functional images. The DWI and lesion masks were co-registered with the realigned EPI images. Spatial normalization to the standard template of the Montreal Neurological Institute (MNI) was achieved through unified segmentation (Ashburner & Friston, 2005). Images were spatially smoothed using an isotropic Gaussian kernel of 8 mm full-width-at-half-maximum (FWHM).

Smoothed EPIs of the fMRI motor task time series were temporally high-pass filtered at 1/128 s. For the first-level analysis, a general linear model (GLM) using box-car vectors for the three experimental conditions (affected hand movement, unaffected hand movement, visual instructions) convolved with a canonical hemodynamic response function was used. Realignment parameters were included as covariates to reduce movement-related variance. For the second-level analysis, the first-level parameter estimates of the conditions “movement of the affected hand” and “movement of the unaffected hand” were entered into a full-factorial design with the within-subject factor “hand” (levels: unaffected vs. affected). The significance threshold for voxel-wise activation was set to $T > 5.1$ ($p < .05$, family-wise error-corrected at the voxel-level).

While trying to keep the preprocessing of resting-state and task-based fMRI data as similar as possible, several methodological idiosyncrasies resulted in subtle differences between both approaches. To remove variance attributable to known confounds from the resting-state time series, we included the six head motion parameters, their squared values and their first-order derivatives, as well as the mean-centered global gray matter, white matter, and cerebrospinal fluid signal intensities per time point obtained by averaging across tissue-class-specific voxels and their squared values as confound regressors into the analysis (Power et al., 2014; Satterthwaite et al., 2013).

Of note, for our primary analyses we did not use PCA-denoising to minimize preprocessing differences of resting-state and task-related data. A temporal bandpass filter was applied, retaining only frequencies between 0.01 and 0.08 Hz (Biswal, Zerrin Yetkin, Haughton, & Hyde, 1995; Fox & Raichle, 2007). To probe for the robustness of our results, we repeated our analyses (a) with PCA-denoising, using the first five principal components extracted by means of a PCA as regressors and (b) without global signal regression (GSR).

2.5 | Estimation of task-related effective connectivity

The analysis of trEC was carried out using DCM as implemented in SPM 12 (SPM12, The Wellcome Centre for Human Neuroimaging, London, UK, <http://www.fil.ion.ucl.ac.uk/>). DCM treats the brain as a deterministic and dynamic system in which inputs, that is, experimental conditions, cause the system to enter a specific state, which hence generates a certain output, that is, the local blood-oxygen-level-dependent signal (Friston et al., 2003). The following bilinear differential state equation expresses state changes over time:

$$\frac{dz}{dt} = \left[A + \sum_{j=1}^m u_j B^{(j)} \right] z + Cu$$

Z represents the neuronal state the system is in, u stands for the experimental input, and A, B, and C are matrices containing the coupling parameters, that is, the rates of change in neuronal population activity that arise from synaptic influences (Stephan et al., 2010; Stephan & Friston, 2010). More specifically, matrix A contains the endogenous connectivity inherent to the system in the absence of external perturbations. Matrix B captures the state changes elicited by external inputs such as experimental conditions, while matrix C contains the corresponding extrinsic influences. Thus, in our case, there were two DCM-B-matrices, one capturing changes elicited by affected hand movements and the other capturing changes related to unaffected hand movements. Of note, DCM is a hypothesis-driven technique that relies on a priori assumptions about the relevant brain regions involved. As computational constraints limit the maximum number of regions, we focused on regions highlighted as essential for the motor recovery process after stroke: bilateral M1, supplementary motor area (SMA), and ventral premotor cortex (PMv) (Grefkes, Nowak, et al., 2008; Grefkes et al., 2010; Rehme, Eickhoff, et al., 2011).

For each region of interest (ROI), we extracted the first eigenvariate of the time series adjusted for effects of interest within a 10 mm sphere around the local activation maximum (see Table S2 for the subject-specific VOI coordinates). The regions were determined individually for each subject by superimposing the subject-specific activation maps showing the contrasts “movement of the unaffected hand vs. rest” for regions in the right hemisphere and “movement of the affected hand vs. rest” for regions in the left hemisphere on a corresponding T1-weighted image. In line with previous work,

definition of local activation maxima was aided by anatomical landmarks (Rehme, Eickhoff, et al., 2011; Volz, Sarfeld, et al., 2015): M1 on the rostral wall of the central sulcus (“hand knob formation”) (Yousry, 1997), SMA on the medial wall within the interhemispheric fissure between the paracentral lobule and the coronal plane running through the anterior commissure (Picard & Strick, 2001), and PMv near the inferior precentral gyrus and pars opercularis (Rizzolatti, Fogassi, & Gallese, 2002). Determining individual ROIs via the local activation maximum enabled us to rule out that ROIs fell into lesioned and therefore no longer functional brain areas.

We computed a total of 44 DCMs that differed concerning their task-related DCM-B matrix, while the fully connected endogenous DCM-A matrix remained constant (Rehme, Eickhoff, et al., 2011; Volz, Sarfeld, et al., 2015). Driving inputs were set on the premotor regions, that is, bilateral SMA and PMv, and the DCM-C matrix was designed accordingly. We generated 44 models differing in task-related connectivity structures (i.e., DCM-B matrix, cf. Figure S1), grouped into four model families differing in terms of lateralization and directionality: (a) nonlateralized/bidirectional, (b) lateralized/bidirectional, (c) non-lateralized/unidirectional, and (d) lateralized/bidirectional. Directionality specified whether M1 only received inputs (unidirectional) or whether there was a feedback onto premotor areas (bidirectional). Lateralization described whether connections targeting bilateral M1 were present in the DCM-B matrix for movements of each hand (nonlateralized) or whether only the M1 contralateral to the moving hand was assumed to interact with premotor areas (lateralized).

To determine the model with the best balance between model fit and generalizability (“winning model”), we performed a Bayesian Model Selection (BMS) random effects analysis across all 44 models (Stephan, Penny, Daunizeau, Moran, & Friston, 2009). Additionally, Bayesian Model Averaging (BMA) was carried out for the model family showing the highest family-wise exceedance probability, and the resulting estimates were entered into a BMS to determine the most suitable model family for the given data. Connections were tested for significance using one-sample *t*-tests ($p < .05$, false discovery rate (FDR)-corrected for multiple comparisons).

2.6 | Estimation of resting-state functional connectivity

rsFC was computed as seed-to-seed correlations between the same motor regions as included in the DCM analysis, using identical individual regional coordinates to allow for comparisons with interregional DCM coupling parameters (Rehme et al., 2013). We used the same approach as defined in the DCM analysis to extract the first eigenvariate within a 10 mm sphere around each seed voxel. Next, we computed Pearson correlations between the time series of all region pairs. The resulting correlation coefficients were Fisher's Z-transformed using the formula $Z = 1/2 * \ln([1+r]/[1-r]) = \text{atanh}(r)$ (Biswal et al., 1995) and tested for significance through one-sample *t*-tests ($p < .05$, FDR-corrected).

2.7 | Estimation of task-related functional connectivity

We computed trFC as seed-to-seed correlations between all possible region pairs individually for each subject. Based on the same coordinates as defined in the DCM- and resting-state analyses, we extracted the first eigenvariate from the time series of each ROI recorded during movement of the affected hand. Pearson correlations were computed on a single-subject level and Fisher's Z-transformed (Biswal et al., 1995). Significance was tested across subjects through one-sample *t*-tests ($p < .05$, FDR-corrected).

2.8 | Explaining motor impairment through connectivity estimates

To assess the relationship between connectivity measures and behavioral performance, we computed Spearman rank correlations between measures of rsFC as well as trEC (i.e., coupling parameters of the DCM-B-affected as well as DCM-B-unaffected matrix) and the composite motor score, as well as the individual motor scores.

Next, we tested to which extent rsFC and trEC explained variance in behavioral performance. We, therefore, computed multiple linear backward regression models with elimination based on the Bayesian information criterion (BIC, $k = \log(n)$ with $n = 26$), using the composite motor score as the outcome variable and either rsFC or trEC measures as predictors. We chose to base the selection of model predictors on the BIC rather than the AIC as the BIC allowed us to account for the relatively small sample size. With respect to the connectivity measures, we decided to focus on connections that have been shown to play a major role in motor network reorganization post stroke, that is, connections between bilateral premotor areas and affected M1 as well as interhemispheric connectivity between bilateral M1. Ideally, one would start the backward elimination process with the same number of connectivity measures in the trEC as in the rsFC-model. However, as trEC is directional whereas rsFC is non-directional, trEC is expressed by two values per region pair, while rsFC only provides one value per region pair. As a result, the trEC starting model automatically contains twice as many values as the rsFC model. In our case, this meant that we started with one model with 10 trEC-coupling parameters and a second model with five rsFC-z-values. To ensure that a potential superiority of the trEC-based model was not merely driven by the difference in dimensionality, we repeated the rsFC-backward regression using a starting model with all 15 rsFC-measures. Moreover, to fully capture the potential of the trEC-based model given its higher granularity and number of connectivity estimates, we computed a trEC-based stepwise backward regression starting with all coupling parameters linked to either of the two M1. To minimize the likelihood of overfitting, model performance was compared via BIC values, penalizing model complexity.

Of note, using backward regression models for a comparison of different connectivity methods has two significant limitations:

First, potential multicollinearity of predictor variables may render inference about the influence of individual connections difficult. Second, as described above, the fact that trEC is directional while rsFC is nondirectional results in a higher number of trEC measures, that is, a higher number of predictors for the corresponding starting model, hindering an unbiased comparison of the explanatory power of rsFC and trEC. To circumvent these limitations, we performed dimensionality reduction for rsFC and trEC by means of PCA, thereby translating measures of both connectivity types into an equal amount of meaningful, independent components. Three separate PCAs were calculated for rsFC as well as trEC, representing (a) ipsilesional, (b) contralesional, and (c) interhemispheric connections separately for rsFC and trEC (cf. Figure 1). Next, the estimated factor scores of the first principal components were used as predictors in the multiple linear regression models. First, each component was entered separately as a predictor to assess how much variance could be explained by each component individually. In other words, we computed three separate simple linear regressions for the rsFC-components and another three for the trEC-components. In a next step, multiple linear regression models were estimated, including the three first principal components of rsFC or trEC, respectively.

2.9 | Association of functional and effective connectivity

We assessed the relationship of rsFC, trEC, and trFC by computing Spearman rank correlations between the three DCM-matrices, the resting-state Z-values and the task-related Z-values for corresponding region pairs. We primarily used coupling parameters of the fully connected DCM-model as its B-matrix contains all connections present in the resting-state network. To ensure the reliability of our findings, we repeated the correlation analysis using (a) the winning model of the BMS, (b) the BMA results of the winning family, as well as resting-state Z-values obtained (c) without GSR and (d) with PCA-denoising. We assessed the significance of the resulting correlation coefficients by performing one-sample *t*-tests ($p < .05$, FDR-corrected).

3 | RESULTS

3.1 | Group-level motor network connectivity

Significant rsFC and trEC group-level averages are shown in Figure 2 and Figure S2. On the group-level, almost all rsFC connections reached statistical significance, resulting in a densely connected resting-state motor network (Figure 2a). DCM group results revealed facilitatory influences from bilateral premotor areas onto the ipsilesional M1 and inhibition from ipsilesional M1 onto premotor areas (Figure 2b) during movements of the paretic hand in line with previous findings (Diekhoff-Krebs et al., 2017; Rehme, Eickhoff, et al., 2011).

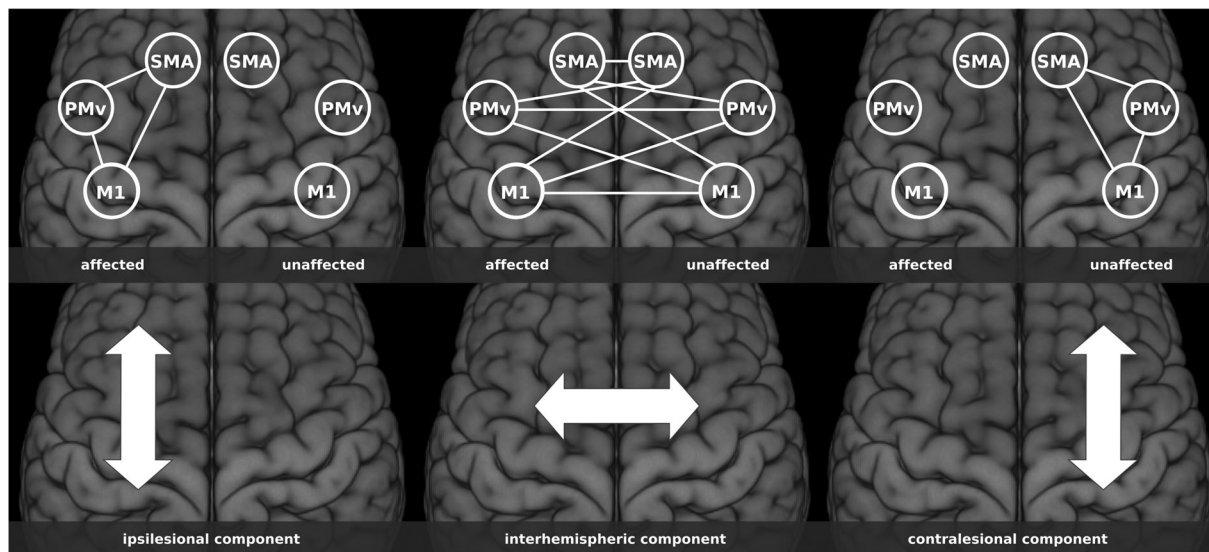


FIGURE 1 Principal components derived via PCA. The figure shows all connections that were summarized via PCAs. For the ipsilesional component, we used all connections between M1, SMA and PMv within the affected hemisphere, that is, three measures in case of rsFC and six measures in case of trEC. The interhemispheric component was derived from all interhemispheric connections, that is, from 9 measures in case of rsFC and 18 in case of trEC. For the contralesional component, all connections between M1, SMA and PMv within the unaffected hemisphere were used, that is, three measures in case of rsFC and six in case of trEC. DCM, dynamic causal modeling; PCA, principal component analysis; PMv, ventral premotor cortex; rsFC, resting-state functional connectivity; SMA, supplementary motor area; trEC, task-related effective connectivity

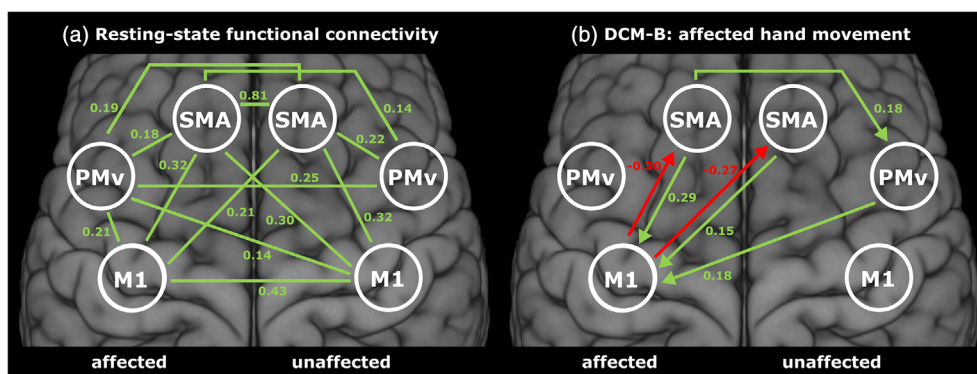


FIGURE 2 Group-level connectivity. Significant connections of the (a) resting-state Z-values and (b) DCM-coupling parameters during movement of the affected hand (DCM-B-affected matrix of the fully connected model), $p < .05$, FDR-corrected for multiple comparisons. The displayed values are group-level averages across patients. Missing connections between the displayed cortical regions did not reach significance after FDR-correction. DCM, dynamic causal modeling

3.2 | Motor impairment and connectivity: Correlation analyses

To address whether specific connections were indicative of motor performance after stroke, Spearman rank correlations were computed to probe for a relationship between the composite motor score with resting-state Z-values as well as coupling parameters modulated during hand movements of the affected or unaffected hand. No significant correlations were observed between rsFC or trEC and motor impairment ($p > .1$, FDR-corrected). Of note, highly similar results were obtained when repeating these analyses using individual

behavioral scores (relative grip strength, ARAT, and JTT scores) rather than the composite motor score.

3.3 | Motor impairment and connectivity: Multiple linear backward regression

As single rsFC or trEC connections were not indicative of motor impairment across patients, multiple linear backward regression models were used to combine information from various connections across the motor network. Regression models obtained through

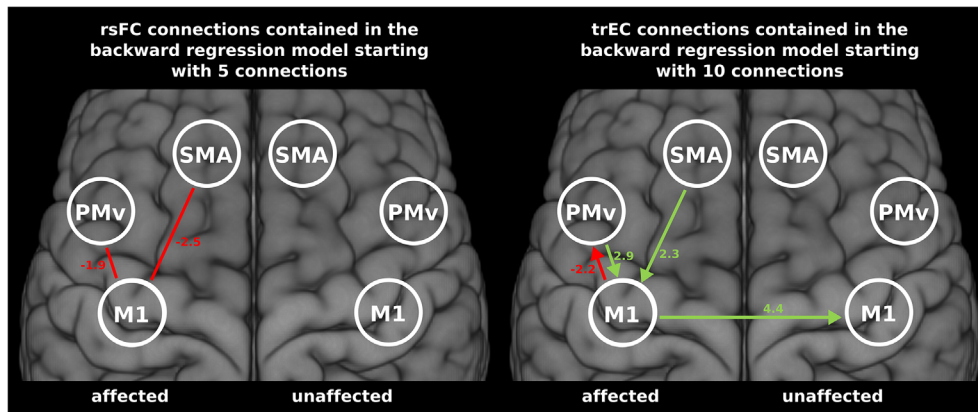


FIGURE 3 Results of the stepwise backward regression. Connections included in the resulting models are displayed with corresponding weights. Both models were able to explain behavioral variance as indicated by the overall model significance (rsFC-based regression model: $R^2 = 33.49\%$, adjusted $R^2 = 27.71\%$, $p = .009$, BIC = 24.25; trEC-based regression model: $R^2 = 55.41\%$, adjusted $R^2 = 46.92\%$, $p = .001$, BIC = 20.37). The connections that remain after backwards elimination are mostly ipsilesional premotor–M1 connections and the interhemispheric M1–M1 connection in case of trEC. rsFC, resting-state functional connectivity; trEC, task-related effective connectivity

stepwise backward elimination (starting with all premotor–M1 and the interhemispheric M1–M1 connection, that is, 10 trEC or 5 rsFC-measures) reached statistical significance for both rsFC and trEC ($p < .05$; see Figure 3). Specifically, the rsFC-model yielded 33.49% explained variance ($p = .009$, adjusted $R^2 = 27.71\%$, BIC = 24.25), while the trEC-based model explained 55.41% ($p = .001$, adjusted $R^2 = 46.92\%$, BIC = 20.37). Interestingly, the final rsFC-model contained only two ipsilesional premotor–M1 connections, highlighting the role of premotor–M1 connectivity within the affected hemisphere (see Equation (1)) early after stroke. While those connections were also included in the resulting trEC-model, it further comprised the interhemispheric M1–M1 connection (see Equation (2)). These findings are well in line with previous findings that stress the importance of those connections for stroke recovery.

$$\text{Motor score} = -2.5M1a - SMAa - 1.9M1a - PMva + 1.2 \quad (1)$$

$$\text{Motor score} = -2.2M1a - PMva + 2.3SMAa - M1a + 2.9PMva - M1a + 4.4M1a - M1u - 1.2 \quad (2)$$

Given the higher adjusted R^2 as well as the lower BIC-value of the final trEC-based model compared to the rsFC-based model, it seems like trEC may be more indicative of motor impairment than resting-state connectivity. To rule out that this finding was driven by the higher number of connectivity measures in the trEC-starting model (10 for trEC vs. 5 for rsFC), we computed an additional backward regression containing all 15 rsFC-measures in the initial model. The resulting model explained 62.67% of behavioral variance ($p = .006$), thereby outperforming the trEC-based model. However, when adjusting for the number of connections in the final model, it performed on a similar level as the trEC-based model according to the adjusted R^2 -value of 48.14% while featuring a higher, that is, worse, BIC (BIC = 25.52). Last, to better capture the full potential of trEC,

we computed a trEC-based backward regression starting with 18 connections that yielded an explained variance of 82.25% ($p < .001$, adjusted $R^2 = 70.42\%$, BIC = 15.97).

In summary, multiple linear backward regression models significantly explained variance in motor impairment across patients for both rsFC and trEC. While for rsFC premotor–M1 connections within the affected hemisphere were sufficient, trEC premotor–M1 coupling parameters and interhemispheric connectivity between bilateral M1 were needed to explain motor impairment.

3.4 | Dimensionality reduction via PCA: Regression results

As highlighted by the backward regression results, a direct comparison between trEC and trFC is hindered by a differing number of connectivity measures per region pair. Thus, we condensed trEC and rsFC into three components each (cf. Figure 1), reflecting ipsilesional, contralesional, and interhemispheric connectivity by performing dimensionality reduction via PCA. The six resulting principal components were entered into linear regression models to explain the composite motor score (see Figure 4 for the explained variance of the individual components). Significant results were exclusively obtained for components derived from rsFC scores: While the principal component of the ipsilesional rsFC values reached 26.98% explained variance ($p = .007$), the interhemispheric component accounted for 21.32% when entered individually into the regression model ($p = .018$). The remaining components did not result in significant regression models. Concerning the overall model including all three principal components, rsFC scores explained 29.35% of variance ($p = .050$), while the model based on trEC did not reach significance. In other words, for rsFC, ipsilesional premotor–M1 connectivity and interhemispheric connectivity could be aggregated to explain motor impairment, while trEC of each category did not sufficiently explain behavioral variance across patients.

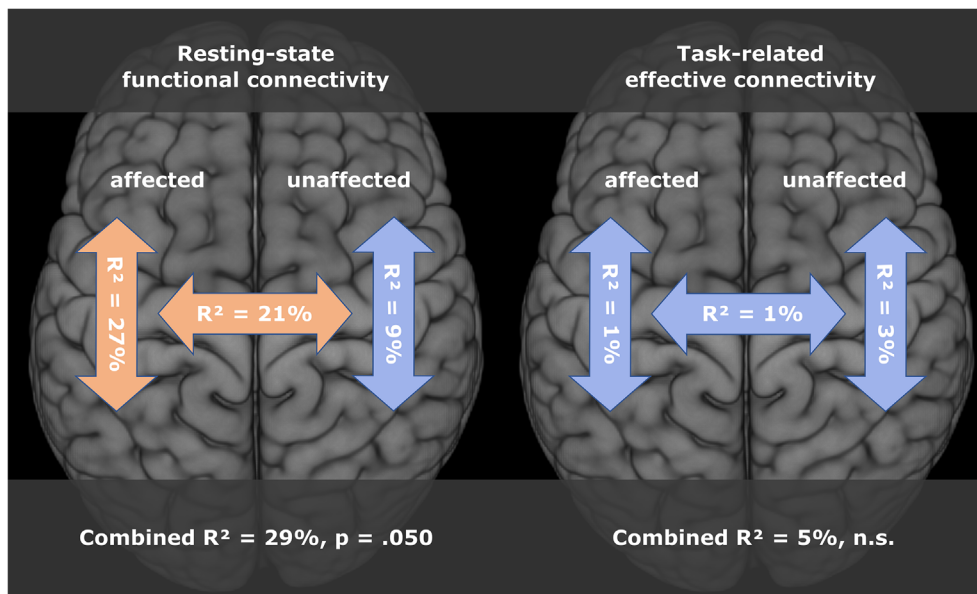


FIGURE 4 Explained motor impairment by individual PCA components. Values within the arrows indicate how much behavioral variance was explained when entering just the respective component into a regression model to predict motor performance. Orange arrows indicate a significant model; blue arrows indicate non-significance (significance threshold: $p < .05$). The combined R^2 denotes explanation of variance when entering all three components simultaneously into a regression model. Hence, the first principal component derived from the three ipsilesional rsFC-measures, as well as the first principal component derived from interhemispheric rsFC-measures significantly explained motor impairment. In general, regression models with PCA components based on resting-state connectivity yielded better results than PCA components based on DCM-coupling parameters, which failed to reach significance. DCM, dynamic causal modeling; PCA, principal component analysis; rsFC, resting-state functional connectivity

3.5 | Comparison of functional and effective connectivity

DCM parameters and resting-state Z-values of the cortical motor network were not significantly correlated (cf. Figure 5). To exclude that this result stemmed from using the fully connected DCM model or a specific resting-state preprocessing approach, we repeated the correlation analyses for (a) the winning model of the BMS, (b) average connection parameters obtained from the BMA procedure of the winning model family (i.e., Family 1), and resting-state Z-values obtained (c) with PCA-denoising and (d) without GSR. For all of these analyses, no significant correlations were observed between trEC and rsFC except for the interhemispheric M1a-PMvu connection, which showed an association between rsFC and trEC values of the DCM-A matrix when using resting-state Z-values obtained without GSR (cf. Figure S3 for correlations of the alternative models).

rsFC and trFC showed significant correlations for the interhemispheric connections of homolog region pairs, while no significant correlations were observed for trFC and trEC (cf. Figure 5, Figure S4). Thus, these results are in line with a mode-dependence of similarity in connectivity after stroke.

4 | DISCUSSION

In the present study, we conducted the first direct comparison of motor network rsFC and trEC in the early subacute stage after stroke. In line

with our hypothesis, trEC was superior in explaining variance in motor performance when capitalizing on its richer informational complexity (i.e., higher number of connections) compared to rsFC. However, when balancing model complexity (i.e., using a similar number of connections), both frameworks explained motor impairment to a similar degree across patients. In line with previous findings, a combination of ipsilesional premotor-M1 connections and interhemispheric M1-M1 connectivity explained behavioral variance. As trEC and rsFC were unrelated for intra-hemispheric as well as most interhemispheric connections, our findings suggest that rsFC and trEC reflect distinct aspects of information integration in the lesioned motor network after stroke, potentially hinting at distinct roles in motor network reorganization. Moreover, the significant associations observed between interhemispheric trFC and rsFC suggest that interhemispheric information integration after stroke might occur in a state-independent fashion, while ipsilesional premotor-M1 connectivity post-stroke seems to be state-dependent. Thus, our findings suggest two distinct aspects of functional network reorganization: (a) task-specific compensation via premotor-M1 in the ipsilesional hemisphere and (b) a more fundamental (i.e., task-independent) change in the interhemispheric interaction of motor homologs.

4.1 | Explaining motor impairment via resting-state vs. task-related connectivity

Both trEC and rsFC significantly explained motor performance, stressing the relevance of functional data as an indicator of motor

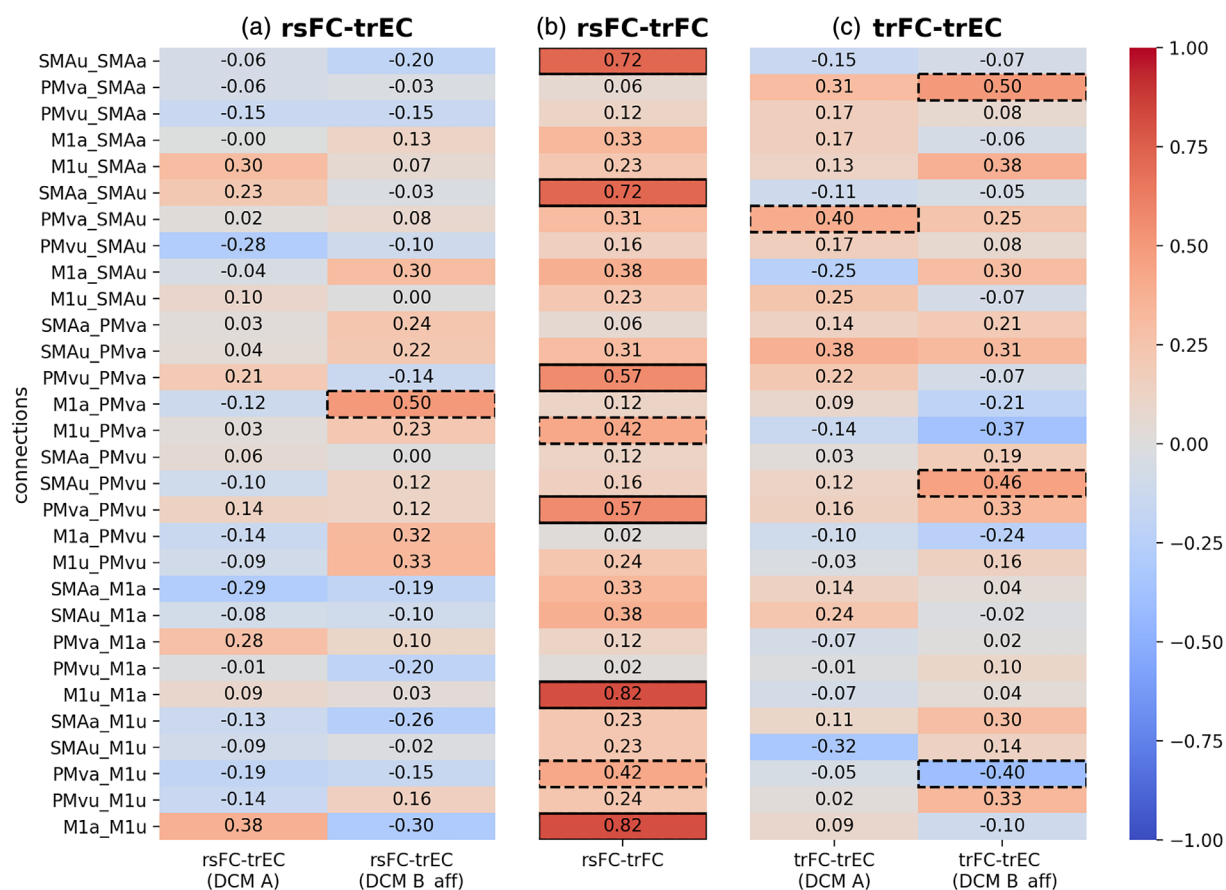


FIGURE 5 Spearman rank correlations between trEC, rsFC, and trFC. The three charts entail correlations between (a) rsFC and trEC, (b) rsFC and trFC, and (c) trFC and trEC. trEC is expressed in terms of coupling parameters of the DCM-A and B-affected matrix. rsFC is expressed as Fisher's Z-scores derived from Pearson correlations of the predefined region pairs. trFC was computed from the time series recorded during movement of the affected hand as Fisher's Z-scores derived from Pearson correlations of the predefined region pairs. Dashed lines indicate significance at an uncorrected level ($p < .05$), solid lines indicate significance after FDR-correction for multiple comparisons ($p < .05$, FDR-corrected). Of note, only rsFC and trFC (depicted in b) showed a significant relationship between interhemispheric homologous connections at a corrected level, suggesting a similarity in functional connectivity during task and rest, that is, depending on the connectivity mode and independent from the brain state. As FC is derived from a purely correlational approach, it is undirected and therefore contains only half as many connections as EC. In other words, while EC differentiates between for instance M1a–M1u and M1u–M1a connectivity, those values are the same for FC. Therefore, in the middle column (b) showing Spearman rank correlations between rsFC and trFC each correlation coefficient is displayed twice. DCM, dynamic causal modeling; FC, functional connectivity; rsFC, resting-state functional connectivity; trEC, task-related effective connectivity

impairment, well in line with previous studies (Baldassarre et al., 2016; Carter et al., 2009; Rehme, Volz, Feis, Eickhoff, et al., 2015; Rehme, Volz, Feis, Bomilcar-Focke, et al., 2015; van Meer et al., 2010; Volz, Sarfeld, et al., 2015). Directly comparing the propensity of rsFC and trEC to explain variance in motor impairment, the trEC-based regression model yielded higher explained variance and superior model evidence, as reflected by BIC (cf. Figure 3). However, the considerable difference in model complexity arising from the distinct number of rsFC and trEC connections renders a direct comparison of both models difficult. Accordingly, when including all rsFC connections and thus increasing their number above the number of trEC connections, the rsFC-based model somewhat surprisingly explained behavioral variance to a similar extent compared to the trEC-based model, yet at the cost of increased model complexity as indicated by a higher

number of connections in the resulting regression model as well as an increased BIC-value.

In summary, when utilizing the higher degree of information contained in trEC, that is, the higher number of connections due to its directionality, it outperformed rsFC in explaining variance of motor performance, in line with our initial hypothesis. However, trEC results are less likely to generalize, given their strong task-dependence and the propensity of more complex statistical models to more easily over-fit the data at hand. When reducing the number of connectivity estimates to enable a more even comparison, rsFC and trEC both significantly explained motor performance to a rather similar degree. Therefore, our results highlight the potential role of both rsFC and trEC as potential biomarkers for motor impairment. Given its superior feasibility in a clinical context, our current findings particularly emphasize the clinical potential of rsFC.

4.2 | Task-related motor network connectivity after stroke

After the advent of fMRI, various studies have conclusively reported increased BOLD-activity levels during paretic hand movements in both the ipsi- and contralesional hemisphere (Rehme, Eickhoff, Rottschy, Fink, & Grefkes, 2012). trEC has often been used to further elucidate the mechanistic underpinnings of such altered activity patterns from a network level-perspective (Grefkes & Fink, 2014). A common finding replicated across studies analyzing trEC in stroke patients highlights the crucial role of excitatory ipsilesional premotor–M1 coupling which is thought to enable movements by driving M1 activity necessary to activate muscles via descending motor activity (Grefkes, Nowak, et al., 2008; Grefkes et al., 2010; Hensel et al., 2021; Rehme, Eickhoff, et al., 2011). In line with this notion, our current analysis implies that stronger excitatory coupling from ipsilesional premotor areas onto the affected M1 as well as stronger inhibitory feedback from the affected M1 back onto the ipsilesional PMv were indicative of better motor performance (cf. Figure 3). Thus, our current findings highlight the functional importance of excitatory premotor–M1 connectivity early after stroke.

Another recurrent, albeit more complex and variable finding lies in altered interhemispheric M1–M1 connectivity. In healthy subjects, unilateral hand movements have repetitively been shown to elicit an inhibitory influence from the *active* M1 (contralateral to the moving hand) onto the *inactive* M1 (ipsilateral to the moving hand; Grefkes, Nowak, et al., 2008; Pool et al., 2013; Pool, Rehme, Fink, Eickhoff, & Grefkes, 2014; Rehme, Eickhoff, et al., 2011; Volz, Hamada, Rothwell, & Grefkes, 2015; Volz, Sarfeld, et al., 2015). After stroke, distinct alterations of M1–M1 trEC have been reported presumably depending on the time-point post stroke and severity of motor impairment, ranging from a lack of inhibition of contralesional M1 by ipsilesional M1 to additional facilitatory influence from the unaffected M1 onto the affected M1 (Hensel et al., 2021; Rehme, Eickhoff, et al., 2011). Accordingly, our present findings also emphasize that interhemispheric M1–M1 connectivity is functionally relevant after stroke. Specifically, stronger excitatory influences from ipsilesional M1 onto contralesional M1 were indicative for better motor performance. From a conceptual perspective, this result may represent a mechanism of task-specific compensation. Mechanistically, pronounced excitation of the contralesional M1 by the ipsilesional would lead to increased activation of the contralesional M1 during paretic hand movements. This finding is well in line with the *vicariation model* (Di Pino et al., 2014), ascribing a supportive role to the over-activation of the contralesional M1 during motor task performance with the paretic hand, as argued by various previous studies (Rehme, Fink, et al., 2011; Tombari et al., 2004; Ward, Brown, Thompson, & Frackowiak, 2003). A similar supportive role of the ipsilateral M1 has also been observed in healthy subjects for complex motor tasks, giving rise to the notion that additional ipsilateral (i.e., contralesional in stroke patients) resources are activated with increased task demands (Verstynen, Diedrichsen, Albert, Aparicio, & Ivry, 2005).

However, the functional role of the contralesional M1 for motor performance of the paretic hand ultimately remains controversial, with evidence from several studies suggesting a maladaptive role of the contralesional M1 (Grefkes et al., 2010; Grefkes, Nowak, et al., 2008; Murase, Duque, Mazzocchio, & Cohen, 2004; Volz et al., 2017; Volz, Sarfeld, et al., 2015). A reason for these diverging findings and interpretations may lie in their dependence on the motor task performed in a given study (Hartwigsen & Volz, 2021; Lotze et al., 2006; Volz et al., 2017). Specifically, stroke patients typically develop individual compensation strategies to master a given movement impacting on trEC. Thus, such specific compensatory efforts of the lesioned motor system might therefore comprise highly individual changes that are less easily captured on the group level. In other words, idiosyncratic patterns of trEC changes may be present in distinct subjects that do not generalize well to the group level.

4.3 | Task-independent motor network connectivity after stroke

By contrast, rsFC offers the opportunity to assess the motor network in a task-independent fashion, allowing for easier generalization of findings and clinical application. After stroke, characteristic changes in rsFC have convergingly been reported across different studies, highlighting a crucial role of interhemispheric M1–M1 connectivity, which has been shown to first decrease and then re-increase alongside functional recovery in both humans and animal models (for references regarding interhemispheric changes, see, e.g., Carter et al., 2009; Golestani et al., 2013; van Meer et al., 2010, 2012). While we did not observe a significant correlation between M1–M1 rsFC-connectivity and motor performance in our current study, variance in motor impairment was significantly explained when entering the first principal component derived from all interhemispheric rsFC-connections into a regression model (cf. Figure 4). In other words, combining interhemispheric connections significantly explained motor impairment, stressing the importance of premotor areas beyond interhemispheric M1–M1 connectivity in rsFC early after stroke. Besides interhemispheric connections, ipsilesional premotor–M1 connectivity also played a major role: regression weights indicated a negative relationship between motor performance and ipsilesional SMA–M1 as well as PMv–M1 connection strength (cf. Figure 3). Moreover, the regression model containing the ipsilesional PCA-component achieved the highest explained variance. While reported less frequently than altered M1–M1 connectivity, previous studies have already outlined the functional significance of premotor–M1 rsFC after stroke. For example, Carter et al. found that interhemispheric rsFC alone was not significantly related to behavioral impairment, yet it explained motor impairment when complemented by intrahemispheric rsFC and lesion size (Carter et al., 2012). Furthermore, Rehme and colleagues reported their machine learning classification to be partially driven by increased connectivity between ipsilesional premotor areas and the affected M1 (Rehme, Volz, Feis, Bomilcar-Focke, et al., 2015). Of note, this evidence supporting a negative relationship between rsFC and motor

performance post-stroke is challenged by data observing the opposite relationship. For instance, a study investigating rsFC in patients within the first 2 weeks post-stroke found a positive association between ipsilesional PMv–M1 connectivity in the acute phase and motor improvement over the course of the next 3 months for a subgroup of severely affected patients (Lee et al., 2017). For the chronic stage, there are also reports of a positive link between premotor–M1 rsFC and motor function (Lam et al., 2018). Thus, the association of altered ipsilesional rsFC post-stroke with motor impairment seems to vary depending on the analytic framework, degree of motor impairment as well as the time since stroke included in a specific study.

In summary, premotor–M1-rsFC within the ipsilesional hemisphere seems to play a crucial role after stroke and should not be neglected next to the commonly reported interhemispheric connectivity changes (Carter et al., 2009; Golestani et al., 2013; van Meer et al., 2010, 2012).

4.4 | Task-specific ipsilesional compensation and general interhemispheric reorganization

We here showed for the first time that ipsilesional and interhemispheric components of both rsFC and trEC readily explained motor impairment post-stroke in the same cohort of patients, while replicating previous findings obtained for either rsFC or trEC in isolation. The observed overlap of explanatory components between rsFC and trEC emphasizes the question whether both similarly capture fundamental aspects of motor network reorganization in a task-independent fashion. Conversely, findings obtained from healthy human subjects support the notion that rsFC and trEC rather reflect differential, state-independent aspects of information integration (Rehme et al., 2013). Our current results revealed a similar lack of overlap between trEC and rsFC in the early phase post-stroke (cf. Figure 5). Thus, despite the fact that stroke-induced changes in motor network connectivity affect highly similar connections, rsFC and trEC seem to reflect largely unrelated aspects of information integration. However, the fact that we observed significant correlations between trFC and rsFC-measures of homologous interhemispheric connections indicates a state-independent similarity of interhemispheric connectivity after stroke (cf. Figure 5). In light of these results, the lack of a relationship between interhemispheric rsFC and trEC seems to depend on the mode, that is, to result at least in part from the methodological approach used to calculate connectivity, rather than the activity state of the brain. In other words, functional connectivity between interhemispheric homologs seems to reflect similar neural interactions post-stroke irrespective of whether the motor system is engaged in task execution or at rest. Taken together, task-independent changes of interhemispheric connectivity may result from a general, task-independent aspect of motor network reorganization. One might speculate that recruiting the computational resources of the functional homolog in the other hemisphere may be a highly efficient and domain-general way of functionally extending the lesioned network by using the pre-existing prominent structural

connections via the corpus callosum allowing for direct information exchange. Support for the notion that involving bilateral functional homologs in the attempt to compensate for tissue loss may be a highly general mechanism derives from the fact that changes in interhemispheric activation and connectivity have been observed in multiple functional systems such as the motor, language and cognitive networks both at rest and during task-performance (Hartwigsen & Volz, 2021).

Conversely, while we found that premotor–M1 connectivity onto ipsilesional M1 crucially contributed to the explanation of motor impairment for both rsFC and trEC, the lack of association between rsFC and trFC suggests that premotor–M1 connectivity may indeed be highly state-dependent. From a mechanistic perspective, this does not seem surprising, given the pivotal role of premotor–M1 connections for the production of voluntary actions such as grasping or reaching movements (Cunnington, Bradshaw, & Iansek, 1996; Davare, 2006; Davare, Lemon, & Olivier, 2008; Kazennikov et al., 1999; Rizzolatti et al., 2002). Conceptually, one might thus assume that the state-dependence of ipsilesional premotor–M1 connectivity reflects the network's attempt to maximize its functionality to serve the specific task at hand. In sum, premotor–M1 connectivity may thus be attributed to task-specific compensation, while interhemispheric connectivity seems to change in a task-independent fashion, potentially reflecting a general aspect of motor network reorganization.

4.5 | Limitations

We here compared the two most commonly used methodological approaches to estimate connectivity from fMRI data in stroke patients. Importantly, while we included trFC to differentiate between state- and mode-specific effects, we refrained from adding resting-state effective connectivity (rsEC) to our analyses. Even though some efforts have been made to estimate effective connectivity from resting-state data using DCM-based approaches (Friston, Kahan, Biswal, & Razi, 2014; Friston, Li, Daunizeau, & Stephan, 2011; Li et al., 2011; Razi, Kahan, Rees, & Friston, 2015), such an approach has to the best of our knowledge never been applied in stroke patients. While the assessment of rsEC after stroke certainly represents a highly interesting scientific question, the focus of the current study was to compare established methodological frameworks which have previously reported similar motor network alterations after stroke. Thus, the first assessment of DCM-based rsEC after stroke is beyond the scope of the current manuscript and should be addressed in future work.

Regression results are heavily influenced by methodological decisions so that the reported connections contributing to the explanation of motor impairment have to be interpreted with caution. For instance, with respect to the stepwise backward regression, other starting models might yield diverging results and other combinations of connectivity measures might achieve similar explanatory power as the ones reported here. An important parameter choice lies in the elimination criterion used in the stepwise backward regression. To account for the

high number of model parameters relative to our sample size we opted for BIC to protect against overfitting. Of note, repeating our analyses using AIC instead of BIC yielded slightly different surviving connections in the final regression model, yet a similar percentage of explained variance, corroborating the robustness of our findings.

Although we here investigated a significantly bigger sample than previous DCM-studies in stroke patients, the limited sample size does still not allow for conclusions regarding the heterogeneity in lesion location and size and the associated variability in reorganization processes. Future research should therefore attempt to recruit larger samples, including patients of the early acute or chronic stage and try to expand the present findings to other functional networks.

5 | CONCLUSION

Comparing trEC and rsFC in the first 2 weeks after stroke, using the superior complexity offered by trEC best explained variance in motor performance. However, when balancing model complexity, connectivity measures of both frameworks explained motor performance in the early subacute phase post-stroke to a similar extent, underscoring the clinical potential of rsFC given its superior feasibility and generalizability. For both approaches, connectivity between ipsilesional premotor-M1 as well as interhemispheric M1-M1 explained motor impairment early after stroke. Besides frequently observed alterations of interhemispheric M1-M1 connectivity, our findings thus particularly highlight the crucial role of premotor-M1 connectivity in early motor network reorganization. From a mechanistic perspective, premotor-M1 connectivity seems to primarily reflect state-dependent compensation, while state-independent interhemispheric connectivity between motor homologs may potentially arise from general aspects of functional motor network reorganization reflected during both task-performance and at rest.

ACKNOWLEDGMENTS

Anne K. Rehme is supported by the Deutsche Forschungsgemeinschaft (DFG, German Research Foundation, RE3014/2-1). Simon B. Eickhoff acknowledges funding through the European Union's Horizon 2020 Research and Innovation Program (grant agreements 785907 [HBP SGA2] and 945539 [HBP SGA3]). Gereon R. Fink and Christian Grefkes are funded by the Deutsche Forschungsgemeinschaft (DFG, German Research Foundation)—Project-ID 431549029—SFB 1451. Gereon R. Fink gratefully acknowledges additional support from the Marga and Walter Boll Stiftung. Open access funding enabled and organized by Projekt DEAL.

DATA AVAILABILITY STATEMENT

The data that support the findings of this study are available from the corresponding author upon reasonable request.

ORCID

Christian Grefkes  <https://orcid.org/0000-0002-1656-720X>

Lukas J. Volz  <https://orcid.org/0000-0002-0161-654X>

REFERENCES

- Ashburner, J., & Friston, K. J. (2005). Unified segmentation. *NeuroImage*, 26(3), 839–851. <https://doi.org/10.1016/j.neuroimage.2005.02.018>
- Baldassarre, A., Ramsey, L., Rengachary, J., Zinn, K., Siegel, J. S., Metcalf, N. V., ... Shulman, G. L. (2016). Dissociated functional connectivity profiles for motor and attention deficits in acute right-hemisphere stroke. *Brain*, 139(7), 2024–2038. <https://doi.org/10.1093/brain/aww107>
- Biswal, B., Zerrin Yetkin, F., Haughton, V. M., & Hyde, J. S. (1995). Functional connectivity in the motor cortex of resting human brain using echo-planar mri. *Magnetic Resonance in Medicine*, 34(4), 537–541. <https://doi.org/10.1002/mrm.1910340409>
- Buxton, R. B., Wong, E. C., & Frank, L. R. (1998). Dynamics of blood flow and oxygenation changes during brain activation: The balloon model. *Magnetic Resonance in Medicine*, 39(17), 855–864. <https://doi.org/10.1002/mrm.1910390602>
- Carter, A. R., Astafiev, S. V., Lang, C. E., Connor, L. T., Rengachary, J., Strube, M. J., ... Corbetta, M. (2009). Resting state inter-hemispheric fMRI connectivity predicts performance after stroke. *Annals of Neurology*, 67(3), 365–375. <https://doi.org/10.1002/ana.21905>
- Carter, A. R., Patel, K. R., Astafiev, S. V., Snyder, A. Z., Rengachary, J., Strube, M. J., ... Corbetta, M. (2012). Upstream dysfunction of Somatomotor functional connectivity after Corticospinal damage in stroke. *Neurorehabilitation and Neural Repair*, 26(1), 7–19. <https://doi.org/10.1177/1545968311411054>
- Cramer, S. C. (2008). Repairing the human brain after stroke: I. Mechanisms of spontaneous recovery. *Annals of Neurology*, 63(3), 272–287. <https://doi.org/10.1002/ana.21393>
- Cunnington, R., Bradshaw, J. L., & Iansek, R. (1996). The role of the supplementary motor area in the control of voluntary movement. *Human Movement Science*, 15(5), 627–647. [https://doi.org/10.1016/0167-9457\(96\)00018-8](https://doi.org/10.1016/0167-9457(96)00018-8)
- Davare, M. (2006). Dissociating the role of ventral and dorsal premotor cortex in precision grasping. *Journal of Neuroscience*, 26(8), 2260–2268. <https://doi.org/10.1523/JNEUROSCI.3386-05.2006>
- Davare, M., Lemon, R., & Olivier, E. (2008). Selective modulation of interactions between ventral premotor cortex and primary motor cortex during precision grasping in humans. *Journal of Physiology*, 586(11), 2735–2742. <https://doi.org/10.1113/jphysiol.2008.152603>
- Di Pino, G., Pellegrino, G., Assenza, G., Capone, F., Ferreri, F., Formica, D., ... Di Lazzaro, V. (2014). Modulation of brain plasticity in stroke: A novel model for neurorehabilitation. *Nature Reviews Neurology*, 10(10), 597–608. <https://doi.org/10.1038/nrneurol.2014.162>
- Diekhoff-Krebs, S., Pool, E. M., Sarfeld, A. S., Rehme, A. K., Eickhoff, S. B., Fink, G. R., & Grefkes, C. (2017). Interindividual differences in motor network connectivity and behavioral response to iTBS in stroke patients. *NeuroImage: Clinical*, 15(June), 559–571. <https://doi.org/10.1016/j.nicl.2017.06.006>
- Duncan, P., Richards, L., Wallace, D., Stoker-Yates, J., Pohl, P., Luchies, C., ... Studenski, S. (1998). A randomized, controlled pilot study of a home-based exercise program for individuals with mild and moderate stroke. *Stroke*, 29(10), 2055–2060. <https://doi.org/10.1161/01.STR.29.10.2055>
- Fox, M. D., & Raichle, M. E. (2007). Spontaneous fluctuations in brain activity observed with functional magnetic resonance imaging. *Nature Reviews Neuroscience*, 8(9), 700–711. <https://doi.org/10.1038/nrn2201>
- Friston, K. J. (1994). Functional and effective connectivity in neuroimaging: A synthesis. *Human Brain Mapping*, 2(1–2), 56–78. <https://doi.org/10.1002/hbm.460020107>
- Friston, K. J., Harrison, L., & Penny, W. (2003). Dynamic causal modelling. *NeuroImage*, 19(4), 1273–1302. [https://doi.org/10.1016/S1053-8119\(03\)00202-7](https://doi.org/10.1016/S1053-8119(03)00202-7)
- Friston, K. J., Kahan, J., Biswal, B., & Razi, A. (2014). A DCM for resting state fMRI. *NeuroImage*, 94, 396–407. <https://doi.org/10.1016/j.neuroimage.2013.12.009>

- Friston, K. J., Li, B., Daunizeau, J., & Stephan, K. E. (2011). Network discovery with DCM. *NeuroImage*, 56(3), 1202–1221. <https://doi.org/10.1016/j.neuroimage.2010.12.039>
- Golestani, A.-M., Tymchuk, S., Demchuk, A., & Goodyear, B. G. (2013). Longitudinal evaluation of resting-state fMRI after acute stroke with hemiparesis. *Neurorehabilitation and Neural Repair*, 27(2), 153–163. <https://doi.org/10.1177/1545968312457827>
- Grefkes, C., Eickhoff, S. B., Nowak, D. A., Dafotakis, M., & Fink, G. R. (2008). Dynamic intra- and interhemispheric interactions during unilateral and bilateral hand movements assessed with fMRI and DCM. *NeuroImage*, 41(4), 1382–1394. <https://doi.org/10.1016/j.neuroimage.2008.03.048>
- Grefkes, C., & Fink, G. R. (2014). Connectivity-based approaches in stroke and recovery of function. *The Lancet Neurology*, 13(2), 206–216. [https://doi.org/10.1016/S1474-4422\(13\)70264-3](https://doi.org/10.1016/S1474-4422(13)70264-3)
- Grefkes, C., Nowak, D. A., Eickhoff, S. B., Dafotakis, M., Küst, J., Karbe, H., & Fink, G. R. (2008). Cortical connectivity after subcortical stroke assessed with functional magnetic resonance imaging. *Annals of Neurology*, 63(2), 236–246. <https://doi.org/10.1002/ana.21228>
- Grefkes, C., Nowak, D. A., Wang, L. E., Dafotakis, M., Eickhoff, S. B., & Fink, G. R. (2010). Modulating cortical connectivity in stroke patients by rTMS assessed with fMRI and dynamic causal modeling. *NeuroImage*, 50(1), 233–242. <https://doi.org/10.1016/j.neuroimage.2009.12.029>
- Grefkes, C., & Ward, N. S. (2014). Cortical reorganization after stroke. *The Neuroscientist*, 20(1), 56–70. <https://doi.org/10.1177/1073858413491147>
- Hartwigsen, G., & Volz, L. J. (2021). Probing rapid network reorganization of motor and language functions via neuromodulation and neuroimaging. *NeuroImage*, 224(October 2020), 117449. <https://doi.org/10.1016/j.neuroimage.2020.117449>
- Hensel, L., Tscherpel, C., Freytag, J., Ritter, S., Rehme, A. K., Volz, L. J., ... Grefkes, C. (2021). Connectivity-related roles of Contralateral brain regions for motor performance early after stroke. *Cerebral Cortex*, 31(2), 993–1007. <https://doi.org/10.1093/cercor/bhaa270>
- Jebsen, R. H., Taylor, N., Trieschmann, R. B., Trotter, M. J., & Howard, L. A. (1969). An objective and standardized test of hand function. *Archives of Physical Medicine and Rehabilitation*, 50(6), 311–319.
- Kazennikov, O., Hyland, B., Corboz, M., Babalian, A., Rouiller, E. M., & Wiesendanger, M. (1999). Neural activity of supplementary and primary motor areas in monkeys and its relation to bimanual and unimanual movement sequences. *Neuroscience*, 89(3), 661–674. [https://doi.org/10.1016/S0306-4522\(98\)00348-0](https://doi.org/10.1016/S0306-4522(98)00348-0)
- Lam, T. K., Dawson, D. R., Honjo, K., Ross, B., Binns, M. A., Stuss, D. T., ... Chen, J. L. J. (2018). Neural coupling between contralateral motor and frontoparietal networks correlates with motor ability in individuals with chronic stroke. *Journal of the Neurological Sciences*, 384 (November 2017), 21–29. <https://doi.org/10.1016/j.jns.2017.11.007>
- Lee, J., Park, E., Lee, A., Chang, W. H., Kim, D. S., & Kim, Y. H. (2017). Recovery-related indicators of motor network plasticity according to impairment severity after stroke. *European Journal of Neurology*, 24(10), 1290–1299. <https://doi.org/10.1111/ene.13377>
- Li, B., Daunizeau, J., Stephan, K. E., Penny, W., Hu, D., & Friston, K. (2011). Generalised filtering and stochastic DCM for fMRI. *NeuroImage*, 58(2), 442–457. <https://doi.org/10.1016/j.neuroimage.2011.01.085>
- Lotze, M., Markert, J., Sauseng, P., Hoppe, J., Plewnia, C., & Gerloff, C. (2006). The role of multiple contralateral motor areas for complex hand movements after internal capsular lesion. *The Journal of Neuroscience: The Official Journal of the Society for Neuroscience*, 26(22), 6096–6102. <https://doi.org/10.1523/JNEUROSCI.4564-05.2006>
- Lyle, R. C. (1981). A performance test for assessment of upper limb function in physical rehabilitation treatment and research. *International Journal of Rehabilitation Research*, 4(4), 483–492.
- Murase, N., Duque, J., Mazzocchio, R., & Cohen, L. G. (2004). Influence of interhemispheric interactions on motor function in chronic stroke. *Annals of Neurology*, 55(3), 400–409. <https://doi.org/10.1002/ana.10848>
- Park, C. H., Chang, W. H., Ohn, S. H., Kim, S. T., Bang, O. Y., Pascual-Leone, A., & Kim, Y.-H. H. (2011). Longitudinal changes of resting-state functional connectivity during motor recovery after stroke. *Stroke*, 42(5), 1357–1362. <https://doi.org/10.1161/STROKEAHA.110.596155>
- Picard, N., & Strick, P. L. (2001). Imaging the premotor areas. *Current Opinion in Neurobiology*, 11(6), 663–672. [https://doi.org/10.1016/S0959-4388\(01\)00266-5](https://doi.org/10.1016/S0959-4388(01)00266-5)
- Pool, E.-M., Rehme, A. K., Fink, G. R., Eickhoff, S. B., & Grefkes, C. (2013). Network dynamics engaged in the modulation of motor behavior in healthy subjects. *NeuroImage*, 82, 68–76. <https://doi.org/10.1016/j.neuroimage.2013.05.123>
- Pool, E.-M., Rehme, A. K., Fink, G. R., Eickhoff, S. B., & Grefkes, C. (2014). Handedness and effective connectivity of the motor system. *NeuroImage*, 99, 451–460. <https://doi.org/10.1016/j.neuroimage.2014.05.048>
- Power, J. D., Mitra, A., Laumann, T. O., Snyder, A. Z., Schlaggar, B. L., & Petersen, S. E. (2014). Methods to detect, characterize, and remove motion artifact in resting state fMRI. *NeuroImage*, 84, 320–341. <https://doi.org/10.1016/j.neuroimage.2013.08.048>
- Razi, A., Kahan, J., Rees, G., & Friston, K. J. (2015). Construct validation of a DCM for resting state fMRI. *NeuroImage*, 106, 1–14. <https://doi.org/10.1016/j.neuroimage.2014.11.027>
- Rehme, A. K., Eickhoff, S. B., & Grefkes, C. (2013). State-dependent differences between functional and effective connectivity of the human cortical motor system. *NeuroImage*, 67, 237–246. <https://doi.org/10.1016/j.neuroimage.2012.11.027>
- Rehme, A. K., Eickhoff, S. B., Rottschy, C., Fink, G. R., & Grefkes, C. (2012). Activation likelihood estimation meta-analysis of motor-related neural activity after stroke. *NeuroImage*, 59(3), 2771–2782. <https://doi.org/10.1016/j.neuroimage.2011.10.023>
- Rehme, A. K., Eickhoff, S. B., Wang, L. E., Fink, G. R., & Grefkes, C. (2011). Dynamic causal modeling of cortical activity from the acute to the chronic stage after stroke. *NeuroImage*, 55(3), 1147–1158. <https://doi.org/10.1016/j.neuroimage.2011.01.014>
- Rehme, A. K., Fink, G. R., von Cramon, D. Y., & Grefkes, C. (2011). The role of the Contralateral motor cortex for motor recovery in the early days after stroke assessed with longitudinal fMRI. *Cerebral Cortex*, 21(4), 756–768. <https://doi.org/10.1093/cercor/bhq140>
- Rehme, A. K., Volz, L. J., Feis, D.-L., Bomilar-Focke, I., Liebig, T., Eickhoff, S. B., ... Grefkes, C. (2015). Identifying neuroimaging markers of motor disability in acute stroke by machine learning techniques. *Cerebral Cortex*, 25(9), 3046–3056. <https://doi.org/10.1093/cercor/bhu100>
- Rehme, A. K., Volz, L. J., Feis, D. L., Eickhoff, S. B., Fink, G. R., & Grefkes, C. (2015). Individual prediction of chronic motor outcome in the acute post-stroke stage: Behavioral parameters versus functional imaging. *Human Brain Mapping*, 36(11), 4553–4565. <https://doi.org/10.1002/hbm.22936>
- Rizzolatti, G., Fogassi, L., & Gallese, V. (2002). Motor and cognitive functions of the ventral premotor cortex. *Current Opinion in Neurobiology*, 12(2), 149–154. [https://doi.org/10.1016/S0959-4388\(02\)00308-2](https://doi.org/10.1016/S0959-4388(02)00308-2)
- Satterthwaite, T. D., Elliott, M. A., Gerraty, R. T., Ruparel, K., Loughhead, J., Calkins, M. E., ... Wolf, D. H. (2013). An improved framework for confound regression and filtering for control of motion artifact in the preprocessing of resting-state functional connectivity data. *NeuroImage*, 64(1), 240–256. <https://doi.org/10.1016/j.neuroimage.2012.08.052>
- Stephan, K. E., & Friston, K. J. (2010). Analyzing effective connectivity with functional magnetic resonance imaging. *Wiley Interdisciplinary Reviews: Cognitive Science*, 1(3), 446–459. <https://doi.org/10.1002/wcs.58>
- Stephan, K. E., Penny, W. D., Daunizeau, J., Moran, R. J., & Friston, K. J. (2009). Bayesian model selection for group studies. *NeuroImage*, 46(4), 1004–1017. <https://doi.org/10.1016/j.neuroimage.2009.03.025>
- Stephan, K. E., Penny, W. D., Moran, R. J., den Ouden, H. E. M., Daunizeau, J., & Friston, K. J. (2010). Ten simple rules for dynamic

- causal modeling. *NeuroImage*, 49(4), 3099–3109. <https://doi.org/10.1016/j.neuroimage.2009.11.015>
- Thiel, A., & Vahdat, S. (2015). Structural and resting-state brain connectivity of motor networks after stroke. *Stroke*, 46(1), 296–301. <https://doi.org/10.1161/STROKEAHA.114.006307>
- Tombari, D., Loubinoux, I., Pariente, J., Gerdelat, A., Albucher, J.-F., Tardy, J., ... Chollet, F. (2004). A longitudinal fMRI study: In recovering and then in clinically stable sub-cortical stroke patients. *NeuroImage*, 23(3), 827–839. <https://doi.org/10.1016/j.neuroimage.2004.07.058>
- van Meer, M. P. A., Otte, W. M., van der Marel, K., Nijboer, C. H., Kavelaars, A., van der Sprenkel, J. W. B., ... Dijkhuizen, R. M. (2012). Extent of bilateral neuronal network reorganization and functional recovery in relation to stroke severity. *Journal of Neuroscience*, 32(13), 4495–4507. <https://doi.org/10.1523/JNEUROSCI.3662-11.2012>
- van Meer, M. P. A., van der Marel, K., Wang, K., Otte, W. M., el Bouazati, S., Roeling, T. A. P., ... Dijkhuizen, R. M. (2010). Recovery of sensorimotor function after experimental stroke correlates with restoration of resting-state Interhemispheric functional connectivity. *Journal of Neuroscience*, 30(11), 3964–3972. <https://doi.org/10.1523/JNEUROSCI.5709-09.2010>
- Verstynen, T., Diedrichsen, J., Albert, N., Aparicio, P., & Ivry, R. B. (2005). Ipsilateral motor cortex activity during unimanual hand movements relates to task complexity. *Journal of Neurophysiology*, 93(3), 1209–1222. <https://doi.org/10.1152/jn.00720.2004>
- Volz, L. J., Hamada, M., Rothwell, J. C., & Grefkes, C. (2015). What makes the muscle twitch: Motor system connectivity and TMS-induced activity. *Cerebral Cortex*, 25(9), 2346–2353. <https://doi.org/10.1093/cercor/bhu032>
- Volz, L. J., Rehme, A. K., Michely, J., Nettekoven, C., Eickhoff, S. B., Fink, G. R., & Grefkes, C. (2016). Shaping early reorganization of neural networks promotes motor function after stroke. *Cerebral Cortex*, 26(6), 2882–2894. <https://doi.org/10.1093/cercor/bhw034>
- Volz, L. J., Sarfeld, A.-S., Diekhoff, S., Rehme, A. K., Pool, E.-M., Eickhoff, S. B., ... Grefkes, C. (2015). Motor cortex excitability and connectivity in chronic stroke: A multimodal model of functional reorganization. *Brain Structure and Function*, 220(2), 1093–1107. <https://doi.org/10.1007/s00429-013-0702-8>
- Volz, L. J., Vollmer, M., Michely, J., Fink, G. R., Rothwell, J. C., & Grefkes, C. (2017). Time-dependent functional role of the contralesional motor cortex after stroke. *NeuroImage: Clinical*, 16(June), 165–174. <https://doi.org/10.1016/j.nicl.2017.07.024>
- Ward, N. S., Brown, M. M., Thompson, A. J., & Frackowiak, R. S. J. (2003). Neural correlates of motor recovery after stroke: A longitudinal fMRI study. *Brain*, 126(11), 2476–2496. <https://doi.org/10.1093/brain/awg245>
- Yousry, T. (1997). Localization of the motor hand area to a knob on the precentral gyrus. A new landmark. *Brain*, 120(1), 141–157. <https://doi.org/10.1093/brain/120.1.141>
- Zheng, X., Sun, L., Yin, D., Jia, J., Zhao, Z., Jiang, Y., ... Fan, M. (2016). The plasticity of intrinsic functional connectivity patterns associated with rehabilitation intervention in chronic stroke patients. *Neuroradiology*, 58(4), 417–427. <https://doi.org/10.1007/s00234-016-1647-4>

SUPPORTING INFORMATION

Additional supporting information may be found online in the Supporting Information section at the end of this article.

How to cite this article: Paul, T., Hensel, L., Rehme, A. K., Tscherpel, C., Eickhoff, S. B., Fink, G. R., Grefkes, C., & Volz, L. J. (2021). Early motor network connectivity after stroke: An interplay of general reorganization and state-specific compensation. *Human Brain Mapping*, 42(16), 5230–5243. <https://doi.org/10.1002/hbm.25612>

Supplementary Material

Supplementary Table 1: Demographical and clinical information of the patient sample; adapted from Volz et al. (2016)

Patient	Age	Sex	Handedness	Lesion side	Lesion location	Days post stroke
1	78	M	R	L	Cortical (frontal)	6
2	45	F	R	L	Cortical (frontal) and WM	5
3	64	M	R	L	Internal capsule	9
4	59	M	R	R	Internal capsule and subcortical WM	5
5	76	F	R	L	Internal capsule and subcortical WM	9
6	59	M	R	L	Internal capsule and subcortical WM	7
7	72	F	L	L	Cortical (frontoparietal) and subcortical WM	1
8	73	M	R	R	Internal capsule	10
9	53	M	R	L	Internal capsule and subcortical WM	13
10	80	F	L	L	Internal capsule and BG	7
11	89	F	R	R	Internal capsule and subcortical WM	7
12	86	M	R	L	Internal capsule and subcortical WM	7
13	72	F	L	L	Internal capsule	6
14	65	M	R	L	Internal capsule	2
15	59	M	R	R	Cortical (frontoparietal) and Subcortical WM	11
16	73	M	R	L	Internal capsule and subcortical WM	4
17	62	M	R	R	Internal capsule	16
18	42	M	R	R	Cortical (frontoparietal) and Subcortical WM	5
19	53	F	L	L	Pons	1
20	89	M	R	L	Internal capsule	4
21	75	F	R	L	Internal capsule and BG	8
22	72	M	R	L	Internal capsule	10
23	58	M	R	L	Internal capsule	11
24	51	M	R	L	Internal capsule and subcortical WM	11
25	83	F	R	L	Internal capsule and BG	8
26	59	M	R	L	Pons	7

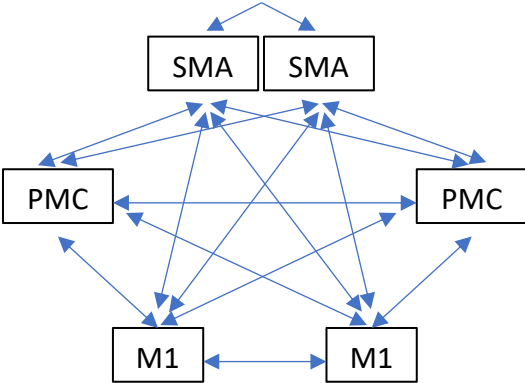
F, female; M, male; R, right; L, left; WM, white matter; BG, basal ganglia

Supplementary Table 2: Subject-specific VOI coordinates used for the calculation of trEC, rsFC and trFC. The coordinates were determined by superimposing the subject-specific activation maps on a corresponding T1-weighted image and finding the local activation maximum within region-specific anatomical constraints.

Subject	M1 aff	M1 unaff	SMA aff	SMA unaff	PMv aff	PMv unaff
1	-36 -28.5 54	28.5 -28.5 69	-13.5 -12 49.5	7.5 -3 64.5	-48 4.5 28.5	43.5 3 27
2	-34.5 -28.5 60	33 -30 60	-4.5 -10.5 51	4.5 -10.5 54	-60 -16.5 24	58.5 13.5 36
3	-33 -22.5 54	34.5 -28.5 52.5	-6 -6 60	4.5 -3 49.5	-54 4.5 43.5	52.5 -4.5 43.5
4	-43.5 -30 58.5	46.5 -27 55.5	-4.5 -12 57	6 -9 52.5	-51 -6 37.5	54 0 39
5	-37.5 -34.5 61.5	39 -34.5 63	-4.5 4.5 55.5	4.5 6 55.5	-52.5 -3 42	52.5 -18 46.5
6	-36 -27 66	37.5 -24 61.5	-6 -18 57	7.5 -1.5 60	-43.5 -6 37.5	49.5 -1.5 37.5
7	-33 -25.5 48	36 -30 46.5	-4.5 -10.5 54	10.5 -6 49.5	-54 1.5 36	46.5 1.5 42
8	-34.5 -19.5 61.5	33 -21 52.5	-7.5 -13.5 57	7.5 -10.5 51	-49.5 -3 40.5	52.5 0 39
9	-39 -22.5 66	48 -21 58.5	-6 -18 54	6 -6 58.5	-57 -9 45	51 3 42
10	-31.5 -25.5 67.5	39 -27 63	-7.5 -7.5 49.5	7.5 -6 46.5	-43.5 -12 48	55.5 1.5 34.5
11	-42 -27 42	34.5 -22.5 52.5	-9 -7.5 49.5	10.5 -12 51	-57 7.5 33	55.5 6 42
12	-34.5 -22.5 55.5	37.5 -25.5 66	-7.5 -4.5 49.5	6 -1.5 48	-54 -4.5 43.5	57 9 39
13	-30 -25.5 60	34.5 -22.5 46.5	-6 -15 57	4.5 -12 63	-46.5 -6 49.5	49.5 -6 31.5
14	-30 -28.5 49.5	34.5 -27 52.5	-4.5 -7.5 64.5	4.5 -1.5 64.5	-46.5 3 37.5	46.5 3 30
15	-39 -30 58.5	40.5 -24 60	-4.5 -10.5 63	9 -1.5 63	-51 0 42	34.5 7.5 48
16	-40.5 -18 54	46.5 -30 60	-4.5 -7.5 52.5	4.5 -9 54	-55.5 -12 40.5	51 -9 45
17	-33 -21 67.5	34.5 -21 63	-9 -4.5 52.5	6 -10.5 52.5	-52.5 -6 39	46.5 -1.5 42
18	-28.5 -27 70.5	39 -30 61.5	-4.5 -4.5 57	4.5 -3 60	-49.5 0 43.5	54 13.5 13.5
19	-31.5 -22.5 69	39 -25.5 60	-4.5 4.5 48	10.5 -3 51	-36 3 58.5	51 -4.5 43.5
20	-37.5 -21 54	36 -24 48	-4.5 -6 54	6 -12 48	-49.5 -1.5 42	51 0 42
21	-37.5 -28.5 58.5	46.5 -28.5 52.5	-4.5 -7.5 48	4.5 -6 49.5	-58.5 -3 15	63 -6 18
22	-36 -27 49.5	36 -28.5 67.5	-6 0 69	10.5 -6 67.5	-51 0 40.5	43.5 7.5 39
23	-33 -27 58.5	37.5 -28.5 57	-4.5 -6 60	7.5 -6 55.5	-52.5 -1.5 39	49.5 0 37.5
24	-31.5 -24 64.5	39 -28.5 55.5	-4.5 -9 58.5	7.5 -1.5 58.5	-55.5 0 39	51 1.5 43.5
25	-36 -25.5 45	42 -21 51	-6 4.5 66	7.5 1.5 60	-51 -4.5 43.5	52.5 -3 49.5
26	-33 -28.5 64.5	39 -30 63	-4.5 -3 52.5	4.5 -6 58.5	-40.5 -6 54	45 4.5 46.5

Supplementary Figure 1: Overview of DCM-models

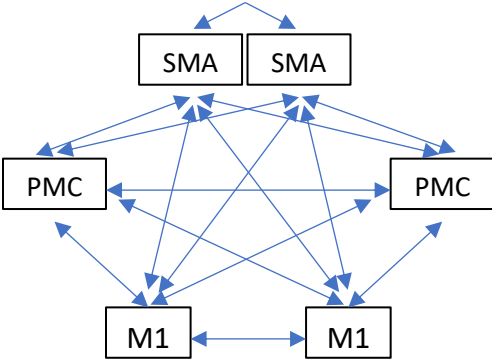
Endogenous connectivity of the DCM-A matrix:



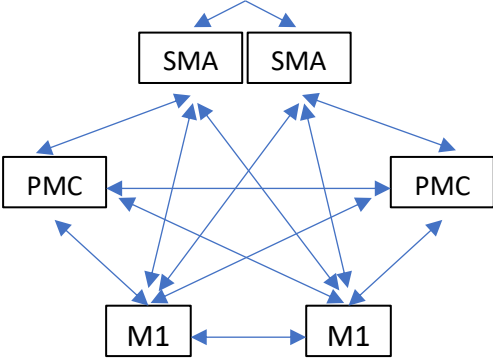
DCM A: Endogenous connectivity

Task-related coupling of the DCM-B matrix:

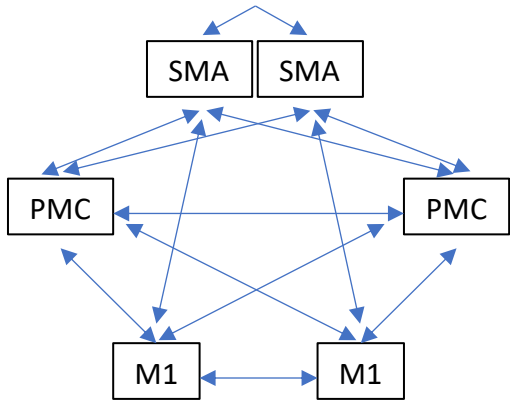
Note that only models containing an M1-M1 connection were tested.



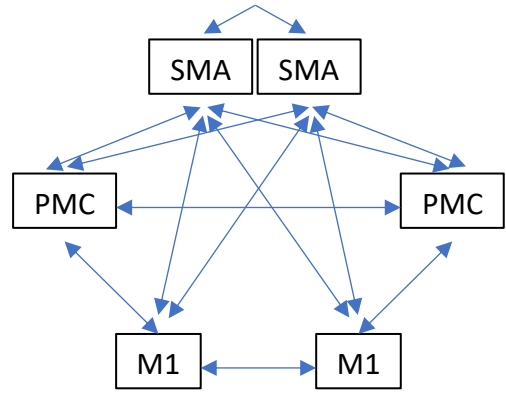
Model 01:
fully connected



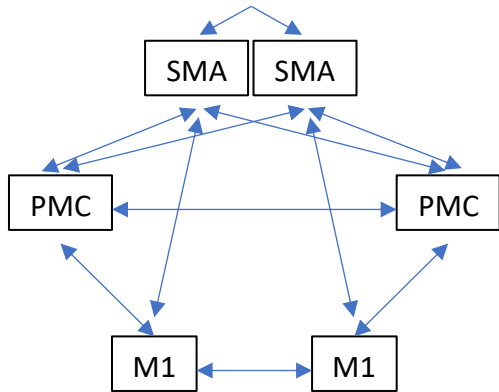
Model 02:
no interhemispheric vPMC-SMA



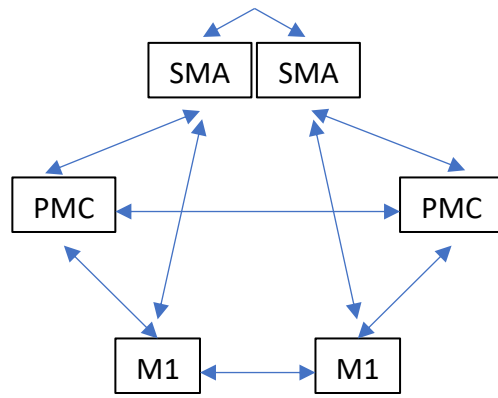
Model 03:
no interhemispheric M1-SMA



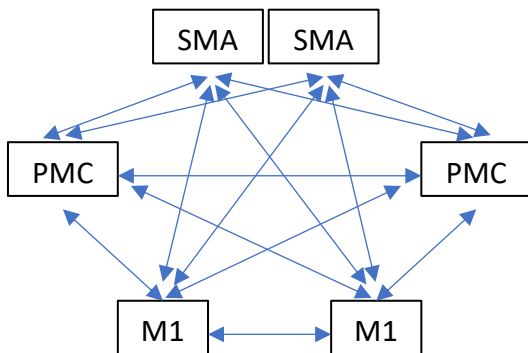
Model 04:
no interhemispheric M1-vPMC



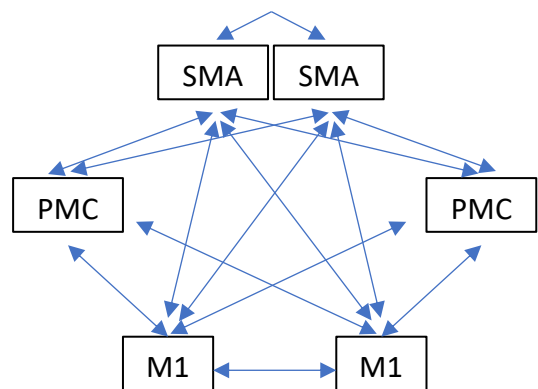
Model 05:
no interhemispheric M1-SMA, M1-vPMC



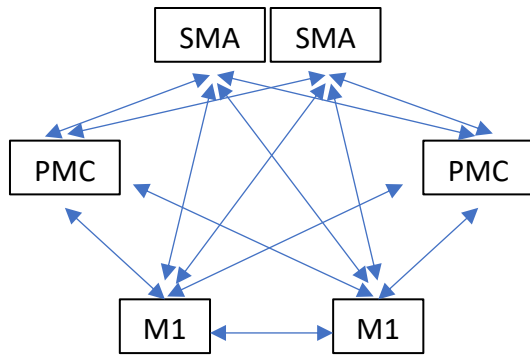
Model 06:
no interhemispheric M1-SMA, M1-vPMC,
SMA-vPMC



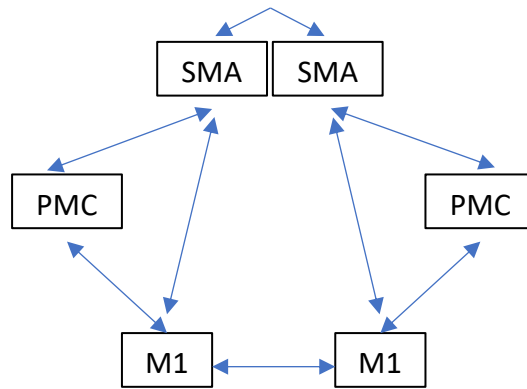
Model 07:
no interhemispheric SMA-SMA



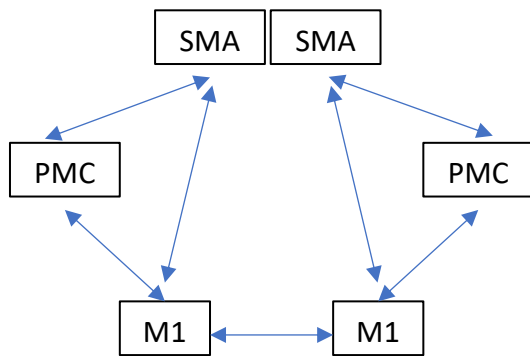
Model 08:
no interhemispheric vPMC-vPMC



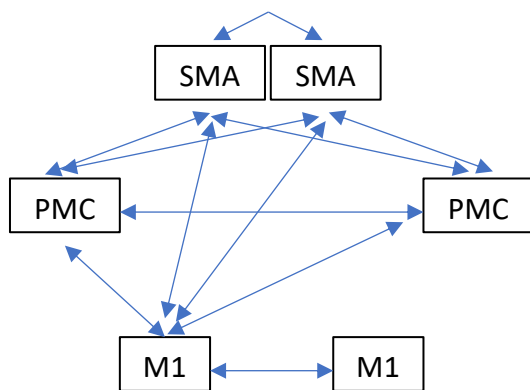
Model 09:
no interhemispheric SMA-SMA,
vPMC-vPMC



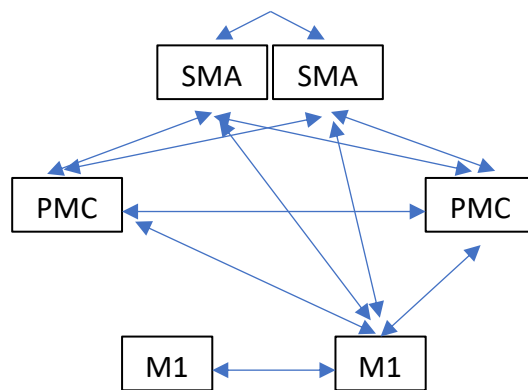
Model 10:
no interhemispheric M1-SMA,
M1-vPMC, SMA-vPMC,
vPMC-vPMC



Model 11:
no interhemispheric M1-SMA,
M1-vPMC, SMA-vPMC,
vPMC-vPMC, SMA-SMA

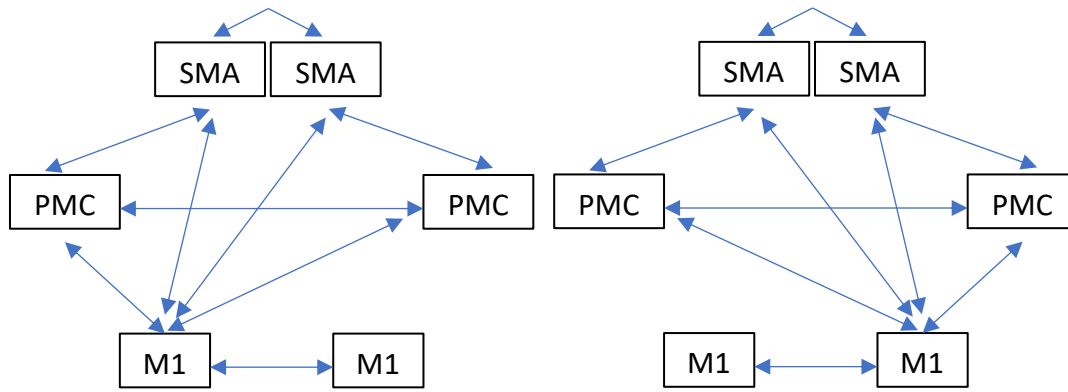


right/affected hand



left/unaffected hand

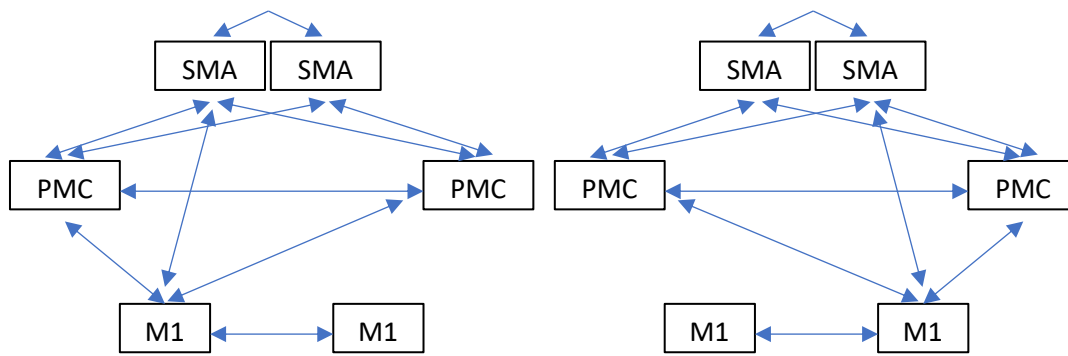
Model 12: as model 01, lateralized
(fully connected)



right/affected hand

left/unaffected hand

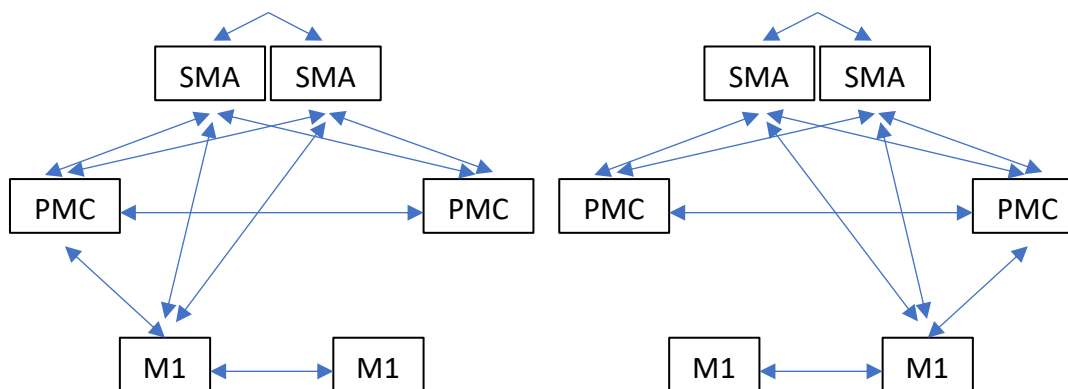
Model 13: as model 02, lateralized
(no interhemispheric vPMC-SMA)



right/affected hand

left/unaffected hand

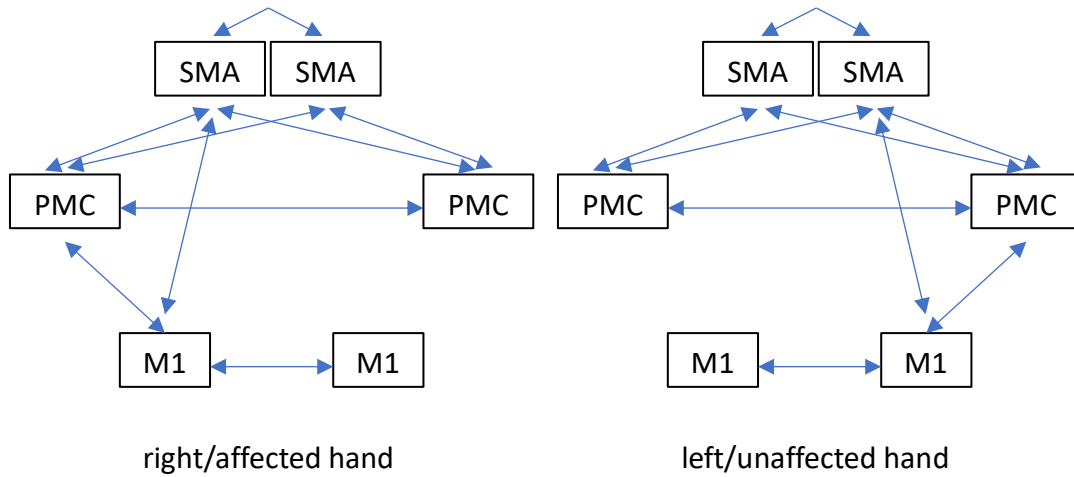
Model 14: as model 03, lateralized
(no interhemispheric M1-SMA)



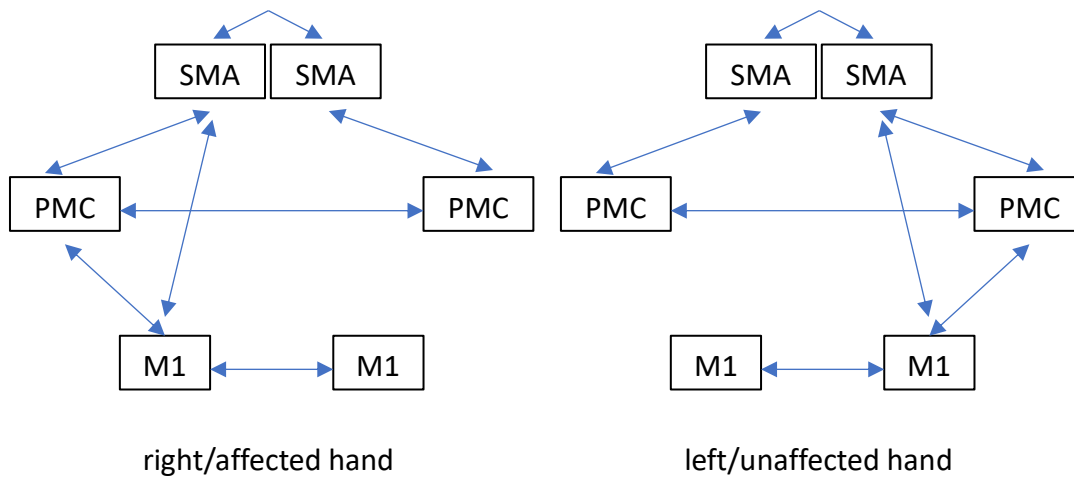
right/affected hand

left/unaffected hand

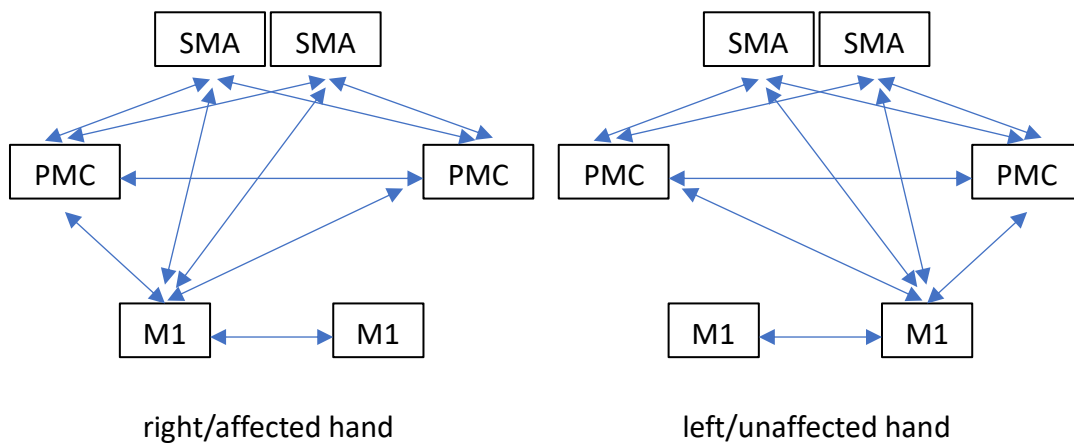
Model 15: as model 04, lateralized
(no interhemispheric M1-vPMC)



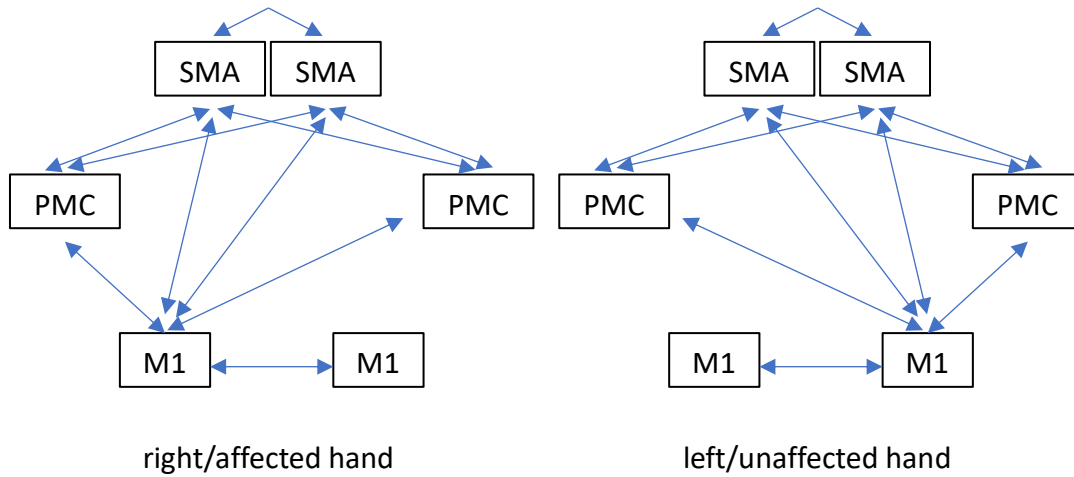
Model 16: as model 05, lateralized
(no interhemispheric M1-SMA, M1-vPMC)



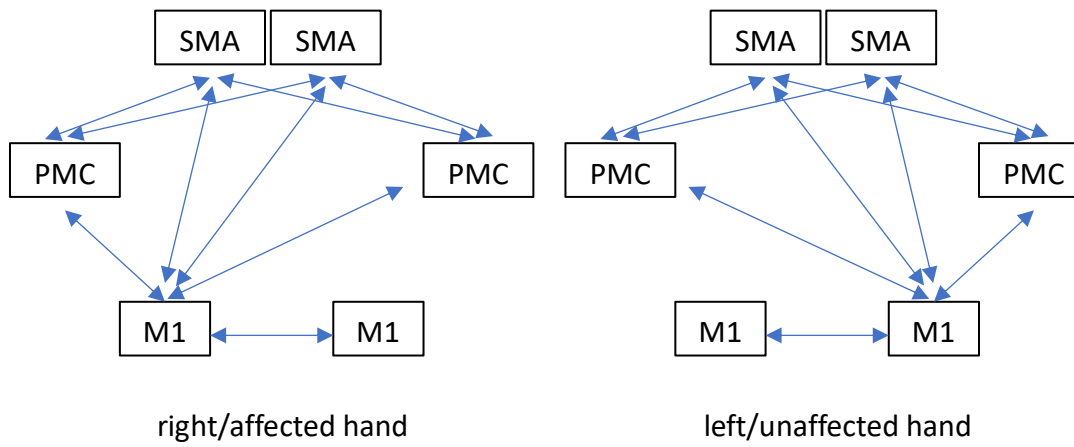
Model 17: as model 06, lateralized
(no interhemispheric M1-SMA, M1-vPMC, SMA-vPMC)



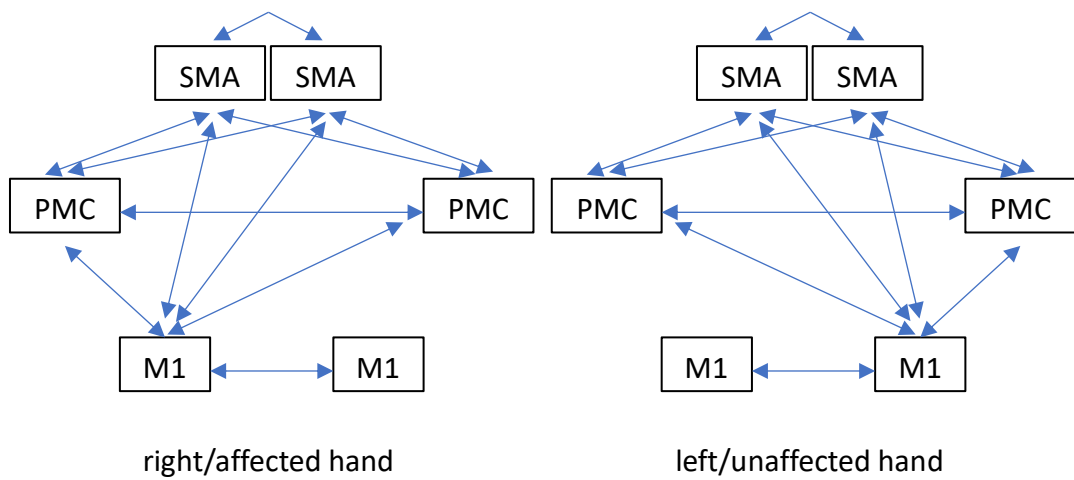
Model 18: as model 07, lateralized
(no interhemispheric SMA-SMA)



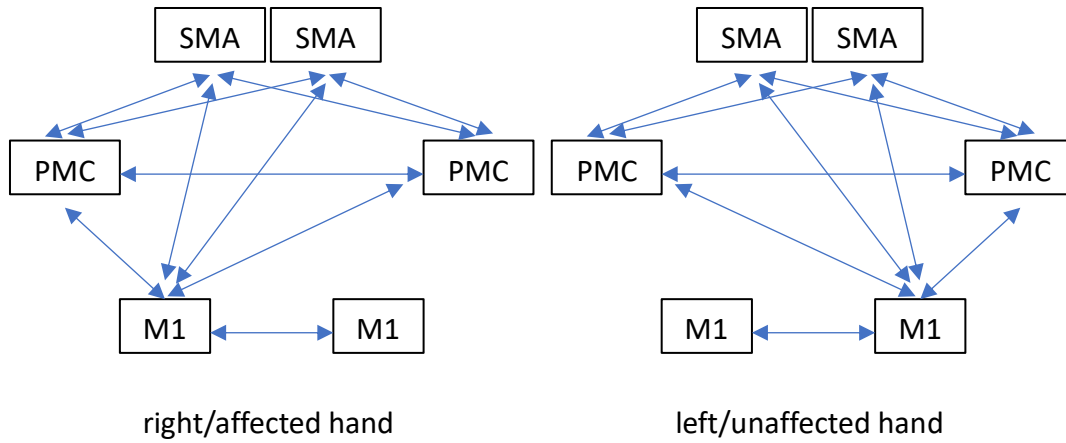
Model 19: as model 08, lateralized
(no interhemispheric vPMC-vPMC)



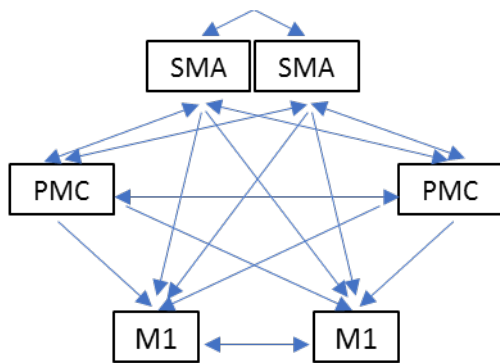
Model 20: as model 09, lateralized
(no interhemispheric SMA-SMA, vPMC-vPMC)



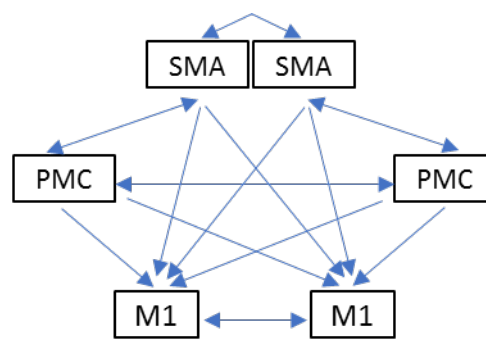
Model 21: as model 10, lateralized
(no interhemispheric M1-SMA, M1-vPMC,
SMA-vPMC, vPMC-vPMC)



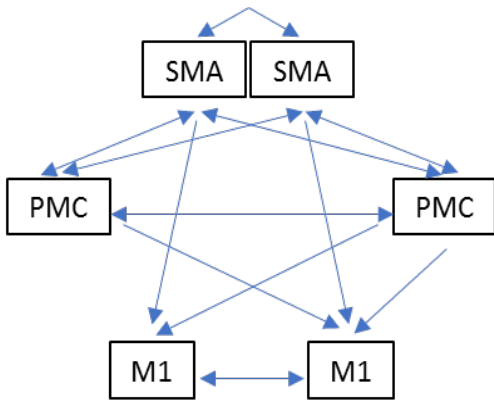
Model 22: as model 11, lateralized
 (no interhemispheric M1-SMA, M1-vPMC,
 SMA-vPMC, vPMC-vPMC, SMA-SMA)



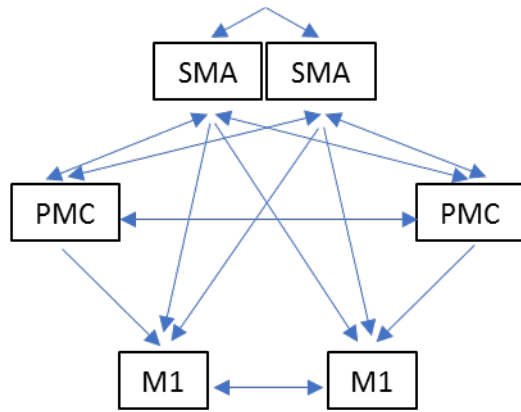
Model 23: as model 01, unidirectional
 (fully connected)



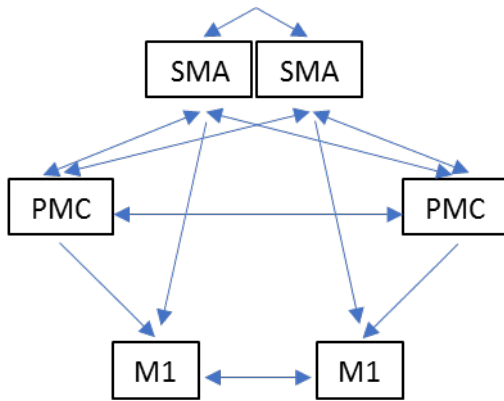
Model 24: as model 02, unidirectional
 (no interhemispheric vPMC-SMA)



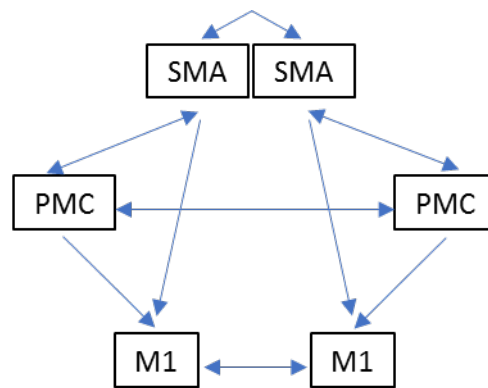
Model 25: as model 03, unidirectional (no interhemispheric M1-SMA)



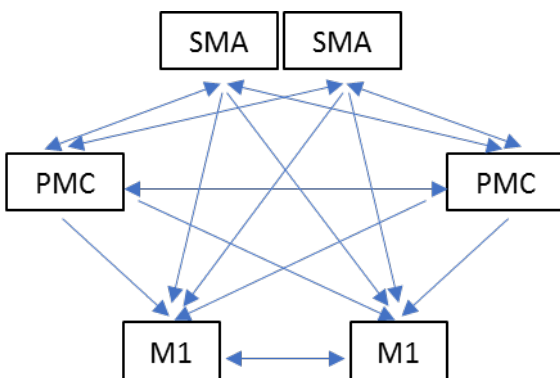
Model 26: as model 04, unidirectional (no interhemispheric M1-vPMC)



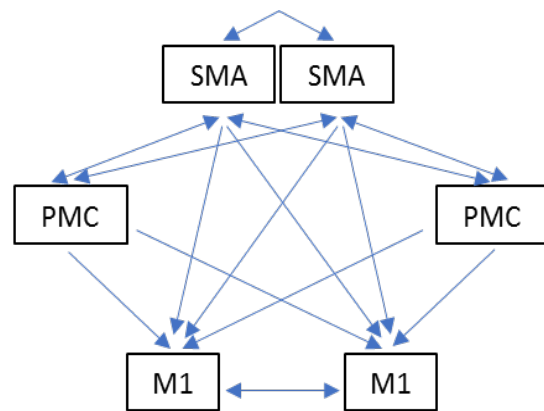
Model 27: as model 05, unidirectional (no interhemispheric M1-SMA, M1-vPMC)



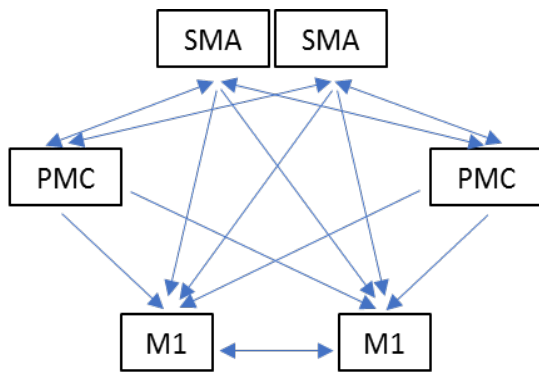
Model 28: as model 06, unidirectional (no interhemispheric M1-SMA, M1-vPMC, SMA-vPMC)



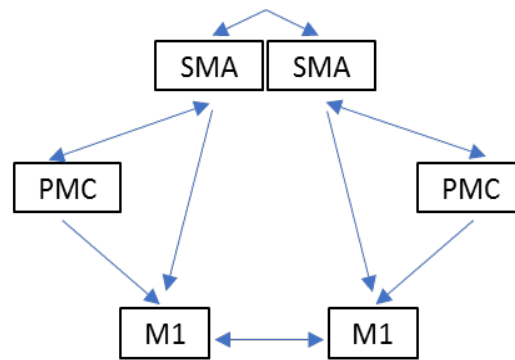
Model 29: as model 07, unidirectional (no interhemispheric SMA-SMA)



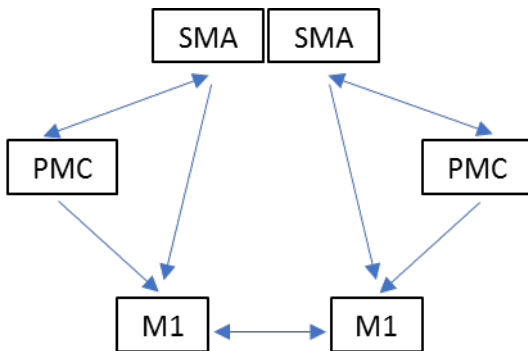
Model 30: as model 08, unidirectional (no interhemispheric vPMC-vPMC)



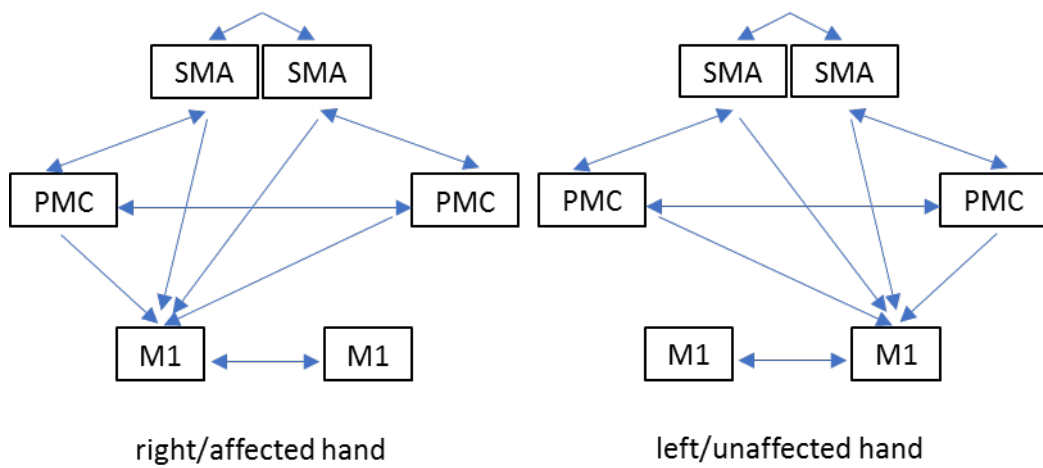
Model 31: as model 09, unidirectional
(no interhemispheric SMA-SMA, vPMC-
vPMC)



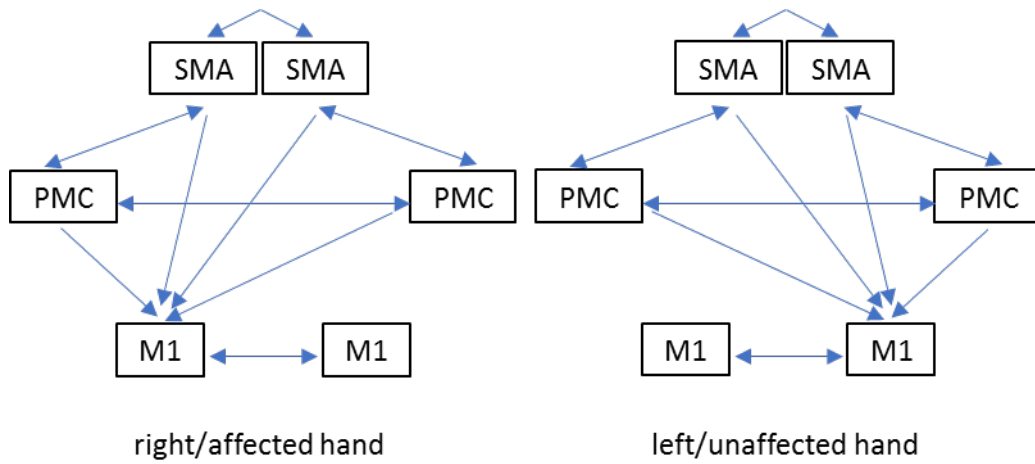
Model 32: as model 10, unidirectional
(no interhemispheric M1-SMA,
M1-vPMC, SMA-vPMC,
vPMC-vPMC)



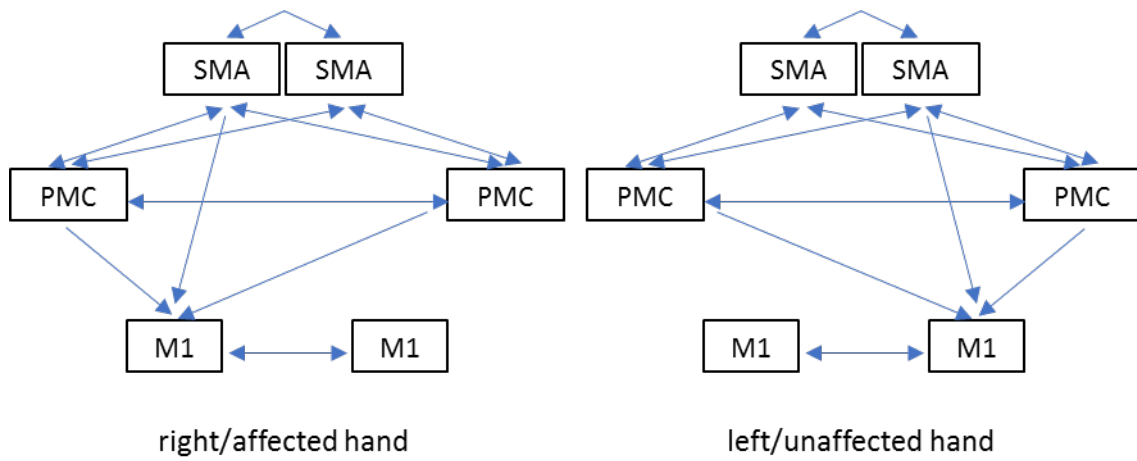
Model 33: as model 11, unidirectional
(no interhemispheric M1-SMA,
M1-vPMC, SMA-vPMC,
vPMC-vPMC, SMA-SMA)



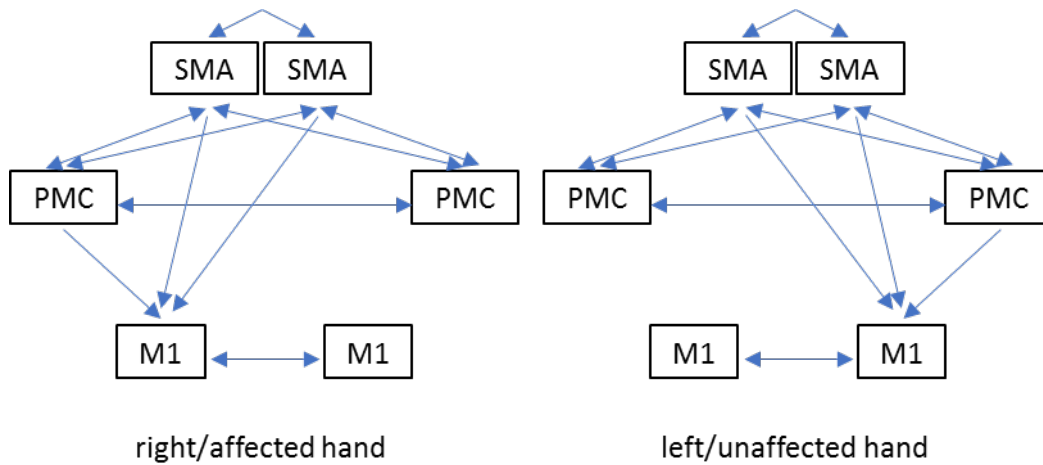
Model 34: as model 12, unidirectional
(fully connected)



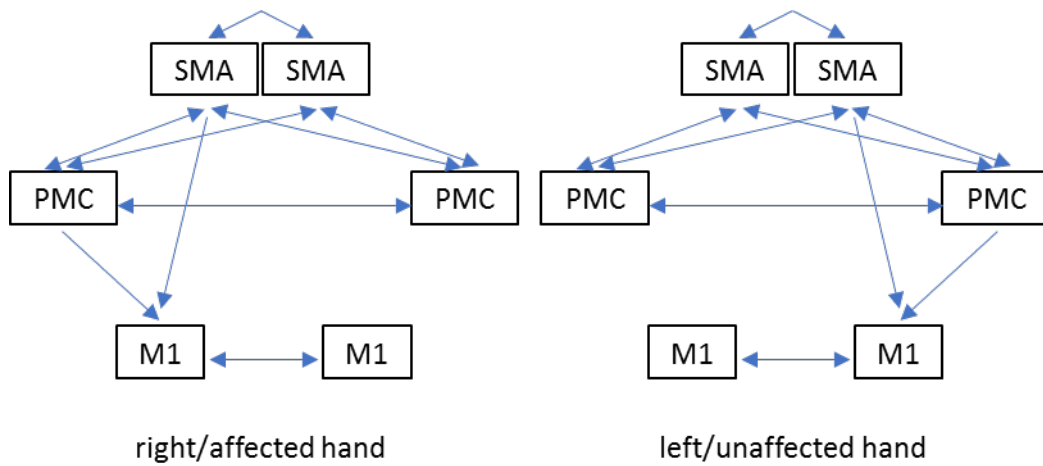
Model 35: as model 13, unidirectional
(no interhemispheric vPMC-SMA)



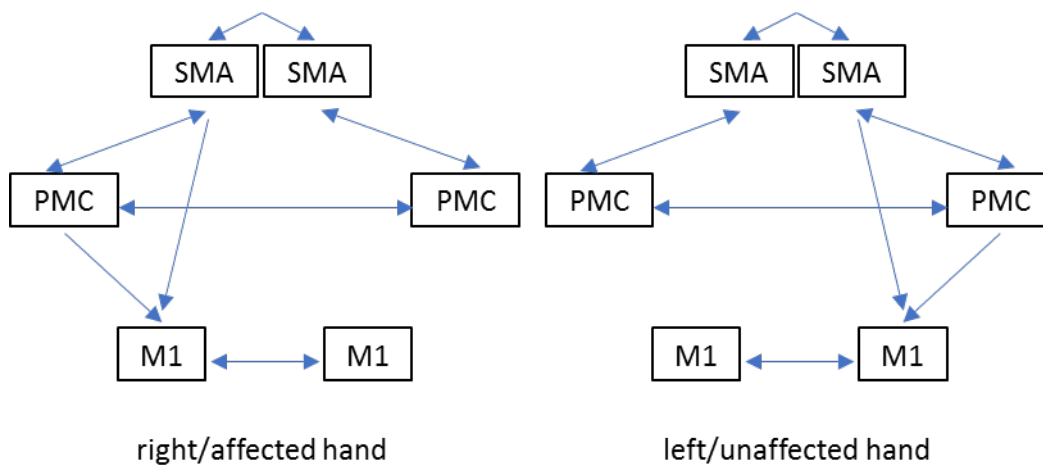
Model 36: as model 14, unidirectional
(no interhemispheric M1-SMA)



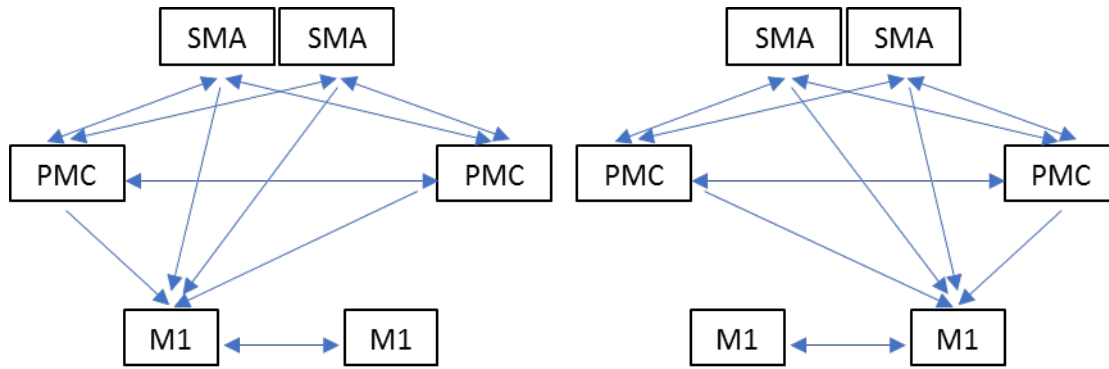
Model 37: as model 15, unidirectional
(no interhemispheric M1-vPMC)



Model 38: as model 16, unidirectional
(no interhemispheric M1-SMA, M1-vPMC)



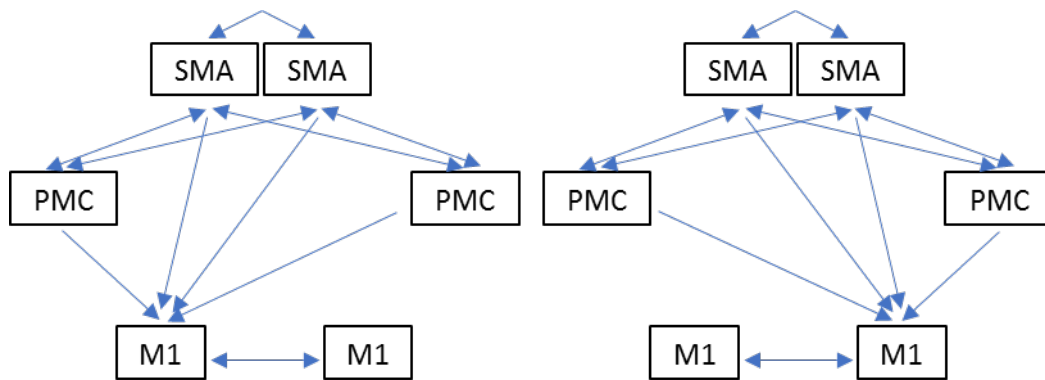
Model 39: as model 17, unidirectional
(no interhemispheric M1-SMA, M1-vPMC, SMA-vPMC)



right/affected hand

left/unaffected hand

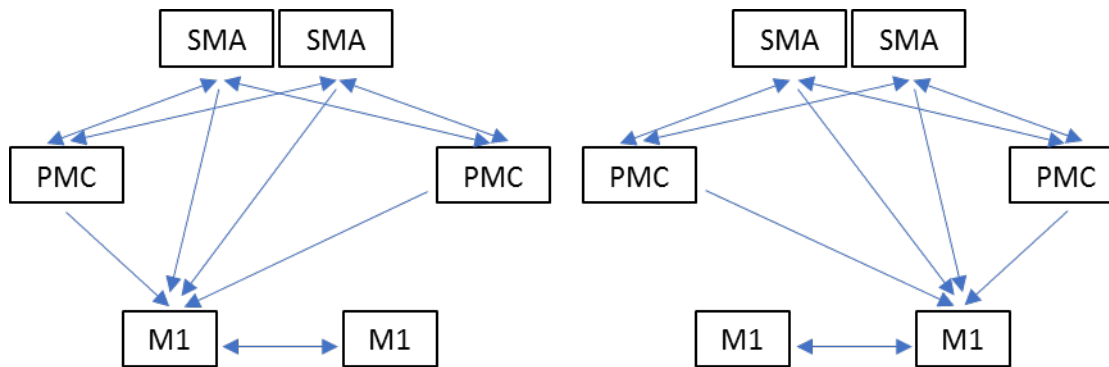
Model 40: as model 18, unidirectional
(no interhemispheric SMA-SMA)



right/affected hand

left/unaffected hand

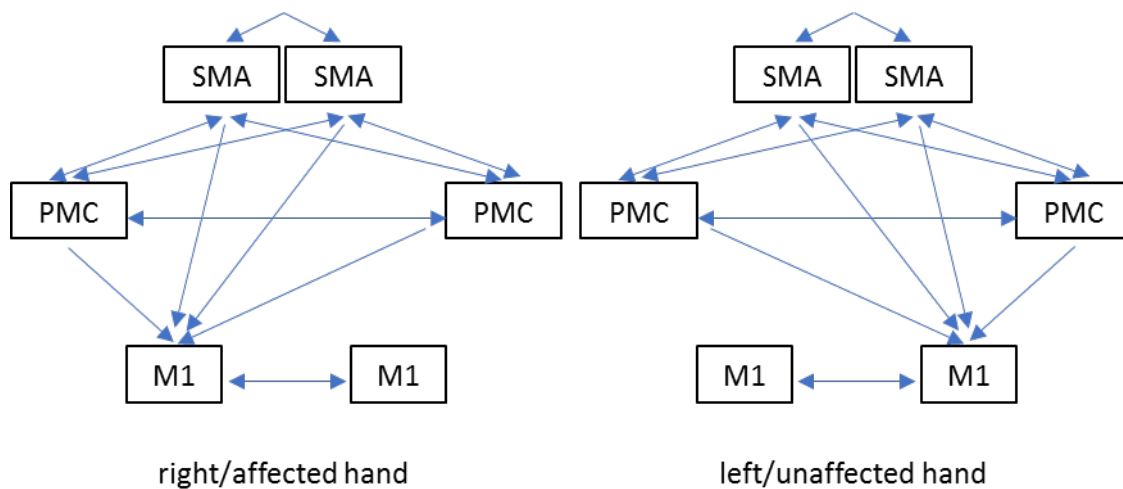
Model 41: as model 19, unidirectional
(no interhemispheric vPMC-vPMC)



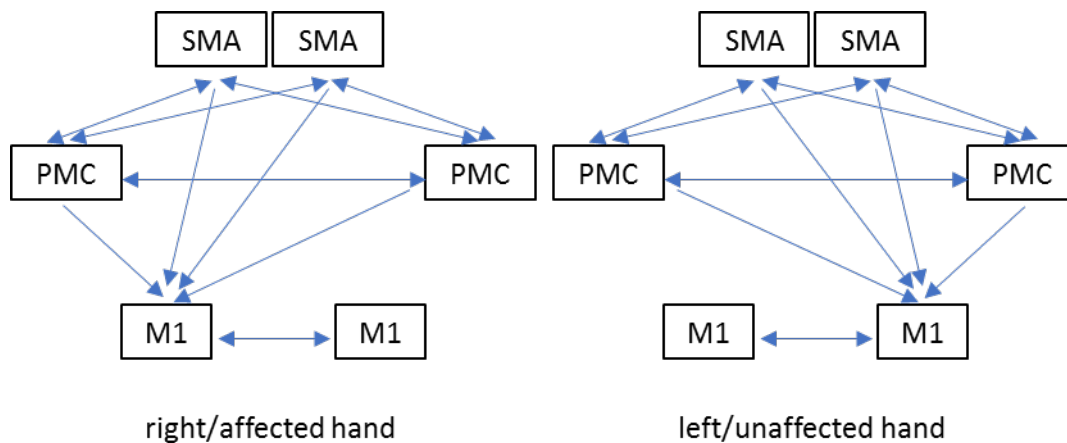
right/affected hand

left/unaffected hand

Model 42: as model 20, unidirectional
(no interhemispheric SMA-SMA, vPMC-vPMC)



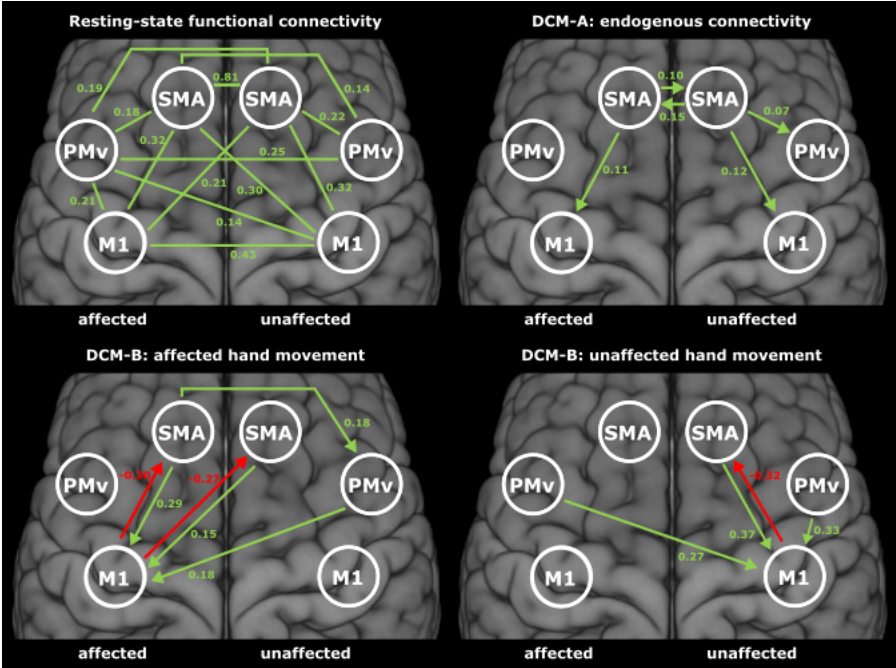
Model 43: as model 21, unidirectional
(no interhemispheric M1-SMA, M1-vPMC,
SMA-vPMC, vPMC-vPMC)



Model 44: as model 22, unidirectional
(no interhemispheric M1-SMA, M1-vPMC,
SMA-vPMC, vPMC-vPMC, SMA-SMA)

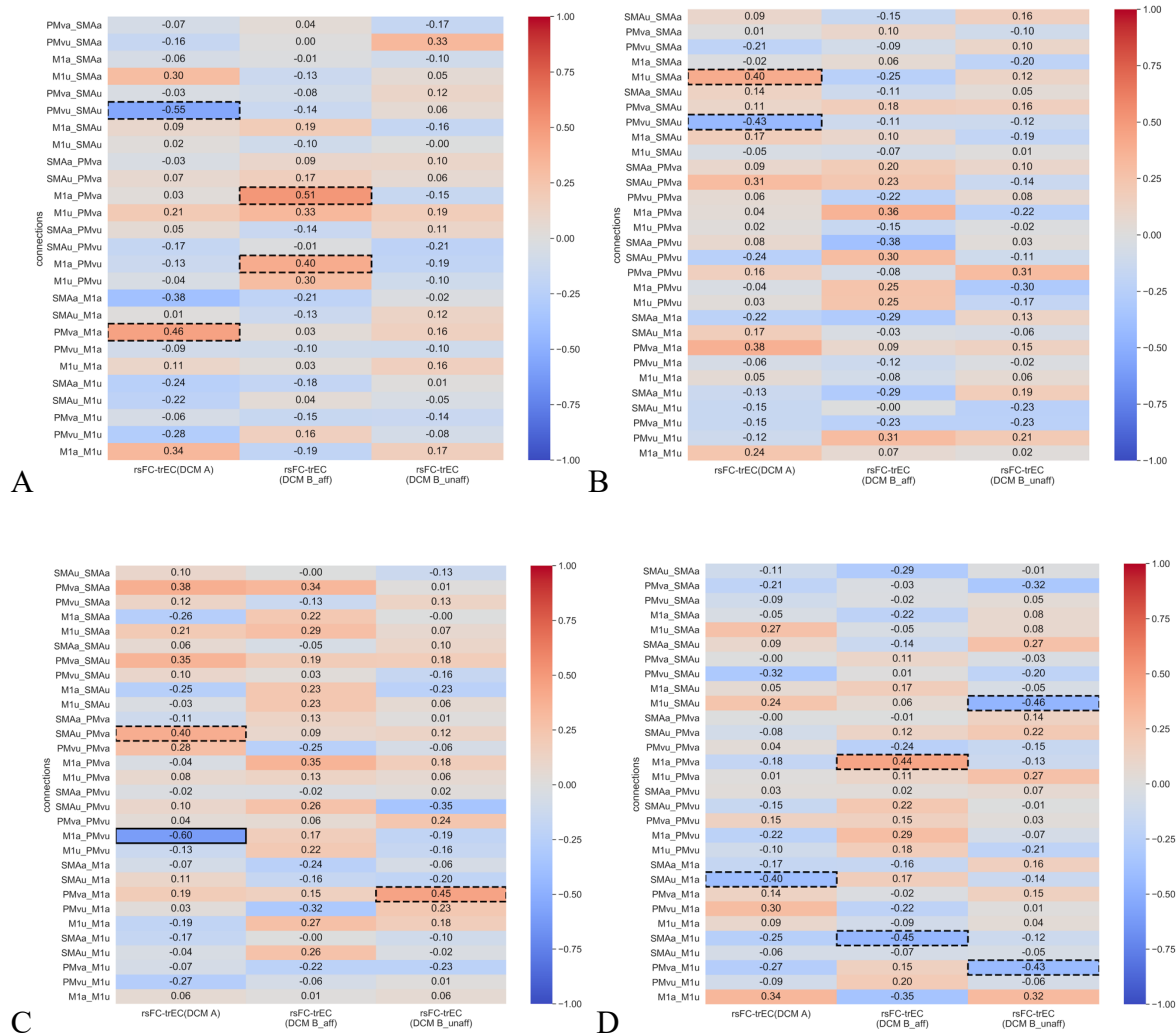
Supplementary Figure 1: Overview of DCM models. For the endogenous connectivity described by matrix A , we assumed a fully connected model. For matrix B , we started with a fully connected model analogous to matrix A from which interhemispheric connections were systematically removed, resulting in 44 models of varying complexity. The resulting models were grouped into four model families consisting of 11 models each, differing in terms of lateralization and directionality: 1) non-lateralized / bidirectional, 2) lateralized / bidirectional, 3) non-lateralized / unidirectional, 4) lateralized / bidirectional. Directionality specifies whether M1 only receives inputs (unidirectional) or whether there is a back-coupling onto premotor areas (bidirectional). Lateralization describes whether connections with both M1 are present in the DCM- B matrix regardless which hand is moved, or whether only the M1 contralateral to the moving hand is connected to premotor areas. While non-lateralized models postulate identical connections in matrix B during movements of either hand, lateralized models assume M1-connections only for the contralateral hemisphere, meaning that the ipsilateral M1 is only connected to its contralateral equivalent.

Supplementary Figure 2: Group-level connectivity



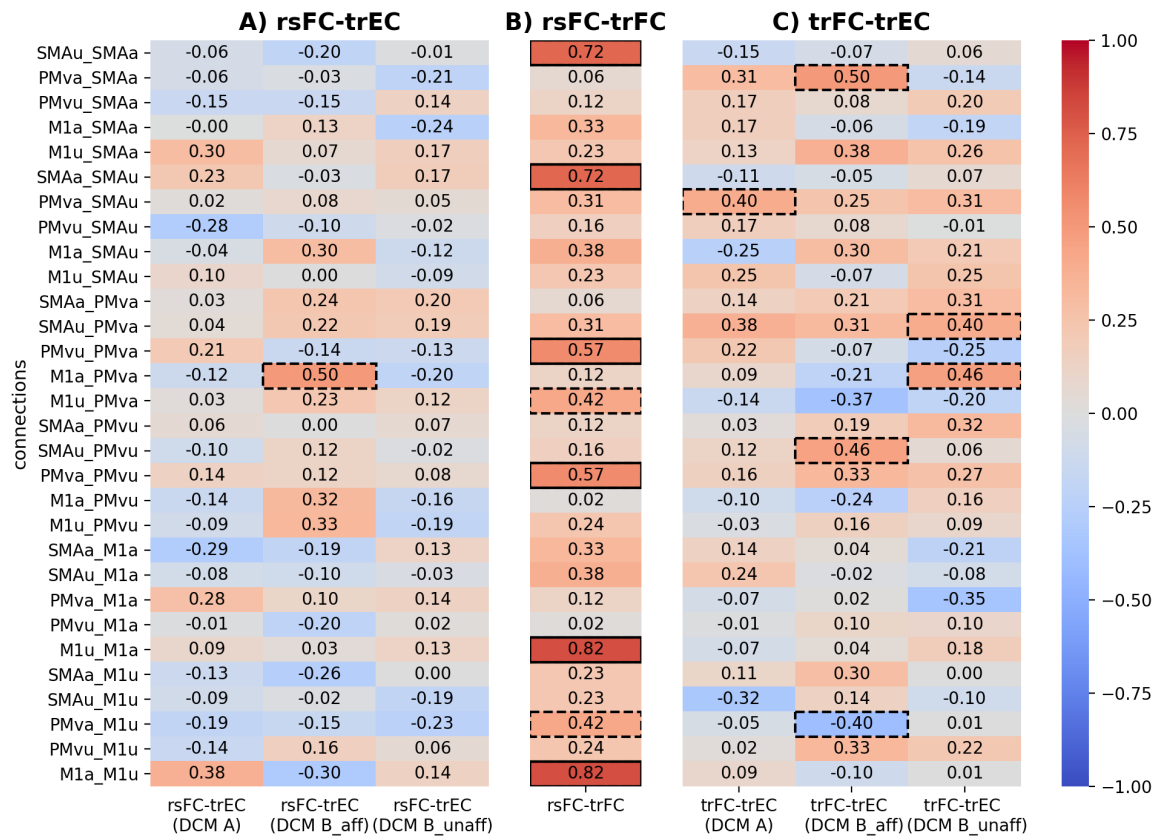
Supplementary Figure 1: Group-level connectivity. Significant connections of the resting-state Z-values, endogenous DCM-connectivity, DCM-coupling parameters during movement of the affected and unaffected hand (DCM-B-affected and DCM-B-unaffected matrix of the fully connected model), $p < .05$, FDR-corrected for multiple comparisons. The displayed values are group-level averages across patients. Missing connections between the displayed cortical regions did not reach significance after FDR-correction across the group.

Supplementary Figure 3: Correlations between functional and effective connectivity for alternative DCMs and resting-state Z-values obtained using different preprocessing methods



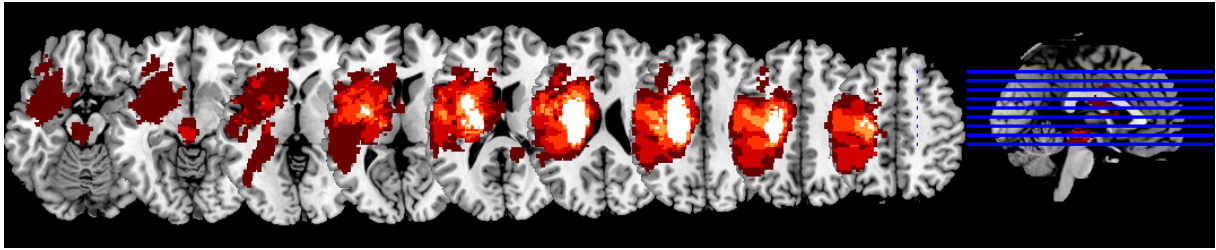
Supplementary Figure 3: Spearman rank correlations between task-related effective connectivity and resting-state functional connectivity of corresponding region pairs. Effective connectivity is expressed in terms of coupling parameters of the DCM-A, B-affected, and B-unaffected matrix. Resting-state functional connectivity is expressed as Fisher's Z-scores derived from Pearson correlations of the predefined region pairs. The values depicted in each cell are the corresponding Spearman rank correlations. Dashed lines indicate significance at an uncorrected level ($p < .05$); solid lines indicate significance at a corrected level ($p < .05$, FDR-corrected for the number of comparisons). The lack of solid lines indicates that no significant correlations between functional and effective connectivity were observed. For the individual comparisons, the following parameters were used: (A) DCM results of the winning model (Model 9), as determined by Bayesian Model Selection (BMS), correlated with resting-state Z-values. (B) DCM coupling parameters derived from Bayesian Model Averaging (BMA) of the winning family (Family 1) correlated with resting-state Z-values. (C) DCM results of the fully connected model correlated with resting-state Z-values obtained without global signal regression. (D) DCM results of the fully connected model correlated with resting-state Z-values obtained with PCA-denoising.

Supplementary Figure 4: Spearman rank correlations between trEC, rsFC, and trFC



Supplementary Figure 4: Spearman rank correlations between trEC, rsFC, and trFC. The three charts entail correlations between A) rsFC and trEC, B) rsFC and trFC, and C) trFC and trEC. trEC is expressed in terms of coupling parameters of the DCM-A, B-affected and B-unaffected matrix. rsFC is expressed as Fisher's Z-scores derived from Pearson correlations of the predefined region pairs. trFC was computed from the timeseries recorded during movement of the affected hand as Fisher's Z-scores derived from Pearson correlations of the predefined region pairs. Dashed lines indicate significance at an uncorrected level ($p < .05$), solid lines indicate significance after FDR-correction for multiple comparisons ($p < .05$, FDR-corrected).

Supplementary Figure 5: Lesion overlay



Supplementary Figure 5: Lesion overlay of all 26 stroke patients. The overlay of all 26 individual lesion maps shows that the greatest lesion overlap is located in the area of the internal capsule, followed by more widespread cortical lesions.

6. General discussion

The present thesis aimed at improving our understanding of mechanisms underlying motor network reorganization after stroke. To this end, we investigated structural and functional properties of the stroke-afflicted motor network and their associations with differential aspects of motor control and impairment. We thereby gained important insights into network mechanisms enabling the recovery of motor functions following stroke. In this section, I will discuss the relevance of our findings in light of the existing literature. I will start by briefly summarizing the main findings of each study before I move on to highlight the benefits of our novel compartmentwise analysis approach for dMRI. I will then continue by discussing potential implications of our results regarding the role of descending motor pathways. Next, I will address the significance of our findings on cortico-cortical connectivity for the task-specificity of post-stroke motor control with a special emphasis on the heavily debated interhemispheric M1-M1 connection. Last, I will illustrate the clinical implications of our findings, address their limitations, and outline suggestions for future research.

6.1. Study-specific key findings

The first study aimed at elucidating the role of different descending motor output pathways in basal and complex motor control of the upper and lower limb. Using a novel compartmentwise analysis approach, we provide evidence for Wallerian degeneration along the entire length of the ipsilesional CST, which constitutes a considerable improvement compared to previous ROI-based approaches. Correlations between two-directional voxels of the extrapyramidal system and basal upper and lower limb motor control point towards specific brain stem structures involved in compensatory processes. Of note, the lack of a difference between patients and age-matched controls with respect to extrapyramidal pathways across all compartments suggests that the observed associations with motor performance stem from the premorbid level of extrapyramidal anisotropy, i.e., the patient's structural reserve, rather than being a result of reorganization reflected by structural changes within the extrapyramidal tracts.

In study 2, we focused on corticospinal output fibers descending from M1, SMA, PMd, and PMv and assessed their relevance for different aspects of motor control after stroke. Our results indicate a dissociation between basal and complex motor skills. While complex motor functions were only correlated with anisotropy derived from premotor subtracts, basal motor control showed positive correlations with both premotor and M1 output pathways. Thus, whereas M1 tract integrity was relevant for any form of muscle activation, premotor pathways

seemed to be primarily involved in shaping complex motor performance. Interestingly, a subgroup analysis revealed that corticospinal premotor tracts might additionally contribute to basal motor control in patients with persistent motor deficits in the chronic stage, which suggests a vicarious role of descending premotor pathways.

In line with our hypotheses, study 3 showed that both ipsilesional premotor-M1 and M1-M1 structural connectivity was significantly correlated with motor impairment. The correlation with complex motor control depended on ipsilesional CST integrity, indicating that complex motor control strongly relies on ipsilesional output fibers. In contrast, the correlations with basal motor functions persisted when controlling for CST integrity, suggesting that basal motor control might be achieved via alternative output routes. As reflected by a subgroup analysis, patients who underwent substantial recovery from the acute to the chronic phase seemed to particularly rely on structural connectivity between bilateral M1, which might help to relay signals via the contralesional M1 and contralesional CST to the spinal level.

In study 4, we conducted a direct comparison of resting-state functional and task-related effective connectivity. Our results showed that both connectivity modes were able to explain motor impairment in the acute phase post-stroke, underlining the clinical potential of fMRI-based approaches. Interestingly, our results suggest a fundamental difference between intrahemispheric and interhemispheric motor network reorganization. While intrahemispheric connectivity depended on the activation state, interhemispheric connectivity was state-independent. Thus, interhemispheric information integration might rely on more general, overarching principles that are reflected across activation states, whereas reorganization of ipsilesional premotor-M1 interactions seems to be state- and task-dependent.

6.2. Advantages of compartmentwise anisotropy in stroke

As described above, reliably estimating anisotropy in voxels with multiple fiber directions, i.e., in voxels containing crossing or kissing fibers, is extremely difficult (Basser et al., 1994; Descoteaux et al., 2006; Volz et al., 2018). Previous research on stroke-related Wallerian degeneration of the ipsilesional CST has therefore commonly employed ROI-based approaches. These approaches are based on the assumption that CST sections of densely packed fibers accurately represent secondary degeneration. Yet the limited number of voxels within each ROI may introduce considerable sampling biases. In study 1, we offered a possible solution to this problem by demonstrating the feasibility of a novel approach to quantify tractwise anisotropy in stroke patients. By categorizing all WM voxels into compartments according to their number of trackable directions, we were able to focus our analyses on a given

directional compartment, e.g., to exclusively include one-directional CST voxels containing descending fibers. Importantly, decreased anisotropy in comparison to healthy age-matched controls was limited to descending fibers (i.e., one-directional voxels) of the ipsilesional CST, whereas age-related reductions in anisotropy could be found ubiquitously across compartments in the left and right CST. Thus, we were able to differentiate between ageing- and stroke-related effects and thereby demonstrated that Wallerian degeneration was specific to the ipsilesional CST. We thereby provide direct evidence for the commonly held view that Wallerian degeneration gives rise to the correlation between ipsilesional CST microstructure and motor impairment. Alternatively, the correlation might have been driven by the level of structural reserve, i.e., the premorbid level of CST fibers. Given the absence of a correlation with the contralesional CST, this alternative interpretation is highly unlikely.

While study 1 provided evidence for Wallerian degeneration along the entire length of the ipsilesional CST, study 2 identified CST sections most indicative of motor performance. Importantly, the analysis of height-dependent differences was only possible because of the compartmentwise approach, as anisotropy in cranial CST sections closer to the cortex tends to be heavily distorted by crossing fibers. Our results revealed a distinction between corticospinal fibers descending from premotor areas and those descending from M1. While both premotor and M1 subtracts showed a strong correlation with motor impairment at the level of the PLIC, the M1 subtract featured an additional section of slices indicative of motor impairment closer to the cortex. These findings might derive from different mechanisms underlying the indicative nature of anisotropy depending on the level of the analyzed CST. Thus, we were able to gain novel insights that were only possible when considering the entire length of the CST.

Of note, the proposed compartmentwise analysis approach did not only offer new mechanistic insights into stroke-related motor system changes but also led to an improved prediction of motor performance. This becomes apparent when comparing the explanation of motor behavior achieved with more conventional ROI-based approaches. As demonstrated in study 1, anisotropy derived from one-directional voxels of the whole CST outperformed anisotropy derived from voxels within the PLIC or located in the CST section ranging from mesencephalon to the cerebral peduncles. The higher ratio of explained variance is like attributable to an enhanced signal-to-noise ratio, which was achieved by two major factors. First, computing mean anisotropy based on a higher number of voxels mitigates the impact of sampling biases like partial volume effects. Second, the focus on one-directional voxels restricts the dilution of anisotropy by crossing fibers. Thus, compartmentwise dMRI analyses constitute a major advancement for improving the signal-to-noise ratio in tractwise analyses of anisotropy.

Importantly, the improvement in signal-to-noise ratio is not limited to descending fiber tracts but also applies to anisotropy derived from cortico-cortical connections as demonstrated in study 3. Certain parts of premotor-M1 connections tend to intersect with other tracts. In consequence, multi-directional voxels are part of most fiber tracts, which impedes a reliable estimation of anisotropy. By limiting the analysis to one-directional voxels, we circumvented this problem by focusing solely on relevant voxels unique to the given connection. This underlines the generalizability of a compartmentwise analysis approach and implies that it can also be used for anisotropy-based analyses of cortico-cortical structures. Moreover, compartmentwise analyses might also be advantageous for applications that go beyond stroke research as an improved signal-to-noise ratio should greatly benefit any tractwise analysis that tries to understand structural alterations in (neurological) diseases.

However, there is one caveat regarding the generalizability to patients in the acute phase. As outlined above, Wallerian degeneration is not a direct effect of the lesion but a secondary degenerative process that occurs over time (Conforti et al., 2014). In consequence, the effects of Wallerian degeneration do not fully materialize in the acute phase but only become apparent over time. This raises the question whether tractwise CST anisotropy is the most suitable measure for a longitudinal prediction of motor performance based on data obtained in the acute phase post-stroke. Empirical studies should therefore address whether tractwise anisotropy, ROI-based anisotropy or a weighted lesion load is better suited for the longitudinal prediction of motor recovery.

6.3. Extrapyramidal output pathways

Another advantage of the compartmentwise approach was that it offered new insights into the role of the extrapyramidal system for motor control in chronic stroke patients. As discussed in detail in section 2.2.4, previous studies have reported inconsistent results regarding the role of extrapyramidal tracts in motor performance after stroke. While some studies argue that output from extrapyramidal pathways supports motor function after stroke, others attribute maladaptive flexor synergies and a loss of finger individuation to an overactive extrapyramidal system (McPherson et al., 2018; Owen et al., 2017; Ruber et al., 2012; Takenobu et al., 2014).

In line with previous findings, we observed a negative correlation with basal upper and lower limb motor control in study 1, suggesting that higher (i.e., better) anisotropy was related to poorer basal motor performance (McPherson et al., 2018; Owen et al., 2017). However, our present findings offer a new perspective on this debate as the correlation with motor performance was driven by voxels containing two dominant fiber directions. While this

complicates the interpretation of the correlation, it also helps to narrow down relevant anatomical structures. First of all, it implies that motor performance was not explained by descending fibers in one-directional voxels (as observed for the ipsilesional CST), but crossing fibers located in specific locations within the brainstem. Overlaying the relevant voxels from compartment 2 on top of a T1-weighted MNI template enabled us to identify these structures as (i) fibers crossing the midline, (ii) fibers potentially transmitting output from brainstem nuclei, and (iii) fibers transferring signals between the extrapyramidal system and the cerebellum. In other words, structural connections that facilitate the communication between extrapyramidal tracts and subcortical structures seemed to be driving the association with basal motor control.

At first glance, these findings might seem at odds with the existing literature as previous studies commonly conclude that the output properties of extrapyramidal tracts are the relevant feature giving rise to the commonly observed association with motor behavior. However, at a closer look, this can be easily reconciled with our present results as previous studies hardly ever focused on the actual reticulospinal or rubrospinal tracts descending from the reticular formation or red nucleus, respectively. Instead, several studies used a priori defined ROIs of the red nucleus or the reticular formation and extracted anisotropy in the vicinity of these ROIs (Owen et al., 2017; Peters et al., 2021). They thereby inadvertently focused on a cluster of mostly two-directional voxels rather than descending extrapyramidal fibers, which is well in line with our findings. Yet the most compelling support for our current results stems from studies applying voxel-wise whole-brain approaches that consistently reveal correlations between motor impairment and clusters of voxels in the periphery of bilateral red nuclei (Ruber et al., 2012; Takenobu et al., 2014). The fact that these whole-brain analyses point towards voxels surrounding the red nucleus without relying on any a priori hypotheses corroborates that the two-directional brainstem voxels identified in our study indeed contribute to motor control after stroke.

In sharp contrast to these findings of very narrowly circumscribed clusters of voxels, another set of studies used relatively wide tract templates that did not discriminate between individual extrapyramidal tracts (Lindenberg et al., 2010, 2012; Schulz et al., 2017a). Of note, these templates also contained cortical projections to the extrapyramidal structures, which means that various unspecific structures were included, and analyses were not limited to descending fibers. Moreover, even the very few studies actually relying on tractwise anisotropy of individual extrapyramidal tracts descending from the brainstem level contained the relevant sections of two-directional voxels (Guo et al., 2019; Karbasforoushan et al., 2019). This leaves

room for speculation whether the observed correlations with motor impairment in these studies might have been driven by the clusters of two-directional voxels identified in study 1.

Having narrowed down the anatomical underpinnings of the observed correlations, we now turn to the issue of directionality. With both positive (Guo et al., 2019; Peters et al., 2021; Ruber et al., 2012; Takenobu et al., 2014) and negative correlations (Owen et al., 2017; Schulz et al., 2017a) between extrapyramidal anisotropy and motor behavior, it is difficult to specify whether the influence of the extrapyramidal system on motor recovery is rather vicarious or maladaptive in nature. Our current results may hold an explanation for these contradictory findings as they might be explained by the fact that the relevant clusters driving the correlation likely contained two-directional voxels. As described in the methods section (see Methods section 4.2.4.), anisotropy in multi-directional voxels cannot be easily quantified and a decrease in only one dominant direction might result in a misleading overall increase of anisotropy. Thus, the directions of the observed correlations have to be interpreted with caution and contradictory results in previous publications might stem from the estimation of anisotropy from two-directional voxels. However, given that we used an advanced DSI protocol which readily differentiates the number of intra-voxel fiber directions, one might cautiously interpret the observed negative correlations in study 1 as tentative evidence for a maladaptive influence of the extrapyramidal system. In other words, if we assumed that higher anisotropy truly reflected better microstructural integrity, then our findings would imply a negative correlation between the integrity of brainstem structures and motor control. This nicely matches the view that an overcompensation by the extrapyramidal system might lead to an increase in strength at the cost of isolated movements (McPherson et al., 2018; Owen et al., 2017). However, improved methods to accurately describe anisotropy in multi-directional voxels are needed to give a definite answer to this question.

6.4. Descending output from premotor regions

Not only the extrapyramidal system plays a role in the compensation of motor impairment, but premotor regions are also thought to be heavily involved in mitigating stroke-induced motor deficits. While previous studies mainly discussed the role of premotor areas in cortico-cortical interactions, we focused on their descending corticospinal output in study 2. Our findings highlight a clear distinction between basal and complex motor control in chronic stroke patients: While M1 was associated with both basal and complex motor skills, premotor subregions were primarily involved in shaping complex motor control. However, patients with persistent motor deficits in the chronic stage also exhibited a correlation between premotor

subtracts and basal motor control. In all cases, higher tractwise anisotropy was observed in patients featuring better motor control. Within the context of functional reorganization, there are three possible interpretations of these findings.

First, they can be interpreted as an indication of vicariation as premotor areas seemed to compensate for basal functions in more severely affected patients. In this case, motor primitives formerly located in M1 might be shifted towards premotor regions. Thus, the retrieval of specific muscle activation patterns would not be found in M1 anymore since the substitute motor primitive would be located in one or even spread across several of the premotor regions. This would enable them to directly shape peripheral activation via their descending outputs. A similar concept has already been considered in the empirical section (study 2) with respect to a maceration of functional segregation between different premotor areas. As we did not observe a clear distinction between the functional relevance of descending output from SMA, PMv, and PMd, it is possible that one region took over certain functions of another to compensate for a region-specific functional loss.

A second explanation for the observed findings would be a relay of motor signals from M1 via premotor areas to the spinal level in the subgroup of patients with persistent deficits. That is to say, motor signals may take a detour to circumvent the damaged M1 output tract but premotor areas themselves would not take over the function of M1. In this case, motor primitives would still be represented in M1 but would be relayed via an alternative output route. In line with this notion, an involvement of the cortico-cortical PMv-M1 connection has been shown to depend on the integrity of CST fibers descending from M1: Only patients with pronounced affection of the CST emerging from M1 showed a correlation between PMv-M1 anisotropy and motor impairment (Schulz et al., 2017b). Of note, our findings of a reliance on premotor-M1 structural connectivity independent of CST integrity in study 3 do not necessarily oppose this view as we controlled for the entire CST in study 3 rather than only for CST fibers descending from M1. Given that we relied on externally validated tract templates in study 2 that included descending sensorimotor tracts but did not include any premotor-M1 connections (Archer et al., 2018), we refrained from testing for an interaction with cortico-cortical connections as we would have had to track these manually without external validation. However, given the observed correlations between premotor-M1 structural connectivity and basal motor performance in study 3, a relay of M1 output via premotor areas to grant M1 access to descending tracts projecting to the spinal level seems logical.

Alternatively, reorganization may also occur at the spinal level. In general, there are two possible ways premotor areas might influence motor control via descending fibers: either via

monosynaptic projections onto lower motor neurons in the ventral horn (Dum & Strick, 2002), or via projections terminating in the intermediate zone of the spinal cord, which modulates M1 output to lower motor neurons targeting arm and hand muscles (Boudrias et al., 2006, 2010). When considering the entire sample, an indirect modulation of M1 output by premotor areas via disynaptic connections seems to be the more likely mechanism as the correlation between motor performance and premotor subtract anisotropy was not independent of M1 subtract integrity. This is well in line with the notion that most projections from premotor areas target spinal interneurons and therefore disynaptically modulate descending motor signals (Strick et al., 2021). Further support for this interpretation stems from the fact that premotor tract integrity only correlated with complex but not basal motor skills, which may require higher levels of additional modulation exerted by disynaptic interneurons in concert with monosynaptic activation of spinal motor neurons. In case of a compensatory influence via monosynaptic premotor projections, one would expect to observe a correlation with basal motor performance as basal motor skills should more strongly rely on such monosynaptic inputs and require less interneuron modulation compared to complex movements. Of note, we observed such an association between premotor subtract anisotropy and basal motor control in patients with persistent deficits. Thus, our current findings may be interpreted as a heavier reliance on monosynaptic projections from premotor areas to the spinal level in patients with persistent motor deficits. Given that monosynaptic transmission of basal motor signals via premotor CST fibers is rather unusual for the human motor system (Strick et al., 2021), this form of mechanistic compensation might be of limited success, which would explain why it was only observed in patients with persistent deficits. At the same time, this form of flexibility underlines the ability of the motor system to maximize motor signal transmission to the spinal level.

6.5. Cortico-cortical structural connectivity

Another commonly discussed alternative to transmit motor signals to the spinal level is via the contralesional CST (Schaechter et al., 2009). While our results on descending motor pathways in study 1 did not show an association between motor control and contralesional CST anisotropy, the lack of a correlation does not necessarily preclude an involvement of the contralesional CST in the transmission of motor output signals. Despite the absence of a correlation, it might still serve as a substitute route, yet independent of its level of microstructural integrity. In that case, neither the premorbid level of the contralesional CST nor potential axonal growth in response to the lesion would be the defining factor for motor recovery. Instead, cortico-cortical structures that enable the relay of information from the ipsi-

to the contralesional motor cortex might be crucial in pre-determining a patient's potential for successful recovery as the transcallosal fibers might help to access the contralesional CST.

Support for this notion stems from study 3, where we observed a correlation between structural M1-M1 connectivity and basal motor control independent of the level of CST integrity. A potential explanation for this finding might lie in a transmission of motor signals from the ipsilesional M1 to the contralesional M1, which may support the generation of descending motor activity via the contralesional CST. Of note, especially patients who underwent substantial motor recovery from the acute to the chronic stage seemed to rely on this alternative route, whereas patients without substantial recovery relied more strongly on ipsilesional premotor-M1 connectivity and the ipsilesional CST. In sum, the recovery of basal motor control might be facilitated by a relay of motor signals via transcallosal fibers to the contralesional M1.

In line with this view, increased activation of the contralesional M1 during paretic hand movements has been associated with anisotropy of the corpus callosum (Wang et al., 2012). Moreover, enhanced effective connectivity from ipsilesional to contralesional M1 during a simple fist closure task performed with the paretic hand correlated positively with motor outcome and anisotropy of the interhemispheric M1-M1 connection, but not with ipsilesional CST integrity (Peng et al., 2019). Therefore, successful recovery of basal motor control might partially arise from the motor system's ability to recruit the contralesional hemisphere and its descending output pathways.

Conversely, the association between bihemispheric premotor areas and the ipsilesional M1 with complex motor control was dependent on the integrity of the ipsilesional CST in study 3. This matches previous reports of a correlation between fMRI-based activation of premotor regions during task execution and CST integrity (Ward et al., 2006). Complex motor control therefore seems to primarily depend on output signals transmitted via the ipsilesional CST which cannot be easily compensated via alternative routes. Support for this view stems from anatomical studies: the ipsilaterally descending portion of the CST mostly innervates proximal muscle groups (Lemon, 2008), which renders a compensation of complex motor skills involving distal control of the hand and fingers via non-crossing fibers of the contralesional CST unlikely. Of note, a strong reliance on premotor areas and ipsilesional corticospinal fibers was not only suggested by the cortico-cortical results in study 3, but study 2 also linked the execution of complex motor skills to the integrity of corticospinal fibers descending from ipsilesional premotor areas. Thus, ipsilesional premotor areas seem to enable complex motor control both via their descending fibers as well as through cortico-cortical interactions with M1.

6.6. Cortico-cortical information integration

Having assessed structural network connectivity in the chronic, i.e., reorganized motor system, the question arises if plastic changes occurring in the early phases of motor recovery may imply similar aspects of motor network reorganization as the observed associations between structural motor network properties and motor control. As early changes in inter-regional communication are likely realized on a functional level rather than through early structural changes such as growing new fiber connections, we focused on fMRI-based data in the acute stage post-stroke.

Changes in functional information integration after stroke have often been probed via resting-state functional or task-related effective connectivity. Using either modality, previous studies in stroke patients have highlighted changes in ipsilesional premotor-M1 and M1-M1 interactions (Golestani et al., 2013; Grefkes, Nowak, et al., 2008; Park et al., 2011; Rehme, Eickhoff, et al., 2011; Volz et al., 2017). In these studies, the same connections also showed an association with motor impairment during task performance and at rest. Similarly, when explaining motor performance in the acute sample in study 4, both resting-state functional and task-related effective connectivity showed a close relationship with motor control. This nicely aligns with our findings in study 2 and 3 as the microstructural integrity of premotor-M1 and M1-M1 pathways was also correlated with motor performance. Thus, both structural and functional MRI data highlight the relevance of these connections for motor control after stroke.

Notably, the observed relationship of motor impairment with structural, functional, and effective connectivity suggests a prominent role of these connections across different activation states of the brain (i.e., task vs. rest). This raises the question whether resting-state functional and task-related effective connectivity might reflect similar processes of information integration. While previous research in healthy subjects did not find such an association (Rehme et al., 2013), it seems possible that stroke-related changes of these specific connections may be reflected by both modalities.

Therefore, we tested for an association between measures of resting-state functional and task-related effective connectivity in our sample of acute stroke patients in study 4. In line with previous findings, measures of either connectivity mode were not correlated. As this negative finding might have also been an effect of the method used to probe connectivity during task and at rest, we conducted an additional analysis and also included task-related functional connectivity. Thereby, we compared non-directional connectivity measures across different activation states. Interestingly, measures of resting-state and task-related functional connectivity yielded significant correlations for interhemispheric motor homologs after stroke,

which had not been observed in the healthy brain (Rehme et al., 2013). In contrast to interhemispheric connectivity between homologs, premotor-M1 connections did not show a relationship between functional connectivity assessed at rest or during task performance. Thus, these results are in line with the notion that premotor-M1 connections may be modulated in a highly task-specific fashion to enable compensation via flexibly adapting to the current demands. Conversely, interhemispheric M1-M1 interactions may undergo a more fundamental form of reorganization that was hence similarly traceable during task performance and at rest. Of note, this view nicely aligns with the findings of study 3 where complex motor skills with more variable task demands relied on ipsilesional premotor-M1 connectivity and only basal aspects of motor control showed a relationship with interhemispheric M1-M1 anisotropy. Moreover, this notion is also in line with the findings of study 2 that suggest flexible compensation processes within the ipsilesional hemisphere to exploit the remaining tissue as efficiently as possible. Thus, the consolidation of our findings implies that post-stroke motor control of complex paretic arm and hand movements relies on a flexible adaptation of network interactions between premotor areas and M1 within the ipsilesional hemisphere, which facilitate task-specific compensation of stroke-induced deficits.

In sum, our findings suggest differential stroke-induced reorganization processes for premotor-M1 and M1-M1 connections. Given the similarity in implications by dMRI and fMRI findings, future research should address the relationship between structural and functional reorganization processes by assessing structural and functional network properties in the same patient cohort.

6.7. Clinical implications

To discuss the clinical implications of the studies presented here, the questions identified by the Stroke Recovery and Rehabilitation Roundtable taskforce provide a useful framework. In their consensus paper, they identified (i) the development of suitable biomarkers to assess a patient's potential for recovery and (ii) individually tailored therapeutic interventions to maximize each patient's functional outcome as the clinically most relevant questions (Boyd et al., 2017).

Given that each patient has a unique lesion pattern and different structural and functional predispositions, personalized outcome predictions remain challenging (Bonkhoff & Grefkes, 2022). As previous studies have mainly focused on the integrity of the ipsilesional CST, the focus of currently accepted biomarkers clearly emphasizes the degree of tract damage and rather ignores the attempts of the reorganizing motor system to compensate for the deficits caused by

the lesion (Boyd et al., 2017; Koch et al., 2016). In line with previous studies showing the superiority of a combination of alternate motor fibers and CST in predicting motor performance (Lindenberg et al., 2010), study 1 emphasized that considering CST and extrapyramidal tractwise anisotropy in concert led to a higher ratio of explained basal upper and lower limb motor performance than any measure alone. Moreover, applying a compartmentwise dMRI-based approach that focuses the analysis on descending CST fibers (i.e., one-directional voxels) and specific clusters of voxels within the extrapyramidal system (i.e., two-directional voxels) was shown to be particularly useful. Notably, our results indicate that the improvement in explained behavioral variance achieved by combining CST with extrapyramidal anisotropy was primarily relevant for basal motor control of the upper and lower limb, whereas complex motor skills showed no association with extrapyramidal anisotropy.

Considering that complex motor skills rely on a more widespread cortical motor network rather than simple output signals descending from M1 (cf. study 2), it seems logical that the prediction of complex motor skills may require a different approach with a stronger emphasis on a wider cortical motor network. According to the results presented in study 3, cortico-cortical structural connectivity constitutes a promising approach to investigate and quantify the cortical structural reserve, which might aid the prediction of motor performance. Such structural measures of the cortico-cortical motor network may be complimented by estimates of fMRI-based connectivity given the associations with motor performance seen in study 4 and in previous findings (Rehme, Volz, Feis, Bomilcar-Focke, et al., 2015; Rehme, Volz, Feis, Eickhoff, et al., 2015). While resting-state scans can be realistically integrated into clinical routines, the application of task-related fMRI in clinical practice is accompanied by several practical challenges. First, it cannot be easily acquired as it strongly depends on patient compliance. This provides a substantial problem for hemiplegic or severely affected patients who are not able to perform even simple tasks such as fist closure movements. Moreover, measures of effective connectivity are highly task-specific, limiting their generalizability. Thus, a multimodal approach combining measures of CST and extrapyramidal anisotropy with cortico-cortical dMRI-based structural and fMRI-based functional connectivity should be considered to predict motor outcome after stroke. As suggested by our current findings, such an approach might even help to delineate specific aspects of motor performance such as basal and complex motor control, which rely on distinct mechanisms of motor control and recovery.

With respect to the second question, i.e., the enhancement of motor recovery through targeted interventions, a promising approach lies in applying repetitive TMS (rTMS) to modulate and increase plasticity within the lesioned motor network. The application of high-

frequency rTMS has been shown to temporarily increase cortical excitability (Di Lazzaro et al., 2008) and especially protocols relying on intermittent theta burst stimulations (iTBS) are thought to induce facilitatory effects for several hours even after a relatively short stimulation period (Huang et al., 2005). While previous studies have adopted a one-size-fits-all approach targeting the same motor region within a specific cohort (Hensel et al., 2019; Volz et al., 2016), our results suggest that the efficiency of TMS-interventions aiming at enhancing motor recovery may be improved by considering patient-specific factors, which is well in line with findings of differential responses to rTMS depending on the lesion location (Ameli et al., 2009).

In more severely affected patients with basal motor impairment, the ipsilesional M1 might be an appropriate target to enhance the transmission of motor output signals to the contralesional hemisphere in line with our findings in study 3. In contrast, moderately affected patients with deficits in complex motor skills might benefit from targeting premotor regions. Moreover, in light of the results from study 2, choosing the cortical target region based on an individual patient's lesion location and his or her specific motor deficit might be a promising approach. As our results suggest that premotor regions compensate for deficits via their descending CST fibers, it might be most beneficial to apply TMS over a premotor region with the best functioning output pathway and the highest level of structural reserve. This might help to relay output signals to the spinal level, thereby bypassing damaged parts of the CST. In addition, it might also be advantageous to integrate fMRI analyses into the selection of the appropriate stimulation target as this might help to assess which premotor area shows the strongest interaction with M1. A future biomarker helping to assign patients to specific interventions should therefore consider the form of motor deficit, lesion location, the structural reserve, and functional interactions between cortical areas in concert.

6.8. Limitations

The presented studies entail several methodological limitations. The most obvious one is likely the relatively small sample size of each study. While this aspect has already been discussed in the study-specific empirical section, the most relevant aspects are revisited here for the sake of completeness. First of all, while 25 chronic and 26 acute patients represent relatively small samples, such sample sizes are all but unusual for hypothesis-driven imaging studies in patient cohorts (see for example Puig et al., 2011; Rehme, Eickhoff, et al., 2011; Ruber et al., 2012; Volz et al., 2016, 2017). Moreover, recruiting a sufficiently large sample of MRI-compatible stroke patients matching all inclusion criteria constitutes a particular challenge. Nonetheless, bigger sample sizes would allow to systematically differentiate

between different lesion locations, which is hardly possible with the current samples. This would have been particularly useful in study 2 as this would have allowed for separate analyses of affected and non-affected corticospinal subtracts. Premotor areas with largely intact descending fibers might take over functions of other premotor fibers with a significantly higher lesion load. This question is particularly relevant as it holds important clinical implications regarding targeted TMS interventions and should hence be addressed by future research.

Another limitation stems from the way cortico-cortical connectivity was quantified in study 3. While tractwise anisotropy derived via the novel compartmentwise approach enabled us to circumvent numerous problems related to dMRI-based connectivity, only pathways that exist in healthy participants were considered due to the template-based approach. However, studies in adult squirrel monkeys suggest that there might be axonal sprouting leading to new connections that usually do not exist in the healthy brain (Dancause, 2005). This process might be of particular relevance for rather short cortico-cortical distances as new connections might accompany cortical remapping. Fiber tracking in each individual patient would be necessary to capture those individual alterations. However, given the current methodological constraints inherent to fiber tracking algorithms, this is hardly possible. First of all, fiber tracking in brains with a significant degree of atrophy is a challenging endeavor per se, rendering fiber tracking on a subject level particularly difficult in a cohort of elderly stroke patients. Second, fiber tracking has the tendency to produce false positive streamlines which makes it almost impossible to distinguish between false positive streamlines and true connections when the anatomical ground truth is unknown (Grisot et al., 2021; Schilling et al., 2020). It will probably take years for tracking algorithms to gain the necessary specificity without incorporating prior anatomical constraints until they can be confidently applied to the problem at hand.

Moreover, while study 1 helped to pinpoint relevant anatomical structures of the extrapyramidal system for post-stroke motor control, the question remains whether its involvement facilitates or hinders motor performance. Due to the advanced DSI protocol and its ability to resolve several intra-voxel fiber directions, we were able to carefully interpret the estimated anisotropy in two-directional brainstem voxels and assess its relationship with motor performance. However, the implications of the observed negative correlation with mean anisotropy derived from two-directional extrapyramidal voxels could not be determined with absolute certainty due to methodological limitations. A complementary approach to address this question may arise from recent studies that assessed the strength of the reticulospinal tract by recording an MEP ipsilateral to a cortically applied TMS-pulse (Hammerbeck et al., 2021; Taga et al., 2021). However, a major limitation of this approach lies in the fact that the TMS-pulse

has to be applied to the cortex rather than eliciting direct reticulospinal output signals in the reticular formation. In consequence, one cannot be sure that the elicited signal only represents properties of the reticulospinal tract as cortical projections might also trigger other descending pathways. dMRI-based approaches are therefore the current gold standard to assess extrapyramidal tracts despite their methodological limitations. Thus, future research using advanced diffusion protocols are needed to address the question whether the observed correlation with motor performance should be interpreted as beneficial or maladaptive.

Another important limitation pertains to the assessment of motor performance. For a differential assessment of motor recovery, longitudinal data on distinct aspects of motor control are needed. However, as studies 1 to 3 were cross-sectional, patients were recruited in the chronic phase post-stroke. Thus, to achieve a longitudinal assessment of motor recovery, we had to rely on the NIHSS scores acquired in an acute setting at the stroke unit of the University Hospital Cologne. The simplicity of the NIHSS arm score prohibits any inference regarding specific aspects of motor control. Moreover, while the elaborate motor tests distinguishing between basal and complex motor skills constitute a significant improvement compared to previous studies, the motor assessments used throughout this thesis still entail certain limitations. For example, motor tests specifically designed to delineate the potential contributions of each premotor area might have been helpful for study 2 and 3 to better distinguish region-specific functional aspects of premotor areas. In particular the surprisingly strong correlation with corticospinal fibers descending from the SMA in study 2 poses the question whether tests that differentiate between reach-to-grasp movements attributed to PMd and PMv (Davare, 2006; Rizzolatti et al., 2002; Rizzolatti & Luppino, 2001) and sequential movements facilitated by the SMA (Gerloff et al., 1997; Lara et al., 2018; Macar et al., 2004) might have led to differential results for individual premotor subtracts. Similarly, even more elaborate tests might have yielded differential results for distinct premotor-M1 connections in study 3. A potential solution for future research would be to distinguish distinct aspects of reach-to-grasp movements for a differential assessment of PMv and PMd and to add a more repetitive task specifically addressing SMA functions.

Finally, study 4 used a PCA-based composite motor score as primary outcome measure rather than the distinction between basal and complex motor skills as the MI was not available. Thus, potential differences between basal and complex aspects of motor control in relation to fMRI readouts could not be assessed. For example, it is possible that resting-state data might reflect basal aspects of motor control more closely than task-related measures. Moreover, our findings in study 1 to 3 indicate fundamental differences between basal and complex motor

control after stroke yet task-related effective connectivity was only assessed based on fist closure movements. Therefore, we can only speculate about the underlying functional interactions within the motor system with regard to other motor tasks. To test our conclusions regarding a differential involvement of the contralesional M1 in basal and complex motor control, it would be highly interesting to see the differences in cortical interactions during the performance of basal (and more proximal) versus complex (and more distal) motor tasks.

6.9. Future perspectives

Our present findings lead to a variety of questions, which provide promising starting points for future research. For example, a highly relevant question pertains to the structure-function relationship in post-stroke motor network reorganization. While structural and functional connectivity are thought to be closely related in the healthy human brain (Fukushima & Sporns, 2020; Rubinov & Sporns, 2010), it remains unclear whether a change in structural connectivity between different motor regions after stroke is necessarily accompanied by a respective decrease or increase in functional or effective connectivity. On the one hand, damage to WM tracts between regions might result in decreased functional information integration between those areas. On the other hand, the motor system might learn to exploit the remaining fibers more efficiently, thereby offsetting the loss of structural connectivity. In this case, successful reorganization might arise from the relationship of changes in functional connection strength relative to the underlying structural connectivity. As structural and functional network properties were assessed in different patient cohorts in the present thesis, no direct comparison of structural and functional connectivity was conducted. For a more coherent interpretation, future research should fully characterize a sample of stroke patients using fMRI and dMRI as suggested in the present thesis and relate readouts of functional cortico-cortical information integration to its structural underpinnings. Moreover, a longitudinal tracking of motor network changes from the acute to the chronic stage using multi-modal imaging techniques will offer valuable insights as this approach might help to clarify whether structural changes precede, coincide with, or predetermine functional reorganization.

Given the observed differences in the compensation of basal and complex motor control and the task-dependent influence of the contralesional M1 (Hensel et al., 2022; Volz et al., 2017), the question arises to which degree changes in information integration between interhemispheric M1-M1 are task-dependent. Or to operationalize it in terms of effective connectivity: Does the coupling between bilateral M1 as assessed via DCM change depending on the level of task complexity? To answer this question, it would be highly interesting to have

patients perform different motor tasks in the scanner with varying levels of complexity. In particular, one may hypothesize that signals are being transmitted from the ipsilesional to the contralesional M1 during basal motor tasks. Thus, coupling parameters from the ipsi- onto the contralesional M1 would be expected to correlate with motor performance. In contrast, I would expect a stronger reliance on the reverse coupling from the contralesional M1 to the ipsilesional M1 for complex motor skills as the main output pathway should be descending fibers from the ipsilesional M1. The latter should be particularly relevant in the acute phase with previous DCM results indicating a beneficial influence from the ipsilesional onto the contralesional M1 (Rehme, Eickhoff, et al., 2011).

Another approach that would nicely complement the present results lies in the validation of compartmentwise anisotropy in acute stroke patients. As described above, Wallerian degeneration occurs over time and has therefore not fully developed in the acute phase post-stroke. Especially with regard to the improvement of biomarkers that rely on a quantification of CST damage, it would be highly relevant to compare the predictive power of compartmentwise anisotropy of the ipsilesional CST to more standard approaches like for example the weighted CST lesion load (Boyd et al., 2017; Feng et al., 2015). Moreover, for a better understanding of stroke-related motor network reorganization over time and the development of suitable biomarkers, longitudinal studies combining different imaging modalities in sufficiently large samples are needed that allow to account for the heterogeneity in lesion distributions and individual differences in structural reserve.

Finally, to date, the majority of studies in stroke has relied on simple motor tasks such as finger tapping, fist closure movements or standardized motor tests (Grefkes & Fink, 2011; Rehme, Eickhoff, et al., 2011; Volz et al., 2016; Volz, Sarfeld, et al., 2015). While the simplicity of such motor tasks allows for an assessment of the ability to initiate and control paretic hand movements, such readouts do not provide any information regarding a patient's ability to learn new motor skill. At the same time, motor learning seems to be particularly relevant in the early phase post-stroke as the motor system lacks relevant motor control policies given the loss of old motor primitives due to the lesion (Krakauer, 2015). As training-dependent motor recovery and the underlying neural changes (Nudo, Wise, et al., 1996; Plautz et al., 2000) are thought to follow similar mechanisms as motor learning in healthy participants (Krakauer, 2006, 2015), incorporating motor learning into future studies might be particularly relevant for an improved understanding of neuroplastic changes in the critical period. Combining dMRI with fMRI readouts during motor learning tasks would offer the chance to answer various questions of clinical relevance: Which structures are involved in training-dependent motor learning after

stroke? How do these structures interact? Do patients with a better structural reserve acquire motor skills more easily? Given the relevance of the cerebellum and basal ganglia for motor learning, it would be particularly interesting to expand DCM and resting-state analyses to subcortical structures and to relate motor learning parameters to cortico-cerebellar structural connectivity.

6.10. Conclusion

The present thesis aimed at furthering our understanding of motor network reorganization underlying different aspects of motor control after stroke. We therefore investigated structural and functional motor network properties in chronic and acute stroke patients and assessed their relationship with measures of basal and complex motor control. To overcome methodological problems inherent to the quantification of anisotropy in voxels with crossing or kissing fibers, we applied a novel compartmentwise analysis approach that allowed us to classify voxels according to their number of trackable directions. We thereby provided evidence for Wallerian degeneration along the length of the entire CST and highlighted its ubiquitous relevance for various aspects of motor control after stroke (study 1). Moreover, we identified extrapyramidal structures relevant for the compensation of basal upper and lower limb motor performance. We further showed that corticospinal fibers descending from premotor areas are critical for shaping complex motor skills (study 2), while additionally supporting the immense flexibility underlying reorganization by adapting a vicarious role when facilitating basal motor control in more severely affected patients. With respect to cortico-cortical structural connectivity, our results offered new insights into the heavily debated role of the contralesional M1 (study 3). While it might help to relay basal motor signals from the ipsilesional M1 to the spinal level, this role seems unlikely for complex motor control. Instead, complex motor control seemed to depend more heavily on ipsilesional premotor-M1 interactions. This is well in line with our fMRI-based findings, which suggest a more fundamental form of information integration for interhemispheric motor homologs and task-specific functional compensation within the ipsilesional hemisphere (study 4). Thus, this thesis offers novel perspectives on motor network reorganization after stroke by combining different connectivity-based analysis approaches and holds important implications for the development of improved biomarkers and personalized therapeutic interventions. Future research should build on this foundation and assess the relationship of stroke-related structural motor network changes and functional information integration over time. Tracking structural and functional alterations simultaneously

while incorporating our current methodological framework will offer new mechanistic insights that might lead to improved treatment options in the long run.

7. References

- Abolins, V., Stremoukhov, A., Walter, C., & Latash, M. L. (2020). On the origin of finger enslaving: control with referent coordinates and effects of visual feedback. *Journal of Neurophysiology*, *124*(6), 1625–1636. <https://doi.org/10.1152/jn.00322.2020>
- Alexander, G. E., & Crutcher, M. D. (1990). Functional architecture of basal ganglia circuits: neural substrates of parallel processing. *Trends in Neurosciences*, *13*(7), 266–271. [https://doi.org/10.1016/0166-2236\(90\)90107-L](https://doi.org/10.1016/0166-2236(90)90107-L)
- Allen, G. I., & Tsukahara, N. (1974). Cerebrocerebellar communication systems. *Physiological Reviews*, *54*(4), 957–1006. <https://doi.org/10.1152/physrev.1974.54.4.957>
- Ameli, M., Grefkes, C., Kemper, F., Riegg, F. P., Rehme, A. K., Karbe, H., Fink, G. R., & Nowak, D. A. (2009). Differential effects of high-frequency repetitive transcranial magnetic stimulation over ipsilesional primary motor cortex in cortical and subcortical middle cerebral artery stroke. *Annals of Neurology*, *66*(3), 298–309. <https://doi.org/10.1002/ana.21725>
- Andersen, K. K., Olsen, T. S., Dehlendorff, C., & Kammersgaard, L. P. (2009). Hemorrhagic and ischemic strokes compared: Stroke severity, mortality, and risk factors. *Stroke*, *40*(6), 2068–2072. <https://doi.org/10.1161/STROKEAHA.108.540112>
- Archer, D. B., Misra, G., Patten, C., & Coombes, S. A. (2016). Microstructural properties of premotor pathways predict visuomotor performance in chronic stroke. *Human Brain Mapping*, *37*(6), 2039–2054. <https://doi.org/10.1002/hbm.23155>
- Archer, D. B., Vaillancourt, D. E., & Coombes, S. A. (2018). A Template and Probabilistic Atlas of the Human Sensorimotor Tracts using Diffusion MRI. *Cerebral Cortex*, *28*(5), 1685–1699. <https://doi.org/10.1093/cercor/bhx066>
- Ashby, F. G. (2011). *Statistical Analysis of fMRI Data* (1st ed.). The MIT Press.
- Baker, S. N. (2011). The primate reticulospinal tract, hand function and functional recovery. *The Journal of Physiology*, *589*(23), 5603–5612. <https://doi.org/10.1113/jphysiol.2011.215160>
- Bammer, R. (2003). Basic principles of diffusion-weighted imaging. *European Journal of Radiology*, *45*(3), 169–184. [https://doi.org/10.1016/S0720-048X\(02\)00303-0](https://doi.org/10.1016/S0720-048X(02)00303-0)
- Bandettini, P. A., Wong, E. C., Hinks, R. S., Tikofsky, R. S., & Hyde, J. S. (1992). Time course EPI of human brain function during task activation. *Magnetic Resonance in Medicine*, *25*(2), 390–397. <https://doi.org/10.1002/mrm.1910250220>
- Bannur, U., & Rajshekhar, V. (2000). Post operative supplementary motor area syndrome: clinical features and outcome. *British Journal of Neurosurgery*, *14*(3), 204–210.

<https://doi.org/10.1080/026886900408379>

- Barker, A. T., Jalinous, R., & Freeston, I. L. (1985). Non-invasive magnetic stimulation of human motor cortex. *The Lancet*, *325*(8437), 1106–1107. [https://doi.org/10.1016/S0140-6736\(85\)92413-4](https://doi.org/10.1016/S0140-6736(85)92413-4)
- Bartels, A., Goense, J., & Logothetis, N. (2012). An introduction to functional magnetic resonance imaging (fMRI) and the origin of the blood oxygen level dependent (BOLD) signal. In *Handbook of Neural Activity Measurement* (Issue 2004).
- Basser, P. J. (1995). Inferring microstructural features and the physiological state of tissues from diffusion-weighted images. *NMR in Biomedicine*, *8*(7), 333–344. <https://doi.org/10.1002/nbm.1940080707>
- Basser, P. J., Mattiello, J., & LeBihan, D. (1994). MR diffusion tensor spectroscopy and imaging. *Biophysical Journal*, *66*(1), 259–267. [https://doi.org/10.1016/S0006-3495\(94\)80775-1](https://doi.org/10.1016/S0006-3495(94)80775-1)
- Basser, P. J., & Özarslan, E. (2014). Introduction to Diffusion MR. In *Diffusion MRI* (pp. 3–9). Elsevier. <https://doi.org/10.1016/B978-0-12-396460-1.00001-9>
- Basser, P. J., & Pierpaoli, C. (1996). Microstructural and Physiological Features of Tissues Elucidated by Quantitative-Diffusion-Tensor MRI. *Journal of Magnetic Resonance, Series B*, *111*(3), 209–219. <https://doi.org/10.1006/jmrb.1996.0086>
- Beaulieu, C. (2002). The basis of anisotropic water diffusion in the nervous system - a technical review. *NMR in Biomedicine*, *15*(7–8), 435–455. <https://doi.org/10.1002/nbm.782>
- Beaulieu, C. (2014). The Biological Basis of Diffusion Anisotropy. In *Diffusion MRI* (Second Edi, pp. 155–183). Elsevier. <https://doi.org/10.1016/B978-0-12-396460-1.00008-1>
- Beck, C. H., & Chambers, W. W. (1970). Speed, accuracy, and strength of forelimb movement after unilateral pyramidotomy in rhesus monkeys. *Journal of Comparative and Physiological Psychology*, *70*(2, Pt.2), 1–22. <https://doi.org/10.1037/h0028698>
- Bernhardt, J., Hayward, K. S., Kwakkel, G., Ward, N. S., Wolf, S. L., Borschmann, K., Krakauer, J. W., Boyd, L. A., Carmichael, S. T., Corbett, D., & Cramer, S. C. (2017). Agreed Definitions and a Shared Vision for New Standards in Stroke Recovery Research: The Stroke Recovery and Rehabilitation Roundtable Taskforce. *Neurorehabilitation and Neural Repair*, *31*(9), 793–799. <https://doi.org/10.1177/1545968317732668>
- Bichat, X. (1805). *Recherches Physiologiques sue la Vie et la Mort* (3rd ed.). Brosson/Gabon.
- Biswal, B., Zerrin Yetkin, F., Haughton, V. M., & Hyde, J. S. (1995). Functional connectivity in the motor cortex of resting human brain using echo-planar mri. *Magnetic Resonance in Medicine*, *34*(4), 537–541. <https://doi.org/10.1002/mrm.1910340409>

- Blumenfeld, H. (2010). *Neuroanatomy through clinical cases* (2nd ed.). Sinauer Associates.
- Boes, A. D., Prasad, S., Liu, H., Liu, Q., Pascual-Leone, A., Caviness, V. S., & Fox, M. D. (2015). Network localization of neurological symptoms from focal brain lesions. *Brain*, *138*(10), 3061–3075. <https://doi.org/10.1093/brain/awv228>
- Bohannon, R. W. (1999). Motricity Index Scores are Valid Indicators of Paretic Upper Extremity Strength Following Stroke. *Journal of Physical Therapy Science*, *11*(2), 59–61. <https://doi.org/10.1589/jpts.11.59>
- Bonita, R., & Beaglehole, R. (1988). Recovery of motor function after stroke. *Stroke*, *19*(12), 1497–1500. <https://doi.org/10.1161/01.STR.19.12.1497>
- Bonkhoff, A. K., Espinoza, F. A., Gazula, H., Vergara, V. M., Hensel, L., Michely, J., Paul, T., Rehme, A. K., Volz, L. J., Fink, G. R., Calhoun, V. D., & Grefkes, C. (2020). Acute ischaemic stroke alters the brain's preference for distinct dynamic connectivity states. *Brain*, *143*(5), 1525–1540. <https://doi.org/10.1093/brain/awaa101>
- Bonkhoff, A. K., & Grefkes, C. (2022). Precision medicine in stroke: towards personalized outcome predictions using artificial intelligence. *Brain*, *145*(2), 457–475. <https://doi.org/10.1093/brain/awab439>
- Borich, M. R., Brown, K. E., & Boyd, L. A. (2014). Motor Skill Learning Is Associated With Diffusion Characteristics of White Matter in Individuals With Chronic Stroke. *Journal of Neurologic Physical Therapy*, *38*(3), 151–160. <https://doi.org/10.1097/NPT.0b013e3182a3d353>
- Borich, M. R., Mang, C., & Boyd, L. A. (2012). Both projection and commissural pathways are disrupted in individuals with chronic stroke: investigating microstructural white matter correlates of motor recovery. *BMC Neuroscience*, *13*(1), 107. <https://doi.org/10.1186/1471-2202-13-107>
- Bortoff, G., & Strick, P. (1993). Corticospinal terminations in two new-world primates: further evidence that corticomotoneuronal connections provide part of the neural substrate for manual dexterity. *The Journal of Neuroscience*, *13*(12), 5105–5118. <https://doi.org/10.1523/JNEUROSCI.13-12-05105.1993>
- Boudrias, M.-H., Belhaj-Saïf, A., Park, M. C., & Cheney, P. D. (2006). Contrasting Properties of Motor Output from the Supplementary Motor Area and Primary Motor Cortex in Rhesus Macaques. *Cerebral Cortex*, *16*(5), 632–638. <https://doi.org/10.1093/cercor/bhj009>
- Boudrias, M.-H., McPherson, R. L., Frost, S. B., & Cheney, P. D. (2010). Output Properties and Organization of the Forelimb Representation of Motor Areas on the Lateral Aspect of the Hemisphere in Rhesus Macaques. *Cerebral Cortex*, *20*(1), 169–186.

<https://doi.org/10.1093/cercor/bhp084>

- Boyd, L. A., Hayward, K. S., Ward, N. S., Stinear, C. M., Rosso, C., Fisher, R. J., Carter, A. R., Leff, A. P., Copland, D. A., Carey, L. M., Cohen, L. G., Basso, D. M., Maguire, J. M., & Cramer, S. C. (2017). Biomarkers of stroke recovery: Consensus-based core recommendations from the Stroke Recovery and Rehabilitation Roundtable. *International Journal of Stroke*, *12*(5), 480–493. <https://doi.org/10.1177/1747493017714176>
- Bright, M. G., Tench, C. R., & Murphy, K. (2017). Potential pitfalls when denoising resting state fMRI data using nuisance regression. *NeuroImage*, *154*(December 2016), 159–168. <https://doi.org/10.1016/j.neuroimage.2016.12.027>
- Broca, P. (1863). Localisation des fonctions cérébrales: siège de langage articulé. *Bulletins de La Société d'Anthropologie de Paris* *4*, 200–208.
- Brott, T., Adams, H. P., Olinger, C. P., Marler, J. R., Barsan, W. G., Biller, J., Spilker, J., Holleran, R., Eberle, R., & Hertzberg, V. (1989). Measurements of acute cerebral infarction: a clinical examination scale. *Stroke*, *20*(7), 864–870. <https://doi.org/10.1161/01.STR.20.7.864>
- Brown-Séquard, C. E. (1875). Séance du 18 décembre. *CR Soc Biol*, *424*.
- Buetefisch, C. M., Revill, K. P., Shuster, L., Hines, B., & Parsons, M. (2014). Motor demand-dependent activation of ipsilateral motor cortex. *Journal of Neurophysiology*, *112*(4), 999–1009. <https://doi.org/10.1152/jn.00110.2014>
- Bullmore, E., & Sporns, O. (2009). Complex brain networks: graph theoretical analysis of structural and functional systems. *Nature Reviews Neuroscience*, *10*(3), 186–198. <https://doi.org/10.1038/nrn2575>
- Buxton, R. B., Wong, E. C., & Frank, L. R. (1998). Dynamics of blood flow and oxygenation changes during brain activation: the balloon model. *Magnetic Resonance in Medicine*, *39*(17), 855–864. <https://doi.org/10.1002/mrm.1910390602>
- Carrera, E., & Ttononi, G. (2014). Diaschisis: past, present, future. *Brain*, *137*(9), 2408–2422. <https://doi.org/10.1093/brain/awu101>
- Cassidy, J. M., & Cramer, S. C. (2017). Spontaneous and Therapeutic-Induced Mechanisms of Functional Recovery After Stroke. *Translational Stroke Research*, *8*(1), 33–46. <https://doi.org/10.1007/s12975-016-0467-5>
- Chauhan, G., & Debette, S. (2016). Genetic Risk Factors for Ischemic and Hemorrhagic Stroke. *Current Cardiology Reports*, *18*(12), 124. <https://doi.org/10.1007/s11886-016-0804-z>
- Chen, J. L., & Schlaug, G. (2013). Resting State Interhemispheric Motor Connectivity and White Matter Integrity Correlate with Motor Impairment in Chronic Stroke. *Frontiers in*

- Neurology*, 4. <https://doi.org/10.3389/fneur.2013.00178>
- Cheney, P. D., Fetz, E. E., & Mewes, K. (1991). Chapter 11 Neural mechanisms underlying corticospinal and rubrospinal control of limb movements (pp. 213–252). [https://doi.org/10.1016/S0079-6123\(08\)63054-X](https://doi.org/10.1016/S0079-6123(08)63054-X)
- Cheng, B., Petersen, M., Schulz, R., Boenstrup, M., Krawinkel, L., Gerloff, C., & Thomalla, G. (2021). White matter degeneration revealed by fiber-specific analysis relates to recovery of hand function after stroke. *Human Brain Mapping*, 42(16), 5423–5432. <https://doi.org/10.1002/hbm.25632>
- Chouinard, P. A., & Paus, T. (2006). The Primary Motor and Premotor Areas of the Human Cerebral Cortex. *The Neuroscientist*, 12(2), 143–152. <https://doi.org/10.1177/1073858405284255>
- Cirstea, M. C., & Levin, M. F. (2000). Compensatory strategies for reaching in stroke. *Brain*, 123(5), 940–953. <https://doi.org/10.1093/brain/123.5.940>
- Cleland, B. T., & Madhavan, S. (2021). Ipsilateral motor pathways to the lower limb after stroke: Insights and opportunities. *Journal of Neuroscience Research*, 99(6), 1565–1578. <https://doi.org/10.1002/jnr.24822>
- Collin, C., & Wade, D. (1990). Assessing motor impairment after stroke: a pilot reliability study. *Journal of Neurology, Neurosurgery & Psychiatry*, 53(7), 576–579. <https://doi.org/10.1136/jnnp.53.7.576>
- Conforti, L., Gilley, J., & Coleman, M. P. (2014). Wallerian degeneration: an emerging axon death pathway linking injury and disease. *Nature Reviews Neuroscience*, 15(6), 394–409. <https://doi.org/10.1038/nrn3680>
- Corbetta, M., & Shulman, G. L. (2002). Control of goal-directed and stimulus-driven attention in the brain. *Nature Reviews Neuroscience*, 3(3), 201–215. <https://doi.org/10.1038/nrn755>
- Cramer, S. C., Weisskoff, R. M., Schaechter, J. D., Nelles, G., Foley, M., Finklestein, S. P., & Rosen, B. R. (2002). Motor cortex activation is related to force of squeezing. *Human Brain Mapping*, 16(4), 197–205. <https://doi.org/10.1002/hbm.10040>
- d’Avella, A. (2009). Muscle Synergies. In M. D. Binder, N. Hirokawa, & U. Windhorst (Eds.), *Encyclopedia of Neuroscience* (pp. 2509–2512). Springer Berlin Heidelberg. https://doi.org/10.1007/978-3-540-29678-2_3678
- Damoiseaux, J. S., Rombouts, S. A. R. B., Barkhof, F., Scheltens, P., Stam, C. J., Smith, S. M., & Beckmann, C. F. (2006). Consistent resting-state networks across healthy subjects. *Proceedings of the National Academy of Sciences*, 103(37), 13848–13853. <https://doi.org/10.1073/pnas.0601417103>

- Dancause, N. (2005). Extensive Cortical Rewiring after Brain Injury. *Journal of Neuroscience*, 25(44), 10167–10179. <https://doi.org/10.1523/JNEUROSCI.3256-05.2005>
- Dancause, N., & Nudo, R. J. (2011). Shaping plasticity to enhance recovery after injury. *Progress in Brain Research*, 192(1), 273–295. <https://doi.org/10.1016/B978-0-444-53355-5.00015-4>
- Davare, M. (2006). Dissociating the Role of Ventral and Dorsal Premotor Cortex in Precision Grasping. *Journal of Neuroscience*, 26(8), 2260–2268. <https://doi.org/10.1523/JNEUROSCI.3386-05.2006>
- de Oliveira-Souza, R. (2012). The human extrapyramidal system. *Medical Hypotheses*, 79(6), 843–852. <https://doi.org/10.1016/j.mehy.2012.09.004>
- Demeurisse, G., Demol, O., & Robaye, E. (1980). Motor Evaluation in Vascular Hemiplegia. *European Neurology*, 19(6), 382–389. <https://doi.org/10.1159/000115178>
- Descoteaux, M. (2015). High Angular Resolution Diffusion Imaging (HARDI). In *Wiley Encyclopedia of Electrical and Electronics Engineering* (pp. 1–25). John Wiley & Sons, Inc. <https://doi.org/10.1002/047134608X.W8258>
- Descoteaux, M., Angelino, E., Fitzgibbons, S., & Deriche, R. (2006). Apparent diffusion coefficients from high angular resolution diffusion imaging: Estimation and applications. *Magnetic Resonance in Medicine*, 56(2), 395–410. <https://doi.org/10.1002/mrm.20948>
- Di Lazzaro, V., Pilato, F., Dileone, M., Profice, P., Capone, F., Ranieri, F., Musumeci, G., Cianfoni, A., Pasqualetti, P., & Tonali, P. A. (2008). Modulating cortical excitability in acute stroke: A repetitive TMS study. *Clinical Neurophysiology*, 119(3), 715–723. <https://doi.org/10.1016/j.clinph.2007.11.049>
- Di Pino, G., Pellegrino, G., Assenza, G., Capone, F., Ferreri, F., Formica, D., Ranieri, F., Tombini, M., Ziemann, U., Rothwell, J. C., & Di Lazzaro, V. (2014). Modulation of brain plasticity in stroke: A novel model for neurorehabilitation. *Nature Reviews Neurology*, 10(10), 597–608. <https://doi.org/10.1038/nrneurol.2014.162>
- Diedrichsen, J. (2006). A spatially unbiased atlas template of the human cerebellum. *NeuroImage*, 33(1), 127–138. <https://doi.org/10.1016/j.neuroimage.2006.05.056>
- Diedrichsen, J., Balsters, J. H., Flavell, J., Cussans, E., & Ramnani, N. (2009). A probabilistic MR atlas of the human cerebellum. *NeuroImage*, 46(1), 39–46. <https://doi.org/10.1016/j.neuroimage.2009.01.045>
- Dobkin, B. H. (2005). Rehabilitation after Stroke. *New England Journal of Medicine*, 352(16), 1677–1684. <https://doi.org/10.1056/NEJMcp043511>
- Doughty, C., Wang, J., Feng, W., Hackney, D., Pani, E., & Schlaug, G. (2016). Detection and

- Predictive Value of Fractional Anisotropy Changes of the Corticospinal Tract in the Acute Phase of a Stroke. *Stroke*, 47(6), 1520–1526. <https://doi.org/10.1161/STROKEAHA.115.012088>
- Dum, R. P., & Strick, P. (1991). The origin of corticospinal projections from the premotor areas in the frontal lobe. *The Journal of Neuroscience*, 11(3), 667–689. <https://doi.org/10.1523/JNEUROSCI.11-03-00667.1991>
- Dum, R. P., & Strick, P. L. (2002). Motor areas in the frontal lobe of the primate. *Physiology & Behavior*, 77(4–5), 677–682. [https://doi.org/10.1016/S0031-9384\(02\)00929-0](https://doi.org/10.1016/S0031-9384(02)00929-0)
- Duncan, P., Richards, L., Wallace, D., Stoker-Yates, J., Pohl, P., Luchies, C., Ogle, A., & Studenski, S. (1998). A randomized, controlled pilot study of a home-based exercise program for individuals with mild and moderate stroke. *Stroke*, 29(10), 2055–2060. <https://doi.org/10.1161/01.STR.29.10.2055>
- Egger, P., Evangelista, G. G., Koch, P. J., Park, C., Levin-Gleba, L., Girard, G., Beanato, E., Lee, J., Choirat, C., Guggisberg, A. G., Kim, Y., & Hummel, F. C. (2021). Disconnectomics of the Rich Club Impacts Motor Recovery After Stroke. *Stroke*, 52(6), 2115–2124. <https://doi.org/10.1161/STROKEAHA.120.031541>
- Einstein, A. (1905). Über die von der molekularkinetischen Theorie der Wärme geforderte Bewegung von in ruhenden Flüssigkeiten suspendierten Teilchen. *Annalen Der Physik*, 322(8), 549–560. <https://doi.org/10.1002/andp.19053220806>
- Feigin, V. L., Stark, B. A., Johnson, C. O., Roth, G. A., Bisignano, C., Abady, G. G., Abbasifard, M., Abbasi-Kangevari, M., Abd-Allah, F., Abedi, V., Abualhasan, A., Abu-Rmeileh, N. M., Abushouk, A. I., Adebayo, O. M., Agarwal, G., Agasthi, P., Ahinkorah, B. O., Ahmad, S., Ahmadi, S., ... Murray, C. J. L. (2021). Global, regional, and national burden of stroke and its risk factors, 1990–2019: a systematic analysis for the Global Burden of Disease Study 2019. *The Lancet Neurology*, 20(10), 795–820. [https://doi.org/10.1016/S1474-4422\(21\)00252-0](https://doi.org/10.1016/S1474-4422(21)00252-0)
- Feng, W., Wang, J., Chhatbar, P. Y., Doughty, C., Landsittel, D., Lioutas, V.-A., Kautz, S. A., & Schlaug, G. (2015). Corticospinal tract lesion load: An imaging biomarker for stroke motor outcomes. *Annals of Neurology*, 78(6), 860–870. <https://doi.org/10.1002/ana.24510>
- Finger, S. (2009). Chapter 51 Recovery of function. In *Handbook of Clinical Neurology* (3rd ed., Vol. 95, Issue C, pp. 833–841). Elsevier B.V. [https://doi.org/10.1016/S0072-9752\(08\)02151-9](https://doi.org/10.1016/S0072-9752(08)02151-9)
- Fonov, V., Evans, A., McKinstry, R., Almli, C., & Collins, D. (2009). Unbiased nonlinear average age-appropriate brain templates from birth to adulthood. *NeuroImage*, 47, S102.

[https://doi.org/10.1016/S1053-8119\(09\)70884-5](https://doi.org/10.1016/S1053-8119(09)70884-5)

- Fox, M. D., & Raichle, M. E. (2007). Spontaneous fluctuations in brain activity observed with functional magnetic resonance imaging. *Nature Reviews Neuroscience*, 8(9), 700–711. <https://doi.org/10.1038/nrn2201>
- Fox, P., Raichle, M., Mintun, M., & Dence, C. (1988). Nonoxidative glucose consumption during focal physiologic neural activity. *Science*, 241(4864), 462–464. <https://doi.org/10.1126/science.3260686>
- Friend, D. M., & Kravitz, A. V. (2014). Working together: basal ganglia pathways in action selection. *Trends in Neurosciences*, 37(6), 301–303. <https://doi.org/10.1016/j.tins.2014.04.004>
- Friston, K. J. (1994). Functional and effective connectivity in neuroimaging: A synthesis. *Human Brain Mapping*, 2(1–2), 56–78. <https://doi.org/10.1002/hbm.460020107>
- Friston, K. J., Ashburner, J., Frith, C. D., Poline, J.-B., Heather, J. D., & Frackowiak, R. S. J. (1995). Spatial registration and normalization of images. *Human Brain Mapping*, 3(3), 165–189. <https://doi.org/10.1002/hbm.460030303>
- Friston, K. J., Fletcher, P., Josephs, O., Holmes, A., Rugg, M. D., & Turner, R. (1998). Event-Related fMRI: Characterizing Differential Responses. *NeuroImage*, 7(1), 30–40. <https://doi.org/10.1006/nimg.1997.0306>
- Friston, K. J., Harrison, L., & Penny, W. (2003). Dynamic causal modelling. *NeuroImage*, 19(4), 1273–1302. [https://doi.org/10.1016/S1053-8119\(03\)00202-7](https://doi.org/10.1016/S1053-8119(03)00202-7)
- Fugl-Meyer, A. R., Jääskö, L., Leyman, I., Olsson, S., & Steglind, S. (1975). The post-stroke hemiplegic patient. 1. a method for evaluation of physical performance. *Scandinavian Journal of Rehabilitation Medicine*, 7(1), 13–31.
- Fukushima, M., & Sporns, O. (2020). Structural determinants of dynamic fluctuations between segregation and integration on the human connectome. *Communications Biology*, 3(1), 606. <https://doi.org/10.1038/s42003-020-01331-3>
- Galea, M. P., & Darian-Smith, I. (1994). Multiple Corticospinal Neuron Populations in the Macaque Monkey Are Specified by Their Unique Cortical Origins, Spinal Terminations, and Connections. *Cerebral Cortex*, 4(2), 166–194. <https://doi.org/10.1093/cercor/4.2.166>
- Garyfallidis, E. (2012). *Towards an accurate brain tractography*. University of Cambridge.
- Gerloff, C., Bushara, K., Sailer, A., Wassermann, E. M., Chen, R., Matsuoka, T., Waldvogel, D., Wittenberg, G. F., Ishii, K., Cohen, L. G., & Hallett, M. (2006). Multimodal imaging of brain reorganization in motor areas of the contralesional hemisphere of well recovered patients after capsular stroke. *Brain*. <https://doi.org/10.1093/brain/awh713>

- Gerloff, C., Corwell, B., Chen, R., Hallett, M., & Cohen, L. G. (1997). Stimulation over the human supplementary motor area interferes with the organization of future elements in complex motor sequences. *Brain*, *120*(9), 1587–1602. <https://doi.org/10.1093/brain/120.9.1587>
- Geyer, S., Matelli, M., Luppino, G., & Zilles, K. (2000). Functional neuroanatomy of the primate isocortical motor system. *Anatomy and Embryology*, *202*(6), 443–474. <https://doi.org/10.1007/s004290000127>
- Glees, P., & Cole, J. (1950). Recovery of skilled motor functions after small repeated lesions of motor cortex in macaque. *Journal of Neurophysiology*, *13*(2), 137–148. <https://doi.org/10.1152/jn.1950.13.2.137>
- Glover, I. S., & Baker, S. N. (2022). Both Corticospinal and Reticulospinal Tracts Control Force of Contraction. *The Journal of Neuroscience*, *42*(15), 3150–3164. <https://doi.org/10.1523/JNEUROSCI.0627-21.2022>
- Golestani, A.-M., Tymchuk, S., Demchuk, A., & Goodyear, B. G. (2013). Longitudinal Evaluation of Resting-State fMRI After Acute Stroke With Hemiparesis. *Neurorehabilitation and Neural Repair*, *27*(2), 153–163. <https://doi.org/10.1177/1545968312457827>
- Goyal, M., Menon, B. K., van Zwam, W. H., Dippel, D. W. J., Mitchell, P. J., Demchuk, A. M., Dávalos, A., Majoie, C. B. L. M., van der Lugt, A., de Miquel, M. A., Donnan, G. A., Roos, Y. B. W. E. M., Bonafe, A., Jahan, R., Diener, H.-C., van den Berg, L. A., Levy, E. I., Berkhemer, O. A., Pereira, V. M., ... Jovin, T. G. (2016). Endovascular thrombectomy after large-vessel ischaemic stroke: a meta-analysis of individual patient data from five randomised trials. *The Lancet*, *387*(10029), 1723–1731. [https://doi.org/10.1016/S0140-6736\(16\)00163-X](https://doi.org/10.1016/S0140-6736(16)00163-X)
- Grafton, S. T., & de C. Hamilton, A. F. (2007). Evidence for a distributed hierarchy of action representation in the brain. *Human Movement Science*, *26*(4), 590–616. <https://doi.org/10.1016/j.humov.2007.05.009>
- Grafton, S. T., & Volz, L. J. (2019). From ideas to action: The prefrontal–premotor connections that shape motor behavior. In *Handbook of Clinical Neurology* (1st ed., Vol. 163, pp. 237–255). Elsevier B.V. <https://doi.org/10.1016/B978-0-12-804281-6.00013-6>
- Graybiel, A. M. (1998). *The Basal Ganglia and Chunking of Action Repertoires*. *136*(70), 119–136.
- Grefkes, C., Eickhoff, S. B., Nowak, D. A., Dafotakis, M., & Fink, G. R. (2008). Dynamic intra- and interhemispheric interactions during unilateral and bilateral hand movements

- assessed with fMRI and DCM. *NeuroImage*, 41(4), 1382–1394.
<https://doi.org/10.1016/j.neuroimage.2008.03.048>
- Grefkes, C., & Fink, G. R. (2005). The functional organization of the intraparietal sulcus in humans and monkeys. *Journal of Anatomy*, 207(1), 3–17. <https://doi.org/10.1111/j.1469-7580.2005.00426.x>
- Grefkes, C., & Fink, G. R. (2011). Reorganization of cerebral networks after stroke: new insights from neuroimaging with connectivity approaches. *Brain*, 134(5), 1264–1276. <https://doi.org/10.1093/brain/awr033>
- Grefkes, C., & Fink, G. R. (2020). Recovery from stroke: current concepts and future perspectives. *Neurological Research and Practice*, 2(1), 17. <https://doi.org/10.1186/s42466-020-00060-6>
- Grefkes, C., Nowak, D. A., Eickhoff, S. B., Dafotakis, M., Küst, J., Karbe, H., & Fink, G. R. (2008). Cortical connectivity after subcortical stroke assessed with functional magnetic resonance imaging. *Annals of Neurology*, 63(2), 236–246. <https://doi.org/10.1002/ana.21228>
- Grefkes, C., Nowak, D. A., Wang, L. E., Dafotakis, M., Eickhoff, S. B., & Fink, G. R. (2010). Modulating cortical connectivity in stroke patients by rTMS assessed with fMRI and dynamic causal modeling. *NeuroImage*, 50(1), 233–242. <https://doi.org/10.1016/j.neuroimage.2009.12.029>
- Grefkes, C., Ritzl, A., Zilles, K., & Fink, G. R. (2004). Human medial intraparietal cortex subserves visuomotor coordinate transformation. *NeuroImage*, 23(4), 1494–1506. <https://doi.org/10.1016/j.neuroimage.2004.08.031>
- Grefkes, C., & Ward, N. S. (2014). Cortical Reorganization After Stroke. *The Neuroscientist*, 20(1), 56–70. <https://doi.org/10.1177/1073858413491147>
- Grisot, G., Haber, S. N., & Yendiki, A. (2021). Diffusion MRI and anatomic tracing in the same brain reveal common failure modes of tractography. *NeuroImage*, 239(January), 118300. <https://doi.org/10.1016/j.neuroimage.2021.118300>
- Guo, J., Liu, J., Wang, C., Cao, C., Fu, L., Han, T., Cheng, J., Yu, C., & Qin, W. (2019). Differential involvement of rubral branches in chronic capsular and pontine stroke. *NeuroImage: Clinical*, 24(154), 102090. <https://doi.org/10.1016/j.nicl.2019.102090>
- Hagmann, P., Jonasson, L., Maeder, P., Thiran, J.-P., Wedeen, V. J., & Meuli, R. (2006). Understanding Diffusion MR Imaging Techniques: From Scalar Diffusion-weighted Imaging to Diffusion Tensor Imaging and Beyond. *RadioGraphics*, 26(suppl_1), S205–S223. <https://doi.org/10.1148/rg.26si065510>

- Hammerbeck, U., Tyson, S. F., Samraj, P., Hollands, K., Krakauer, J. W., & Rothwell, J. (2021). The Strength of the Corticospinal Tract Not the Reticulospinal Tract Determines Upper-Limb Impairment Level and Capacity for Skill-Acquisition in the Sub-Acute Post-Stroke Period. *Neurorehabilitation and Neural Repair*, 35(9), 812–822. <https://doi.org/10.1177/15459683211028243>
- Hartwigsen, G., & Volz, L. J. (2021). Probing rapid network reorganization of motor and language functions via neuromodulation and neuroimaging. *NeuroImage*, 224(October 2020), 117449. <https://doi.org/10.1016/j.neuroimage.2020.117449>
- Hayward, K., Ferris, J. K., Lohse, K. R., Borich, M. R., Borstad, A., Cassidy, J. M., Cramer, S. C., Dukelow, S. P., Findlater, S. E., Hawe, R. L., Liew, S.-L., Neva, J. L., Stewart, J. C., & Boyd, L. A. (2022). Observational Study of Neuroimaging Biomarkers of Severe Upper Limb Impairment After Stroke. *Neurology*, 1–42. <https://doi.org/10.1212/WNL.0000000000200517>
- He, S., Dum, R., & Strick, P. (1995). Topographic organization of corticospinal projections from the frontal lobe: motor areas on the medial surface of the hemisphere. *The Journal of Neuroscience*, 15(5), 3284–3306. <https://doi.org/10.1523/JNEUROSCI.15-05-03284.1995>
- Heffner, R., & Masterton, B. (1975). Variation in Form of the Pyramidal Tract and Its Relationship to Digital Dexterity. *Brain, Behavior and Evolution*, 12(3), 188–200. <https://doi.org/10.1159/000124403>
- Hensel, L., Grefkes, C., Tscherpel, C., Ringmaier, C., Kraus, D., Hamacher, S., Volz, L. J., & Fink, G. R. (2019). Intermittent theta burst stimulation applied during early rehabilitation after stroke: study protocol for a randomised controlled trial. *BMJ Open*, 9(12), e034088. <https://doi.org/10.1136/bmjopen-2019-034088>
- Hensel, L., Lange, F., Tscherpel, C., Viswanathan, S., Freytag, J., Volz, L. J., Eickhoff, S. B., Fink, G. R., & Grefkes, C. (2022). Recovered grasping performance after stroke depends on interhemispheric frontoparietal connectivity. *Brain*, 1–15. <https://doi.org/10.1093/brain/awac157>
- Hensel, L., Tscherpel, C., Freytag, J., Ritter, S., Rehme, A. K., Volz, L. J., Eickhoff, S. B., Fink, G. R., & Grefkes, C. (2021). Connectivity-Related Roles of Contralateral Brain Regions for Motor Performance Early after Stroke. *Cerebral Cortex*, 31(2), 993–1007. <https://doi.org/10.1093/cercor/bhaa270>
- Henson, R., Buechel, C., Josephs, O., & Friston, K. J. (1999). The slice-timing problem in event-related fMRI. *NeuroImage*, 9, 125–125.

- Hsieh, C. L., Hsueh, I. P., Chiang, F. M., & Lin, P. H. (1998). Inter-rater reliability and validity of the action research arm test in stroke patients. *Age and Ageing*, *27*(2), 107–113. <https://doi.org/10.1093/ageing/27.2.107>
- Hsu, J.-L., Leemans, A., Bai, C.-H., Lee, C.-H., Tsai, Y.-F., Chiu, H.-C., & Chen, W.-H. (2008). Gender differences and age-related white matter changes of the human brain: A diffusion tensor imaging study. *NeuroImage*, *39*(2), 566–577. <https://doi.org/10.1016/j.neuroimage.2007.09.017>
- Huang, Y.-Z., Edwards, M. J., Rounis, E., Bhatia, K. P., & Rothwell, J. C. (2005). Theta Burst Stimulation of the Human Motor Cortex. *Neuron*, *45*(2), 201–206. <https://doi.org/10.1016/j.neuron.2004.12.033>
- Hylton, N. M., & Crooks, L. E. (1991). Principles of Magnetic Resonance Imaging. In S. Ueno & M. Sekino (Eds.), *Vascular Imaging by Color Doppler and Magnetic Resonance* (pp. 127–155). Springer Berlin Heidelberg. https://doi.org/10.1007/978-3-642-76194-2_5
- Ito, K. L., Kim, B., Liu, J., Soekadar, S. R., Winstein, C., Yu, C., Cramer, S. C., Schweighofer, N., & Liew, S.-L. (2021). Corticospinal Tract Lesion Load Originating From Both Ventral Premotor and Primary Motor Cortices Are Associated With Post-stroke Motor Severity. *Neurorehabilitation and Neural Repair*, 154596832110684. <https://doi.org/10.1177/15459683211068441>
- Jayaram, G., Stagg, C. J., Esser, P., Kischka, U., Stinear, J., & Johansen-Berg, H. (2012). Relationships between functional and structural corticospinal tract integrity and walking post stroke. *Clinical Neurophysiology*, *123*(12), 2422–2428. <https://doi.org/10.1016/j.clinph.2012.04.026>
- Jebsen, R. H., Taylor, N., Trieschmann, R. B., Trotter, M. J., & Howard, L. A. (1969). An objective and standardized test of hand function. *Archives of Physical Medicine and Rehabilitation*, *50*(6), 311–319.
- Jin, Z., Bao, Y., Wang, Y., Li, Z., Zheng, X., Long, S., & Wang, Y. (2019). Differences between generalized Q-sampling imaging and diffusion tensor imaging in visualization of crossing neural fibers in the brain. *Surgical and Radiologic Anatomy*, *41*(9), 1019–1028. <https://doi.org/10.1007/s00276-019-02264-1>
- Jones, D. K. (2008). Studying connections in the living human brain with diffusion MRI. *Cortex*, *44*(8), 936–952. <https://doi.org/10.1016/j.cortex.2008.05.002>
- Jones, D. K. (2014). Gaussian Modeling of the Diffusion Signal. In *Diffusion MRI* (Second Edition, pp. 87–104). Elsevier. <https://doi.org/10.1016/B978-0-12-396460-1.00005-6>
- Karbasforoushan, H., Cohen-Adad, J., & Dewald, J. P. A. (2019). Brainstem and spinal cord

- MRI identifies altered sensorimotor pathways post-stroke. *Nature Communications*, *10*(1), 3524. <https://doi.org/10.1038/s41467-019-11244-3>
- Kelley, S., Plass, J., Bender, A. R., & Polk, T. A. (2021). Age-Related Differences in White Matter: Understanding Tensor-Based Results Using Fixel-Based Analysis. *Cerebral Cortex*, *31*(8), 3881–3898. <https://doi.org/10.1093/cercor/bhab056>
- Kennard, M. A. (1936). Age and other factors in motor recovery from precentral lesions in monkeys. *American Journal of Physiology-Legacy Content*, *115*(1), 138–146. <https://doi.org/10.1152/ajplegacy.1936.115.1.138>
- Kennard, M. A. (1938). Reorganization of motor function in the cerebral cortex of monkeys deprived of motor and premotor areas in infancy. *Journal of Neurophysiology*, *1*(6), 477–496. <https://doi.org/10.1152/jn.1938.1.6.477>
- Kiebel, S. J., & Holmes, A. P. (2004). The General Linear Model. In R. Frackowiak, K. J. Friston, C. Frith, R. Dolan, C. Price, J. Ashburner, W. D. Penny, & S. Zeki (Eds.), *Human Brain Function* (2nd ed., pp. 725–760). Elsevier. <https://doi.org/10.1016/B978-012264841-0/50039-1>
- Kim, B., Fisher, B. E., Schweighofer, N., Leahy, R. M., Haldar, J. P., Choi, S., Kay, D. B., Gordon, J., & Winstein, C. J. (2018). A comparison of seven different DTI-derived estimates of corticospinal tract structural characteristics in chronic stroke survivors. *Journal of Neuroscience Methods*, *304*, 66–75. <https://doi.org/10.1016/j.jneumeth.2018.04.010>
- Klomjai, W., Katz, R., & Lackmy-Vallée, A. (2015). Basic principles of transcranial magnetic stimulation (TMS) and repetitive TMS (rTMS). *Annals of Physical and Rehabilitation Medicine*, *58*(4), 208–213. <https://doi.org/10.1016/j.rehab.2015.05.005>
- Koch, P. J., Park, C. H., Girard, G., Beanato, E., Egger, P., Evangelista, G. G., Lee, J., Wessel, M. J., Morishita, T., Koch, G., Thiran, J. P., Guggisberg, A. G., Rosso, C., Kim, Y. H., & Hummel, F. C. (2021). The structural connectome and motor recovery after stroke: Predicting natural recovery. *Brain*, *144*(7), 2107–2119. <https://doi.org/10.1093/brain/awab082>
- Koch, P. J., Schulz, R., & Hummel, F. C. (2016). Structural connectivity analyses in motor recovery research after stroke. *Annals of Clinical and Translational Neurology*, *3*(3), 233–244. <https://doi.org/10.1002/acn3.278>
- Krakauer, J. W. (2006). Motor learning: its relevance to stroke recovery and neurorehabilitation. *Current Opinion in Neurology*, *19*(1), 84–90. <https://doi.org/10.1097/01.wco.0000200544.29915.cc>

- Krakauer, J. W. (2015). The applicability of motor learning to neurorehabilitation. In V. Dietz & N. Ward (Eds.), *Oxford Textbook of Neurorehabilitation* (Vol. 1). Oxford University Press. <https://doi.org/10.1093/med/9780199673711.001.0001>
- Krakauer, J. W., & Carmichael, S. T. (2017). *Broken Movement*. The MIT Press. <https://doi.org/10.7551/mitpress/9310.001.0001>
- Küchler, M., Fouad, K., Weinmann, O., Schwab, M. E., & Raineteau, O. (2002). Red nucleus projections to distinct motor neuron pools in the rat spinal cord. *Journal of Comparative Neurology*, *448*(4), 349–359. <https://doi.org/10.1002/cne.10259>
- Kwon, H. G., Lee, D. G., Son, S. M., Byun, W. M., Hong, C. P., Lee, D. H., Kim, S., & Jang, S. H. (2011). Identification of the anterior corticospinal tract in the human brain using diffusion tensor imaging. *Neuroscience Letters*, *505*(3), 238–241. <https://doi.org/10.1016/j.neulet.2011.10.020>
- Kwong, K. K., Belliveau, J. W., Chesler, D. A., Goldberg, I. E., Weisskoff, R. M., Poncelet, B. P., Kennedy, D. N., Hoppel, B. E., Cohen, M. S., & Turner, R. (1992). Dynamic magnetic resonance imaging of human brain activity during primary sensory stimulation. *Proceedings of the National Academy of Sciences*, *89*(12), 5675–5679. <https://doi.org/10.1073/pnas.89.12.5675>
- Lang, C. E., Wagner, J. M., Bastian, A. J., Hu, Q., Edwards, D. F., Sahrman, S. A., & Dromerick, A. W. (2005). Deficits in grasp versus reach during acute hemiparesis. *Experimental Brain Research*, *166*(1), 126–136. <https://doi.org/10.1007/s00221-005-2350-6>
- Langhorne, P., Bernhardt, J., & Kwakkel, G. (2011). Stroke rehabilitation. *The Lancet*, *377*(9778), 1693–1702. [https://doi.org/10.1016/S0140-6736\(11\)60325-5](https://doi.org/10.1016/S0140-6736(11)60325-5)
- Lara, A. H., Cunningham, J. P., & Churchland, M. M. (2018). Different population dynamics in the supplementary motor area and motor cortex during reaching. *Nature Communications*, *9*(1), 2754. <https://doi.org/10.1038/s41467-018-05146-z>
- Lauterbur, P. C. (1973). Image Formation by Induced Local Interactions: Examples Employing Nuclear Magnetic Resonance. *Nature*, *242*(5394), 190–191. <https://doi.org/10.1038/242190a0>
- Lawrence, D. G., & Kuypers, H. G. J. M. (1968a). The Functional Organization of the Motor System in the Monkey: I. The effects of bilateral pyramidal lesions. *Brain*, *91*(1), 1–14. <https://doi.org/10.1093/brain/91.1.15>
- Lawrence, D. G., & Kuypers, H. G. J. M. (1968b). The Functional Organization of the Motor System in the Monkey: II. The Effects of lesions of the descending brain-stem pathways.

- Brain*, 91(1), 15–36. <https://doi.org/10.1093/brain/91.1.15>
- Le Bihan, D., Poupon, C., Amadon, A., & Lethimonnier, F. (2006). Artifacts and pitfalls in diffusion MRI. *Journal of Magnetic Resonance Imaging*, 24(3), 478–488. <https://doi.org/10.1002/jmri.20683>
- Lee, J., Park, E., Lee, A., Chang, W. H., Kim, D. S., & Kim, Y. H. (2017). Recovery-related indicators of motor network plasticity according to impairment severity after stroke. *European Journal of Neurology*, 24(10), 1290–1299. <https://doi.org/10.1111/ene.13377>
- Lemon, R. N. (2008). Descending Pathways in Motor Control. *Annual Review of Neuroscience*, 31(1), 195–218. <https://doi.org/10.1146/annurev.neuro.31.060407.125547>
- Lindenberg, R., Renga, V., Zhu, L. L., Betzler, F., Alsop, D., & Schlaug, G. (2010). Structural integrity of corticospinal motor fibers predicts motor impairment in chronic stroke. *Neurology*, 74(4), 280–287. <https://doi.org/10.1212/WNL.0b013e3181ccc6d9>
- Lindenberg, R., Zhu, L. L., Rüber, T., & Schlaug, G. (2012). Predicting functional motor potential in chronic stroke patients using diffusion tensor imaging. *Human Brain Mapping*, 33(5), 1040–1051. <https://doi.org/10.1002/hbm.21266>
- Liu, J., Wang, C., Qin, W., Ding, H., Guo, J., Han, T., Cheng, J., & Yu, C. (2020). Corticospinal Fibers With Different Origins Impact Motor Outcome and Brain After Subcortical Stroke. *Stroke*, 51(7), 2170–2178. <https://doi.org/10.1161/STROKEAHA.120.029508>
- Logothetis, N. K., Auguth, M., Oeltermann, A., Pauls, J., & Trinath, T. (2001). A neurophysiological investigation of the basis of the BOLD signal in fMRI. *Nature*, 412(6843), 150–157.
- Lotze, M., Markert, J., Sauseng, P., Hoppe, J., Plewnia, C., & Gerloff, C. (2006). The role of multiple contralesional motor areas for complex hand movements after internal capsular lesion. *The Journal of Neuroscience : The Official Journal of the Society for Neuroscience*, 26(22), 6096–6102. <https://doi.org/10.1523/JNEUROSCI.4564-05.2006>
- Lyle, R. C. (1981). A performance test for assessment of upper limb function in physical rehabilitation treatment and research. *International Journal of Rehabilitation Research*, 4(4), 483–492. <https://doi.org/10.1097/00004356-198112000-00001>
- Macar, F., Anton, J.-L., Bonnet, M., & Vidal, F. (2004). Timing functions of the supplementary motor area: an event-related fMRI study. *Cognitive Brain Research*, 21(2), 206–215. <https://doi.org/10.1016/j.cogbrainres.2004.01.005>
- McDonnell, M. N., & Stinear, C. M. (2017). TMS measures of motor cortex function after stroke: A meta-analysis. *Brain Stimulation*, 10(4), 721–734. <https://doi.org/10.1016/j.brs.2017.03.008>

- McMorland, A. J. C., Runnalls, K. D., & Byblow, W. D. (2015). A Neuroanatomical Framework for Upper Limb Synergies after Stroke. *Frontiers in Human Neuroscience*, 9(FEB), 1–6. <https://doi.org/10.3389/fnhum.2015.00082>
- McPherson, J. G., Chen, A., Ellis, M. D., Yao, J., Heckman, C. J., & Dewald, J. P. A. (2018). Progressive recruitment of contralesional cortico-reticulospinal pathways drives motor impairment post stroke. *The Journal of Physiology*, 596(7), 1211–1225. <https://doi.org/10.1113/JP274968>
- Merzenich, M. M., Nelson, R. J., Stryker, M. P., Cynader, M. S., Schoppmann, A., & Zook, J. M. (1984). Somatosensory cortical map changes following digit amputation in adult monkeys. *The Journal of Comparative Neurology*, 224(4), 591–605. <https://doi.org/10.1002/cne.902240408>
- Middleton, F. (2000). Basal ganglia and cerebellar loops: motor and cognitive circuits. *Brain Research Reviews*, 31(2–3), 236–250. [https://doi.org/10.1016/S0165-0173\(99\)00040-5](https://doi.org/10.1016/S0165-0173(99)00040-5)
- Moura, L. M., Luccas, R., Paiva, J. P. Q. de, Amaro, E., Leemans, A., Leite, C. da C., Otaduy, M. C. G., & Conforto, A. B. (2019). Diffusion Tensor Imaging Biomarkers to Predict Motor Outcomes in Stroke: A Narrative Review. *Frontiers in Neurology*, 10(MAY), 1–17. <https://doi.org/10.3389/fneur.2019.00445>
- Murase, N., Duque, J., Mazzocchio, R., & Cohen, L. G. (2004). Influence of interhemispheric interactions on motor function in chronic stroke. *Annals of Neurology*, 55(3), 400–409. <https://doi.org/10.1002/ana.10848>
- Murphy, K., Birn, R. M., Handwerker, D. A., Jones, T. B., & Bandettini, P. A. (2009). The impact of global signal regression on resting state correlations: Are anti-correlated networks introduced? *NeuroImage*, 44(3), 893–905. <https://doi.org/10.1016/j.neuroimage.2008.09.036>
- Murphy, K., & Fox, M. D. (2017). Towards a consensus regarding global signal regression for resting state functional connectivity MRI. *NeuroImage*, 154(November 2016), 169–173. <https://doi.org/10.1016/j.neuroimage.2016.11.052>
- Nijland, R., van Wegen, E., Verbunt, J., van Wijk, R., van Kordelaar, J., & Kwakkel, G. (2010). A comparison of two validated tests for upper limb function after stroke: The Wolf Motor Function Test and the Action Research Arm Test. *Journal of Rehabilitation Medicine*, 42(7), 694–696. <https://doi.org/10.2340/16501977-0560>
- Nudo, R. J. (2003). Adaptive plasticity in motor cortex: implications for rehabilitation after brain injury. *Journal of Rehabilitation Medicine*, 35(41), 7–10. <https://doi.org/10.1080/16501960310010070>

- Nudo, R. J. (2006a). Plasticity. *NeuroRX*, 3(4), 420–427. <https://doi.org/10.1016/j.nurx.2006.07.006>
- Nudo, R. J. (2006b). Mechanisms for recovery of motor function following cortical damage. *Current Opinion in Neurobiology*, 16(6), 638–644. <https://doi.org/10.1016/j.conb.2006.10.004>
- Nudo, R. J. (2013). Recovery after brain injury: mechanisms and principles. *Frontiers in Human Neuroscience*, 7(DEC), 1–14. <https://doi.org/10.3389/fnhum.2013.00887>
- Nudo, R. J., & Masterton, R. B. (1990). Descending pathways to the spinal cord, IV: Some factors related to the amount of cortex devoted to the corticospinal tract. *The Journal of Comparative Neurology*, 296(4), 584–597. <https://doi.org/10.1002/cne.902960406>
- Nudo, R. J., Milliken, G., Jenkins, W., & Merzenich, M. (1996). Use-dependent alterations of movement representations in primary motor cortex of adult squirrel monkeys. *The Journal of Neuroscience*, 16(2), 785–807. <https://doi.org/10.1523/JNEUROSCI.16-02-00785.1996>
- Nudo, R. J., Wise, B. M., SiFuentes, F., & Milliken, G. W. (1996). Neural Substrates for the Effects of Rehabilitative Training on Motor Recovery After Ischemic Infarct. *Science*, 272(5269), 1791–1794. <https://doi.org/10.1126/science.272.5269.1791>
- O'Donnell, L. J., & Pasternak, O. (2015). Does diffusion MRI tell us anything about the white matter? An overview of methods and pitfalls. *Schizophrenia Research*, 161(1), 133–141. <https://doi.org/10.1016/j.schres.2014.09.007>
- Ogawa, S., Lee, T. M., Kay, A. R., & Tank, D. W. (1990). Brain magnetic resonance imaging with contrast dependent on blood oxygenation. *Proceedings of the National Academy of Sciences*, 87(24), 9868–9872. <https://doi.org/10.1073/pnas.87.24.9868>
- Ogawa, S., Tank, D. W., Menon, R., Ellermann, J. M., Kim, S. G., Merkle, H., & Ugurbil, K. (1992). Intrinsic signal changes accompanying sensory stimulation: functional brain mapping with magnetic resonance imaging. *Proceedings of the National Academy of Sciences*, 89(13), 5951–5955. <https://doi.org/10.1073/pnas.89.13.5951>
- Overduin, S. A., D'Avella, A., Roh, J., Carmena, J. M., & Bizzi, E. (2015). Representation of Muscle Synergies in the Primate Brain. *Journal of Neuroscience*, 35(37), 12615–12624. <https://doi.org/10.1523/JNEUROSCI.4302-14.2015>
- Owen, M., Ingo, C., & Dewald, J. P. A. (2017). Upper Extremity Motor Impairments and Microstructural Changes in Bulbospinal Pathways in Chronic Hemiparetic Stroke. *Frontiers in Neurology*, 8(JUN), 1–10. <https://doi.org/10.3389/fneur.2017.00257>
- Park, C., Chang, W. H., Ohn, S. H., Kim, S. T., Bang, O. Y., Pascual-Leone, A., & Kim, Y.-H.

- H. (2011). Longitudinal Changes of Resting-State Functional Connectivity During Motor Recovery After Stroke. *Stroke*, 42(5), 1357–1362. <https://doi.org/10.1161/STROKEAHA.110.596155>
- Penfield, W., & Boldrey, E. (1937). Somatic motor and sensory representation in the cerebral cortex of man as studied by electrical stimulation. *Brain*, 60(4), 389–443. <https://doi.org/10.1093/brain/60.4.389>
- Peng, Y., Liu, J., Hua, M., Liang, M., & Yu, C. (2019). Enhanced Effective Connectivity From Ipsilesional to Contralesional M1 in Well-Recovered Subcortical Stroke Patients. *Frontiers in Neurology*, 10(AUG), 1–8. <https://doi.org/10.3389/fneur.2019.00909>
- Penny, W. D., Stephan, K. E., Mechelli, A., & Friston, K. J. (2004). Comparing dynamic causal models. *NeuroImage*, 22(3), 1157–1172. <https://doi.org/10.1016/j.neuroimage.2004.03.026>
- Pesce, M., Repetti, A., Auría, A., Daducci, A., Thiran, J.-P., & Wiaux, Y. (2021). Fast Fiber Orientation Estimation in Diffusion MRI from kq-Space Sampling and Anatomical Priors. *Journal of Imaging*, 7(11), 226. <https://doi.org/10.3390/jimaging7110226>
- Peters, D. M., Fridriksson, J., Richardson, J. D., Stewart, J. C., Rorden, C., Bonilha, L., Middleton, A., & Fritz, S. L. (2021). Upper and Lower Limb Motor Function Correlates with Ipsilesional Corticospinal Tract and Red Nucleus Structural Integrity in Chronic Stroke: A Cross-Sectional, ROI-Based MRI Study. *Behavioural Neurology*, 2021, 1–10. <https://doi.org/10.1155/2021/3010555>
- Peters, D. M., Fridriksson, J., Stewart, J. C., Richardson, J. D., Rorden, C., Bonilha, L., Middleton, A., Gleichgerrcht, E., & Fritz, S. L. (2018). Cortical disconnection of the ipsilesional primary motor cortex is associated with gait speed and upper extremity motor impairment in chronic left hemispheric stroke. *Human Brain Mapping*, 39(1), 120–132. <https://doi.org/10.1002/hbm.23829>
- Phan, T. G., van der Voort, S., Chen, J., Beare, R., Ma, H., Clissold, B., Ly, J., Foster, E., Thong, E., & Srikanth, V. (2013). Impact of corticofugal fibre involvement in subcortical stroke. *BMJ Open*, 3(9), e003318. <https://doi.org/10.1136/bmjopen-2013-003318>
- Plautz, E. J., Milliken, G. W., & Nudo, R. J. (2000). Effects of Repetitive Motor Training on Movement Representations in Adult Squirrel Monkeys: Role of Use versus Learning. *Neurobiology of Learning and Memory*, 74(1), 27–55. <https://doi.org/10.1006/nlme.1999.3934>
- Poldrack, R. A., Nichols, T., & Mumford, J. (2011). *Handbook of Functional MRI Data Analysis*. Cambridge University Press. <https://doi.org/10.1017/CBO9780511895029>

- Pool, E.-M., Rehme, A. K., Eickhoff, S. B., Fink, G. R., & Grefkes, C. (2015). Functional resting-state connectivity of the human motor network: Differences between right- and left-handers. *NeuroImage*, *109*, 298–306. <https://doi.org/10.1016/j.neuroimage.2015.01.034>
- Pool, E.-M., Rehme, A. K., Fink, G. R., Eickhoff, S. B., & Grefkes, C. (2013). Network dynamics engaged in the modulation of motor behavior in healthy subjects. *NeuroImage*, *82*, 68–76. <https://doi.org/10.1016/j.neuroimage.2013.05.123>
- Pool, E.-M., Rehme, A. K., Fink, G. R., Eickhoff, S. B., & Grefkes, C. (2014). Handedness and effective connectivity of the motor system. *NeuroImage*, *99*, 451–460. <https://doi.org/10.1016/j.neuroimage.2014.05.048>
- Power, J. D., Barnes, K. A., Snyder, A. Z., Schlaggar, B. L., & Petersen, S. E. (2012). Spurious but systematic correlations in functional connectivity MRI networks arise from subject motion. *NeuroImage*, *59*(3), 2142–2154. <https://doi.org/10.1016/j.neuroimage.2011.10.018>
- Power, J. D., Mitra, A., Laumann, T. O., Snyder, A. Z., Schlaggar, B. L., & Petersen, S. E. (2014). Methods to detect, characterize, and remove motion artifact in resting state fMRI. *NeuroImage*, *84*, 320–341. <https://doi.org/10.1016/j.neuroimage.2013.08.048>
- Puig, J., Blasco, G., Daunis-I-Estadella, J., Thomalla, G., Castellanos, M., Figueras, J., Remollo, S., van Eendenburg, C., Sánchez-González, J., Serena, J., & Pedraza, S. (2013). Decreased Corticospinal Tract Fractional Anisotropy Predicts Long-term Motor Outcome After Stroke. *Stroke*, *44*(7), 2016–2018. <https://doi.org/10.1161/STROKEAHA.111.000382>
- Puig, J., Pedraza, S., Blasco, G., Daunis-i-Estadella, J., Prados, F., Remollo, S., Prats-Galino, A., Soria, G., Boada, I., Castellanos, M., & Serena, J. (2011). Acute Damage to the Posterior Limb of the Internal Capsule on Diffusion Tensor Tractography as an Early Imaging Predictor of Motor Outcome after Stroke. *American Journal of Neuroradiology*, *32*(5), 857–863. <https://doi.org/10.3174/ajnr.A2400>
- Puig, J., Pedraza, S., Blasco, G., Daunis-i-Estadella, J., Prats, A., Prados, F., Boada, I., Castellanos, M., Sánchez-González, J., Remollo, S., Laguillo, G., Quiles, A. M., Gómez, E., & Serena, J. (2010). Wallerian degeneration in the corticospinal tract evaluated by diffusion tensor imaging correlates with motor deficit 30 days after middle cerebral artery ischemic stroke. *American Journal of Neuroradiology*, *31*(7), 1324–1330. <https://doi.org/10.3174/ajnr.A2038>
- Radlinska, B. A., Blunk, Y., Leppert, I. R., Minuk, J., Pike, G. B., & Thiel, A. (2012). Changes

- in Callosal Motor Fiber Integrity after Subcortical Stroke of the Pyramidal Tract. *Journal of Cerebral Blood Flow & Metabolism*, 32(8), 1515–1524. <https://doi.org/10.1038/jcbfm.2012.37>
- Raichle, M. E. (2009). A Paradigm Shift in Functional Brain Imaging. *Journal of Neuroscience*, 29(41), 12729–12734. <https://doi.org/10.1523/JNEUROSCI.4366-09.2009>
- Ramnani, N. (2006). The primate cortico-cerebellar system: anatomy and function. *Nature Reviews Neuroscience*, 7(7), 511–522. <https://doi.org/10.1038/nrn1953>
- Rehme, A. K., Eickhoff, S. B., & Grefkes, C. (2013). State-dependent differences between functional and effective connectivity of the human cortical motor system. *NeuroImage*, 67, 237–246. <https://doi.org/10.1016/j.neuroimage.2012.11.027>
- Rehme, A. K., Eickhoff, S. B., Rottschy, C., Fink, G. R., & Grefkes, C. (2012). Activation likelihood estimation meta-analysis of motor-related neural activity after stroke. *NeuroImage*, 59(3), 2771–2782. <https://doi.org/10.1016/j.neuroimage.2011.10.023>
- Rehme, A. K., Eickhoff, S. B., Wang, L. E., Fink, G. R., & Grefkes, C. (2011). Dynamic causal modeling of cortical activity from the acute to the chronic stage after stroke. *NeuroImage*, 55(3), 1147–1158. <https://doi.org/10.1016/j.neuroimage.2011.01.014>
- Rehme, A. K., Fink, G. R., von Cramon, D. Y., & Grefkes, C. (2011). The Role of the Contralateral Motor Cortex for Motor Recovery in the Early Days after Stroke Assessed with Longitudinal fMRI. *Cerebral Cortex*, 21(4), 756–768. <https://doi.org/10.1093/cercor/bhq140>
- Rehme, A. K., Volz, L. J., Feis, D.-L., Bomilcar-Focke, I., Liebig, T., Eickhoff, S. B., Fink, G. R., & Grefkes, C. (2015). Identifying Neuroimaging Markers of Motor Disability in Acute Stroke by Machine Learning Techniques. *Cerebral Cortex*, 25(9), 3046–3056. <https://doi.org/10.1093/cercor/bhu100>
- Rehme, A. K., Volz, L. J., Feis, D. L., Eickhoff, S. B., Fink, G. R., & Grefkes, C. (2015). Individual prediction of chronic motor outcome in the acute post-stroke stage: Behavioral parameters versus functional imaging. *Human Brain Mapping*, 36(11), 4553–4565. <https://doi.org/10.1002/hbm.22936>
- Riley, J. D., Le, V., Der-Yeghiaian, L., See, J., Newton, J. M., Ward, N. S., & Cramer, S. C. (2011). Anatomy of Stroke Injury Predicts Gains From Therapy. *Stroke*, 42(2), 421–426. <https://doi.org/10.1161/STROKEAHA.110.599340>
- Rizzolatti, G., Fogassi, L., & Gallese, V. (2002). Motor and cognitive functions of the ventral premotor cortex. *Current Opinion in Neurobiology*, 12(2), 149–154. [https://doi.org/10.1016/S0959-4388\(02\)00308-2](https://doi.org/10.1016/S0959-4388(02)00308-2)

- Rizzolatti, G., & Luppino, G. (2001). The Cortical Motor System. *Neuron*, 31(6), 889–901. [https://doi.org/10.1016/S0896-6273\(01\)00423-8](https://doi.org/10.1016/S0896-6273(01)00423-8)
- Roh, J., Rymer, W. Z., & Beer, R. F. (2015). Evidence for altered upper extremity muscle synergies in chronic stroke survivors with mild and moderate impairment. *Frontiers in Human Neuroscience*, 9(FEB), 1–14. <https://doi.org/10.3389/fnhum.2015.00006>
- Ruber, T., Schlaug, G., & Lindenberg, R. (2012). Compensatory role of the cortico-rubro-spinal tract in motor recovery after stroke. *Neurology*, 79(6), 515–522. <https://doi.org/10.1212/WNL.0b013e31826356e8>
- Rubinov, M., & Sporns, O. (2010). Complex network measures of brain connectivity: Uses and interpretations. *NeuroImage*, 52(3), 1059–1069. <https://doi.org/10.1016/j.neuroimage.2009.10.003>
- Salat, D. H., Tuch, D. S., Greve, D. N., van der Kouwe, A. J. W., Hevelone, N. D., Zaleta, A. K., Rosen, B. R., Fischl, B., Corkin, S., Rosas, H. D., & Dale, A. M. (2005). Age-related alterations in white matter microstructure measured by diffusion tensor imaging. *Neurobiology of Aging*, 26(8), 1215–1227. <https://doi.org/10.1016/j.neurobiolaging.2004.09.017>
- Satterthwaite, T. D., Elliott, M. A., Gerraty, R. T., Ruparel, K., Loughead, J., Calkins, M. E., Eickhoff, S. B., Hakonarson, H., Gur, R. C., Gur, R. E., & Wolf, D. H. (2013). An improved framework for confound regression and filtering for control of motion artifact in the preprocessing of resting-state functional connectivity data. *NeuroImage*, 64(1), 240–256. <https://doi.org/10.1016/j.neuroimage.2012.08.052>
- Schaechter, J. D., Fricker, Z. P., Perdue, K. L., Helmer, K. G., Vangel, M. G., Greve, D. N., & Makris, N. (2009). Microstructural status of ipsilesional and contralesional corticospinal tract correlates with motor skill in chronic stroke patients. *Human Brain Mapping*, 30(11), 3461–3474. <https://doi.org/10.1002/hbm.20770>
- Schilling, K. G., Daducci, A., Maier-Hein, K., Poupon, C., Houde, J.-C., Nath, V., Anderson, A. W., Landman, B. A., & Descoteaux, M. (2019). Challenges in diffusion MRI tractography – Lessons learned from international benchmark competitions. *Magnetic Resonance Imaging*, 57(October 2018), 194–209. <https://doi.org/10.1016/j.mri.2018.11.014>
- Schilling, K. G., Petit, L., Rheault, F., Remedios, S., Pierpaoli, C., Anderson, A. W., Landman, B. A., & Descoteaux, M. (2020). Brain connections derived from diffusion MRI tractography can be highly anatomically accurate—if we know where white matter pathways start, where they end, and where they do not go. *Brain Structure and Function*,

- 225(8), 2387–2402. <https://doi.org/10.1007/s00429-020-02129-z>
- Schlemm, E., Schulz, R., Bönstrup, M., Krawinkel, L., Fiehler, J., Gerloff, C., Thomalla, G., & Cheng, B. (2020). Structural brain networks and functional motor outcome after stroke—a prospective cohort study. *Brain Communications*, 2(1), 1–13. <https://doi.org/10.1093/braincomms/fcaa001>
- Schubotz, R. I., & Von Cramon, D. Y. (2003). Functional-anatomical concepts of human premotor cortex: Evidence from fMRI and PET studies. *NeuroImage*, 20(SUPPL. 1), 120–131. <https://doi.org/10.1016/j.neuroimage.2003.09.014>
- Schulz, R., Braass, H., Liuzzi, G., Hoerniss, V., Lechner, P., Gerloff, C., & Hummel, F. C. (2015). White matter integrity of premotor–motor connections is associated with motor output in chronic stroke patients. *NeuroImage: Clinical*, 7, 82–86. <https://doi.org/10.1016/j.nicl.2014.11.006>
- Schulz, R., Koch, P., Zimmerman, M., Wessel, M., Bönstrup, M., Thomalla, G., Cheng, B., Gerloff, C., & Hummel, F. C. (2015). Parietofrontal motor pathways and their association with motor function after stroke. *Brain*, 138(7), 1949–1960. <https://doi.org/10.1093/brain/awv100>
- Schulz, R., Park, C.-H., Boudrias, M.-H., Gerloff, C., Hummel, F. C., & Ward, N. S. (2012). Assessing the Integrity of Corticospinal Pathways From Primary and Secondary Cortical Motor Areas After Stroke. *Stroke*, 43(8), 2248–2251. <https://doi.org/10.1161/STROKEAHA.112.662619>
- Schulz, R., Park, E., Lee, J., Chang, W. H., Lee, A., Kim, Y.-H., & Hummel, F. C. (2017a). Synergistic but independent: The role of corticospinal and alternate motor fibers for residual motor output after stroke. *NeuroImage: Clinical*, 15(April), 118–124. <https://doi.org/10.1016/j.nicl.2017.04.016>
- Schulz, R., Park, E., Lee, J., Chang, W. H., Lee, A., Kim, Y.-H., & Hummel, F. C. (2017b). Interactions Between the Corticospinal Tract and Premotor–Motor Pathways for Residual Motor Output After Stroke. *Stroke*, 48(10), 2805–2811. <https://doi.org/10.1161/STROKEAHA.117.016834>
- Seunarine, K. K., & Alexander, D. C. (2013). Multiple Fibers. Beyond the Diffusion Tensor. In *Diffusion MRI: From Quantitative Measurement to In vivo Neuroanatomy: Second Edition* (Second Edi). Elsevier. <https://doi.org/10.1016/B978-0-12-396460-1.00006-8>
- Shadmehr, R., Smith, M. A., & Krakauer, J. W. (2010). Error correction, sensory prediction, and adaptation in motor control. *Annual Review of Neuroscience*, 33, 89–108. <https://doi.org/10.1146/annurev-neuro-060909-153135>

- Sherrington, C. S., & Grunbaum, A. S. F. (1901). An address on Localisation in the “motor” cerebral cortex. *BMJ*, *2*(2139), 1857–1859. <https://doi.org/10.1136/bmj.2.2139.1857>
- Sivapatham, T., & Melhem, E. R. (2011). Physical Principles of Diffusion Imaging. In *Functional Neuroradiology* (pp. 3–11). Springer US. https://doi.org/10.1007/978-1-4419-0345-7_1
- Sladky, R., Friston, K. J., Tröstl, J., Cunnington, R., Moser, E., & Windischberger, C. (2011). Slice-timing effects and their correction in functional MRI. *NeuroImage*, *58*(2), 588–594. <https://doi.org/10.1016/j.neuroimage.2011.06.078>
- Smith, Y., Bevan, M. D., Shink, E., & Bolam, J. P. (1998). Microcircuitry of the direct and indirect pathways of the basal ganglia. *Neuroscience*, *86*(2), 353–387. [https://doi.org/10.1016/s0306-4522\(98\)00004-9](https://doi.org/10.1016/s0306-4522(98)00004-9)
- Soltmann, O. (1876). Experimentelle Studien über die Funktionen des Grosshirns der Neugeborenen. *Jahrbuch Der Kinderheilkunde*, *9*, 106–148.
- Stejskal, E. O., & Tanner, J. E. (1965). Spin Diffusion Measurements: Spin Echoes in the Presence of a Time-Dependent Field Gradient. *The Journal of Chemical Physics*, *42*(1), 288–292. <https://doi.org/10.1063/1.1695690>
- Stephan, K. E., & Friston, K. J. (2010). Analyzing effective connectivity with functional magnetic resonance imaging. *Wiley Interdisciplinary Reviews: Cognitive Science*, *1*(3), 446–459. <https://doi.org/10.1002/wcs.58>
- Stephan, K. E., Penny, W. D., Daunizeau, J., Moran, R. J., & Friston, K. J. (2009). Bayesian model selection for group studies. *NeuroImage*, *46*(4), 1004–1017. <https://doi.org/10.1016/j.neuroimage.2009.03.025>
- Stephan, K. E., Penny, W. D., Moran, R. J., den Ouden, H. E. M., Daunizeau, J., & Friston, K. J. (2010). Ten simple rules for dynamic causal modeling. *NeuroImage*, *49*(4), 3099–3109. <https://doi.org/10.1016/j.neuroimage.2009.11.015>
- Stewart, J. C., Dewanjee, P., Tran, G., Quinlan, E. B., Dodakian, L., McKenzie, A., See, J., & Cramer, S. C. (2017). Role of corpus callosum integrity in arm function differs based on motor severity after stroke. *NeuroImage: Clinical*, *14*, 641–647. <https://doi.org/10.1016/j.nicl.2017.02.023>
- Stinear, C. M., Barber, P. A., Petoe, M., Anwar, S., & Byblow, W. D. (2012). The PREP algorithm predicts potential for upper limb recovery after stroke. *Brain*, *135*(8), 2527–2535. <https://doi.org/10.1093/brain/aws146>
- Stinear, C. M., Byblow, W. D., Ackerley, S. J., Smith, M.-C., Borges, V. M., & Barber, P. A. (2017). PREP2: A biomarker-based algorithm for predicting upper limb function after

- stroke. *Annals of Clinical and Translational Neurology*, 4(11), 811–820.
<https://doi.org/10.1002/acn3.488>
- Stoodley, C. J., & Schmammann, J. D. (2010). Evidence for topographic organization in the cerebellum of motor control versus cognitive and affective processing. *CORTEX*, 46(7), 831–844. <https://doi.org/10.1016/j.cortex.2009.11.008>
- Strick, P. L., Dum, R. P., & Rathelot, J.-A. (2021). The Cortical Motor Areas and the Emergence of Motor Skills: A Neuroanatomical Perspective. *Annual Review of Neuroscience*, 44(1), 425–447. <https://doi.org/10.1146/annurev-neuro-070918-050216>
- Taga, M., Charalambous, C. C., Raju, S., Lin, J., Zhang, Y., Stern, E., & Schambra, H. M. (2021). Corticoreticulospinal tract neurophysiology in an arm and hand muscle in healthy and stroke subjects. *The Journal of Physiology*, 599(16), 3955–3971. <https://doi.org/10.1113/JP281681>
- Takenobu, Y., Hayashi, T., Moriwaki, H., Nagatsuka, K., Naritomi, H., & Fukuyama, H. (2014). Motor recovery and microstructural change in rubro-spinal tract in subcortical stroke. *NeuroImage: Clinical*, 4, 201–208. <https://doi.org/10.1016/j.nicl.2013.12.003>
- Thomalla, G., Glauche, V., Koch, M. A., Beaulieu, C., Weiller, C., & Röther, J. (2004). Diffusion tensor imaging detects early Wallerian degeneration of the pyramidal tract after ischemic stroke. *NeuroImage*, 22(4), 1767–1774. <https://doi.org/10.1016/j.neuroimage.2004.03.041>
- Thomalla, G., Simonsen, C. Z., Boutitie, F., Andersen, G., Berthezene, Y., Cheng, B., Cheripelli, B., Cho, T.-H., Fazekas, F., Fiehler, J., Ford, I., Galinovic, I., Gellissen, S., Golsari, A., Gregori, J., Günther, M., Guibernau, J., Häusler, K. G., Hennerici, M., ... Gerloff, C. (2018). MRI-Guided Thrombolysis for Stroke with Unknown Time of Onset. *New England Journal of Medicine*, 379(7), 611–622. <https://doi.org/10.1056/NEJMoa1804355>
- Thomas, C., Ye, F. Q., Irfanoglu, M. O., Modi, P., Saleem, K. S., Leopold, D. A., & Pierpaoli, C. (2014). Anatomical accuracy of brain connections derived from diffusion MRI tractography is inherently limited. *Proceedings of the National Academy of Sciences*, 111(46), 16574–16579. <https://doi.org/10.1073/pnas.1405672111>
- Tombari, D., Loubinoux, I., Pariente, J., Gerdelat, A., Albucher, J.-F., Tardy, J., Cassol, E., & Chollet, F. (2004). A longitudinal fMRI study: in recovering and then in clinically stable sub-cortical stroke patients. *NeuroImage*, 23(3), 827–839. <https://doi.org/10.1016/j.neuroimage.2004.07.058>
- Tower, S. S. (1940). Pyramidal lesion in the monkey. *Brain*, 63(1), 36–90.

<https://doi.org/10.1093/brain/63.1.36>

- Traversa, R., Cicinelli, P., Pasqualetti, P., Filippi, M., & Rossini, P. M. (1998). Follow-up of interhemispheric differences of motor evoked potentials from the “affected” and “unaffected” hemispheres in human stroke. *Brain Research*, *803*(1–2), 1–8. [https://doi.org/10.1016/S0006-8993\(98\)00505-8](https://doi.org/10.1016/S0006-8993(98)00505-8)
- Trepel, M. (2017). *Neuroanatomie: Struktur und Funktion* (7th ed.). Elsevier.
- Tuch, D. S. (2004). Q-ball imaging. *Magnetic Resonance in Medicine*, *52*(6), 1358–1372. <https://doi.org/10.1002/mrm.20279>
- Turner, R. S., & Desmurget, M. (2010). Basal ganglia contributions to motor control: A vigorous tutor. *Current Opinion in Neurobiology*, *20*(6), 704–716. <https://doi.org/10.1016/j.conb.2010.08.022>
- van der Vliet, R., Selles, R. W., Andrinopoulou, E., Nijland, R., Ribbers, G. M., Frens, M. A., Meskers, C., & Kwakkel, G. (2020). Predicting Upper Limb Motor Impairment Recovery after Stroke: A Mixture Model. *Annals of Neurology*, *87*(3), 383–393. <https://doi.org/10.1002/ana.25679>
- van Dijk, K. R. A., Sabuncu, M. R., & Buckner, R. L. (2012). The influence of head motion on intrinsic functional connectivity MRI. *NeuroImage*, *59*(1), 431–438. <https://doi.org/10.1016/j.neuroimage.2011.07.044>
- van Meer, M. P. A., Otte, W. M., van der Marel, K., Nijboer, C. H., Kavelaars, A., van der Sprenkel, J. W. B., Viergever, M. A., & Dijkhuizen, R. M. (2012). Extent of Bilateral Neuronal Network Reorganization and Functional Recovery in Relation to Stroke Severity. *Journal of Neuroscience*, *32*(13), 4495–4507. <https://doi.org/10.1523/JNEUROSCI.3662-11.2012>
- van Meer, M. P. A., van der Marel, K., Wang, K., Otte, W. M., el Bouazati, S., Roeling, T. A. P., Viergever, M. A., Berkelbach van der Sprenkel, J. W., & Dijkhuizen, R. M. (2010). Recovery of Sensorimotor Function after Experimental Stroke Correlates with Restoration of Resting-State Interhemispheric Functional Connectivity. *Journal of Neuroscience*, *30*(11), 3964–3972. <https://doi.org/10.1523/JNEUROSCI.5709-09.2010>
- van Zijl, P. C. M., Hua, J., & Lu, H. (2012). The BOLD post-stimulus undershoot, one of the most debated issues in fMRI. *NeuroImage*, *62*(2), 1092–1102. <https://doi.org/10.1016/j.neuroimage.2012.01.029>
- Volz, L. J., Cieslak, M., & Grafton, S. T. (2018). A probabilistic atlas of fiber crossings for variability reduction of anisotropy measures. *Brain Structure and Function*, *223*(2), 635–651. <https://doi.org/10.1007/s00429-017-1508-x>

- Volz, L. J., Eickhoff, S. B., Pool, E.-M., Fink, G. R., & Grefkes, C. (2015). Differential modulation of motor network connectivity during movements of the upper and lower limbs. *NeuroImage*, *119*, 44–53. <https://doi.org/10.1016/j.neuroimage.2015.05.101>
- Volz, L. J., Rehme, A. K., Michely, J., Nettekoven, C., Eickhoff, S. B., Fink, G. R., & Grefkes, C. (2016). Shaping Early Reorganization of Neural Networks Promotes Motor Function after Stroke. *Cerebral Cortex*, *26*(6), 2882–2894. <https://doi.org/10.1093/cercor/bhw034>
- Volz, L. J., Sarfeld, A.-S., Diekhoff, S., Rehme, A. K., Pool, E.-M., Eickhoff, S. B., Fink, G. R., & Grefkes, C. (2015). Motor cortex excitability and connectivity in chronic stroke: a multimodal model of functional reorganization. *Brain Structure and Function*, *220*(2), 1093–1107. <https://doi.org/10.1007/s00429-013-0702-8>
- Volz, L. J., Vollmer, M., Michely, J., Fink, G. R., Rothwell, J. C., & Grefkes, C. (2017). Time-dependent functional role of the contralesional motor cortex after stroke. *NeuroImage: Clinical*, *16*(June), 165–174. <https://doi.org/10.1016/j.nicl.2017.07.024>
- von Monakow, C. (1914). *Die Lokalisation im Grosshirn und der Abbau der Funktion durch kortikale Herde*. Bergmann, J. F.
- Wade, D. T. (1989). Measuring arm impairment and disability after stroke. *International Disability Studies*, *11*(2), 89–92. <https://doi.org/10.3109/03790798909166398>
- Wang, L. E., Tittgemeyer, M., Imperati, D., Diekhoff, S., Ameli, M., Fink, G. R., & Grefkes, C. (2012). Degeneration of corpus callosum and recovery of motor function after stroke: A multimodal magnetic resonance imaging study. *Human Brain Mapping*, *33*(12), 2941–2956. <https://doi.org/10.1002/hbm.21417>
- Ward, N. S., Brown, M. M., Thompson, A. J., & Frackowiak, R. S. J. (2003). Neural correlates of motor recovery after stroke: A longitudinal fMRI study. *Brain*, *126*(11), 2476–2496. <https://doi.org/10.1093/brain/awg245>
- Ward, N. S., Newton, J. M., Swayne, O. B. C., Lee, L., Thompson, A. J., Greenwood, R. J., Rothwell, J. C., & Frackowiak, R. S. J. (2006). Motor system activation after subcortical stroke depends on corticospinal system integrity. *Brain*, *129*(3), 809–819. <https://doi.org/10.1093/brain/awl002>
- Wedeen, V. J., Hagmann, P., Tseng, W.-Y. I., Reese, T. G., & Weisskoff, R. M. (2005). Mapping complex tissue architecture with diffusion spectrum magnetic resonance imaging. *Magnetic Resonance in Medicine*, *54*(6), 1377–1386. <https://doi.org/10.1002/mrm.20642>
- Wedeen, V. J., Wang, R. P., Schmahmann, J. D., Benner, T., Tseng, W. Y. I., Dai, G., Pandya, D. N., Hagmann, P., D’Arceuil, H., & de Crespigny, A. J. (2008). Diffusion spectrum

- magnetic resonance imaging (DSI) tractography of crossing fibers. *NeuroImage*, 41(4), 1267–1277. <https://doi.org/10.1016/j.neuroimage.2008.03.036>
- Wigan, A. L. (1844). *A New View of Insanity: The Duality of the Mind*. Longman, Brown, Green and Longmans.
- Willis, T. (1664). *Cerebri Anatome*. Martyn and Allestry.
- Xu, H., Qin, W., Chen, H., Jiang, L., Li, K., & Yu, C. (2014). Contribution of the resting-state functional connectivity of the contralesional primary sensorimotor cortex to motor recovery after subcortical stroke. *PLoS ONE*, 9(1), 1–9. <https://doi.org/10.1371/journal.pone.0084729>
- Yang, H.-S., Kwon, H. G., Hong, J. H., Hong, C. P., & Jang, S. H. (2011). The rubrospinal tract in the human brain: Diffusion tensor imaging study. *Neuroscience Letters*, 504(1), 45–48. <https://doi.org/10.1016/j.neulet.2011.08.054>
- Yeh, F.-C., Panesar, S., Fernandes, D., Meola, A., Yoshino, M., Fernandez-Miranda, J. C., Vettel, J. M., & Verstynen, T. (2018). Population-averaged atlas of the macroscale human structural connectome and its network topology. *NeuroImage*, 178(April), 57–68. <https://doi.org/10.1016/j.neuroimage.2018.05.027>
- Yeh, F.-C., Wedeen, V. J., & Tseng, W.-Y. I. (2010). Generalized q-Sampling Imaging. *IEEE Transactions on Medical Imaging*, 29(9), 1626–1635. <https://doi.org/10.1109/TMI.2010.2045126>
- Yu, C., Zhu, C., Zhang, Y., Chen, H., Qin, W., Wang, M., & Li, K. (2009). A longitudinal diffusion tensor imaging study on Wallerian degeneration of corticospinal tract after motor pathway stroke. *NeuroImage*, 47(2), 451–458. <https://doi.org/10.1016/j.neuroimage.2009.04.066>
- Zaaimi, B., Edgley, S. A., Soteropoulos, D. S., & Baker, S. N. (2012). Changes in descending motor pathway connectivity after corticospinal tract lesion in macaque monkey. *Brain*, 135(7), 2277–2289. <https://doi.org/10.1093/brain/aws115>
- Zalesky, A., Fornito, A., Cocchi, L., Gollo, L. L., van den Heuvel, M. P., & Breakspear, M. (2016). Connectome sensitivity or specificity: which is more important? *NeuroImage*, 142, 407–420. <https://doi.org/10.1016/j.neuroimage.2016.06.035>
- Zheng, X., Sun, L., Yin, D., Jia, J., Zhao, Z., Jiang, Y., Wang, X., Wu, J., Gong, J., & Fan, M. (2016). The plasticity of intrinsic functional connectivity patterns associated with rehabilitation intervention in chronic stroke patients. *Neuroradiology*, 58(4), 417–427. <https://doi.org/10.1007/s00234-016-1647-4>
- Zimny, A., Neska-Matuszewska, M., Bladowska, J., & Sasiadek, M. J. (2015). Intracranial

lesions with low signal intensity on T2-weighted MR images - review of pathologies.
Polish Journal of Radiology, 80(1), 40–50. <https://doi.org/10.12659/PJR.892146>

8. Personal contributions

In study 1 to 3, I contributed to the conception and design of the studies and acquired a substantial amount of the data.

In study 1 and 2, preprocessing and analyses of the data were carried out by me under the supervision of Dr. Lukas Volz and in collaboration with Dr. Matt Cieslack for specific questions regarding the preprocessing and reconstruction of dMRI data. I drafted the first version of the manuscripts and refined them together with Dr. Lukas Volz while receiving helpful feedback from all co-authors.

Study 3 was a shared first authorship project with Valerie Wiemer, a Phd student in our lab. She assisted me with data acquisition in study 1 to 3. I performed the data preprocessing for study 3. Data analyses in study 3 were largely based on my analysis scripts and carried out together with Valerie Wiemer under the supervision of Dr. Lukas Volz. For study 3, I drafted the first version of the introduction and discussion section, while Valerie Wiemer drafted the first version of methods and results. Together with Dr. Lukas Volz, we carefully revised the manuscript and incorporated feedback from all co-authors.

Study 4 relied on data formerly acquired by Dr. Lukas Volz. In study 4, I carried out the preprocessing and analyses of the data under the supervision of Dr. Lukas Volz. I wrote the first draft of the manuscript, which I then refined together with Dr. Lukas Volz. All co-authors provided valuable feedback throughout the process.